POLYTECHNIQUE MONTRÉAL
affiliée à l'Université de Montréal

On Topology Optimization in the Generative Design Framework: Use on Aircraft Structure Design

JEAN-FRANÇOIS GAMACHE
Département de génie mécanique

Thèse présentée en vue de l'obtention du diplôme de *Philosophiæ Doctor*
Génie mécanique

Août 2021

© Jean-François Gamache, 2021.

POLYTECHNIQUE MONTRÉAL
affiliée à l'Université de Montréal

Cette thèse intitulée :

On Topology Optimization in the Generative Design Framework: Use on Aircraft Structure Design

présentée par **Jean-François GAMACHE**
en vue de l'obtention du diplôme de *Philosophiæ Doctor*
a été dûment acceptée par le jury d'examen constitué de :

Daniel THERRIAULT, président
Sofiane ACHICHE, membre et directeur de recherche
Aurelian VADEAN, membre et codirecteur de recherche
Frederick GOSSELIN, membre
Michael KOKKOLARAS, membre externe

DEDICATION

To my parents Louise and Denis,
my brothers David and Vincent,
thank you for your support.

ACKNOWLEDGEMENTS

The final year of working on this thesis has been a real challenge for all of us, with the Covid-19 confinement. Working with such a wonderful palette of unique people have helped me tremendously to push through the last year.

First and foremost, I want to thank both of my advisors, Prof. Sofiane Achiche and Prof. Aurelian Vadean, if not for them, I would not have had the chance to pursue this amazing project. Your trust and patience has been felt throughout the many years I've worked with you. Your guidance has pushed me through the difficult path of research.

I also want to thank Stelia Canada, but especially the people I've worked with. Émeric for starting the project that became the subject of my thesis. Nicolas for its continuous help, support and engagement in my project. I also want to thank my colleagues for their advice: Aniello, Simon, Daniel, and Patrick.

My colleagues in the CoSIM laboratory are the reason I choose to pursue the PhD at Polytechnique. I would not be presenting this thesis without you guys. You are the best venting group ever. Thank you for the good times, I wish we could have played cards at lunch until the end.

I want to acknowledge the help I got from interns and other graduate students throughout my project. Patrick, Peter, Steve, Kevin and Clément have been incredible colleagues that have helped me advance my project much faster. I want to especially note Mario and Thomas which have helped me through the end of my project. I wish you good luck in pursuing your degrees and your research in the ever interesting domain of topology optimization.

Finally, I really want to thank my family and friends for their support and encouragement. My time away from my project has always been a good time because of all of you. You gave me the energy to push through and kept me motivated until the end.

RÉSUMÉ

La conception des ailes d'avion est un projet pluridisciplinaire complexe qui demande une collaboration importante entre tous les groupes de développement. Un des membres principaux de cette équipe pluridisciplinaire est l'équipe de conception structurelle. Depuis quelques années, l'optimisation topologique est de plus en plus utilisée par les ingénieurs structuraux puisque c'est un outil qui leur permet de diminuer significativement la masse des composantes structurelles.

Ce projet de doctorat s'inscrit dans le cadre du projet de grande envergure MuFox, qui regroupe plusieurs partenaires académiques et industriels du domaine aéronautique canadien. L'objectif de MuFox est de développer un cadre d'optimisation multidisciplinaire pour les caissons de voilure d'avions commerciaux. C'est dans ce contexte que ce projet cherche à développer des méthodes et des outils pour intégrer l'optimisation topologique dans le processus de conception des caissons de voilure et plus spécifiquement des panneaux raidis. En effet, plusieurs tentatives dans la littérature et dans l'industrie ont démontré que l'utilisation actuelle de l'optimisation topologique sur les panneaux raidis ne permet aucun gain de masse significatif et que son utilisation dans le processus de conception reste laborieux.

Dans cette thèse, nous avons identifié plusieurs limitations au niveau du processus de conception basé sur l'optimisation topologique pour l'optimisation de structures aéronautiques. C'est pourquoi nous proposons un cadre de conception générative (generative design), afin de mieux étudier l'effet de l'optimisation topologique, qui est alors considéré comme un système génératif (generative system). La conception générative peut être décrite comme l'automatisation du design conceptuel par des règles implémentées sur ordinateur. Les systèmes génératifs ont trois propriétés clefs, soit la génération, la représentation et l'exploration.

Nous notons un déséquilibre de ces trois propriétés pour l'optimisation topologique appliquée aux structures aéronautiques, principalement lors de la prise en compte de l'instabilité liée au flambement. L'inclusion du flambement amplifie ce déséquilibre relié à l'utilisation de la génération implicite qui rend l'implémentation d'analyses de plus haute fidélité très difficile. C'est ce que nous mettons de l'avant dans deux articles qui discutent des méthodes basées sur la densité et sur le « Ground-Structure ». Dans les deux cas, il apparaît primordial d'inclure un processus de validation pour être capable d'évaluer la performance réelle des solutions que l'optimisation topologique génère. Les résultats de ces études montrent aussi que la complexité des solutions proposées rend la validation difficile. Nous avons aussi mis de l'avant la taille impressionnante de l'espace de conception lors de l'optimisation topologique.

Afin de faciliter le processus d'interprétation et de validation de la performance au travers de ce large espace de conception, nous proposons un algorithme basé sur la vision par ordinateur qui peut automatiquement reconnaître une structure explicite, donc d'identifier le graphe de connexions, à partir de la distribution de matière implicite.

Finalement, pour parer les déséquilibres des algorithmes d'optimisation topologique actuels, nous proposons un nouvel algorithme qui tient en compte la complexité des solutions et la taille de l'espace de conception. Le développement de cet algorithme a pour but de développer une manière efficace d'utiliser une génération explicite et une exploration axées sur la diversité. Nous avons nommé cet algorithme « Complexity-Driven Conceptual Exploration for Aircraft Structures » (CD-CEAS). C'est donc un algorithme qui vise d'abord l'aide à la conception puis l'optimisation, contrairement à l'optimisation topologique classique qui vise un résultat "optimal", avec des contraintes de conception. CD-CEAS est basé sur plusieurs disciplines de l'ingénierie, incluant le design axiomatique pour évaluer la complexité fonctionnelle, les systèmes génératifs axés sur la performance, la grammaire basée sur les graphes et la recherche stochastique. Les résultats de deux études de cas sont présentés et montrent un avantage marqué par rapport à l'optimisation topologique autant au niveau de la vitesse d'exécution que de l'exploration. Par exemple, dans un cas de design de panneau de type « bulkhead », on peut faire apparaître un compromis de 1% de masse, pour une réduction de 70% de complexité. Pour la génération de panneau compressé avec contrainte de flambement, 500 solutions ont été créés et dimensionnées en seulement 6 heures. Pour l'équivalent avec l'optimisation topologique par densité, le temps de calcul est plutôt de 3 à 4 jours.

ABSTRACT

Aircraft wing design is a complex multidisciplinary task which requires a close collaboration between multiple engineering groups. A main actor of aircraft design is the team of design and analysis of the structure. Engineers have come to rely on many structural optimization tools, and more recently topology optimization has seen an increase usage. Topology optimization has shown to be an effective tool to significantly reduce the weight of simple structural components.

This doctoral project is part of the multidisciplinary optimization project MuFox, which is a large partnership with the Canadian aeronautic industry and academic partners. The objective of MuFox was to develop a multidisciplinary optimization framework for the design of aircraft wing box. It is in this context that we developed our work of wing box topology optimization for aircraft design, and more specifically for stiffened panel design. There exists several publications in academia and industry for stiffened panel topology optimization but current results show no significant reduction of weight with respect to conventional designs, as well as they are unable to demonstrate either time reduction or simplification of the design process.

In our work, we have identified multiple limitations in the design process based on topology optimization for aircraft structural component. This is why we propose to use a generative design framework to categorize topology optimization as a generative system and improve its capabilities within this framework. Generative design can be summarized as the automation of conceptual design via the use of a generative system. Generative systems have three key properties: generation, representation and exploration.

We note that these properties are not balanced for topology optimization when used for the design of aircraft structures, which is mainly driven by buckling instabilities prevention. Buckling analysis amplifies the unbalance of the implicit generation used in topology optimization when trying to use high-fidelity models. This is put forward in two articles of this thesis which concern two algorithms: the density-based approach and the ground-structure approach. In both cases, the importance of validation with high-fidelity models is put forward to ensure performance is conserved when the topologies are interpreted and designed. The results have shown that validation and interpretation is made more difficult by the complexity of material distributions. Another challenging aspect is the enormous size of the design space of topology optimization, which requires many evaluations to understand. Exploration with these algorithms is minimal.

To automate validation and exploration of this large design space, we propose a tool based on computer vision. The algorithm we have developed allows the computer to automatically translate the implicit model used in continuous topology optimization towards an explicit model that can be used directly for high-fidelity validation modeling.

Finally, with the identified unbalance of topology optimization as a generative system, we propose a new algorithm for aircraft structural optimization. This new algorithm takes into account the complexity and size of the design and solution space to help designers navigate and reach optimal solutions. We have named the algorithm "Complexity-Driven Conceptual Exploration for Aircraft Structures" (CD-CEAS). The main development driver was to build an explicit generation method that can easily consider high-fidelity models and an exploration algorithm that is focused on diversity rather than intensification. Consequently, CD-CEAS is focused on design first and optimization second, whereas topology optimization is focused on optimization first and design second.

CD-CEAS includes many engineering methods, as in axiomatic design, performance-based generative systems, graph-grammars and stochastic search. Results from two case studies have shown a clear advantage of CD-CEAS with respect to current topology optimization approaches in terms of speed of execution (including all aspects of generation, representation, and exploration) and in terms of solution diversification. We have found that by adapting the balance of generation, representation and exploration to the specific problem of stiffened panel design, we can obtain a better tool for supporting the design process. For example, in the case of the pressurized bulkhead, CD-CEAS showed a compromise of about 1% of weight, with a reduction of 70% of complexity. Furthermore, in the case the compressed stiffened panel CD-CEAS generated and sized 500 feasible layouts in only 6 hours. An equivalent exploration had taken multiple days with a commercial software.

TABLE OF CONTENTS

DEDICATION iii

ACKNOWLEDGEMENTS iv

RÉSUMÉ v

ABSTRACT vii

TABLE OF CONTENTS ix

LIST OF TABLES xiii

LIST OF FIGURES xiv

LIST OF SYMBOLS AND ACRONYMS xx

CHAPTER 1 INTRODUCTION **1**

1.1 Context 1

1.1.1 Aircraft Design 2

1.2 Definitions and concepts 3

1.2.1 Aircraft Assemblies 4

1.2.2 Stiffened Panels 5

1.2.3 Structural Optimization 6

1.2.4 Design Theories 7

1.2.5 Generative Design 8

1.3 Problematic 10

1.4 Research Objectives 12

1.5 Thesis Outline 13

CHAPTER 2 LITERATURE REVIEW **14**

2.1 Analyzing and Sizing Stiffened Panels 15

2.1.1 Challenges of Stiffened Panel Design 15

2.1.2 Buckling 16

2.1.3 Post-Buckling 20

2.1.4 Sizing Aircraft Structures 21

2.2 Structural Optimization Algorithms 22

2.3 Novel Stiffening Patterns for Compressed Stiffened Panels 23
2.3.1 Buckling Containment Features (BCF) 24
2.3.2 Curvilinear Stiffeners 24
2.4 Generative Design 26
2.4.1 Classification of Generative Systems 26
2.4.2 Integrating Generative Systems in the Generative Design Approach . 31
2.5 Topology Optimization Methods and Aircraft Applications 33
2.5.1 Continuum Methods 33
2.5.2 Truss Optimization (Ground-Structure) 36
2.5.3 Level-Set Methods 37
2.5.4 Moving Morphable Components 39
2.5.5 Novel Topology Optimization Approaches 41
2.5.6 Challenges of Nonlinear Constraints in Topology Optimization 42
2.6 Conclusion on State-of-the-Art 43

CHAPTER 3 GENERATIVE DESIGN APPROACH FOR STIFFENED PANELS **45**
3.1 Generative Design Framework 45
3.2 Summary of Articles 46

CHAPTER 4 Article 1: Image-based Truss Recognition for Density-Based Topology Optimization Approach **49**
4.1 Introduction 50
4.2 Literature Review 51
4.3 Methodology 53
4.3.1 Step 1: Image Acquisition & Pre-Processing 54
4.3.2 Step 2: Binary Image Skeletonization Method 54
4.3.3 Step 3: Node Position 56
4.3.4 Step 4: Node Connectivity 57
4.3.5 Step 5: Image Segmentation 58
4.3.6 Step 6: Truss Stabilization 60
4.4 Skeletonization Comparison 62
4.4.1 Comparison with Bremicker 63
4.4.2 Comparison with Gedig 64
4.5 Case Study 65
4.5.1 Optistruct Results 67
4.5.2 Truss Recognition Discussion 67
4.6 Conclusion 71

CHAPTER 5 Article 2: On Generating Stiffening Layouts with Density-Based Topology Optimization Considering Buckling **72**
5.1 Introduction . . . 72
5.1.1 Aerospace Applications of Topology Optimization . . . 73
5.1.2 Topology Optimization . . . 74
5.1.3 This Work . . . 76
5.1.4 Case Study . . . 77
5.2 Setting Up Topology Optimization . . . 79
5.2.1 The Reference Material Distribution . . . 82
5.2.2 Parameter and Formulation Analysis . . . 83
5.2.3 Randomized Initial Values Topology Optimization . . . 86
5.3 Interpretation, Sizing and Validation . . . 91
5.3.1 Sizing the "New" Stiffened Panels . . . 91
5.3.2 Validating the Stiffening Layouts . . . 94
5.4 Conclusion . . . 96

CHAPTER 6 Article 3: Topology Optimization for Stiffened Panels: A Ground-Structure Method **100**
6.1 Introduction . . . 100
6.1.1 Optimization with a Buckling Constraint . . . 102
6.1.2 Ground Structure Topology Optimization for Stiffened Panels . . . 103
6.2 Case Study . . . 103
6.3 Ground Structure Method for Stiffened Panels Design . . . 104
6.3.1 Setting-up Ground Structure Topology Optimization . . . 106
6.3.2 Solving Ground-Structure Topology Optimization . . . 109
6.3.3 Interpreting and Sizing Proposed Layouts . . . 111
6.4 Discussion . . . 113
6.4.1 Topology Optimization Setup . . . 114
6.4.2 Computing Topology Optimization . . . 114
6.4.3 Interpretation and Sizing . . . 115
6.4.4 Possibilities of Improvement . . . 115
6.5 Conclusion . . . 116

CHAPTER 7 Article 4: Complexity-Driven Conceptual Exploration for Aircraft Structures (CD-CEAS) **117**
7.1 Introduction . . . 117
7.1.1 Generative Design . . . 118

7.1.2 Topology Optimization 120
7.1.3 Conventional and Performance-based Generative Systems 121
7.1.4 Scope of this Work 122
7.2 Complexity Measures for Optimization 123
7.2.1 Introduction to Axiomatic Design 124
7.2.2 Complexity Measure for Complexity-Driven Exploration 127
7.3 Performance Evaluation Implementation for Stiffened Panels 129
7.4 Graph-Grammar for Stiffened Panels 131
7.5 Complexity-Driven Basic Burst-Algorithm 134
7.6 Case Studies of CD-CEAS 136
7.6.1 Pressure Bulkhead with Out-of-plane Loading 136
7.6.2 Compressed Stiffened Panel, with In-plane Loading 140
7.7 Discussion and Limitations 146
7.8 Conclusion 148

CHAPTER 8 GENERAL DISCUSSION **150**
8.1 Industrial Deliverable 151
8.2 Contributions and Importance of Research 151
8.3 Limitations 152

CHAPTER 9 CONCLUSION & FUTURE WORK **155**

REFERENCES 158

LIST OF TABLES

Table 4.1: HyperMesh model geometry and optimization parameters 66
Table 5.1: Sizing optimization formulation 79
Table 5.2: Aluminum 7075 properties 80
Table 5.3: Baseline dimensions [in.] from different optimization methods 81
Table 5.4: Baseline load values, with integrated safety factors. 81
Table 5.5: Baseline properties with a 4-stiffener orthogrid layout. Two sizing optimization were completed, with the handbook sizing allowing for a controlled skin buckling. 81
Table 5.6: Comparison of baseline and reference material distribution 84
Table 5.7: Optimization parameters for random initial value TO 87
Table 5.8: Sizing optimization formulation 92
Table 5.9: Properties of each interpreted panels 94
Table 5.10: Non-linear validation of each interpreted panels in name order 97
Table 6.1: Aluminum 7075 properties 104
Table 6.2: Baseline properties 105
Table 6.3: Properties of some layouts obtained with density-based optimization compared to the baseline obtained with handbook methods. 106
Table 6.4: The relation between density (ρ_x) and height (H_x) variables for each stiffener (SAV_X) variable 109
Table 6.5: Comparison of stiffening layouts 113
Table 7.1: Aluminum 7075 properties 137
Table 7.2: Properties of the model created from an SIMP interpretation 137
Table 7.3: Baseline properties 141
Table 8.1: All scientific publications completed during this PhD. 153
Table 8.2: Major contributions by communities 154

LIST OF FIGURES

Figure 1.1: Aircraft design phases and relative time and cost escalation 2

Figure 1.2: Evolution of knowledge during the design process. It shows that during design, knowledge of the product comes later at which point freedom has already been limited by previous decisions. [1]. 3

Figure 1.3: Stiffened panel assembly with an orthogrid layout, meaning all stiffeners are orthogonal. 4

Figure 1.4: Wing box assembly. 4

Figure 1.5: Different types of structural optimizations [2]. (A) Design space (B) Size optimization (C) Shape optimization (D) Topology optimization. 6

Figure 1.6: Top-down vs bottom-up design approaches 8

Figure 2.1: Illustration of complexities in the structural engineering world 15

Figure 2.2: Possible buckling modes for stiffened panels 18

Figure 2.3: Skin variables that affect buckling resistance 18

Figure 2.4: Illustration of the BCF as sub-stiffening elements in an orthogrid stiffened panel. [3] 24

Figure 2.5: Unitized panel with curvilinear stiffeners 25

Figure 2.6: Classification of generative systems. Note that the categories used are conventional ones, found in the literature. The classification has no "hard" boundaries, they are placed qualitatively. All of the tools included in this figure are discussed in the next sub-sections. From left to right, increasingly explicit definition of topological variables. The current research trends, encouraged by the ever increasing computing powers, has pushed recent research in topology optimization towards more and more explicit generation. From bottom to top, you get towards exploration vs performance focus. The difference between research communities is mostly driven in this axis. Topology optimization is rather focused on find the "optimal" results and driven by applied science teams, whereas generative systems are more focused on helping designers and driven by design science teams. 28

Figure 2.7: Design method with topology optimization 32

Figure 2.8: Illustration of density in a SIMP topology optimization [2]. The values represent the resulting density of each element, thus changing the Young's modulus of said elements. The force F is applied at the middle of the exterior face. 35
Figure 2.9: The ground structure [2] (left) and a result of truss area optimization from the ground structure (right). The design variables in this example are the thickness of the trusses, illustrated with varying thicknesses of lines. The force F is applied at the middle of the exterior face. . . . 37
Figure 2.10: The level-set method with initial hole positions (left) and a result of optimization (right) [4]. In green, where material is "full" and the other regions are considered "void". The force F is applied at the middle of the exterior face. 39
Figure 2.11: MMC method with initial member positions (left), a result of optimization (right) and commonly used design variables for each morphable components (bottom) [5]. In red, where material is considered "full" and the rest is considered "void. Where F is the applied force. The other variable are the explicit topological variables of each components, where θ is the angle, x and y the position, W and L the width and length. 40
Figure 3.1: Balancing topology optimization towards a focus on exploration using more explicit generation. This approach has helped the algorithm use higher fidelity models which reduces the amount of rework required in preliminary and detailed design. 48
Figure 4.1: The different steps of the truss recognition algorithm 55
Figure 4.2: Cantilever beam design space, this structure problem is used as an illustration throughout this section with L/D ratio of 2. 56
Figure 4.3: Inputs image for the cantilever beam 57
Figure 4.4: Steps of the skeletonization process. (a) Unloaded edges, used as sources for geodesic distances, (b) The geodesic distance of the edges in the binary topology image (the darker the color, the farther it is from an unloaded edge), (c) The watershed image. The ridges (in black) can be interpreted as the image skeleton, (d) The skeleton obtained using our proposed skeletonization method. 58
Figure 4.5: The intersections and endpoints of the binary skeleton are considered nodes of the skeletal structure 59

Figure 4.6: Node connectivity method. (a) Find nodes on image skeleton. (b) Remove nodes and segment each lines. (c) draw aura around each lines and detect which lines connects to the same nodes. The step is repeated for each lines (d) The connectivity of each nodes is extracted as a graph. 60
Figure 4.7: Results of recognition of node positions and connections on the cantilever use case. In gray, the initial material distribution and the recognized trusses superimposed on it. 61
Figure 4.8: Segmentation results of the cantilever beam 61
Figure 4.9: Stabilized structure. The short unstable trusses of fig. 4.7 were removed. 62
Figure 4.10: A comparison of different skeletonization results, note that skeletons have been dilated for illustration purpose.(a) Bremicker's cantilever beam results with homogenization method [6], (b) Bremicker's skeleton [6], (c) MATLAB bwmoprh skeleton with thinning, (d) Skeleton using the method presented in this work. 64
Figure 4.11: A comparison with Gedig's work, note that skeletons have been dilated for illustration purpose. (a) Gedig's beam results with SIMP method [7] (b) Gedig's skeleton [7] (c) MATLAB bwmorph skeleton with thinning (d) Skeleton using the method presented in this work 65
Figure 4.12: HyperMesh model of loaded rib. 66
Figure 4.13: Binarization of ribs material distribution. (a) Optimal material distribution using Optistruct (b) Binarization of material distribution with a low threshold (All pixels with density value over 0.01) (c) Binarization of material distribution with a high threshold (All pixels with density value over 0.98) 68
Figure 4.14: Rib's material distribution connectivity with low threshold. (a) Connectivity results (b) Image segmentation 69
Figure 4.15: Rib's material distribution connectivity with high threshold. (a) Connectivity results. (b) Image segmentation. 70
Figure 5.1: Research method used in this research project. Including validation of stiffened panels has shown that topology optimization need to consider buckling. 78
Figure 5.2: Sub-Components of the Stiffened Panel 78

Figure 5.3: Boundary and loading conditions of the case study. U_x,U_y,U_z are the displacement conditions and R_x,R_y,R_z the rotation conditions. F_y is the chord-wise compression, F_x is the span-wise compression, τ_{xy} Shear. 80
Figure 5.4: Baseline Dimensions. Where is W the panel width, b the bay width, L the panel length, p the pad-up width, h the stiffener height, f the free-flange width. 80
Figure 5.5: Stiffened panel topology design space 82
Figure 5.6: Boundary and loading conditions of the design space for topology optimization of the panel. (a) Boundary conditions on the design space. (b) Loading conditions on the design space. Where F_y is chord-wise compression, F_x is span-wise compression, τ_{xy} is shear, U_x,U_y,U_z are displacement conditions, R_x,R_y,R_z are rotation conditions 83
Figure 5.7: Reference material distribution 84
Figure 5.8: Material distributions of compliance only optimization (a) modeling compared to the optimization with an additional buckling constraint (c). The results with random initial density values with compliance only (b) and added buckling (d). Where T is the design space thickness. 87
Figure 5.9: The effect of three different fully random initial values on TO. On top, the random initial value distribution of three examples. On the bottom line, their respective optimized material distribution. 89
Figure 5.10: Frequency of different families of topology distribution for 500 random initial values 89
Figure 5.11: A sample of the family of “4 stiffeners” material distribution. These material distributions all have the same topology. (a) A sample of "4-stiffeners" material distributions. (b) First buckling modes of respective "4-stiffeners" material distribution. The total displacement of each node is illustrated. 90
Figure 5.12: The effect of initial values on the convergence of TO with buckling constraints. The color of each curve is related to each material distribution (box of the same color). 92
Figure 5.13: Interpretation into Stiffened Panels of the different Layout Families . 93
Figure 5.14: Non-linear analysis using the RIKS method for the baseline with sized with handbook methods. Note that there is a separation between initial buckling and collapse, this is the stable post-buckling. 96
Figure 5.15: Evolution of the stress range of the baseline 97

Figure 5.16: Non-linear relation between displacement and applied load for all layouts. The analysis stops at numerical instability or when collapse is reached. See fig. 5.13 for definition of layouts. 98
Figure 6.1: Four-stiffeners (Baseline) sub-components of the stiffened panel . . . 105
Figure 6.2: Loads applied on the baseline stiffened panel 105
Figure 6.3: The stiffened panel ground-structure 107
Figure 6.4: The design variables for the ground-structure topology optimization. 108
Figure 6.5: The relation between density and height variables for each stiffener . 110
Figure 6.6: Distribution of results from a 100 random initial values ground-structure topology optimization. 111
Figure 6.7: Ground-Structure lightest layouts, color indicate regions affected by different variables. 112
Figure 6.8: Interpretation of stiffening layouts. The interpretation process uses engineering knowledge to modify the results towards more classical solutions. ISA has 5 stiffeners and is interpreted from GSA and GSD and ISB has 6 stiffeners and is interpreted from GSB and GSC. . . . 112
Figure 7.1: General process of the CD-CEAS approach. 124
Figure 7.2: Sub-Components of the Stiffened Panel 129
Figure 7.3: Generation of graph representation and conversion to FEM from the application of the action “CreateStiffener”. We show the application of the same action on two different nodes. On top, we see that there are no intersections, as such the grammar rules allows the grid to adapt to the stiffener with "Offset Nodes". On the bottom, two stiffeners intersect, and the grammar rule forces the node to get back to its initial position as an "Active node". The illustrated model has an aspect ratio of 1:1, but it is possible to easily change the conversion to other surfaces. 133
Figure 7.4: Our implementation of the basic Burst algorithm. [8] 135
Figure 7.5: Test case of a stiffened panel with a uniform pressure, with simply supported boundary conditions. (a) The pressure load is applied uniformly on the whole panel. (b) The panel dimensions. Where U_z is the imposed displacement. 137
Figure 7.6: (a) Material Distribution using SIMP (b) Interpretation as a stiffened panel, shown as a graph. 137
Figure 7.7: Solutions on the Pareto front for the pressurized stiffened panel exploration. 139

Figure 7.8: Results of the compliance-based run for the pressure case study. For this run, the sizing optimization uses a compliance minimization with a weight constraint of 5.0 lb. Burst size: 8, Archive has 500 layouts, relaxation is set to 3 and the grid size is 10x10. Symmetry on both axis is active. (a) Pareto front for the pressurized stiffened panel exploration. (b) Convergence of compliance for the Pressure Bulkhead. 139
Figure 7.9: Second set of solutions of the Pareto front for the pressurized stiffened panel exploration. The optimization parameters are the same as of fig. 7.8 140
Figure 7.10: Test case of an axially compressed stiffened panel, with simply supported boundary conditions. (a) The applied load. (b) The design space dimensions. Where, U_z, U_x are imposed displacement, and F_x is the applied force on a RBE2. 142
Figure 7.11: Compression baseline layout from a commercial aircraft, sized with handbook methods. Where t_{Stiff} and t_{Skin} are respectively the thickness variables for stiffeners and skin sections. 142
Figure 7.12: Layouts on the Pareto front for the compliance-based compression case. 143
Figure 7.13: Results of the compliance-based run of the compression case study. For this run, the sizing optimization uses a compliance minimization with a weight constraint of 5.0 lb. Burst size: 8, Archive has 500 layouts, relaxation is set to 3 and the grid size is 10x10. Symmetry on both axis is active. (a) Scatter of the archive of all layouts created in this compliance-based run. (b) Layouts on the Pareto front for the compliance-based compression case. 144
Figure 7.14: Sizing optimization with weight minimization and a buckling constraint ($\lambda_1 = 1.0$ for all layouts) for the layouts proposed by CD-CEAS for the search with compliance only. 144
Figure 7.15: Layouts on the Pareto front for the buckling-based compression case. 145
Figure 7.16: Results of the buckling-based run of the compression case study. For this run, the sizing optimization uses a weight minimization with a buckling constraint of $\lambda > 1.0$ and a weight constraint of 5.0 lb. Burst size: 8, Archive has 500 layouts, relaxation is set to 3 and the grid size is 10x10. Symmetry on both axis is active. (a) Scatter of the archive of all layouts created in the buckling-based run. (b) Convergence of weight in the buckling-based run. 146

LIST OF SYMBOLS AND ACRONYMS

CAD	Computer Aided Design
CD-CEAS	Complexity-Driven Conceptual Exploration for Aircraft Structures
DFEM	Detailed FEM
DOE	Design of Experiment
DP	Design Parameter
FEM	Finite Element Model
FEA	Finite Element Analysis
FR	Functional Requirement
GFEM	General FEM
GSM	Ground-Structure Method
LSM	Level-Set Method
MDO	Multi-Disciplinary Optimization
MMC	Moving Morphable Components
OT	Optimized Topology
SIMP	Solid Isotropic Material with Penalization
TO	Topology Optimization

CHAPTER 1 INTRODUCTION

1.1 Context

Airplanes have tremendously changed how people travel, which propelled the human civilization into a globalized society [9]. Flying, be it for leisure or business reaches nearly 4.1 billion passengers in 2017 [10]. Keeping its current growth, the aviation sector will have three times more passengers by 2050 [10]. Furthermore, since emissions of CO_2 from aircraft is directly released in the upper atmosphere, its lifecycle is longer and thus has much more impact on climate change than ground emissions [10]. In 2000, the aviation sector has contributed to 0.8% of total anthropogenic warming (with an impact of 0.009°C of warming) [10]. In 2050, if the efficiency of aircraft keeps increasing at its current pace, the aviation sector could reach 1.4% of anthropogenic warming (0.04°C of warming) and 5.2% (up to 0.1°C) in 2100 [10]. The Paris Agreement on climate seeks to limit the warming of the planet at 2°C and aviation will be a major contributor to it's success.

The threat caused by climate change makes it important, if not urgent, to reduce the consumption of fuel to decrease the greenhouse gas emission in the aviation sector. The aircraft and engine manufacturers are currently working on a large and diversified portfolio of projects to achieve the environmental transition required for the 21st century. There are projects of electrification and hybridization of propulsion [11], changes of materials and structures [12, 13], biofuels [14], new types of configurations [15] and new lifecycle design methods [16]. Innovation is not the work of a single team or discipline any more, making it even more complicated. Combining multiple disciplines and expertize with emergent tools in a multidisciplinary design, analysis and optimization approaches is the primary research axis of the last decade [17–19].

This PhD project is part of the structural optimization package of a multidisciplinary optimization project, in direct partnership with the Research & Tools (R&T) team at Stelia Canada. The global project *MUltidisciplinary Framework for Optimization of wing box* (MuFOX) is overseen by the *Consortium de Recherche et d'Innovation en Aéronautique du Québec* (CRIAQ).

MuFOX originated from a need to redefine the preliminary and conceptual design phases of aircraft with modern collaborative tools. MuFOX challenges existing design and research methods in both academia and industry. Therefore, it includes two industrial partners, Bombardier Aéronautique and Stelia Canada, and two academic partners, Carleton University

and Polytechnique Montreal. MuFOX touches many different disciplines of aircraft engineering, such as optimization, aerodynamics, load, structures and design. For this PhD project on structural optimization, topology optimization had been identified as a promising tool to redefine conceptual design. The challenges related to topology optimization in aircraft design are at different levels: design theory, exploratory optimization and structural analysis. Accordingly, the goal of the project is to identify challenges of design using topology optimization during the early phases of the conception and develop solutions for these main bottlenecks.

1.1.1 Aircraft Design

The complete design of an aircraft is complex and expensive; it takes many years and costs billions of dollars for a new program to go from an idea to delivery [20]. A typical design cycle of an aircraft is illustrated in fig. 1.1. To reduce design time and also to minimize the budget, the different design phases are usually done concurrently, using the Concurrent Engineering or Collaborative Engineering design theories [21–23]. The challenge of concurrent engineering is that important decisions have to be made very early in the design phase, when knowledge may be incomplete. This is crucial for complex multi-domain systems such as aircraft [24].

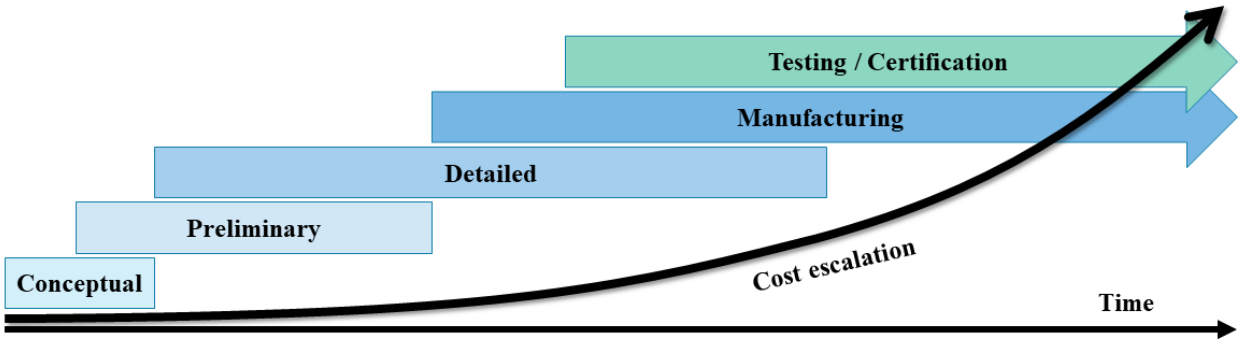


Figure 1.1 Aircraft design phases and approximate time and cost escalation, timescale typically 2-5 years. [21]

As illustrated in fig. 1.2, the design process is about balancing the decisions that reduce design freedom and increase new knowledge to advance the design process. In this thesis, we define design freedom as the remaining possible design modification that can be done with low cost. For example, in the concurrent engineering process, some components are ordered during the preliminary design phase in order to reduce design time. As the design advances engineers acquire new knowledge on the product and processes, it is already too late to make significant changes to the design because it has become too costly to cancel or modify already

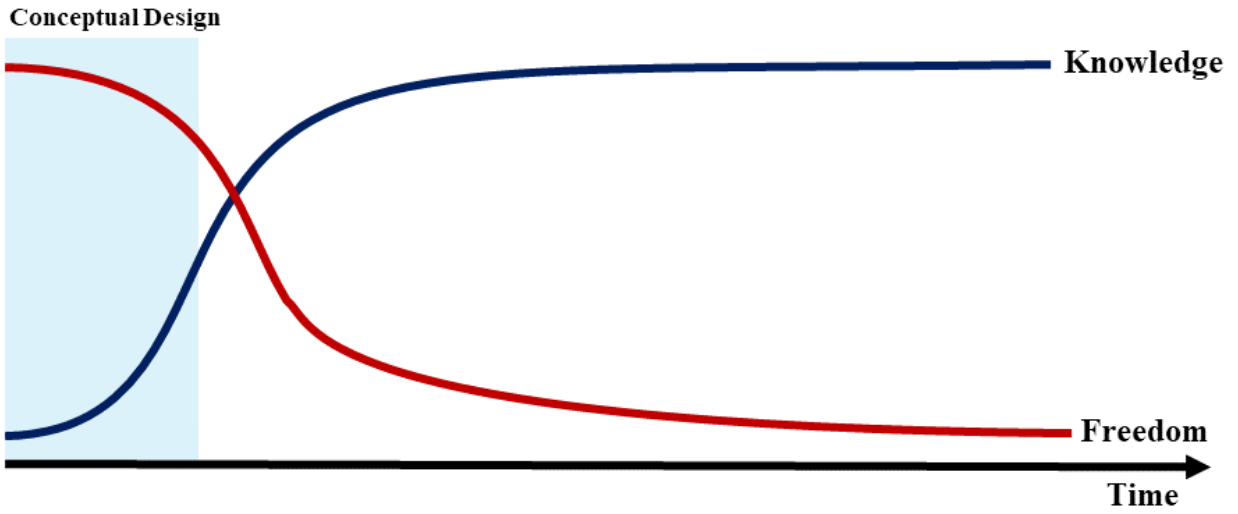


Figure 1.2 Evolution of knowledge during the design process. It shows that during design, knowledge of the product comes later at which point freedom has already been limited by previous decisions. [1].

manufactured components. This project is rooted in the creation of new ideas and improving the knowledge of designers during the conceptual design phase, by leveraging computing power and generative systems, such as topology optimization. The use of computer-aided engineering design (CAED) during the conceptual design phase has been identified as an active challenge in research [25]

This chapter first introduces the most important concepts and definitions related to the context of the project. From there, we identify the main limitations of current practices and finally limit the scope of the project to the identified challenges.

1.2 Definitions and concepts

This section introduces the most important concepts of this thesis which are required to understand the context and research objectives. A comprehensive literature review is presented in chapter 2.

We first present the standard wing assembly used in civil aircraft. From there, the stiffened panel and its functions are described. We then discuss current structural optimization tools, including topology optimization. Then, general design theories are introduced to provide a common language for design. Finally, we position all of these concepts within the generative design framework.

1.2.1 Aircraft Assemblies

Aircraft structures have a relatively simple role in the design of aircraft: to ensure the integrity of the aircraft during all operational procedures (taxi, take-off, climb, cruise, descent and landing) [26]. As this work is in collaboration with a commercial aircraft manufacturer, this project focuses on traditional aircraft configuration.

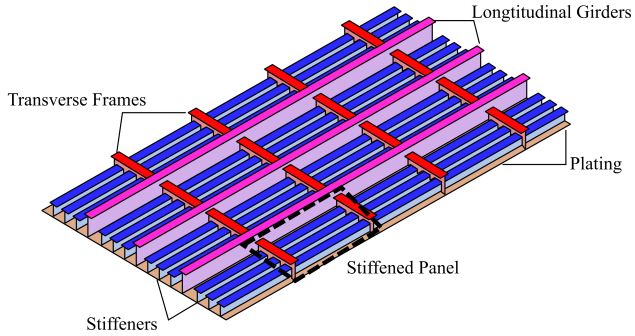


Figure 1.3 Stiffened panel assembly with an orthogrid layout, meaning all stiffeners are orthogonal.

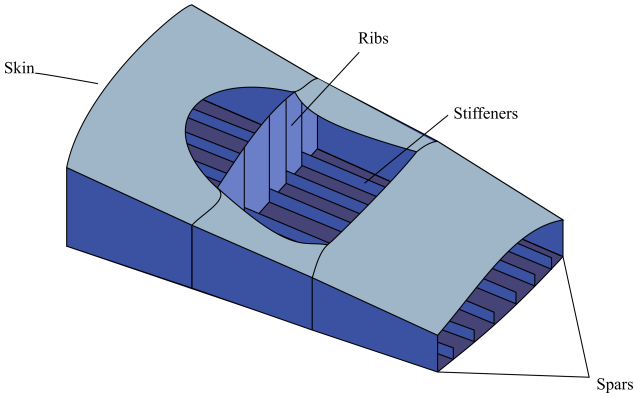


Figure 1.4 Wing box assembly.

What is important to note is that every structural assemblies in modern aircraft are built from specialized stiffened panels, which are usually stiffened as an orthogrid configuration (see fig. 1.3). This configuration requires that all stiffening components are perpendicular to one another. In the fuselage, these stiffeners are called frames, stringers and girders. In the wing box, similar functions are attained by the ribs, stringers and spars (see fig. 1.4).

1.2.2 Stiffened Panels

Orthogrid stiffened panels have been used in the aeronautics, aerospace and shipbuilding industries for decades due to their high strength/weight ratio. This layout consists of stiffeners always placed orthogonal to one another. One of our goals is to challenge the use of orthogrid configuration and seek to improve the strength/weight ratio of structural assemblies. However, due to the scope of the project, we mainly focus on stiffened panels used for the wing box assembly.

Stiffened panels are generally built with the orthogrid configuration for three reasons. First, there are very few unconventional configurations that have challenged it [27, 28] and from these, local improvements were made with a trade-off of significantly increasing manufacturing complexity and cost. Secondly, traditional analysis tools for stiffened panels are simple, but also narrow in application. They are based on analytical and semi-empirical calculations (see Sec. 2.1). More advanced analysis tools, such as finite-element method, allow more flexibility, but at an increased computational cost [29]. Finally, even though there are many academic tools to help design and/or optimize the stiffening layouts, very few have made their way to industrial applications [29, 30]. The complexity due to the interactions between tasks of design, manufacturing and analysis is identified as the main reason to explain the lack of innovation.

Most recent developments in reducing the weight of stiffened panels have been related to improved manufacturing techniques. Improvements in layered composite materials have seen a widespread application in newer civil aircraft [31, 32]. New joining and fabrication techniques have also been studied, such as friction stir welding [33, 34], electron beam free forming fabrication [35] and additive manufacturing [36]. These manufacturing techniques have opened the possibility of innovative stiffening layouts [30] which are not limited to straight, orthogonal stiffeners. However, increased freedom in manufacturing capabilities must now be matched by new and reliable techniques that allow this expanded design space to be explored in a systematic and reliable manner.

Another challenge associated with stiffened panels in aeronautic structure is their multiple roles in the assemblies. In addition to ensuring structural integrity, they often serve secondary functions, such as containing fuel, providing attachment points for systems or limiting the deformation of aerodynamic surfaces. As these different secondary functions are usually only considered in later design phases, they can create situations where design limitations only appear after design decisions are made. The next section introduces structural optimization tools that seek to improve the performance structural components, including stiffened panels.

1.2.3 Structural Optimization

Structural optimization is a sub-area of optimization that specializes in improving the performance of structures in terms of weight and resistance. There are multiple optimization formulations available to structural engineers at different stages of the design. They are often classified into three families: size, shape and topology optimization [37], as illustrated in fig. 1.5.

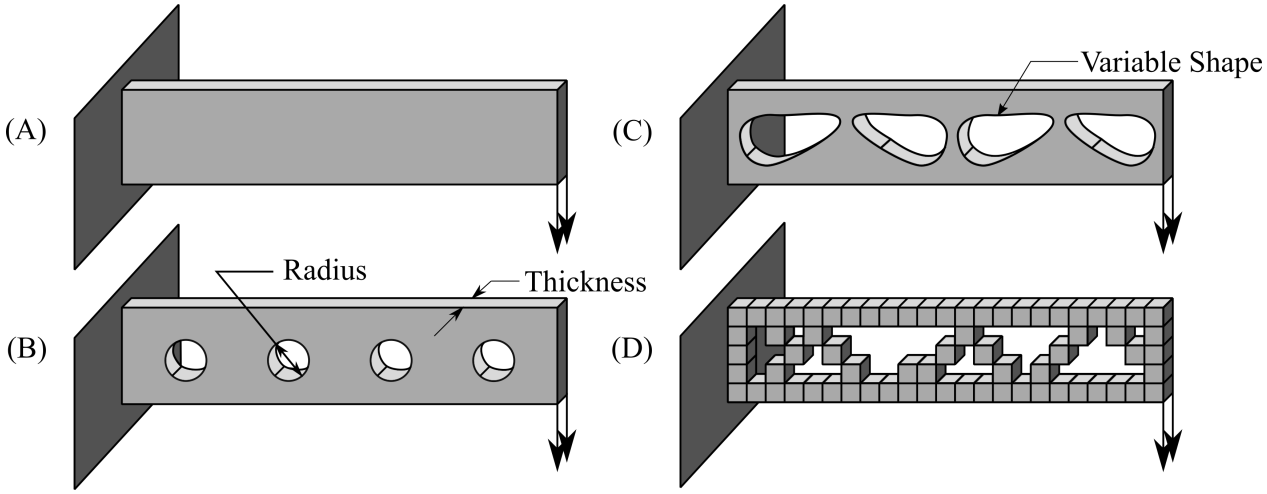


Figure 1.5 Different types of structural optimizations [2]. (A) Design space (B) Size optimization (C) Shape optimization (D) Topology optimization.

These methods all have in common that they start from an already defined design space that requires improvements, in terms of strength, rigidity (or its inverse compliance), stability or weight. The only differences are in the way they handle the design variables, and thus the design space. The design space is characterized as the mathematical space in which all the design possibilities, with respect to the chosen variables may be achieved.

When it comes to size optimization (fig. 1.5.B), the goal is to find the ideal size of a specific component with respect to material and assembly limits. For example, the thickness of a plate, the size of a bracket or the radius of a hole. It is a highly parametrized and rigid formulation that is very useful during the final design phase. As such, the design space, models and variables are known *a priori* and are thus fixed during optimization [37].

For shape optimization (fig. 1.5.C), the contour and surfaces are not fixed and become the design variables. A good use of this approach is to optimize the shape of holes or fillets to reduce stress concentrations. The domain changes are usually limited to small variations, to ensure that no topological changes happen.

Finally, topology optimization (fig. 1.5.D) offers the largest design space, by allowing the

topology of the solution to change iteratively. In its largest definition, topology optimization seeks an optimal material distribution in a given geometrical space. There are many algorithms, formulations, and methods for topology optimization, which are discussed in depth in section 2.5.

The different types of structural optimization have their use in each design phases. Topology optimization is generally used early in the design process to inspire engineers to promote innovative structures. Size and shape optimization are used in the preliminary and detailed design phase using low to high-fidelity structural models. Density-based topology optimization, especially with the solid isotropic material penalty (SIMP) formulation, has been widely used in the industry and in applications found in the academic literature [13, 38–40]. An impressive example using billions of design variables for the optimization of a complete wing box has been published in *Nature* in 2017 [39]. Even with this impressive optimization problem, only marginal weight saving was achieved after the interpretation of the results into complex wing box shapes [39]. Other attempts of topology optimization of smaller scale have yielded better results, with an average expected results of reducing the weight by at least 10% [13, 38, 41]. However, these projects did not optimize main structural assemblies but rather focused on single components such as floor reinforcements, brackets and attachment systems which have a simple, single function: ensure structural integrity.

1.2.4 Design Theories

Optimization is only one of the tools in the engineer toolbox. Engineers are not only analysts, they are also designers and creators. The design process is the act of using experience and intuition in addition to the analysis and optimization tools. Design theory is the study of the design process, from which methodologies are proposed to help engineers improve their design.

Concurrent engineering was mentioned in the aircraft design section for the general aircraft design. Considering the large scope of aircraft design, concurrent engineering has proven an effective tool to reduce design cost and the design-to-deliver timeline [21].

In collaborative engineering, concurrent engineering, infused design theory and C-K theory, design is defined as a social collaborative process [19, 42–44]. It involves a non-linear process where the design progresses with the exchange of information between the stakeholders: customers, designers, analysts, managers, etc [42, 43]. The challenges put forward in social design theories are related to the complexities of communication between disciplines. This fact has also been emphasized in multidisciplinary optimization problems where communication is required between programs for optimization [45].

There are also more systematic design theories, such as axiomatic design. Axiomatic design has seen a significant number of publications [46,47] and has its roots in mechanical engineering design. In axiomatic design theory, design is defined as the process of identifying *needs* that must be satisfied with *functions* to create an *innovation* [46].

1.2.5 Generative Design

In presented conventional design theories, the design process is started from the *requirements*, *specifications* or *needs* of the customer or other stakeholders. For example, in axiomatic design, the design process is split into *doing the right things* (first axiom) and *doing things right* (second axiom) [48]. This process is considered *first time right* and thus considers a good design process a design that did not require any redesign [49]. In the Infused Design, the requirements evolves during the design process, until requirements, knowledge and functions of all the design teams matches [42]. As such, conventional design theories are "top-down" approaches, creating solutions from the knowledge of designers and customers requirements.

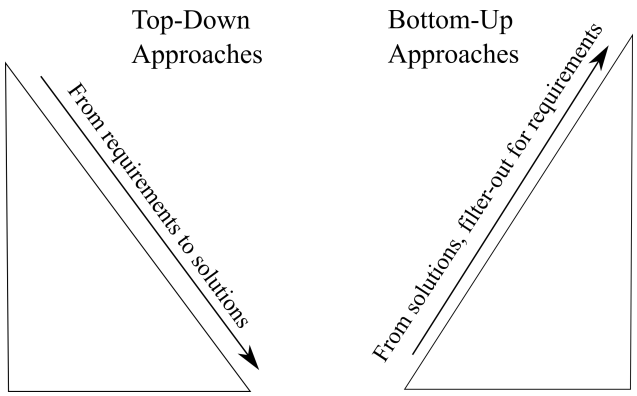


Figure 1.6 Top-down vs bottom-up design approaches

In this sub-section, we discuss generative design (sometimes also called computational design synthesis [50, 51]) which uses a "bottom-up" approach (see fig. 1.6). This time, starting from possible solutions and filtering them out until only feasible solutions are available. Generative design is a design approach that leverages computational power to generate virtual artifacts. However, as far as we know, generative design has not been studied as part of a design theory. We think generative design offers great potential for the design of complex and multidisciplinary systems [52].

In this thesis, we have defined three essential disciplines that are part of this project, namely structure, optimization and design theories. These three disciplines have different views and very different languages to describe their processes. For example, for design theorist (depending on the framework) the language tends to use words such as concepts, functions, ideas or

organizations. Optimization specialists think in terms of objectives, programming, variables and constraints. Structure engineers will think in terms of process, computation, stress and stability. As put forward in social design theories, the interface and language of multiple disciplines and the organization of design can be at the same time limiting aspects (concurrent engineering) but also exploratory spaces for emergent solutions (infused design).

Generative design, as used in the literature, offers a solution to leverage the language barriers of multidisciplinary design [53]. The term generative design has been used in different ways in the last decades, sometimes in computer-aided design (CAD) software [53] and often in the architectural/civil engineering journals and conferences [54]. A common aspect of generative design literature, is that it focuses on the use of computer systems capable of generating concepts (be it structures, ideas, layout, shapes, graphs, etc.) to inspire the designers to innovate and think outside the usual available solutions. It leverages the engineers experience and intuition by acting like a *Rorschach* test, but instead of finding psychological patterns in patients, we explore the creativity of professional designers. To explore properly, the generative design framework must include different disciplines in the design process to create opportunities of conflict with different disciplines, and thus improved design.

Let's define what generative design is for us: *A generative design approach leverages generative systems to generate solutions, from which the best are filtered and then selected by computer-assisted experts*. From there, a common definition of generative systems includes important properties [54]:

Generative system Generative systems are computational algorithms that are used to create design solutions from rules, evolution or optimization. They have four main properties [54]:

1. Ability to generate complexity from simple rules (the systems uses base components to create emergent properties from the assembly);
2. Generated solutions have forms that are interconnected with their environment;
3. Ability for self-maintenance and self-repair;
4. Novel forms, behaviors and outcomes are expected results.

Let's break down this definition into its most important components. First, the generative design is simply an approach that uses tools (generative systems) in a systematic way. Secondly, generative systems are computer programs that uses simple components to create

novel, complex and stable artefacts. And finally, generative design leads the engineers toward a solution space that requires filtering and selections. The strength of generative design is that it leaves the engineer the job to explore the solution instead of the design space, which greatly reduce the space to explore. Still, smart computer filters can greatly help engineers reduce the amount of solutions even further. As such, there is the nuance between conventional generative systems and performance-based generative systems that leverages optimization techniques to generate only efficient solutions.

For an efficient, generative systems must balance **representation, generation and design** exploration in pursuit of innovative and original design solutions [55]. This balance is important to ensure a flexible generative design. Representation ensures that the generated solutions correctly reflect the design intent and that accurate information might be extracted from the generated results. The generative portion in generative systems is central to the concept, still if too much effort is put into creating innovative concepts, the good solutions will be lost in the sea of bad solutions. A good generative systems can create more feasible than bad solutions. Finally, a good generative system is not too focused on finding the best solution, as in the conceptual design phase, many hypothesis are required. As such, it balances optimal and exploratory solution to provide opportunities for engineers, as the maturity of the project reduces the number of design hypothesis.

From these definitions of generative systems, it appears that for the design of complex products, such as stiffened panels used for aerostructures, topology optimization is a generative system that focuses only on close optimal solutions. This is done at the cost of proper representation of the structure, for example, it is difficult to capture buckling accurately in density-based approaches. Moreover, this reduces the capacity for exploration which is virtually non-existent in topology optimization literature. We think that exploration is barely leveraged in topology optimization because it has been developed for convex optimization problems (an optimization problem with only one global minima).

1.3 Problematic

This introduction has discussed the roles of structural assemblies in keeping the integrity of the aircraft in all operating conditions. Stiffened panels are an essential component of modern aircraft assemblies and there's currently new manufacturing capabilities that are not properly leveraged due to limitations in generation and analysis of innovative stiffening layouts.

Topology optimization has been identified multiple times in the literature as a promising tool to inspire structural designers to create innovative, strong and light structures. There

are currently no adequate design theories that may properly leverage topology optimization for structural design, but the generative design framework identifies important limitations of current design methods based on topology optimization. A good generative design approach balances representation, generation and design search. Currently, topology optimization as a generative system focuses on the concept generation by optimal material distribution. However, as not all the design requirements are integrated in the optimization process, the performance is only focused on stiffness. As such, for stiffened panel design, layouts obtained with topology optimization offers a sub-par strength/weight ratio compared to conventional orthogrid panels. There is a need to re-imagine topology optimization as a generative systems and re-balance it toward better representation and exploration.

The current generation methods in the most used topology optimization algorithms are implicit, which makes the interpretation tedious and the use of higher fidelity models (better representation) challenging. Moreover, there are few works focusing on exploratory topology optimization.

This leads to the following challenges for the design of stiffened panels with generative design:

Challenge 1 Current topology optimization algorithms are not suitable to represent stiffened panels and their non-linear constraints due to their implicit generation of the design.

Challenge 2 Designing innovative stiffened panels requires extensive design space search and exploration. Design with current topology optimization algorithms, also requires a lot of manual work, interpretation and performance-analysis. There is no guarantee that requirements are met by the single proposed material distribution. All of this makes design space exploration tedious, non-systematic and inefficient.

The first challenge is linked to the way topology optimization uses implicit variables to ease the optimization problem. Still, it can only be effectively used for finding the main load-paths, that is finding how the primary loads travel in the continuum design space. Furthermore, the design interpretation process takes time and it is difficult to properly evaluate the design with an best suited model for high fidelity analysis. Interpretation requires evaluating the material distribution, turning it into something manufacturable and reanalyzing it with constraints not previously considered.

This leads to the second challenge associated with topology optimization. The current methods rely on the expertise of engineers and their intuition to choose the right formulation and hypothesis, then parametrize optimizations properly. Each decision on the parameters and

formulations lead to only one "new" result, which may or may not be a feasible result when considering all design requirements. All design requirements not considered during topology optimization usually include more complex limitations such as post-buckling stability, damage tolerance, manufacturing limitations or even economical or environmental considerations. By looking at the big picture, it is clear that by finding only one "optimal" material distribution, there is a high risk of missing a solution that might later be a better compromise. Balancing exploration and optimality in topology optimization (when used as a generative system) should help engineers find more innovative designs.

These challenges foresee avenues for improvement: make the design space exploration more efficient, automate interpretation of implicit variables, filter models before manual intervention, etc.

1.4 Research Objectives

With the research challenges identified, we are set to define a general research question as follows:

> How can topology optimization be leveraged in a generative design framework to reduce the weight of stiffened panels used in commercial aircraft?

From this research question, objectives and sub-objectives are defined. These objectives are related to the research question and the identified challenges and expressed as mission statements.

Main Objective (MO) Develop a generative design method for stiffened panels based on topology optimization to minimize their weight.

Secondary Objective 1 (SO1) Characterize the impact of optimization formulation and parameters on the behavior of topology optimization with a buckling constraint.

Secondary Objective 2 (SO2) Develop a tool to automatically read and segment discrete components from a density-based topology optimization result.

Secondary Objective 3 (SO3) Develop a tool to determine complexity levels and synthesize innovative stiffening layouts.

From the main objective, we keep in mind that the goal of the project is to find a way to reduce the structural weight of stiffened panels. The selected generative system is topology

optimization, for which different algorithms are tested. The improvements are measured by comparing innovative panels strength/weight ratio with the orthogrid configuration that is optimized with only size and shape optimization.

SO1 is related to challenge 1, which identifies that current topology optimization algorithms use implicit generation of structures which makes higher fidelity constraints more difficult to implement. This first sub-objective seeks to understand how this implicit generation affects the results of topology optimization using non-linear constraints, especially buckling.

SO2 and SO3 are related to challenge 2, which shows limitations to the search and exploration of the design space. SO2 focuses on the challenge of interpretation for density-based topology optimization by automating the extraction of the discrete components in the material distribution. SO3 seeks to create a tool for the designers, helping them for the analysis and synthesis of the large amount of solutions.

1.5 Thesis Outline

We have discussed the industrial and academic context of the project in this chapter. Important challenges have been identified that limits innovation for stiffened panels, and thus aircraft structural assemblies.

The next chapter focuses on the literature review of the project, from which we identify research opportunities and solutions. Chapter 3 makes a synthesis of the methodology, solutions and articles presented in this thesis. It also presents the generative design framework that has driven the research presented in this thesis. Chapter 4 shows the development and use of a computer vision tool that automates generation with a commercial topology optimization software. Chapter 5 and 6 use and implement buckling into the widely used topology optimization methods of Solid Isotropic Material with Penalization and of the Ground-Structure method respectively. In both work, the use of the implicit generation shows several limitations when coupled with linear buckling constraints. Chapter 7 leverages lessons learned from the previous work to create an innovative complexity-driven design exploration method.

A discussion on the generative design method and associated generative systems is located in Chapter 8. Finally, the conclusion offers insight on the limitations of this work and discusses possible future work.

CHAPTER 2 LITERATURE REVIEW

In the early 2000s, Venkataraman noticed that even though the available computational power has increased exponentially, the time required for a given structural optimization has stayed roughly the same over twenty years (1980–2000) [56]. Engineers have used simulations that run overnight, no matter the exponential increase in speed of modern computers, as with more powerful computers, more complexity is introduced in simulations. With anecdotal evidence gathered with industrial partners, this seems to remain true in 2021. Venkataraman defines design complexity as the sum of challenges required to achieve a task [56]. As time goes on, the requirements for different complexities, precisely the optimization, modeling and analysis complexities have increased, creating an ever-expanding demand for more computation power [56]. As such, solving a complex analysis, requires advanced numerical techniques, powerful computers and/or intensive pre-process effort.

Even with recent advances in computations, combining complex optimization with complex modeling and complex analysis remains cumbersome. Most recent advances in the literature challenge only one aspect (optimization, modeling or analysis) at a time. The combination of multiple complexities in a single problem is rarely explored. This is illustrated in fig. 2.1 where the blue area denotes the explored areas and the point P the unexplored area with multiple complexities.

In essence, the challenges we have identified in the introduction chapter are related to the combination of these different complexities. As an example, considering the complexity of the topology optimization problem, it is necessary to use simplifying assumptions for both analysis and modeling; otherwise the optimization problem is unmanageable. Stiffened panels, especially in vehicle assemblies, are complex models that require multiscale optimization, complicated assemblies and interfaces with multiple systems. Finally, stiffened panels require increasingly complex analysis methods to consider stability (buckling and post-buckling), fatigue and crack propagation.

These three complexities can be related to the balance in generative design we have identified in sec 1.2.5. For example, the decision to reduce the complexity of the analysis and automated modeling penalizes the generative representation and exploration but creates a much easier optimization problem. Thus, tackling all complexities in a single problem requires a difficult act of balancing what is left in and what is left out.

In this chapter, we will review the available literature on how these challenges have been tackled. First, we discuss the current design, optimization and analysis method for conventional

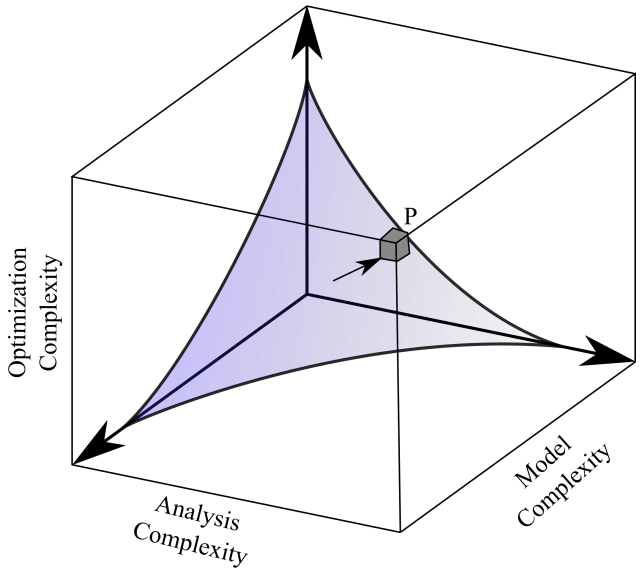


Figure 2.1 Illustration of complexities in the structural engineering world [56]

stiffened panels. A state-of-the-art review on structural optimization algorithms and techniques reviews the latest advancements. From there, methods for innovative layouts and new analysis algorithms are presented. Our classification of generative systems for structural design, for which we include topology optimization, is proposed as part of the generative design approach. Finally, an exhaustive review of current trends in structural topology optimization puts forward current limitations.

2.1 Analyzing and Sizing Stiffened Panels

Stiffened panels have been introduced in the section 1.2.2. The discussion in this section is more specifically about the identified challenges linked to the analysis (representation) complexities of stiffened panels. The orthogrid configuration has been predominantly used in the aerospace industry, and as such this section focuses on it. Innovative layouts are presented in the section 2.3.

2.1.1 Challenges of Stiffened Panel Design

The orthogrid stiffened panels are highly efficient and relatively easy to design [56]. Their analysis requires good understanding of specific conditions, such as [29]:

- Kinematics of the stiffeners, relative to the mid-plane of the plate;
- Boundary conditions at the plate/stiffener junctions;

- Stiffener geometric parameters (flexural, torsional, warping, etc.).

As noted in [29], using the orthogrid layout reduces considerably the modeling complexity, as it may be considered as a monolithic, orthotropic structure [29] with the mentioned hypothesis constant throughout the panels. Difficulties in the analysis of non-orthogrid panels arise as it changes the hypothesis [29]. For example, using curved stiffeners locally changes the torsional resistance across the panels, making the simple monolithic approach inadequate.

The first challenge of the design of stiffened panels is related to ultimate limit states. For most shell design problems, designing with limit state in mind (buckling and material yield) is the easiest evaluation [57]. However, experiments have shown that important weight saving (of the order of 20%) may be achieved by designing with ultimate strength in mind (post-buckling stability and material ultimate strength). At this level, considering material non-linearity is important, such as the cladding of aluminum [58]. For example, with aluminum-alloy there is a second stable slope of material that can be defined using the Ramberg-Osgood factor (n) [59].

Scale is also a challenge, as global and local buckling modes must be considered, multiscale analysis is required. The scaling problem makes numerical techniques quickly prohibitive compared to simple analytical equations [60]. Approximate modeling of panels have been used to reduce the modeling complexity, at the cost of increasing analysis complexity (e.g., smeared approaches) [61].

Furthermore, stiffened panels are very sensitive to geometric imperfections [29]. These imperfections might arise from some unexpected deflections or welding residual stresses [62]. These imperfections are difficult to predict, making buckling initiation and growth somewhat unpredictable [57]. Integrated extruded or machined stiffeners are less prone to the effects of imperfections relative to traditional welded or riveted assemblies, which is another advantage of using modern manufacturing technologies [62].

Finally, for minimal weight panels, the closeness of multiple buckling modes can lead to instability earlier than numerical techniques predicts [57]. For this challenge, semi-empirical techniques have been developed to account for experimental data. Some important equations are presented in this section.

2.1.2 Buckling

Current design methods considering buckling rely on well understood analytic and semi-empirical formulations [26]. These measures for traditional configuration help reduce the analysis complexity, especially for large-scale structures. Basic equations for buckling failure

evaluation are presented in this section.

First, we have to acknowledge that buckling encompasses multiple types of modes, and not all modes lead directly to collapse [26]. It is the combination of the plate, stiffeners and layout properties that influence the shapes and limits of the different modes [29]. See fig. 2.2 for a non-exhaustive illustration of common buckling modes. Fig. 2.2.(a) shows a global buckling mode, which arises when stiffeners only offer a small flexural rigidity; thus the whole structure buckles together. Fig. 2.2.(b) and (c) shows the buckling modes associated with high flexural or high rotational rigidity of the stiffeners; the local buckling modes. Finally, modes in fig. 2.2(d) and (e) shows rotational buckling around the stiffener axis. This may happen if the junction of the plate/stiffener is not stiff enough, or if the stiffeners are too slender.

There has been a continuous effort to create more precise and/or more flexible analytical tools, as shown by more than 400 papers found in [29] between 1950 and 2007. In summary, the early methods studied the differential equations and energy formulations to create buckling charts and rules that may be used for plates and stiffeners alike [29]. Later methods focus on numerical methods such as FEM and the finite-strip method (FSM), which have been studied extensively [29, 57].

Analytic and semi-empirical methods

We will note some important equations developed by the NACA in the 1950s that are still largely used today for buckling evaluation [58]. The first important equation describes the critical stress associated with skin buckling, which has been derived from the total potential energy equation and transformed into a double trigonometrical series [58]. As an example, the equation for a skin supported on all sides is presented in equations 2.1 and 2.2, see fig. 2.3 for an illustration of variables.

$$N_{x,CR} = \pi^2 a^2 D \frac{1}{m^2} \left(\frac{m^2}{a^2} + \frac{n^2}{b^2} \right)^2 \tag{2.1}$$

$$D = \frac{Et^3}{12(1-\nu^2)} \tag{2.2}$$

where $N_{x,CR}$ is the critical load, a and b are respectively the length and width of the plate, ν is the poisson ratio of the material and t the thickness of the skin. Finally, m and n are the indices related to the longitudinal and transversely modes.

If we choose $n = 1$ to observe the buckling modes in only the loading direction, it is possible to reduce the equation to:

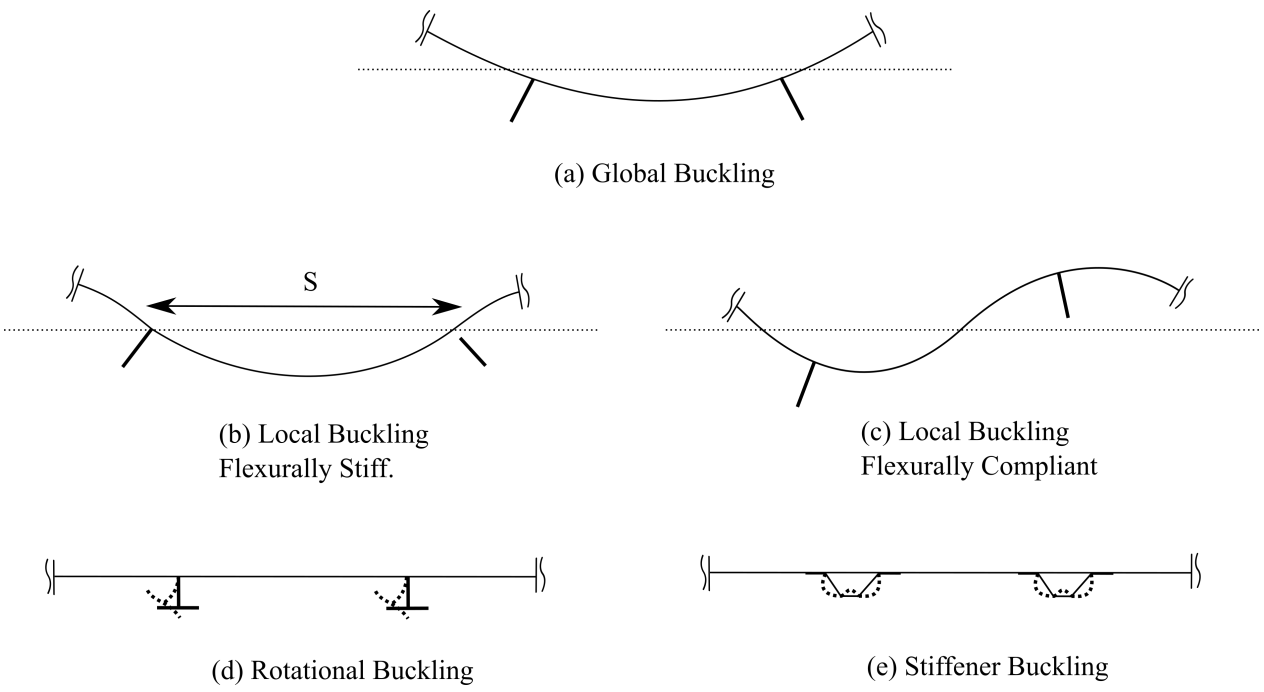


Figure 2.2 Possible buckling modes for stiffened panels [29]

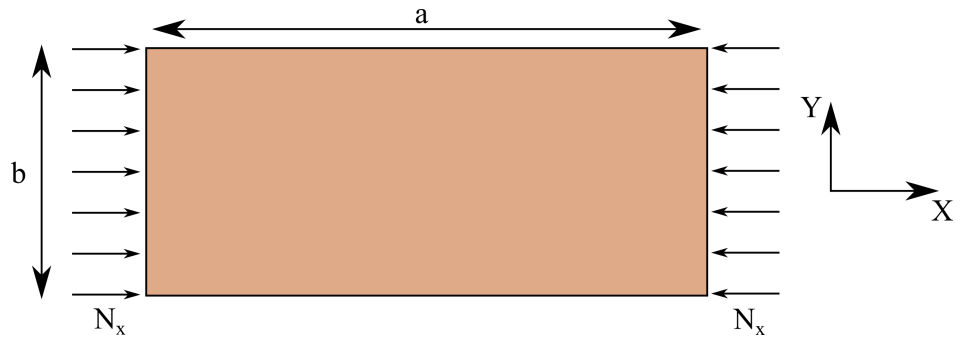


Figure 2.3 Skin variables that affect buckling resistance where N_x is the applied load, a and b are respectively the length and width of the plate. [26]

$$N_{x,CR} = \frac{k\pi^2 D}{b^2} \quad \text{where} \quad k = \left(\frac{mb}{a} + \frac{a}{mb}\right)^2 \tag{2.3}$$

From these equations, it is possible to simply plot the resulting effect with respect to the a/b fraction. The buckling factor k converges for $a/b > 1$ toward 4 for simple supported skins. Other boundary conditions produce other buckling constants.

Combining equations 2.3 and 2.2, we finally obtain the final critical skin buckling stress:

$$\sigma_{cr,skin} = \frac{k\pi^2 E}{12(1-\nu^2)} \left(\frac{t}{b}\right)^2 \tag{2.4}$$

We can see that uniaxial buckling is mainly driven by the skin thickness (t) and its width (b).

In a similar fashion, it is possible to introduce the Euler column buckling equation [26].

$$\sigma_{cr,euler} = \frac{\pi^2 E}{\frac{l_e}{r^2}} \tag{2.5}$$

where, $\sigma_{cr,euler}$ is the critical Euler stress of a single column, which depends on the ratio l_e/r^2. l_e is the effective length of the column (which depends on the actual length and boundary conditions) and r the buckling radius which is affected by the area of inertia of the column's cross-section [26]. Contrary to skin buckling, Euler buckling is inherently unstable and is to be avoided [26].

In stiffened panels, local buckling of short columns (also called crippling) can also be problematic. This local instability depends on the shape (*L, Z, J,* Ω, etc.) and properties of the stiffeners. There exists multiple methods proposed in the literature, based on empirical data, though there is still universal acceptance on a particular method [26]. Need-ham and Gerard methods are usually presented in coursebooks [26, 58].

Numerical methods

Numerical methods are used primarily for smaller components, as their use for large-scale structures can quickly become prohibitive [62]. Still, they allow for a much more flexible control over geometry, boundary conditions, loads and materials [62].

Using the FEM method for the evaluation of buckling resistance starts with the assembled

stiffness matrix. Using the equilibrium equation from the FEM (eq. 2.6), it is possible to create an eigenvalue problem (eq. 2.7) to identify the different critical load factors and their associated modes that may be extracted from the eigenvectors [63].

$$\mathbf{f_0} = \mathbf{K}\mathbf{u_0} \tag{2.6}$$

where f_0 is the critical load, $\mathbf{K} \in \mathbb{R}_{n\times n}$ is the stiffness matrix and $\mathbf{u_0} \in \mathbb{R}_n$ is the displacement vector.

$$[\mathbf{K} + \lambda\mathbf{K}_\sigma(\mathbf{u_0})]\varphi = \mathbf{0}, \qquad \varphi \neq \mathbf{0} \tag{2.7}$$

where $\mathbf{K}_\sigma(\mathbf{u_0})$ is the stress stiffness matrix used for the generalized eigenvalue problem which may be solved using classic numerical methods. Solving the eigenvalue problem results in the eigenpairs $(\lambda_i, \varphi_\mathbf{i}p)$ which represent respectively the critical load factors and its associated buckling modes.

There is abundant literature on numerical techniques to efficiently evaluate buckling [57]. Some work focuses on new finite-element formulations [57]. Some focus on the effect of local and global imperfections (related to geometry, manufacturing or heat adverse effects) [57]. There are also the smeared approaches that create approximations for out-of-design areas, allowing a focus only in a given design space [61].

A common challenge is to capture both local and global buckling mode accurately. A solution for this is an alternative formulation from strong form equations and differential quadrature methods [64]. Finite and exact strip approaches also provide efficient evaluations for the orthogrid configuration [64].

Still, all of these techniques, except FEM, are focused on orthogrid stiffened panels [62]. It appears that both efficient and flexible tools for buckling evaluation are still under development.

2.1.3 Post-Buckling

Well-designed stiffened panels control not only the safety factor of each buckling mode, but also sets the load factors of each mode. A usual design method consists of setting the critical load associated with skin buckling (which is stable) earlier than the other buckling modes [65]. This creates a new post-buckling equilibrium that is characterized by a load redistribution from the skins to the stiffeners, with skins still able to provide significant stiffness. The stiffener and the buckled skin together are sometimes called the “super-stiffener”

[66]. Nevertheless, designing for post-buckling equilibrium requires more complicated analysis tools than simple buckling.

For the analytical methods, some semi-empirical equations are available for orthogrid panels. Post-buckling failure arises from the coupling of slender buckling (Euler, eq. 2.5) and short column buckling (or crippling) in a failure mode characterized by the Euler-Johnson equation, eq. 2.8 [67]. This failure mode is also called the intermediate column failure [67].

$$\sigma_{cr} = \sigma_{cc} - \frac{\sigma_{cc}^2}{4\pi E}\left(\frac{L'}{\rho}\right)^2 \tag{2.8}$$

where, σ_{cr} is the Euler-Johnson critical stress. σ_{cc} is the critical crippling stress evaluated from semi-empirical methods such as Needham or Gerard. L' is the effective column length (which depend on actual length and boundary conditions) and ρ the radius of gyration.

For orthogrid stiffened panels, FEM and Finite Strips methods are also capable of modeling the post-buckling failure. Again, for non-orthogrid stiffened panels, only FEM allows for a flexible solution.

For post-buckling analysis, a time dependence requires nonlinear numerical methods [65]. There are multiple solutions for nonlinear solving, though the Rikz arc-length time-step method is usually preferred in the literature [65, 68].

To consider post-buckling in optimization, some approximation techniques are proposed in [69, 70].

2.1.4 Sizing Aircraft Structures

The sizing of stiffened panels is choosing the right thicknesses and shapes of stiffeners and skin segments in the general assembly.

A common approach for detailed design is to use the analytical and semi-empirical equations into simple margin of security calculations tools. These calculations are often done directly on Excel spreadsheets, with each section of the wing and fuselage having their own dedicated section in the workbook. More modern approaches use object-oriented programming. The calculations include the buckling, discussed earlier, and also fatigue, damage tolerance, stress, etc. The sizing of components are modified whenever a design change is required, and the engineers verify that margins stay positive.

Optimization techniques, including mathematical programming and meta-heuristic methods, are now used at the conceptual and preliminary stage of aircraft design [57, 71]. This can be

leveraged in multidisciplinary optimization where it becomes possible to include structure, aerodynamics and control into a single aeroservoelastic problem [72]. These techniques are discussed in the next section.

2.2 Structural Optimization Algorithms

Optimization, in its broadest definition, is the study of the minimization/maximization of a set of cost functions under a given context [73]. With the advent of numerical methods and the exponential rise in computational powers, optimization has become more and more popular in design and structural engineering [73].

However, as often stated in any optimization work: *there is no free lunch* [73]. That is, there is no perfect algorithm for all optimization problems. The compromises are generally defined by the problem's number of variables, the nature of the constraints and/or properties of the objective functions [73]. Optimization complexity is thus mainly related to the implementation of the optimization problem, in terms of solver, objective functions, constraint evaluations and gradient computation or approximations. This subsection presents a quick overview of state-of-the-art optimization techniques, with a focus on mathematical programming and meta-heuristics approaches commonly used in structural optimization packages.

Under the mathematical programming techniques, the *method of moving asymptotes* (MMA) [74] and its evolution the *globally convergent MMA* (GCMMA) have been used extensively in the structural optimization (especially for the topology optimization) community [75, 76]. Due to the convexity of the sub-problems, MMA and more so the GCMMA have excellent convergence properties, with GCMMA being guaranteed to converge toward an optimum (not necessarily global) in a finite amount of time steps [77].

More general techniques include the methods of feasible directions (MFD) and sequential quadratic programming (SQP) [78]. MFD uses first-order derivatives to find an efficient solution in the feasible zone [73]. SQP resolves a quadratic subproblem to find the most efficient descent direction and step size [73]. Both algorithms are often used in commercial packages [78, 79]. MFD is most efficient if you know a feasible starting point and you are not too far from optimality, each iteration requires less computation than SQP. However, SQP is more efficient in non-feasible regions and even though each iteration is longer to compute, it often requires fewer iterations. Generally, SQP is considered more efficient than MFD [73].

There are multiple algorithms available for global optimization, that is algorithms that search for the global minimum, and not just the closest minimum. There is no algorithm that is used preferably in structural optimization, though multiple are available in different commercial

optimization packages. Response surface methods (RSM) use surrogate models to decide the new evaluation points and use these new points to improve the surrogate models [80]. The DIRECT algorithm splits the design space into a hypercube then searches smaller and smaller areas as a deterministic-search algorithm [77]. The Mesh Adaptative Direct Search (MADS) is very useful for black-box optimization problems [81].

Meta-heuristic methods use arbitrary rules to define the behavior of the optimization process [73]. These rules are often inspired by nature and mimic it to create a flexible optimization process. The most well-known meta-heuristic method is the genetic algorithm, which mimics the evolution of species. With a set of solutions, it selects and reproduces "individuals" of a species into better and better solutions [73]. Another well-known algorithm is the Simulated Annealing which mimics the cooling of metals to find global optimum [73]. Some algorithms simulate the movement of insects or birds to balance search and exploration (Particle Swarm Optimization, Ant Colony, Crow Search, Firefly, etc.) [73]. These algorithms are usually easily adapted for parallel computing, and they generally do not require gradient [73]. They do, however, require an enormous amount of evaluation which can make convergence rather slow. Still, with enough time and computation power, they generally converge toward a global minimum [73].

Global optimization schemes and meta-heuristic methods are *zero order* approaches, that is they do not use gradients at all to decide which points to evaluate next. However, most structural optimization problems have available gradients, even though they can be expensive to evaluate. As MMA uses gradient approximations to leverage the gradient without evaluating them at each iteration, it is often considered the most efficient algorithm for large-scale structural optimizations. Nevertheless, contrary to global and meta-heuristic approaches, they are highly likely to find sub-optimal local minima rather than the global minimum. A reasonable approach used is to use global schemes to find initial values, then use gradient descent to polish the results into feasible optimum [77].

2.3 Novel Stiffening Patterns for Compressed Stiffened Panels

In section 2.1, we discussed advances in the modeling, analysis and optimization of commonly used stiffened panels. There are few works that challenge the orthogrid configuration and in this section we discuss some innovative patterns that have been studied in the literature. The patterns presented here have not been obtained by topology optimization, but have been designed from the experience of industrial and academic researchers. In this shortlist of innovative panels, we find the buckling containment features (BCF) [82], and the curvilinear stiffening patterns [83, 84].

2.3.1 Buckling Containment Features (BCF)

The idea of using sub-stiffening patterns to reinforce the buckling of plates has first been introduced in [28] as a way to leverage new discoveries in aluminum properties that were able to increase significantly the damage tolerance and limit residual stresses. Sub-stiffening patterns were developed in the hope of reducing the possible propagation of cracks into the panels [28]. In this early work, the sub-stiffening patterns were simple extra thickness located in the middle of the plate sections.

From there, the research into BCF (See fig. 2.4) stiffened panels have been encouraged by the development of new manufacturing techniques such as high-speed machining, welding, and panel extrusion [85]. It is now possible to create prismatic sub-stiffeners that act as smaller stiffeners that are able to increase the buckling, fatigue and crack propagation in lowly loaded panels [86].

BCF have been analyzed experimentally and numerically studied in aerospace applications [3, 87, 88]. The finite-strip method has been the preferred method of analysis for this type of panel [87]. Design guidelines have also been issued, in a similar fashion to the usual tables generally used for stiffened panel design [88]. In a full design activity, the team at Queen's University of Belfast was able to reduce the weight of a commercial airplane wing box, by 11% using BCFs [3].

More recent works have also explored more complex sub-stiffening patterns with particle swarm optimization [84, 89].

2.3.2 Curvilinear Stiffeners

The goal of using curvilinear stiffening patterns comes from the advent of the electron beam free fabrication forming (EBF3). The idea of developping a design and optimization tool

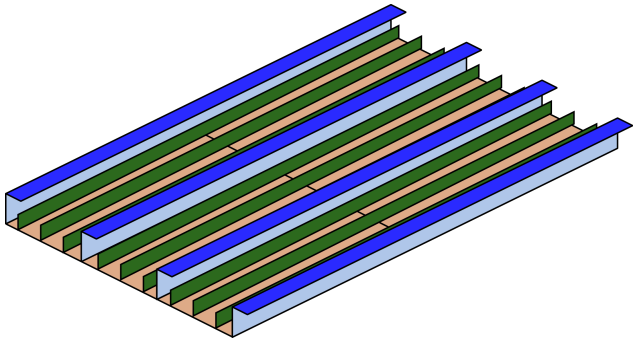


Figure 2.4 Illustration of the BCF as sub-stiffening elements in an orthogrid stiffened panel. [3]

based on EBF3 dates from 2005, and most work has been initially done on this idea at Virginia Polytechnic Institute [27, 82]. See fig. 2.5

Since 2005, EBF3 optimization has been extended by multiple new research groups. For recent analysis improvements a meshfree application has also been proposed in [90], a direct Ritz in application [91] and an isogeometric analysis that combines modeling and analysis in [92].

New optimization schemes have also been proposed [83, 93–95]. The one that shows the most promises is the one proposed by Mulani & al. [30]. This scheme uses a two-level optimization. On the first level one only keeps topological variables, such as position, orientation and curvature [30]. And the second-level focuses on the sizing of the stiffeners and panels [30]. This allows the mass to be explicitly optimized while doing a proper evaluation of local/global buckling and fatigue constraints [30]. However, these techniques have limited possible topological changes, as the number of variables/stiffeners is fixed before the optimization (It is not recommended to go over six (!) stiffeners for an acceptable convergence rate [96]). Some meta-heuristics and deep-learning approaches have shown more efficient convergence, but are still fairly limited [96, 97]. The use of curvilinear stiffeners described with splines is challenging due to the introduction of many variables for each stiffener, creating an enormous and complicated optimization problem [30].

Another approach for curvilinear optimization is to use a grid layout and use the spacing of each component as the design variables. This adds the possibility of curvilinear stiffeners, while limiting the amount of design variables. However, this technique doesn't allow for any topological changes [84, 98–100].

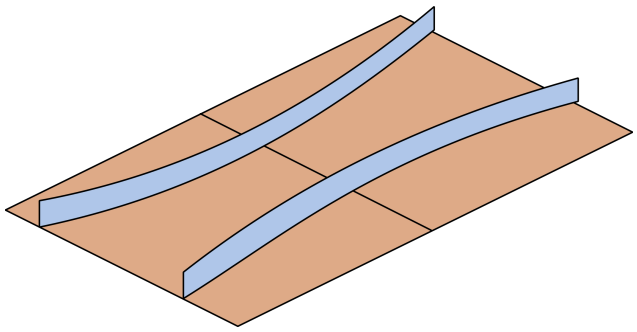


Figure 2.5 Unitized panel with curvilinear stiffeners [27]

2.4 Generative Design

Generative design, and its related generative systems, are introduced in section 1.2.5. We have defined generative design as the process by which generative systems are used to explore the space of possible designs. Generative systems have been defined by their ability, among others, to generate complex solutions from simple variables, rules or properties. This section explores different generative systems across disciplines and how they are used. This helps us position topology optimization as a generative system, and use lessons from generative design to improve the search of a systematic search of innovative stiffening layouts.

A particularity of generative design is its use of computational tools during the conceptual phase of design, whereas more traditional design processes use computational tools, such as optimization, when the design is more advanced: in the preliminary or more often the detailed design phase. As such, the challenge of generative systems is not only to find a minimum value for a set of variables, but also to choose which variables to optimize. That is why you will find algorithms in the literature simply named "generative design" [101] instead of "generative system" or "computation design synthesis." Their authors consider that their algorithm does "design," not only optimization.

In a recent review, there has been an interesting classification of generative systems in the architectural/engineering/construction domain [54]. The classification is based on the differences between "conventional" and "performance-based" generative systems [54]. Performance-based systems are focused on finding the best and optimal solution, generally by using different optimization techniques whereas conventional systems focus on generating solutions first, then evaluating the performance in the generated solutions.

2.4.1 Classification of Generative Systems

Viewing topology optimization as a generative system allows us to group together optimization and exploration techniques that are generally not presented as a single family. This will help the reader understand the process, ideas and concepts presented in this thesis. To illustrate these families, we propose the classification of fig. 2.6.

Generative systems have three main characteristics, similar to the structural complexities identify in the introduction of this review.

Generation The generation capability of a generative system refers to the way it infers the structure or architecture of the solution from the description of design variables. Existing systems use a range from completely implicit to detailed explicit descriptions of the sub-components of the topology. As an example,

density-based topology optimization uses an implicit generation as there a no defined components, whereas the moving morphable component algorithms defines explicitly the position of the sub-components.

Representation The representation is the degree of fidelity to reality used by the generative system. That is, using a high-fidelity model captures more physics based phenomena, but at the cost of increasing computational costs.

Exploration In generative systems, the focus can either be on finding a close-by feasible solutions, on finding a global minimum or on only exploring a large design space. This encompasses a range of systems that can generally only perform well for one type of task.

On the vertical axis of fig. 2.6, there is the exploration vs. performance focus. What we mean by that is that some generative systems are more focused on exploring and generating plenty of solutions, with different levels of performance evaluations, whereas some generative systems use performance evaluations at each iteration with the objective of finding the best, and only the best, concept for a given objective. The different optimization algorithms presented in sec. 2.2 may be used to move along the vertical axis, gradient-based algorithms are focused on finding the closest local minima. Global search tries to find the global optimum by balancing exploration and search (global search includes meta-heuristic optimization methods). Evolutive algorithms (not to mix with genetic algorithms) make solutions evolve (adapt topology) from a given set of rules, based on performance evaluations. Finally, the most exploratory-focused algorithms are based on grammars to describe and adopt solutions.

On the horizontal axis of fig. 2.6, there is the level of abstraction of the generation in the generative systems. On the left, we have very implicit topological variables, that is generally local size variables that change from zero (no material) to one (full material). From this distribution of implicit variables, it is possible to qualitatively evaluate the topology, which is usually reinterpreted. Examples of fully implicit variables are the continuum methods of topology optimization (see 2.5.1). Further to the right, the topological variable gets increasingly explicit, with the end right being a direct topological graph generation. At this level of abstraction, not only are components positioned in the design space, the way they are connected also evolves directly in a connection graph. That is, the algorithm (be it exploratory or performance-focused) can directly measure which variables have an impact one another.

Furthermore, the graph shows the different families, or the way the systems are usually separated in the literature depending on the colors. We have already discussed layout optimization for stiffeners in sections 2.3. Topology optimization algorithms classified in fig. 2.6 are discussed on their own, in the section 2.5. While a different area of research, topology op-

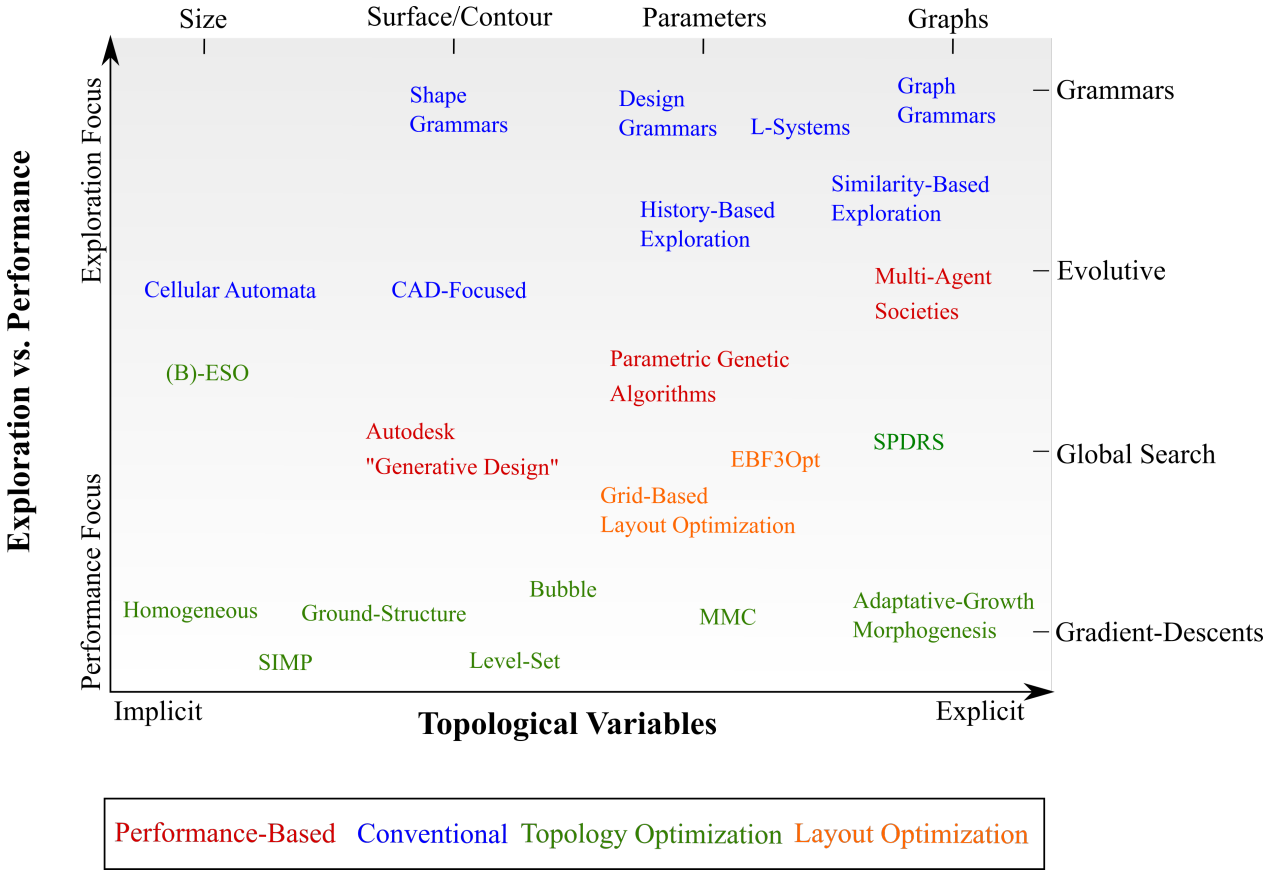


Figure 2.6 Classification of generative systems. Note that the categories used are conventional ones, found in the literature. The classification has no "hard" boundaries, they are placed qualitatively. All of the tools included in this figure are discussed in the next sub-sections. From left to right, increasingly explicit definition of topological variables. The current research trends, encouraged by the ever increasing computing powers, has pushed recent research in topology optimization towards more and more explicit generation. From bottom to top, you get towards exploration vs performance focus. The difference between research communities is mostly driven in this axis. Topology optimization is rather focused on find the "optimal" results and driven by applied science teams, whereas generative systems are more focused on helping designers and driven by design science teams.

timization can be considered a performance-based generative systems as it uses performance evaluation at each iteration to create a single optimal result [102–104].

The graph of fig. 2.6 doesn't include the representation property of generative systems, as different levels of simulations were used for a wide range of generative systems. Still, higher fidelity representations usually require more explicit generation for accurate capture of the physics of the problems.

The next subsection discusses generative systems that are traditionally found as generative systems in the literature, split into conventional and performance-based generative systems.

Conventional Generative Systems

Conventional generative systems are defined by their lack of performance evaluation driving the generation of concepts. The performance is still evaluated, but only once all concepts have been generated. As such, the biggest advantage of conventional generative systems is that they are capable of quickly generating innovative geometry even if performance is expensive to evaluate [53]. However, including these systems in the generative design process is challenging hence smart "filter and select" algorithm are required to navigate the solution space [105].

In architecture, generative systems are used to inspire architects to find innovative urban layouts, façades, or buildings [106]. Shape grammars have seen interest in this research area [106]. However, they are considered challenging to create, as computers are more agile working with symbols than with shapes [107]. Shape grammars rely on shape generation rules to iteratively explore novel shapes [107]. Their current implementations are usually limited to certain architectural types, but are very useful to explore new variations of known styles [106]. Another use case for shape grammars are wheel design, in which combining shape grammar, topology optimization and deep learning, it is possible to explore the design space extensively [108].

L-Systems are another type of grammar that allows for parallel rules to be applied simultaneously [109]. They are systems that try to mimic the growth mechanism of plants and have a basis in mathematics [109]. They have been used as generative systems in multiple work [110–112].

In a broader term, there are also graph grammars (also called design or generative grammar) that explores the design space in a similar way, but with more explicit variables [113–115]. Simply put, a graph-grammar relies on the description of a solution being fully defined by a graph, including components description (nodes in the graph) and their relationship (vertices of the graph) [113]. Starting from any graph, a set of rules (grammar) is defined that can

alter the graph in a specific way [113]. Graph-grammars have been used with success for the design of hybrid power trains and the synthesis of gearboxes [113]. However, they are largely unsystematic and there is no consensus on which strategy to adopt for rigorous writing of the grammars [116]. Some recent work has put forward some rigorous design methods for graph-grammar [50, 113]. Graph-Grammars are more powerful than shape grammars, due to their capacity of creating with two sets of rules: the topological rules and the parametric rules [50, 117].

Some work in generative design is focused on the aesthetic of the solutions or on creating CAD-friendly structures, using NURBS, splines and other mathematical descriptions as the design elements [118]. Some CAD-focused solutions also focuses on simpler parametric systems [119]. The challenge associated with these systems is building the link between CAD and CAE systems, which can be helped by sequential convergence/divergence processes [118].

Although barely studied as a generative system, "cellular automata" have fascinated computer scientists for decades [120]. They have been more recently fitted for architectural design [120, 121]. Cellular automata are a distributed grid of cellular "robots" that responds to specific rules toward their environment [121]. They are better known in a popular "game" called the game of life [122], in which specific local rules create complex behaviors.

To help the designers navigate enormous design spaces, some strategies have also been developed to identify similarities between solutions [123, 124]. Similarity-based algorithm allows the computer program to skim through all proposed solutions and ensure that say, the ten presented solutions to the designer are all significantly different. A similar idea is pushed through history-based filtering that is very useful for parametric approaches [125, 126].

Performance-Based Generative Systems

Performance-based generative systems offers more robustness to the generative systems, by using performance analysis throughout the design process [127]. This allows the system to generate mostly feasible solutions, making the job of engineers during the generative design process easier, with less filtering and selecting to do [127]. Still, this comes at the cost of much more computing power which reduces the total number of solutions. Depending on the generative system, this can greatly reduce the innovation of the systems. Meta-heuristic algorithms, such as the genetic algorithm and particle swarm optimization, and evolutive patterns are generally used for the design exploration [128, 129].

The link between the generative systems and the performance evaluation is generally a major limitation to the implementation of such systems [128]. Still, it offers a main advantage over

conventional topology optimization: An explicit description of the design problem [128].

Multi-agent societies are another approach to push the generative system toward interesting solutions, especially in the applications of problems where the best compromise is not obvious [130]. Combining agents with deep-learning techniques has shown get promises [131, 132].

AutoDesk has seen some recent papers using their so-called generative design tools, with a robotic manipulator and a wind turbine design [133,134]. The tool has shown interesting and unique results, but since it is a black box for users and researchers, the papers note that the control of the output is difficult to manage and explain.

Some work combines more conventional approaches with a heuristic analysis. In [135], projected internal forces are used in combination with shape grammars to decide where to add new components. In [136], displacement fields are translated into design rules and tree searches.

2.4.2 Integrating Generative Systems in the Generative Design Approach

The biggest difference between the generative design approach and more traditional design theories is that instead of starting from requirements and creating feasible solutions, the designers use generative systems to create solutions that are then filtered. The design process then becomes mainly centered around *navigating and exploring* the solution space and adapting the generative systems if solutions are not acceptable [137].

An experiment with senior designers shows that most designers follow a similar pattern for navigation. First, observing and learning about the proposed solution, *what can they learn from the available solutions?* Secondly, they set qualitative criteria that allows them to segment solutions into subgroups. Some subgroups are quickly eliminated, others put forward. Subgroups are then made into smaller sub-groups. This process usually goes on until some solutions are considered convincing [137]. This study puts forwards the need to help designers cluster the solutions and display them in efficient manners to avoid overloading the designers [137]. Similarity-Based generative systems are especially useful for helping engineers navigate the solution space [124]. Other solutions include interactive displays, galleries and performance mapping [138].

In multi-objective optimization, the generative problem has also been raised. In this research area, the solutions are displayed on Pareto fronts, showing optimal compromises of certain solutions. However, for more than two, sometimes three objectives, it becomes increasingly complex to understand the compromises being made on the Pareto Front [139].

Two cases studies are discussed in [55], in both technical and artistic applications. We focus

on three challenges identified in the paper. First, pre-processing, that is choosing the right parameters, design space and which performance measures to be left evaluated by the user or automatically evaluated. Secondly, choosing the right optimization parameters and the right generation (implicit or explicit?) is challenging. Finally, integrating generative systems in the current design process is made more difficult by the integration with commercial design and analysis tools. In summary, generative systems require a completely different approach to design than traditional design, which makes it difficult to be integrated into current design teams [55].

In topology optimization, current design methods simply include a few topology optimization runs before going to the more detailed design [140]. This allows for an easier integration with the current design process. However exploration is very limited with this approach.

An adequate generative design approach should include aspects of both systematic design theories and social design theories, as discussed in the section 1.2.4. In fact, designing the generative systems becomes the act of design per se. The systematic approach is done by the generative systems, letting the computer and its algorithm explore the design space according to the developed rules. And the rules are developed not only by coding the engineers first intuition, but including a social process of discussing and developing the generative rules. This process becomes closer to a brainstorm, or political debate, rather than a systematic design approach. As stated in collaborative engineering [19], infused design [42] and C-K theory [43], it is in this conflict of ideas that we could be able to open up new creative design rules and grammars, opening up innovating possibilities.

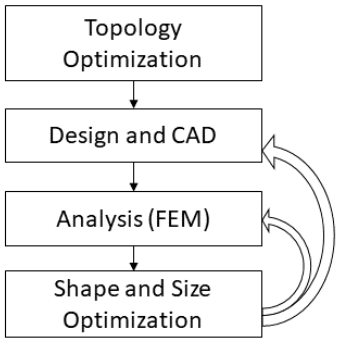


Figure 2.7 Design method with topology optimization during the conceptual design phase [140]

2.5 Topology Optimization Methods and Aircraft Applications

Topology optimization, in its widest definition, is an optimization tools that seeks an optimized topology or a functional material distribution with respect to a set of objectives and constraints. It has been used in multiple disciplines such as structures, radio and heat distribution [141, 142]. This thesis, and literature review, focus sorely on structural applications of topology optimization. Moreover, there are multiple approaches to topology optimization. This section of the literature review explores those approaches through the algorithms and their use in the design of structural components.

Historically, topology optimization has emerged from structural optimization research [2]. Prior research areas are defined as *size* and *shape* optimizations. However, both of these structural optimization tools are usually used more down the road during the detailed design phase, whereas topology optimization is used at the conceptual design phase. At this stage of design, there is still a significant amount of uncertainty in the project. Still, this is where topology optimization has proven to be especially useful in improving performance and/or reducing the weight of components [13, 38]. Topology optimization has seen more and more popularity in industrial applications due to innovation in manufacturing techniques, such as electron beam free-form fabrication and additive manufacturing [36].

Throughout the last decades, there has been a lot of new approaches that have been proposed, and this section will discuss the main ones. Some less popular approaches are also discussed at the end. As noted by Ole Sigmund in his review, most of these methods seeks to find the best topology, they are not designed as exploration tools [76]. This is why in this work topology optimization is placed low on the exploration axis of the classification of generative systems (see fig. 2.6).

As such, we will discuss topology optimization methods from most implicit to most explicit.

1. Continuum methods
2. Ground-structure methods
3. Level-set methods / Phase-Field
4. Moving Morphable Components
5. Novelty Approaches

2.5.1 Continuum Methods

The continuum methods have been at the forefront of research for a while now [76] and have been the flagship of topology optimization in industrial applications [141] and commercial

software [79, 143].

These methods breakdown as: Homogeneous, hard-kill and density-based approaches [141]. Homogeneous is the "ancestor" of continuum methods and is rarely used in recent research [144]. It consisted of assigning a microstructure to each element of the FEM and optimizing for the microstructure properties [144]. Hard-kill methods such as evolutionary structural optimization (ESO) and its more recent version bidirectional-ESO (B-ESO) make regular appearances in the literature, but are generally considered less performant in convergence and stability than density-based methods [76, 145, 146]. They are heuristic methods based on "evolutive" rules [146]. Finally, density-based is the most popular algorithm and is used widely, especially using the Solid Isotropic Material Penalization (SIMP) formulation [76].

The strength of SIMP relies on an implicit variable description of local density (varying from 0 to 1) assigned to each element of a finite-element model [2]. With the density variable, it changes the constitutive equation of the model for each element with equation 2.9.

$$E_i = E_0 {\rho_i}^P \tag{2.9}$$

where E_i is the Young's modulus of the element x, E_0 the material's Young's modulus, ρ the density variable of elements i and P the penalization factor.

The penalization factor is the main success driver of SIMP. It allows a continuous density variable, which allows gradient-based optimization solver to be used, while ensuring that most elements will have easily interpretable void ($\rho = 0$) or full ($\rho = 1$) density. As seen in fig. 2.8, the only intermediate density (0.3 to 0.7) is at the boundaries of full/void elements. Using qualitative assessments, it is possible to extract visually the topologies that are proposed by SIMP.

SIMP offers a tremendous design freedom to find innovative, and sometimes organic, material distributions [147]. The main strength is its ease of use and implementation. Multiple academic codes, such as the 99-line MATLAB implementation has tremendously helped the development of the technique [148]. SIMP also has some limitations.

First, due to the implicit nature of the design variables, it is limited to low-fidelity analysis. Using compliance as the optimization objective and volume (or weight) as constraints offers relatively quick and stable convergence. However, using more complex constraints, such as stress, buckling or fatigue leads to convergence challenges [2, 149]. Multiple objectives and multiple load scenarios have also been studied [149].

Also, again due to the implicit nature of the material distribution, it often arises that the interpretation of the result yields lesser improvements than what might be expected [39].

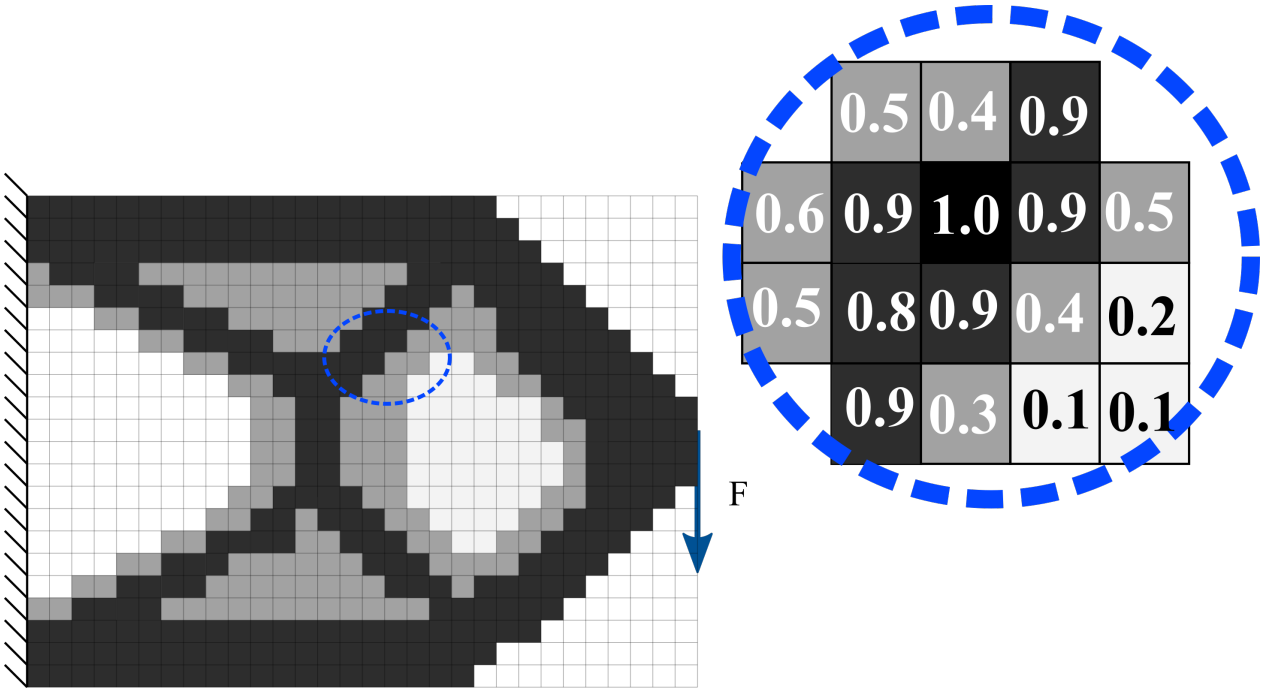


Figure 2.8 Illustration of density in a SIMP topology optimization [2]. The values represent the resulting density of each element, thus changing the Young's modulus of said elements. The force F is applied at the middle of the exterior face.

Finally, SIMP (as well as B-ESO) requires important regularization schemes to ensure convergence toward proper results [150]. Complex manufacturing filters are also required to ensure results which comply with more standard manufacturing techniques, such as extrusion and casting [143]. Still, additive manufacturing has shown incredible promises when combined with SIMP [150].

Due to the interpretation time, design and analysis automation are very difficult to achieve. Depending of the size and complexity of the problem at-hand, an adequate interpretation can take multiple hours to a couple of days by experienced engineers. In most cases, interpretation is driven by other design constraints, based on product knowledge, manufacturing or other criteria that can hardly be coded directly in the optimization algorithm. Multiple works have been done to answer this challenge [151, 152], but none has proposed a complete framework.

SIMP has been used in many applications for the aerospace industry, Zhu proposes a large review on the subject [13]. More recent work includes the Giga-Voxel project which used billions of design variables for the optimization of a complete wing box [39]. Stiffened panel optimizations focusing on the optimization of existing stiffeners (these works do not change the existing layout) [153, 154]. In [155], the design space of a wing box has been segmented

at the existing ribs for a buckling optimization. Finally, works discussed in [156] proposes an optimization of stiffener placements for ribs that also optimizes the loads from multi-fastener joints.

2.5.2 Truss Optimization (Ground-Structure)

Truss topology optimization, also often called the ground-structure method, is the oldest topology optimization method and is still relevant today [157]. The first algorithm with continuous variables is proposed in 1964 [158] and the first discrete algorithm in 1968 [159]. Contrary to continuum topology optimization techniques, truss topology optimization uses an already defined design space containing all the possible trusses, this is the so-called ground structure (see fig. 2.9).

Due to its long history, it has been noted that techniques and algorithms are often *rediscovered* in this field, with new researcher generations recreating old algorithms, simply taking advantage of the better computational power [157]. Still, new ground-structure algorithms and applications are presented regularly [157]. Ground structure has mainly been used for the design and analysis of large-scale structures such as bridges, cranes and buildings [160].

Even though the ground-structure approach limits the design freedom, compared to continuum methods, it allows an efficient gradient descent with explicit components. This allows more complex physics to be accounted during optimization [157]. However, the problem with ground-structure variables is that it doesn't scale particularly well with denser ground structures. The number of design variables increases exponentially, and even for the case with available analytic gradients, the evaluation of each gradient becomes prohibitive [157].

For these problems, there has been a continued interest in derivative-free techniques using discrete variables [157]. Contrary to discrete continuum methods ((B)-ESO), the discrete approaches in ground-structure approaches have had success in finding interesting topologies with an acceptable convergence rate [157]. Meta-heuristic solvers are relatively popular with discrete topology optimization, such as the genetic algorithm, particle swarm optimization, ant colony search, etc. [157].

For discrete ground-structure problems, global optimization schemes using mixed-integer variations have proven to be effective at small scales, but also suffers from large ground structures [157]. Deterministic heuristics while not very efficient at researching the design space, offers an efficient method that converges quickly [157]. An example of a deterministic heuristic methods is presented in [161], where all design variables are scaled to $[-1, 1]$ and using a gradient evaluation, trusses are removed or added iteratively.

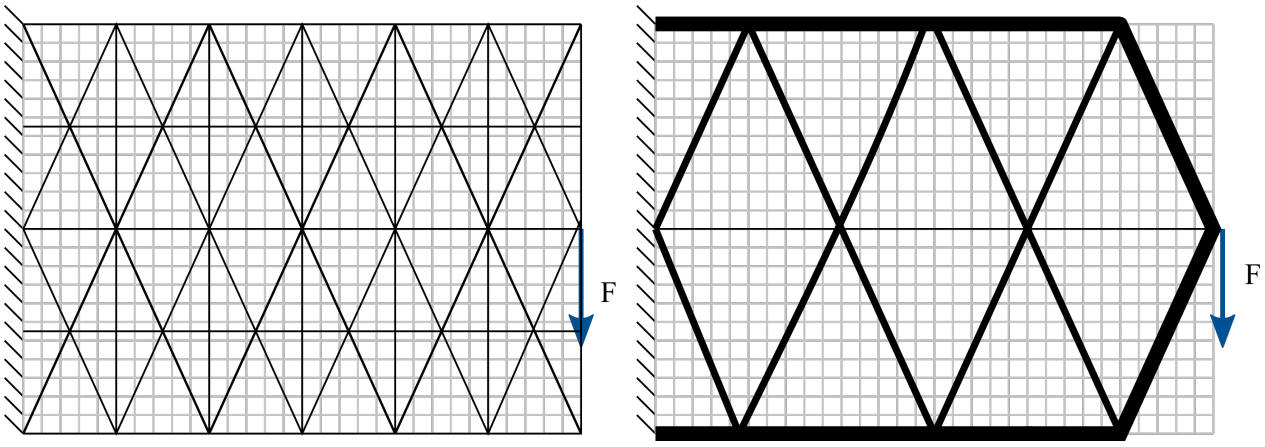


Figure 2.9 The ground structure [2] (left) and a result of truss area optimization from the ground structure (right). The design variables in this example are the thickness of the trusses, illustrated with varying thicknesses of lines. The force F is applied at the middle of the exterior face.

Not all truss topology optimization approaches are based on the ground-structure methods. There has been some work to "free" the trusses from the original grid. This allows more freedom while keeping the number of design variables low. A good example is presented in [162] where the ground structure expands during the optimization as more trusses are required and using a mixed-integer approach to choosing the activated trusses. In [163], the planar truss optimization is enhanced with grammatical evolution. This method is similar to some design grammars discussed in some traditional performance-based generative systems.

As noted earlier, ground-structure methods are mostly used on large-scale structures. Still, some works have used the method for aerospace structures. In [164], a mixed-integer approach using multi-level optimizations seeks to optimize not only structure, but also operations during topology and sizing optimization. In [165] [166] and [167], the ground structure is used to position the ribs in a commercial aircraft wing box. There has also been applications in morphing wing design [168].

2.5.3 Level-Set Methods

Level-set functions have first been used to model the evolution of interfaces in multi-phase flows and in image segmentation [4]. Then, in optimization, the nature of the level-set has evolved from shape optimization toward topology optimization when it gained more design freedom. It still uses shape derivatives to drive the optimization, but allows interfaces to disappear (and some algorithm allows re-apparition, but this hasn't been shown as efficient) [4]. Put another way, the level-set method for topology optimization is a generalized shape

optimization.

Level-set is usually also classified in the continuum topology optimization, but there is a fundamental difference with this method which sets it in its own category. Continuum and truss methods use comparatively implicit topological variables (i.e., density or thickness). Whereas for the level-set methods the contours of the material distributions are used for layout generation [76]. Still, the contours are not described as explicitly as in CAD software (which uses mathematical lines and surfaces tools such as b-splines) but with an implicit generation from the level-set functions [76]. As such, in the generative system classification (fig. 2.6), we position the level-set methods at the right of continuum and ground-structure methods.

Having a clear boundary definition is one of the main strength of the level-set methods, which allows for a crisp definition of the material distribution and no interpretation of half-density (fig. 2.10). It works by defining level-set functions in the design space and setting a threshold on full and void elements. The level-set functions are aggregate of local basis functions, often a radial basis function [4].

The level-set method is relatively complex and requires multiple steps, including regularization schemes like the density-based methods. It is able to have stable convergence in a larger and more complex physics than other continuum methods [169]. However, there are still major setbacks in the use of level-set in a design process.

The algorithm is highly dependent toward the initial interfaces in the design space, all results are local minima. The design space is highly concave [4]. Secondly, nonlinear constraints tend to create oscillations on the interfaces, which makes the optimization stuck in loops without proper convergence of optimization [4]. Still, tools like Fusion 360 by AutoDesk leverages this dependency toward initial values in their generative design [101]. This allows for a more exploratory approach to the usual "optimal" approach used in topology optimization.

Some recent work includes a rewrite of the algorithm for GPU solving [170]. These methods leverage an isogeometric analysis instead of a finite-element analysis, which allows a very quick rewrite of the static problem using the level-set directly. Level-set by optimizing directly with surfaces allows for an easier implementation with CAD software, as described in [171]. A multi-material method is proposed in [172].

For the design of aircraft, the level-set method has been applied to some projects. Using the level-set method, Townsend proposes a stiffened panel and wing box optimization method including buckling, however it still uses implicit modeling, which only captures the buckling of the skin [173]. In [174], the level-set method is used for multidisciplinary optimization, where

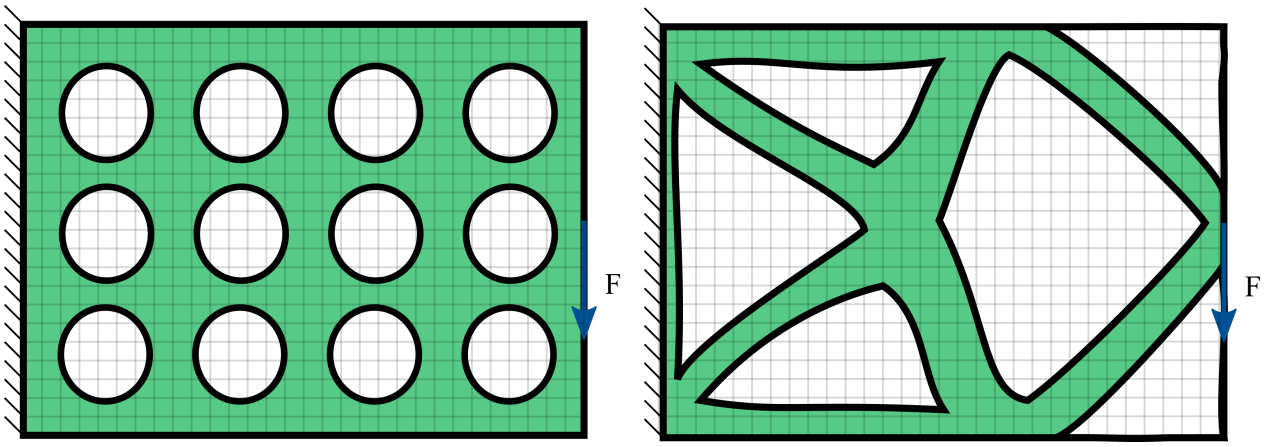


Figure 2.10 The level-set method with initial hole positions (left) and a result of optimization (right) [4]. In green, where material is "full" and the other regions are considered "void". The force F is applied at the middle of the exterior face.

not only is compliance studied, but the coupling with aerodynamics allows for interesting results. A topology optimization of ribs in [175] has leveraged the level-set method to minimize the dynamic effect of fuel moving in the wing (called *slushing*).

2.5.4 Moving Morphable Components

The moving morphable component (MMC) method is the youngest topology optimization method, and continues the trend of using more explicit optimization variables [5]. Due to its very recent introduction, there is no current review or state-of-the-art available. It has been first introduced in 2014 [5], and very similar method has been presented shortly after from a different research group [176]. The main advantage of the MMC method is that they consider variables explicitly, with only angle, position and morphing variables, as shown in fig. 2.11 [5]. They use a projection scheme and the ersatz material to create the analysis models on a fixed grid [5].

There have been many papers by the main research team at Dalian University of Technology since its introduction. Here is a non-exhaustive list of interesting papers for research in MMC topology optimization [177–181].

The main current challenges are related to the number of iterations required for convergence. For example, the 99-line SIMP MATLAB code from the Denmark Technical University requires about 30 iterations for complete convergence, with a very quick gradient evaluation [148]. The equivalent code proposed by Zhang in [182] takes a few hundred iterations for the same problem, with a very similar solution.

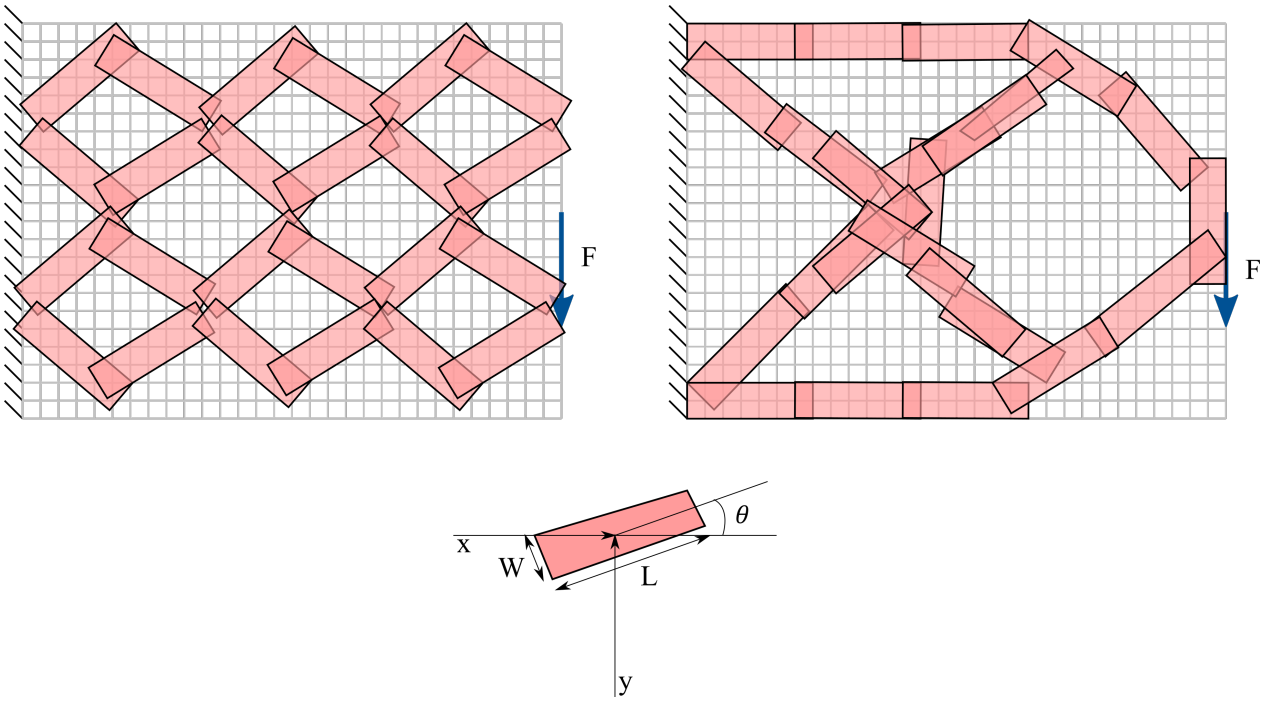


Figure 2.11 MMC method with initial member positions (left), a result of optimization (right) and commonly used design variables for each morphable components (bottom) [5]. In red, where material is considered "full" and the rest is considered "void. Where F is the applied force. The other variable are the explicit topological variables of each components, where θ is the angle, x and y the position, W and L the width and length.

Nevertheless, the main advantage of this method is the explicit description of the topological variables, which allows for more complex analysis tools to be used directly during the optimization [179]. Placing the MMC on our generative system classification still is not completely on the explicit right, as the connections between components is still not explicit. To remove material in the design space, the MMC relies on "hiding" superfluous components between useful components. This creates a similar problem to the level-set methods, where "hidden" components have no active gradients, which does not allow them to reappear in the solution, if required.

Since its recent introduction, it has also been used in many different areas of applications. For aircraft design, it has been used for stiffened plate optimization with buckling constraints only in 2020 [183]. This application, while promising, suffers from difficult convergence, no exploration and an implicit buckling buckling of the skin only.

2.5.5 Novel Topology Optimization Approaches

This subsection mentions some approaches that have been published in recent years. These methods are also placed in the generative system classification of fig. 2.6. Some of them get outside the scope of usual topology optimization with more exploration than performance focus.

Notable mentions are two recent bio-inspired methods, adaptative morphogenesis [184, 185] and space colonization algorithms [186]. The adaptative morphogenesis has been applied for stiffened panel design [184]. It works by starting from "seeds" and having them grow iteratively to create complex stiffening patterns [184].

L-Systems have been discussed in conventional generative systems. In a recent work, Bielefeldt has proposed an L-system generative system (called SPIDRS) for aeroelastic topology optimization [187]. Contrary to more traditional L-Systems, they have coupled the system with a performance focused genetic algorithm rather than an exploration [187]. This required more than a thousand design candidates per generation for a thousand generations [187].

There is also the graph-based optimization algorithm [188] and more recently [136]. In [136], the topology optimization process is based on graph-grammars (discussed in section 2.4). Using a seed and a displacement field, it uses the grammar to choose where to place new edges. It does not use a genetic algorithm to optimize the sequence of the grammar, but rather uses the stochastic decisions combined with the grammar to explore the design space thoroughly, by ensuring every change has an effect on the topology [136]. As the design space is explored, he then optimizes in the solution space rather than the design space. Since generation and

optimization are separated, the process is rather efficient and the results impressive. A more recent work by short has tried to increase the efficiency of the exploration phase by improving decisions as a tree search algorithm [189].

2.5.6 Challenges of Nonlinear Constraints in Topology Optimization

All techniques of topology optimization presented above were first born as compliance minimization problems. Compliance is often measured as the sum of strain energy present in all elements [2]. By minimizing the compliance, we ensure the minimal displacement of the nodes for which loads are applied, that is we ensure structural integrity [2]. This formulation is usually capped by a volume fraction constraint which is chosen by the user, allowing a proper control of weight of new components. This formulation has the main advantage of being convex for continuum optimization techniques, which ensures a quick and global convergence [141].

Compliance only does not always yield optimal structures, other structural considerations are essential for proper material/component distribution such as stress and stability (buckling) and must be considered for really optimal solutions [190]. These are considered nonlinear optimization constraints as there is a high coupling between design variables and the resulting stress and stability responses [66]. They create three main identified problems for gradient descent: The singularity problem, the local nature of stress constraints (and thus buckling), the nonlinear nature of stress behavior [190].

The singularity problem has been generally solved in the literature using relaxation or penalization techniques [190]. The local nature of stress is circumvented using aggregation techniques such as the P-Norm or the Kreisselmeier-Steinhauser (K-S) techniques [190]. Those same techniques can be used to aggregate the eigenvalues to help with buckling convergence [191]. Aggregation techniques are not perfect, though, they offer poor control on stress levels and a high nonlinearity in the aggregation functions may create unstable convergence [190]. Block and cluster aggregation may help with the convergence instability [192].

General optimization considering buckling constraints are also prone to mode switching and repeated eigenvalues [190]. This can generally be alleviated by using many eigenvalue modes (over 50 is reported) rather than the usual 10 which are often found in the literature [193]. In addition to this, for topology optimization, pseudo-buckling modes can arise in "empty" elements of the design space. This creates convergence issues and erroneous measures of the sensitivities, which leads to slow convergence [190].

2.6 Conclusion on State-of-the-Art

We have first discussed the object of the design problem: the structure of the wing box, and more precisely its main components the stiffened panels. The current challenges of innovation for stiffened panels are linked to general structural complexities related to analysis, model and optimization. For each of these complexities, current methods may easily tackle one at a time, but no techniques can handle the three of them. This leads towards rigid computational tools, greatly limiting innovation to known solutions.

The limitations we have identified in structural design are faced in any design problems that rely intensively on computations to evaluate new designs. A key takeaway, is that without infinite computing power, any generative systems have to compromise between the representation (analysis complexity), the generation (modeling complexity) and the exploration (optimization complexity).

The current big families of generative systems are positioned according to their choice in the matter of exploration, conventional systems are focused on exploration and performance-based systems are focused on local optimization.

We have positioned current topology optimization approaches as part of the performance-based family, as it greatly focuses on finding a local optima, rather than exploring the design space towards innovative solutions. The current trends in topology optimization have seen the focus change from implicit generation (SIMP) towards explicit boundary conditions (level-set method) and now explicit position and rotations of components (MMC). This more explicit generation, in time, should also make higher fidelity representation easier to implement, including stress, buckling and fatigue. Still, a major limitation of current topology optimization lies in the fact that the focus is on local optimization. Yet, in industry and in design articles, topology optimization is often used as an exploratory tool to inspire designers during the conceptual design phase [143]. More specifically, using topology optimization has shown multiple challenges for the design of stiffened panels. A higher-fidelity representation is necessary to capture buckling accurately, which makes the addition of exploration even more difficult.

Integrating generative systems such as topology optimization in the design process is part of generative design. As generative design uses a bottom-up approach to design, it is not necessary to implement all the requirements directly into the generative system. Using this systematic approach to explore ensures a more thorough exploration of the design space. The new conflicting solutions should hopefully spark creative ideas and allow the creation of efficient solutions.

In architecture and aesthetic design, the conventional generative systems with no performance

analysis provide a useful solution space from which to select innovative layouts. However, in mechanical design, performance-based generative systems are necessary to provide a good framework to find mostly feasible solutions quickly. There are multiple lessons to be learned from these generative systems to improve topology optimization of stiffened panels. Still, it should be noted that generative systems are developed for ad-hoc applications, and as such a difficult to generalize for different problems. As such, the work in this thesis focuses only on aircraft stiffened panel design.

The next section will discuss the scope of the project that has arisen from using topology optimization to find innovative stiffened panels. We give a brief presentation of the overarching ideas of the thesis and a summary of the articles to help the reader navigate the thesis.

CHAPTER 3 GENERATIVE DESIGN APPROACH FOR STIFFENED PANELS

In the last chapter, we discussed the trends and limitations of topology optimization when used as a generative system for the design of stiffened panels. For generative system, three key properties are put forward, that is representation, generation and exploration. For topology optimization, current techniques focuses only on improving the flexibility of generation at the expanse of representation and exploration. On the other side, conventional generative systems focus on exploration and finally performance-based generative systems focus on good representation and balanced exploration.

To use generative design for the application on stiffened panels layout, a rebalance of the three key properties of the generative system is required and as such, this research project seeks to evaluate different ways to do so.

3.1 Generative Design Framework

Through the work presented in this thesis, we assess and develop different computational and design tools to enhance and rebalance existing generative systems based on topology optimization. We think it is central to improving the efficiency of these tools within the generative design framework. While the focus of this thesis is on layout optimization of stiffened panels, we developed at the same time a comprehensive design and optimization workflow for any generative design. The proposed generative design framework is split in two processes: Deployment/Design of the generative system and the filter/validation process.

The choice of the generative system really depends on the problem at hand, as such the deployment strategy for generative systems is mainly centered around identifying and choosing the right one. As such, the workflow is described as follows:

1. Set the product/system requirements: functions, components, design rules, boundaries, etc.,
2. Explore different types of generative systems and evaluate their properties: **representation, exploration and generation**,
3. Discuss expected results with field experts,
4. Implement a generative system,
5. Develop an interpretation, filtering and validation process, automatic or not,

6. Adapt or change the generative system if results are not satisfying.

Within this strategy, the layout optimization of aircraft stiffened panels becomes:

1. Define the boundary conditions, manufacturing rules, design rules,
2. Explore different types of generative systems and evaluate their abilities with respect to generation, representation and exploration,
3. Discuss expected results with aircraft experts (designers, analysts, manufacturers),
4. Develop an interpretation process of optimization results in FEM,
5. Implement topology and sizing optimization,
6. Use nonlinear post-buckling for validation,
7. Adapt or change the generative systems if results are not satisfying with their performance, feasibility or innovation.

Our design requirements have been defined by a succession of discussions with engineering experts at Stelia Aéronautique Canada, our project partner in the MuFox collaborative project, and were revised regularly as the project progressed. The articles presented in this thesis put forward multiple tools, lessons and algorithm for different aspects of generative design specific to aircraft structure design. For every proposed tools we evaluate their capabilities to meet design requirements and constraints, by following a precise sequence of steps:

1. Generate concept/topologies/layouts (Using any generative system),
2. Filter infeasible concepts,
3. Use size and shape optimization (Using explicit models and medium fidelity representation models),
4. Filter low-performing concepts,
5. Validate promising concepts for requirements that are more expensive to evaluate (Using explicit models with the highest fidelity representation models).

3.2 Summary of Articles

In the first article, *Image-based Truss Recognition for Density-Based Topology Optimization Approach* we have worked on automating the integration of density-based topology optimization into the generative design approach. This work uses the SIMP method, a topology

optimization algorithm that uses implicit generation, low fidelity representation and gradient-based optimization. Integrating the implicit results from SIMP into a filter and validation process is an active challenge for automation. Still, we have shown that it is possible to extract an explicit model from an image of the density distribution. This can be used to automate the sizing and validation steps of generative design. Note that at the time of publication, we discussed "low/high level of abstraction" instead of implicit/explicit generation.

In the second article, *On Generating Stiffening Layouts with Density-Based Topology Optimization Considering Buckling* we attempt to use medium cost representation in the implicit generation of SIMP, while leveraging different initial values to increase exploration. In the approach presented in this article, randomized initial points are used to improve exploration, rather than just changing the optimization parameters which is commonly done in the industry. The article includes a simple case study, which explores on the properties of the design space of a seemingly simple case. In an experiment of 500 runs, the best performing minima is found only a few times, whereas sub-performing topologies are found often. Using these results, it is concluded that using SIMP for generation while increasing representation and exploration is possible, but computationally expensive and inefficient.

In the third article, *Topology Optimization for Stiffened Panels: A Ground-Structure Method* we propose a ground-structure method for stiffened panels. A ground-structure like approach is chosen for its ease of implementation and for its more explicit generation that allows for an easier use of buckling representation during optimization. The ground-structure approach uses a predefined set of possible reinforcement in the design space, which is decided explicitly by the designer. From this general approach, we developed a specific method for stiffened panels by combining density and sizing optimization variables. Like in the previous article, randomized initial points increases exploration of the design space. For our simple test case computation time is rather high, though comparable to SIMP. Still, results are more varied, coherent and easier to interpret, which is an improvement over SIMP for our application.

In the final article, *Complexity-Driven Conceptual Exploration for Aircraft Structure (CD-CEAS)* we combine multiple approaches to again try to find an improved balance of generative system properties within a new algorithm. With CD-CEAS, we propose to leverage complexity analysis to ensure simpler and more robust solutions. The algorithm allows for an efficient search using the basic Burst algorithm and an explicit generation using a graph-grammar. As the generation is completely explicit, using higher fidelity representation is possible, though computation cost increases quickly. We showcase the efficiency of the algorithm with case studies commonly used in stiffened panels optimization problems. Using complexity, it appears that even without assessing buckling during optimization, the new layouts can easily

be adapted as they were kept with low complexity.

In summary, the articles of this thesis discusses balancing representation, generation and exploration. For this purpose, new algorithms and tools were implemented as illustrated in fig. 3.1.

In the figure, it appears that making SIMP and ground-structure more exploratory led to new computation challenges and the original approaches were not adapted for this balance. The proposed algorithm to ease interpretation automation of SIMP results has proven to be efficient as post-processing tool. Despite that, we see that SIMP major weakness is in the design space exploration capability. An algorithm which automate the search by starting from multiple initial points, showed to be blocked by the nature of the implicit representation, which suffers local minima road-blocks. Thus, we didn't find a real potential in revealing useful unexpected information in the application of SIMP in this test case. Finally, the most effective approach is done using a layout optimization specific algorithm (EBF3) for representation and creating a novel generation and exploration algorithm that we named CD-CEAS.

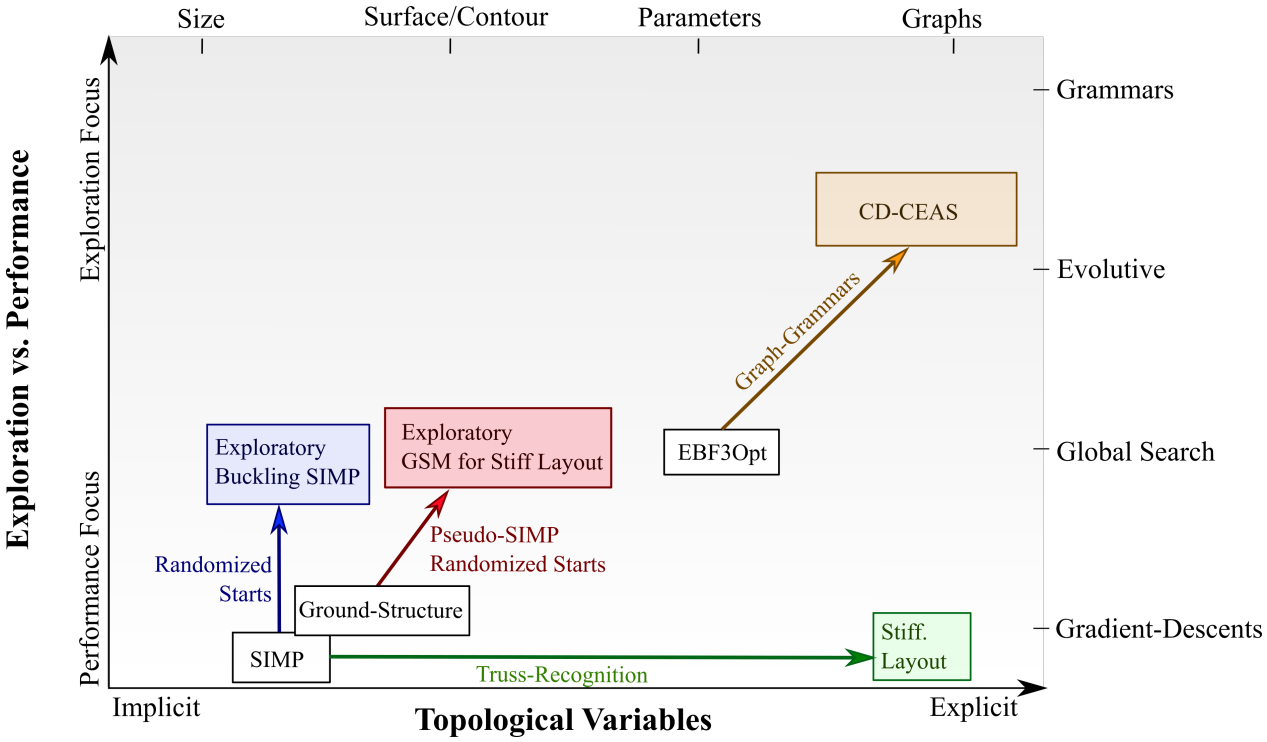


Figure 3.1 Balancing topology optimization towards a focus on exploration using more explicit generation. This approach has helped the algorithm use higher fidelity models which reduces the amount of rework required in preliminary and detailed design.

CHAPTER 4 Article 1: Image-based Truss Recognition for Density-Based Topology Optimization Approach

Jean-François Gamache[a], Aurelian Vadean[a], Émeric Noirot-Nérin[b], Dominique Beaini[a] and Sofiane Achiche[a]

[a]Polytechnique Montreal, 2900 Edouard Montpetit Blvd, Montreal, Québec, Canada
[b]Stelia Aéronautique Canada, Research & Technology, 12000 rue Henry Giffard, Mirabel, Québec, Canada.

Published in *Structural and Multidisciplinary Optimization*, Vol. 58, 2018

Abstract

Topology optimization is a tool that supports the creativity of structural-designers and is used in various industries, from automotive to aeronautics, to reduce design iterations towards obtaining the optimal structure layout. However, this tool requires both time and experience to interpret the results into manufacturable and reliable structure layout. To improve this aspect, an interpretation support tool is being developed by our research team based on industrial knowledge and axiomatic design principles. This design tool will be very useful for aircraft structure development, for instance, as it aims to help the structural designer in the conception of stiffened panels. The tool has been divided into three modules: feature recognition, feature analysis and design support. This paper presents the first of the three modules that identifies the trusses of the optimized topology in terms of truss recognition algorithms. The purpose of the truss recognition algorithm is to translate the densities of the element of the optimized topology (low-level abstraction) to a skeletal structure (high-level abstraction) that contains nodes and branches that describe the same topology as the optimized topology. It should also ensure that the structural skeleton retains connectivity with loads and boundary conditions. The information may then be used by the design support tool for analysis, comparison, decision-making, design and optimization purposes. To do so, a novel image-based method using a binary skeleton is proposed. For this work, we identified multiple limitations existing in similar solutions and we mitigated them. Therefore, a new skeletonization method is proposed, which is specifically designed for truss recognition in the optimized topology. The capabilities of the skeletonization method are demonstrated by comparing it with existing methods, and the truss recognition algorithm is used with a test case exhibiting the algorithm's capabilities on an airplane wing box rib.

4.1 Introduction

Topology optimization while technically challenging, can help achieve great economic gains by allowing more freedom to the optimization process [146]. The goal of topology optimization is to find the optimal material distribution for a given set of boundary conditions [2]. It is a powerful tool to support design creativity and offer solutions that are not initially apparent to the structural designer [38, 194]. Its impact on a design is more noticeable when used from the beginning of the design process, i.e. the conceptual phase [195]. A common technique implemented in multiple Finite Element Model (FEM) commercial software is Solid Isotropic Material with Penalization (SIMP) [141]. Optistruct from Altair uses this algorithm and is used in this work to generate the topologies used for the truss recognition.

The following procedure defines the design work that integrates topology optimization. It is a simplified version of the procedures from Buchanan and Bremicker [6, 140].

1. Problem definition/pre-processing
2. Topology Optimization
3. Design interpretation (From the study of topology results, design a feasible structure)
4. Sizing
5. Computer Assisted Design (CAD) prototype definition

Including topology optimization into the design process has proven to be very challenging. This is mainly due to the design interpretation step. Furthermore, due to its nature, topology optimization proposes "optimal" shapes, thus it is important to understand that only the **topology or the layout** should be used. In addition, the resulting shapes should not be directly used as structures [194, 195]. Topology optimization remains a source of inspiration, for design engineers, to discover new topologies; hence, the interpretation will be different depending on the user.

Topology optimization requires extensive knowledge of both the problem at hand and the optimization process [38]. One design strategy, developed by Dugre et al. [196], is based on axiomatic design and topology optimization. This strategy analyzes multiple Optimized Topology (OT) to define the function of each component. The interpretation of OTs is looped back to the initial objectives of the optimization defined through axiomatic design mapping. The results are conclusive, even for a complex problem such as a pressure bulkhead submitted to an out-of-plane loading. Furthermore, optimization design like the work published in Zhang et al. [197] have manually interpreted their OTs with skeleton information. Automating this step would have been useful for this work.

The work presented in this paper details the first step in developing a tool to support structural engineers in the interpretation of topology optimization results. The goal is to ease the design interpretation process for standard recurrent aircraft components, such as airplane wing box ribs.

There are two recognized family of methods of OT interpretation, the most popular one are the shape interpolation schemes, but there are also the skeletal interpretation methods. Ultimately, we would want our design tool to integrate both shape interpolation and truss recognition. Shape interpolation schemes are well understood and multiple tools already exist in this area, while truss recognition schemes are more rare and much less robust. This is why truss recognition is developed in this paper.

Furthermore, it is to be noted that this work is not grounded into a mathematical or theoretical background, but based on the engineering process that has been built throughout years of experience and research work. As such, it will try to mimic the analysis and synthesis the work of engineers [38, 196].

One of the key aspects of the interpretation step is the optimization parameters analysis, that is, the work carried out to understand the impact of the different parameters on the design. Among these parameters are the meshing, the filters and the optimization parameters. This step is hard to automate because the results from topology optimization are presented in the form of a finite-element model, which offers only the optimized density values of each element, considered as low-level information. In other words, there is no level of abstraction to manipulate the object so it cannot be easily converted into an object-oriented design tool. For a design support tool, it is necessary to allow the extraction of high-level information from the FEM, such as nodes and branches that are easy to handle by the object-oriented approach.

This paper is divided into four sections. First, the current methods of topology optimization integration, interpretation, and recognition are discussed in a brief literature review. Second, the developed algorithm is presented and applied to a cantilever beam, as an example. Third, a comparison with existing skeleton-based recognition methods is done to provide insight on the advances achieved by the method proposed in this work. Finally, a case study is carried-out using an airplane rib to illustrate the industrial potential of the proposed method.

4.2 Literature Review

Topology interpretation algorithms are generally divided into two main groups. The first group algorithms concentrate on the extraction of truss topology, while the second group

algorithms extract the shape information from OTs.

Algorithms in the first group use methods that seek to extract a skeletal structure (frame and truss configurations), such as the image skeleton extraction [6,7,198,199], the contour derivatives methods [200] and the active contour method [201]. Skeletal interpretation methods seek to extract low-level information from OTs and convert it into a high-level abstraction. High-level information consists of skeletal nodes, as well as the relationship between branches and their preliminary size. These results may also be easily combined with analytical methods for stress, buckling or fatigue analysis. Extracted skeletal structures have also recently been used as explicit length scale control for SIMP and level-set methods [5, 177]. Finally, it is worth noting that truss recognition is used only for low volume fraction topology optimization [6]. Currently, one of the downsides of the skeletal interpretation in the literature is the loss of boundary information after the interpretation, which means there are no guarantees that the structural skeleton connects with every loads and boundary conditions.

Algorithms in the second group keep low-level information from the FEM and directly translate it back to FEM by only extracting the shape of the material distribution. These methods include, among others, B-spline extraction [202], pre-defined shape recognition [203], neural-network feature recognition [204], 3D contour extraction [205], surface reconstruction [206] and 3D reconstruction via template sweeps [207, 208].

Shape interpretation has a main advantage in that it can be used directly with additive manufacturing making the design interpretation easier. However, these techniques do not perform on a complete analysis of the structure; they simply translate the OT directly into a CAD. Because of this, the results should be used with caution. Consequently, the use of shape extraction is limited to simple components, such as fixtures [209]. There are commercially available tools that use shape interpretation, for example, the OSSmooth module from Altair's optimization suite, which is based on B-Spline smoothing [143].

It is important to note that the methods used in each of the two algorithm groups provide crucial information for the development of the final design support tool. The skeletal interpretation focuses on recognizing the features available from the material distribution and extracting them into a high-level abstraction composed of nodes and branches. On the other hand, the shape interpretation focuses on defining the edges of the material distribution and integrating them with shape optimization. Mass & Amir [210] combine both skeletal and shape approaches to develop a tool that uses topology optimization to create 3D files to be used with additive manufacturing. Their method resolves the overhang and boundary definition problems. While both shape and skeletal information will be integrated into our final tool, the fact that existing skeletal recognition methods lose information about their context

after the process needed more research attention.

The work presented in this paper is developed and then tested to recognize trusses in the results from the SIMP topology optimization method, owing the the fact that SIMP is a method commonly used in the industry. The authors are aware that a new optimization method, the Moving Morphable Compoments (MMC) method, optimizes directly a set of discretized components with promising results [5, 176, 180]. However, the tool developed in this project seeks to combine knowledge from multiple optimization runs and analysis. The main application of the developed tool is for aerospace stiffened panel design, which is a complex assembly of panels and stiffeners with a behavior that is hard to simulate. Our usage of topology optimization is to use as a design initiator, to be used with stiffened panels optimization algorithms (e.g. [82]).

Among the skeletal recognition methods, the image skeleton extraction method is chosen because it is the easiest to implement numerically and its limitations can be mitigated by altering the existing algorithms. The skeleton-based implementations require the use of a binary image skeletonization method, which currently limits the capabilities of the truss recognition. There are four limitations due to image skeletonization, which are [6, 7]:

1. high dependence on the quality of the material distribution,
2. necessity of smoothing the edges, because skeletonization are usually very sensitive to jagged boundaries,
3. boundary conditions information cannot be retained,
4. superposed trusses cannot be recognized as two different trusses.

In this paper, a new skeletonization method specifically adapted for OT is developed due to these limitations. The skeleton is also used to discretize the binary image into the different sub-components, branches and nodes, of the structure.

4.3 Methodology

The OT may be obtained from a multitude of different topology optimization algorithms, which are all presented the same way, i.e. with a gray scale image that represents the density value of each element of the design space. For this paper, Optistruct is used to optimize the topology [78]. The OT obtained from Optistruct is the input of our truss recognition algorithm. We used MATLAB, due to its extensive and easy-to-use computer vision toolbox, to implement our work. However, a more versatile coding language like Python could easily be

used as well. The different steps that we followed are explained in this section, each one with their specificities and challenges. Fig. 4.1 illustrates the workflow of the proposed algorithm.

To exemplify the use of the developed algorithm, the classical problem of the cantilever beam optimized for compliance is used. This problem is considered as a benchmark in topology optimization [2]. It is defined as a simple rectangle that is fully constrained on one side with a downward force on the opposite side, as illustrated on fig. 4.2.

4.3.1 Step 1: Image Acquisition & Pre-Processing

The first step of the proposed algorithm is acquiring and pre-processing the OT images. Using the HyperView module of Altair HyperWorks suite [143], the topology shape is extracted for a given arbitrary threshold, which in this example is 0.5.

The images are pre-processed by binarizing and cropping software related pixels (fig. 4.3.a), such as the density scale. It is important to note that in the image of the OT a pixel, which is the basic unit of computer images, and finite-elements are not the same. The image is of higher resolution than the finite-element model, which means that there are many more pixels than elements resulting in a smoother resolution.

It is also necessary to extract the image of the loaded edges (fig. 4.3.b) and the design space (fig. 4.3.c) to ensure connectivity with boundary conditions. The edges are then extracted for each image, as shown on fig. 4.4.a.

4.3.2 Step 2: Binary Image Skeletonization Method

Once the images are pre-processed, the algorithm extracts the skeleton of the image. The goal of skeletonization is finding a simplified version of the image that can be further analyzed.

Most skeletonization methods, including the one implemented in MATLAB, use a thinning algorithm which seeks to preserve the number of holes and branches present in the original image. This is problematic since the skeletonization algorithm cannot recognize trusses as two different features, even with pixel connectivity. Also, the information from the skeleton should be able to be integrated directly into the design space with the appropriate boundary conditions. Another important aspect is that the skeleton should be free of spurs and imperfections that are due to image information rather than the structure itself, especially since jagged images are always present due to the nature of finite elements.

To achieve these goals, our method uses two key pieces of information, geodesic distances and lake filling. This will be carried out using two computer vision functions from MATLAB:

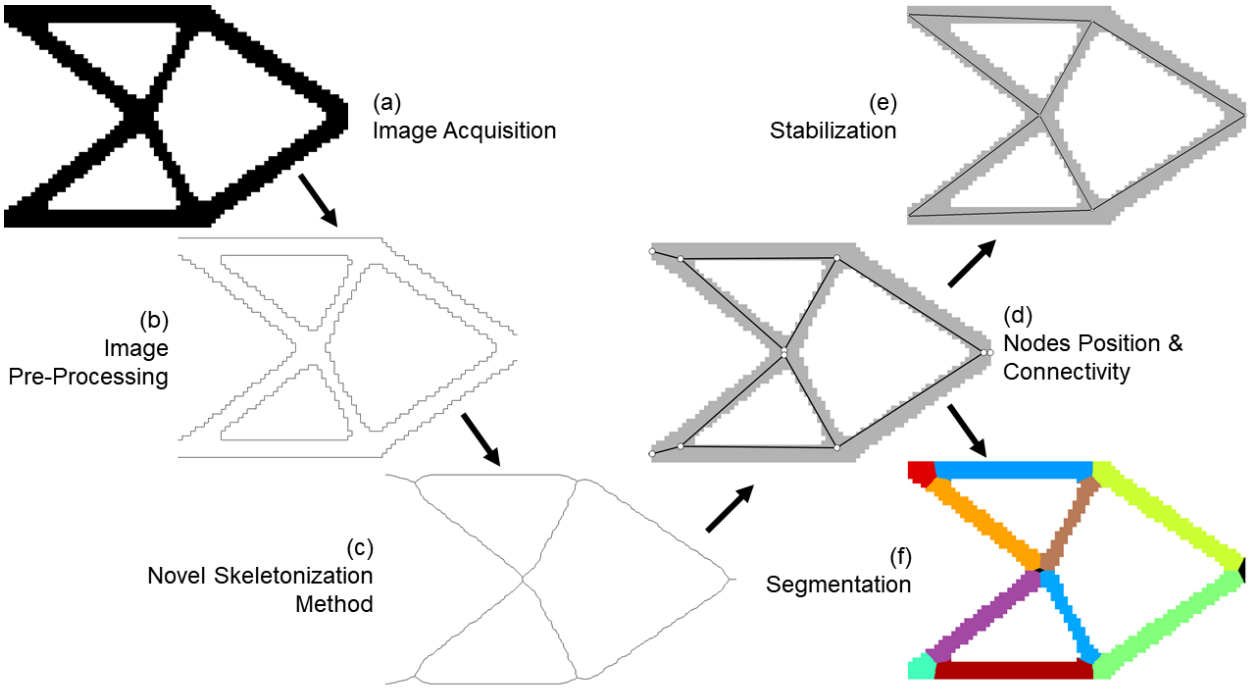


Figure 4.1 The different steps of the truss recognition algorithm

bwdistgeodesic() and *watershed()*.

The *bwdistgeodesic* function is used to compute the geodesic distance of each non-loaded edges (fig. 4.4.a). into the shape of the OT (fig. 4.3.a). Fig. 4.4.b illustrates the geodesic distance of the cantilever beam results. By removing the loaded edges from the images the branches can grow to the boundary conditions thus insuring a closed and coherent skeleton.

The geodesic distances of non-loaded edges can be illustrated as mountains as they form ridges in the middle of each branch of the OT. The *watershed()* function then fills every lake. The lakes are the lowest points (minimum geodesic distance value) in the local region. Since all lakes fill at the same rate, common edges are found at the ridges of the mountains (maximum geodesic distance value). This intermediate result is illustrated in fig. 4.4.c. Then, the ridges are simply extracted using an equality filter; MATLAB defines ridges with a value of 0. The ridges common with the design space are removed. The resulting skeleton is presented in fig. 4.4.d. The watershed function is used instead of the traditional gradient-technique because of the numerical noise on the edges.

The algorithm is presented in the following pseudo-code:

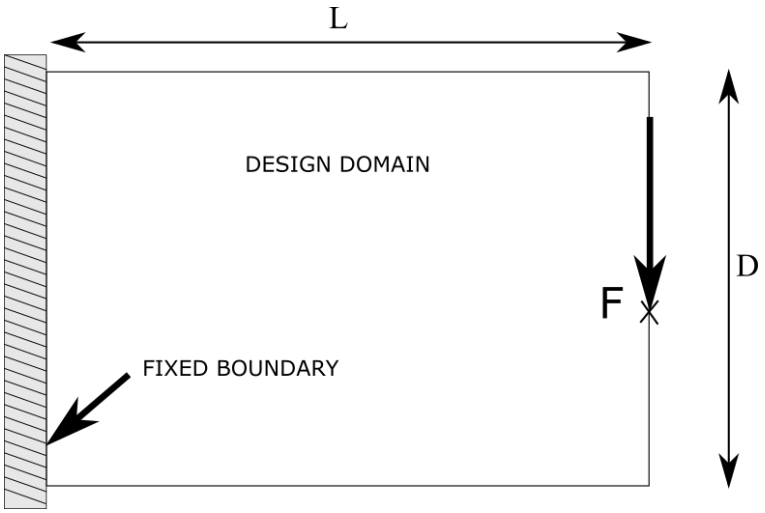


Figure 4.2 Cantilever beam design space, this structure problem is used as an illustration throughout this section with L/D ratio of 2.

Algorithm 1 Skeletonization

Require: Im1, Im2, Im3
Map1 = BWDISTGEODESIC(Im1, Im2)
Map2 = $Map1 + Im3$
Map3 = WATERSHED(Map2)
Skeleton = $(Map3 == 0) \cap (Im3 == 0)$
return Skeleton

where Im1 is the black and white image of the topology (Fig. 4.3.a), Im2 is the edges of the domain, without the loaded edges (Fig. 4.4.a) and Im3 is the contour of the design space. Map1 is the map of geodesic distances from Im1 and Im2 (Fig. 4.4.b). Map2 is an intermediate result with geodesic and the contour. Map3 is the watershed of Map2 (Fig. 4.4.c). Finally, the skeleton is the ridges of the watershed, which have a value of 0 in MATLAB. The contour of the design space also has a value of 0, which is therefore removed from the skeleton.

In summary, this skeletonization method resolves multiple limitations of skeletonization for topology optimization making its use in our truss recognition algorithm viable. Each issues will be discussed in section 4.4.

4.3.3 Step 3: Node Position

As stated above, the skeleton is defined by two types of sub-components: the nodes and branches. In the binary image skeleton the different branches appear clearly, see fig. 4.5. However, they are not recognized as different entities yet. The skeleton image analysis starts

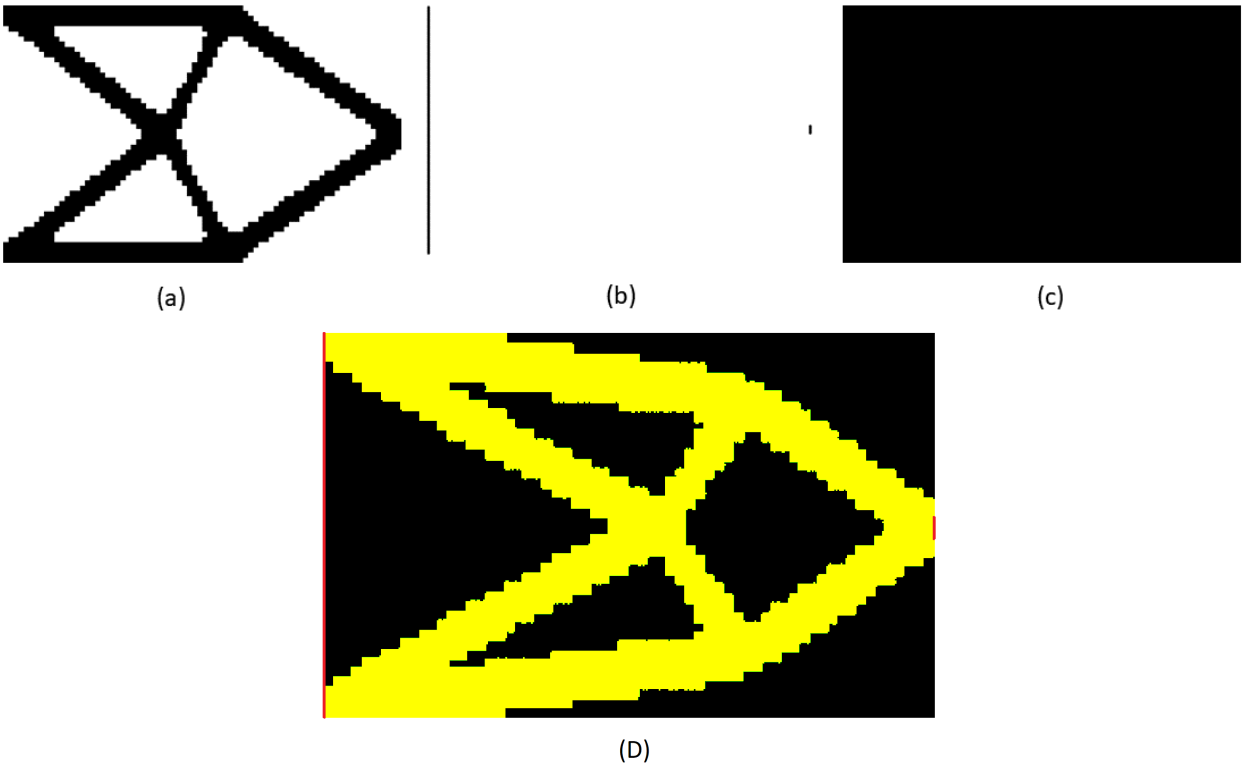


Figure 4.3 Inputs image for the cantilever beam. (a) Optimized topology from with a threshold of 0.5 (b) Pixels under load or constraint. Pixels have been enlarged for illustration purposes (c) Design Space (d) Superimposed image with all three inputs.

by finding the nodes at the intersection of the different branches of the image and at the end points of the free spurs.

Finding the position of the nodes in a binary skeleton image is a straightforward task using image analysis.

In MATLAB, the binary image analysis function *bwmorph()* is used on the binary image skeleton. This function provides the different branch points at the intersection of three or more image branches, and the end points at the end of each free spur. However, when two nodes are very close to each other this function might recognize them as two different entities. To avoid this problem, the nodes are filtered with a distance filter; nodes closer than 2 pixels are merged together. This ensures that the branches are identified correctly.

4.3.4 Step 4: Node Connectivity

The next step is to recognize the different branches of the structural skeleton. This is done by analyzing the relation between the different nodes in the binary skeleton.

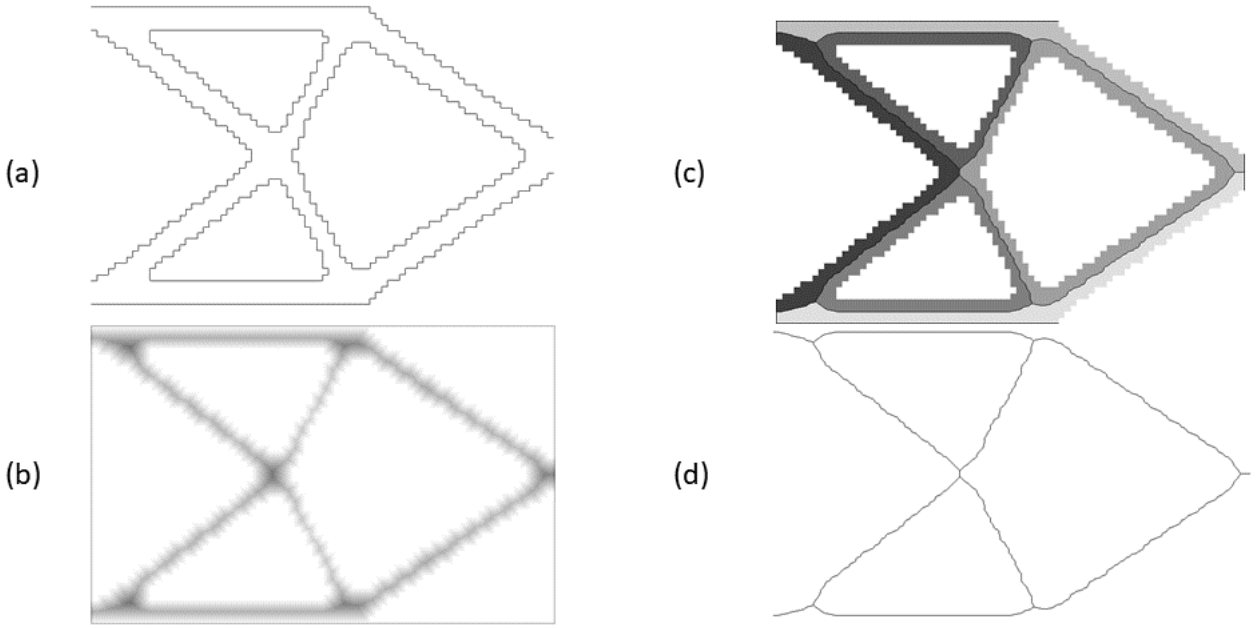


Figure 4.4 Steps of the skeletonization process. (a) Unloaded edges, used as sources for geodesic distances, (b) The geodesic distance of the edges in the binary topology image (the darker the color, the farther it is from an unloaded edge), (c) The watershed image. The ridges (in black) can be interpreted as the image skeleton, (d) The skeleton obtained using our proposed skeletonization method.

Fig. 4.6 illustrates this process using the central section of the OT of the cantilever beam fig. 4.6.a. First, the binary skeleton is cut using the position of the nodes and removing any pixels around it, as illustrated in fig. 4.6.b. Then, each branch identified with different colors is used for morphological dilatation (fig. 4.6.c). The position of each node is then compared to the image dilated branches and the nodes, that are part of the image, are connected with the structural branch.

4.3.5 Step 5: Image Segmentation

The goal of the image segmentation is to associate element data of the OT, such as stress, displacement, strain energy, density, with each branch. This step provides the link between the FEM results, the image pixels and the recognized branches.

This step is usually ignored by recognition algorithms [6, 7, 211], since they usually stop when the nodes and branches are identified without looking for their role. It seems that it is because these algorithms make the hypothesis that the recognition of a single OT is enough for a suitable design. Industrial partners and literature [196] agree that a single topology optimization in not enough for design. By ignoring this step, a lot of information about

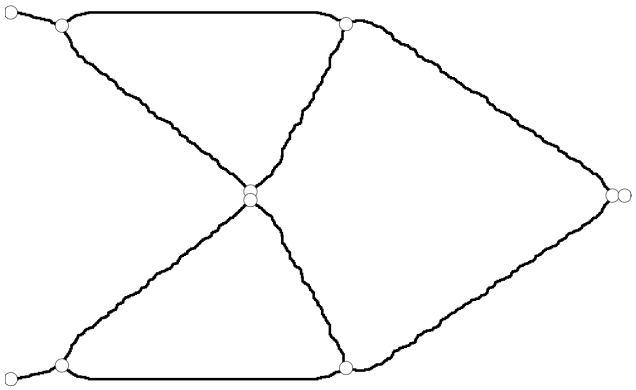


Figure 4.5 The intersections and endpoints of the binary skeleton are considered nodes of the skeletal structure

how the optimization problem behaves is lost. Connecting the information from the FEM to the high level information will allow our tool to use Axiomatic Design in its interpretation process.

To carry out the segmentation, a geodesic distance is computed for each branch of the binary skeleton image. This provides a distance map that is used to find the closest branch for each pixel of the OT. A pseudo-code of step 5 is presented below:

Algorithm 2 Image segmentation

```
Require: Im1, List1
  List2 = emptyList
  List3 = emptyList
  for all branch in List1 do
      Map1 = BWDISTGEODESIC(Im1, branch)
     List2 ← Map1
  end for
  for all pixel in Im1 do
      Parent = FINDCLOSESTBRANCH(pixel, List2)
     List3 ← Parent
  end for
      return List3
```

In the pseudo-code, the variable Im1 refers to the black and white image of the OT. List1 is a list of all individual images of the skeletal branches. List2 is the list containing the maps of distances for each branch, Map1. The Parent variable contains a pointer to the parent branch of the pixel in the topology image and List3 contains Parent for each pixels of the topology image. The function FINDCLOSESTBRANCH uses the maps from List2 and the position of pixel to find the closest branch.

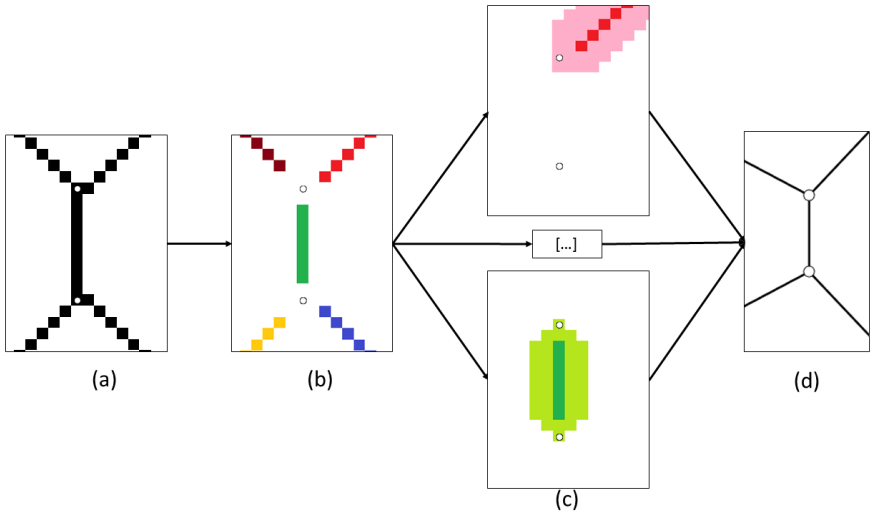


Figure 4.6 Node connectivity method. (a) Find nodes on image skeleton. (b) Remove nodes and segment each lines. (c) draw aura around each lines and detect which lines connects to the same nodes. The step is repeated for each lines (d) The connectivity of each nodes is extracted as a graph.

The results for the cantilever beam are presented in fig. 4.8.a. Fig. 4.8.b illustrates an ideal case of segmentation. An ideal case is where all the discrete members are correctly identified and the load paths are separated between the trusses accordingly. The main differences are caused by the small branches of the binary skeleton that do not play a structural role.

With the information obtained from the image segmentation step, it is possible to extract geometric data such as branch orientation, area and contour. Also, it makes it possible for the engineer to better understand the role of each branch, whether it is in tension or compression, in specific load cases. Overall, this step will allow the FEM to feed data directly to the interpretation support tool to be developed in future work.

It is important to note that the image segmentation, due to the fact that it is image based, is done before truss stabilization. In addition, since the stabilization process alters the position of the nodes, the segmentation would not be capable of associating the shape with the right branches. More work is needed to improve segmentation and obtain something that is closer to the ideal case.

4.3.6 Step 6: Truss Stabilization

As reported in Chiredast et. al. [212], the stability of an interpreted structure should be verified, especially if it is to be interpreted as a truss structure. It has been found that even if the structure is interpreted as a frame, the truss interpretation yields results closer to

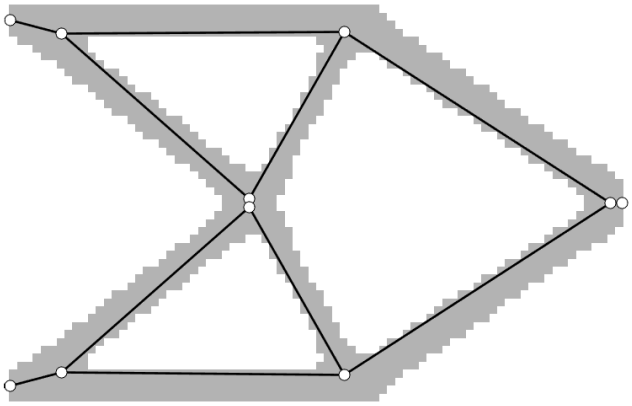


Figure 4.7 Results of recognition of node positions and connections on the cantilever use case. In gray, the initial material distribution and the recognized trusses superimposed on it.

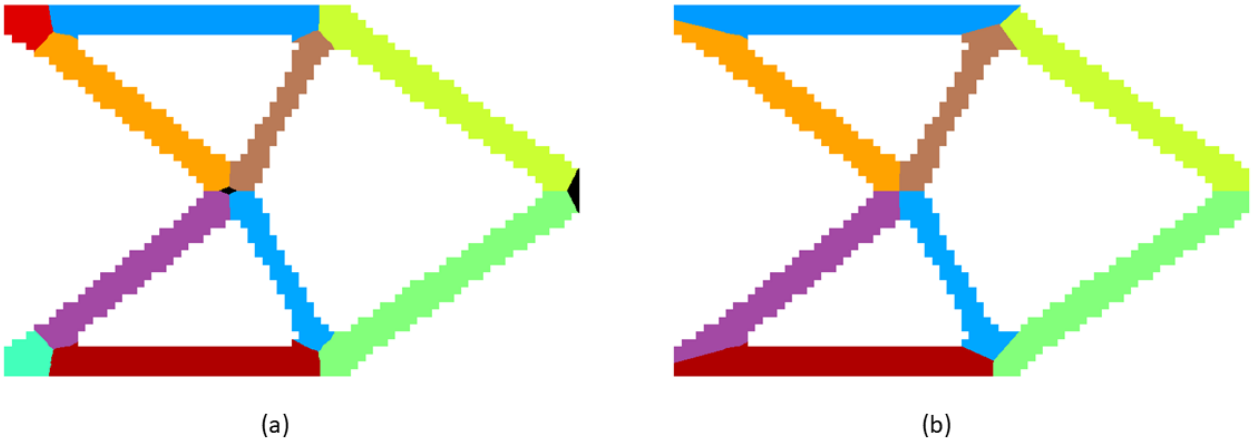


Figure 4.8 Segmentation results of the cantilever beam. (a) Results obtained with the image segmentation algorithm (b) Ideal results with a manual interpretation done by the authors.

the concept proposed by continuous topology optimization. Therefore, this step is crucial in ensuring accurate truss recognition. If the structure is to be interpreted as a beam, instead of a truss, this step can be skipped.

This process will ensure that the structure is stable, i.e. it will not collapse on itself under external forces. In previous approaches, this step was usually replaced with geometry optimization [6, 7] , which is computationally expensive and does not add any value to the concept or solution proposed by topology optimization. Since the main benefit of topology optimization is providing new concepts for the design engineer, geometry optimization should be avoided if possible. Hence, stabilization should stay a simple heuristic process that ensures stability at a minimum cost. Equation 4.1 presents the stability conditions for a truss structure:

$$s + z \geq 2k \tag{4.1}$$

where s is the number of bars/trusses, z is the number of reaction forces and k is the number of nodes [6].

This process is iterative; at each iteration the smallest bar that will not remove a truss triangle is deleted until stability is obtained. Triangles are shapes created by multiple trusses that have only 3 sides. They are the base of a stable skeletal structure and therefore, they are never altered. The only trusses to be modified are the ones that will increase the internal stability of the structure. With the first results from fig. 4.7 the algorithm is able to obtain the skeletal structure presented in fig. 4.9. It can be seen that small and unstable branches are removed and all that is left is a stabilized and simplified structure that retains only the critical branches.

4.4 Skeletonization Comparison

Analysis of topology optimization with computer vision has already been done in the past [6, 7], however the novelty of the work presented in this paper lies in the skeletonization method. Our approach, allows the rapid recognition of the different branches and the way they connect with each other while considering the boundary conditions, and other issues associated with skeletonization. This section will compare the skeletonization process results with both Bremicker's and Gedig's skeletons [6,7]. Both of the latter works use skeletonization and computer vision to integrate topology optimization with their design tool.

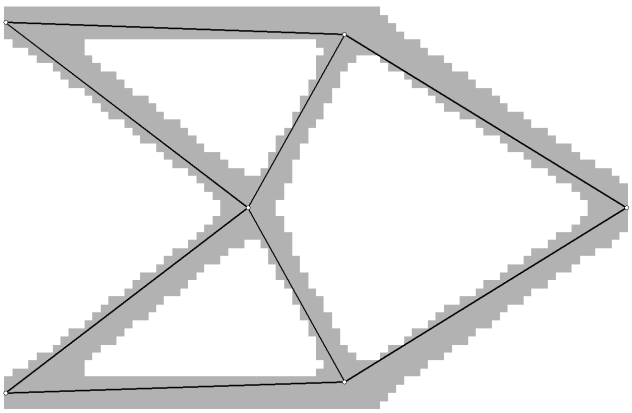


Figure 4.9 Stabilized structure. The short unstable trusses of fig. 4.7 were removed.

4.4.1 Comparison with Bremicker

Bremicker was the first scientist to have worked on topology optimization skeletonization in 1991 [6]. At the time, the main topology optimization algorithm used was the homogenization method which is the precursor of SIMP. Even though this algorithm was developed in 1991, it remains crucial to benchmark our proposed solution against it. Indeed, there is still a large gap of research in the area of image-based recognition, and using modern computer vision tools mitigates the limits of the method developed in 1991 and therefore extends its relevance to this day.

For a fair comparison, the topology optimization image used in [6] was reproduced as close as possible to the original. A comparison between Bremicker's skeleton, MATLAB's thinning algorithm, and the skeletonization method presented in this paper are illustrated in fig. 4.10. Bremicker uses a traditional thinning method, as presented in Arcelli's et al. [213].

The advantage of our developed solution is presented in this comparison. First, the skeleton created using our algorithm is connected to the edge of the design space, in a position that makes sense regarding boundary conditions (fig. 4.10.d), which shows improvement toward issue 3. When looking at fig. 4.10.b and 4.10.c the skeletons created using Bremicker's method and MATLAB respectively, the boundary conditions are not represented as they should be. In fig. 4.10.b, the skeleton is doubled and does not touch the edges of the design space. In fig. 4.10.c some of the branches touch the edges of the material distribution. However, the edges does not correlate with the existing boundary conditions.

Secondly, one can see in both fig. 4.10.b and 4.10.c that these methods are sensitive to jagged boundaries, described as the issue 2. Due to the nature of FEM, the OT will always have jagged edges unless smoothing is applied. Skeletonization methods tend to mistakenly recognize these sharp corners as branches, and as it can be seen in fig. 4.10.c. This is much more noticeable in the MATLAB results, while it is not an issue in this work, as shown in fig. 4.10.

For issues 1 and 4, threshold dependency and superposed trusses are not an issue in the cantilever beam problem. As such, it is not sensitive to the threshold choice and there are no sub-structures in this case that could create superposed trusses.

Also, since both Bremicker and Matlab use similar thinning algorithms, it may be assumed that similar results could be observed with Bremicker's algorithm at high resolutions. However, our algorithm is less robust at lower resolutions, similar to the one used by Bremicker. It indeed requires at least 5 pixels-wide features to recognize effectively.

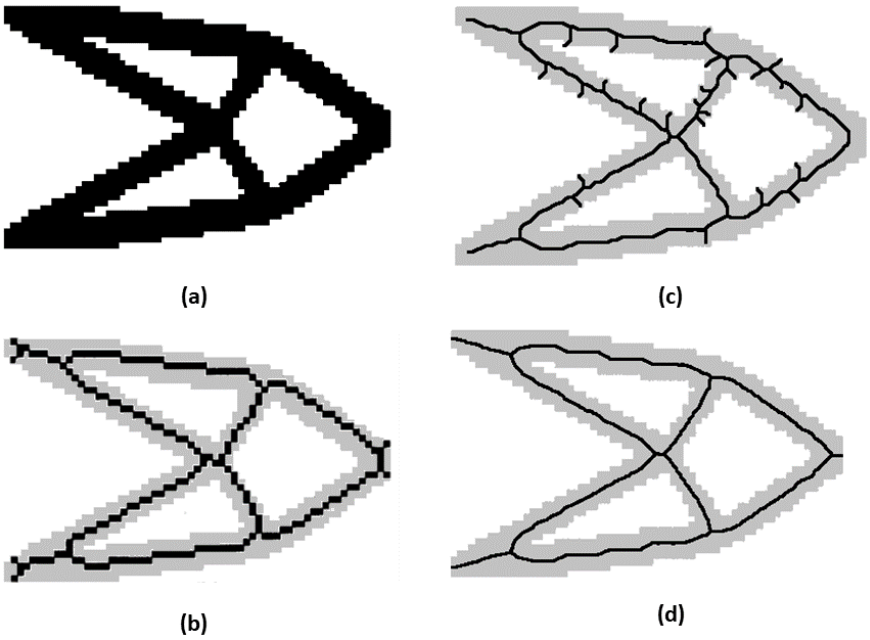


Figure 4.10 A comparison of different skeletonization results, note that skeletons have been dilated for illustration purpose.(a) Bremicker's cantilever beam results with homogenization method [6], (b) Bremicker's skeleton [6], (c) MATLAB bwmoprh skeleton with thinning, (d) Skeleton using the method presented in this work.

4.4.2 Comparison with Gedig

Gedig [7] presented an integrated framework for the design of steel beam assemblies. He has used the SIMP method to obtain his topology optimization results. Once again, topology optimization results were obtained as close as possible from the original work of Gedig [7], see fig. 4.11.a.

Notice in fig. 4.11.a that the result of the topology optimization has been smoothed to prevent the appearance of unwanted spurs. For every skeletonization method, the results are spur-free due to this pre-processing step, as seen in fig. 4.11.b, c and d, which is another method to resolve issue 2.

In addition, it can be observed that Gedig's method (fig. 4.11.b) can give results similar to those given by the MATLAB thinning algorithm fig. 4.11.c. The only visible difference between the results of this method and the results of our work is our work's ability to reach the boundary conditions completely, as shown in fig. 4.11.c. This small difference makes the integration with a FEM software much easier, as described with issue 3.

Gedig [7] developed a skeletonization method based on traditional thinning methods, but added a special weight to pixels near the boundary conditions. This has two advantages: first,

no spurs appear in random locations, which is a frequent problem with thinning algorithms, second, it allows spurs to grow only in the direction of the boundary conditions. While being effective at eliminating issue 3, it doesn't address the issue 4 for superposed trusses and issue 1 for threshold dependency.

In summary, Gedig's [7] solution is close to a functional skeletonization method, but its results are not easily integrated with FEM software due to the lack of fully using the boundary conditions. Furthermore, this solution cannot properly treat jagged edges and a smoothing of the image is required before the recognition step.

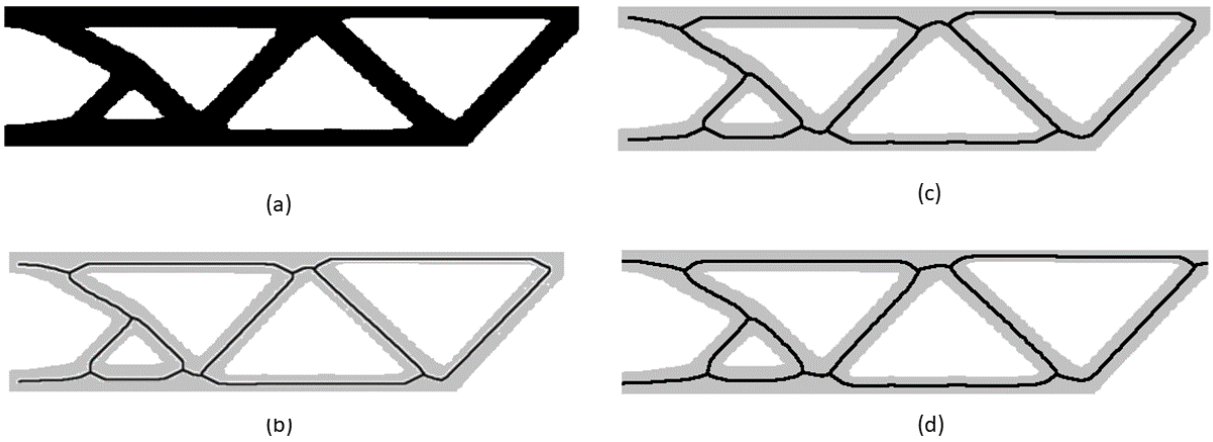


Figure 4.11 A comparison with Gedig's work, note that skeletons have been dilated for illustration purpose. (a) Gedig's beam results with SIMP method [7] (b) Gedig's skeleton [7] (c) MATLAB bwmorph skeleton with thinning (d) Skeleton using the method presented in this work

4.5 Case Study

As stated earlier, the long-term goal of our research team is to develop a support tool to be used in the design process of standard, recurring aircraft components such as ribs and spars of a wing box. This design support tool would be particularly useful since there is not yet such tool for hybrid structures. An example of an hybrid structure is the stiffened panels, the main construction block of most modern aircraft [58].

The following section will present an example of the results obtained for a topology optimization case study using a simply loaded airplane rib. The FEM is illustrated in fig. 4.12 and defined by the parameters in table 4.1.

The model is built with a parameterizable FEM generator for ribs written as a TCL/TK macro in HyperMesh [143]. This specific case study was chosen because its material dis-

Table 4.1 HyperMesh model geometry and optimization parameters

Parameters	Value
Airfoil Profile	NACA 2412
Load - Compression	500 lb
Load - Shear	125 lb
Volume Fraction	0.3
Length	65"
Height	10"
Constraints	x-y-z at bottom left y-z at bottom right x at top left
Minimum Member Size	1"

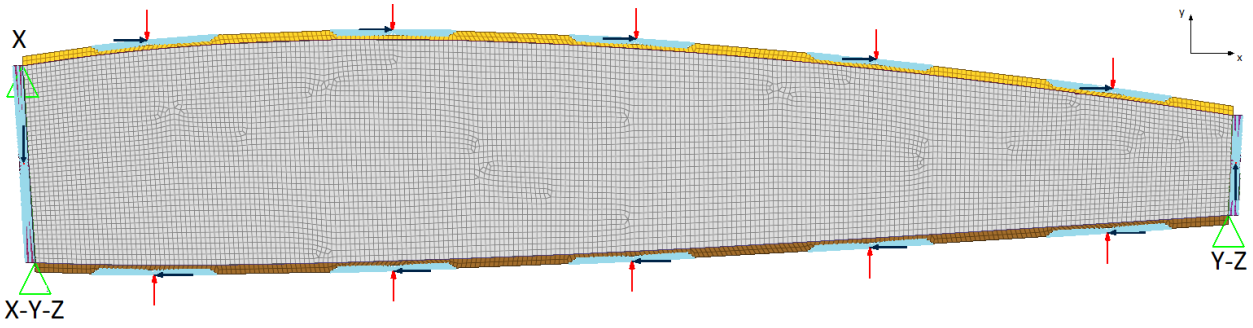


Figure 4.12 HyperMesh model of loaded rib.

tribution has important characteristics that expose some interesting aspects of the truss recognition. The design space is limited to the web only; the rest of the FEM is defined as non-designable and is used to distribute the load.

4.5.1 Optistruct Results

This section presents the raw results read with the HyperView software [143]. One of the commonly used parameters, that engineers need to explore more in depth, is the density. Fig. 4.13.a illustrates the density in the design space. Two different thresholds were used to show their impact on the truss recognition. Fig. 4.13.b illustrates the low threshold result and fig. 4.13.c shows the high threshold result. One can notice that the high threshold only keeps elements with a full density of 1.0, and the low threshold keeps everything except elements with density of 0.0.

An aspect of these results that is interesting, compared to the literature cases, is the quality of the results. They present multiple zones with intermediate values which makes the choice of the threshold critical. By allowing our tool to analyze different level of threshold, we expect to be able to find an appropriate topology. Also, the test case chose has two branches that share the same end point, which usually cause issue 4.

4.5.2 Truss Recognition Discussion

The discussion of the results of the recognition is divided into two parts: the first part deals with the low threshold results, and the second part deals with the high threshold results.

There are two images that are interesting to study in detail after the interpretation. The first one exhibits the connectivity results, as shown in fig. 4.14.a.

Upon examination of the connections, it appears that the trusses that could have been interpreted intuitively are all present. The skeletonization has yielded satisfactory results, even with the jagged edges of the material distribution and the superposed columns on the two last columns on the right side. The test case is a good example illustrating issue 4, that appears in real-life cases, and don't appear in the examples usually used in the literature. The boundary conditions of the rib design space are well considered for each recognized truss.

The second interesting image to study in more detail, which is the result of image segmentation, also provides us with further important information, as shown in Fig. 4.14.b. As explained in the methodology, image segmentation allows the recognition process to associate shape and contour information to the appropriate branches and nodes. For example, in this case we could find the trusses that are loaded in compression, decide of a column profile,

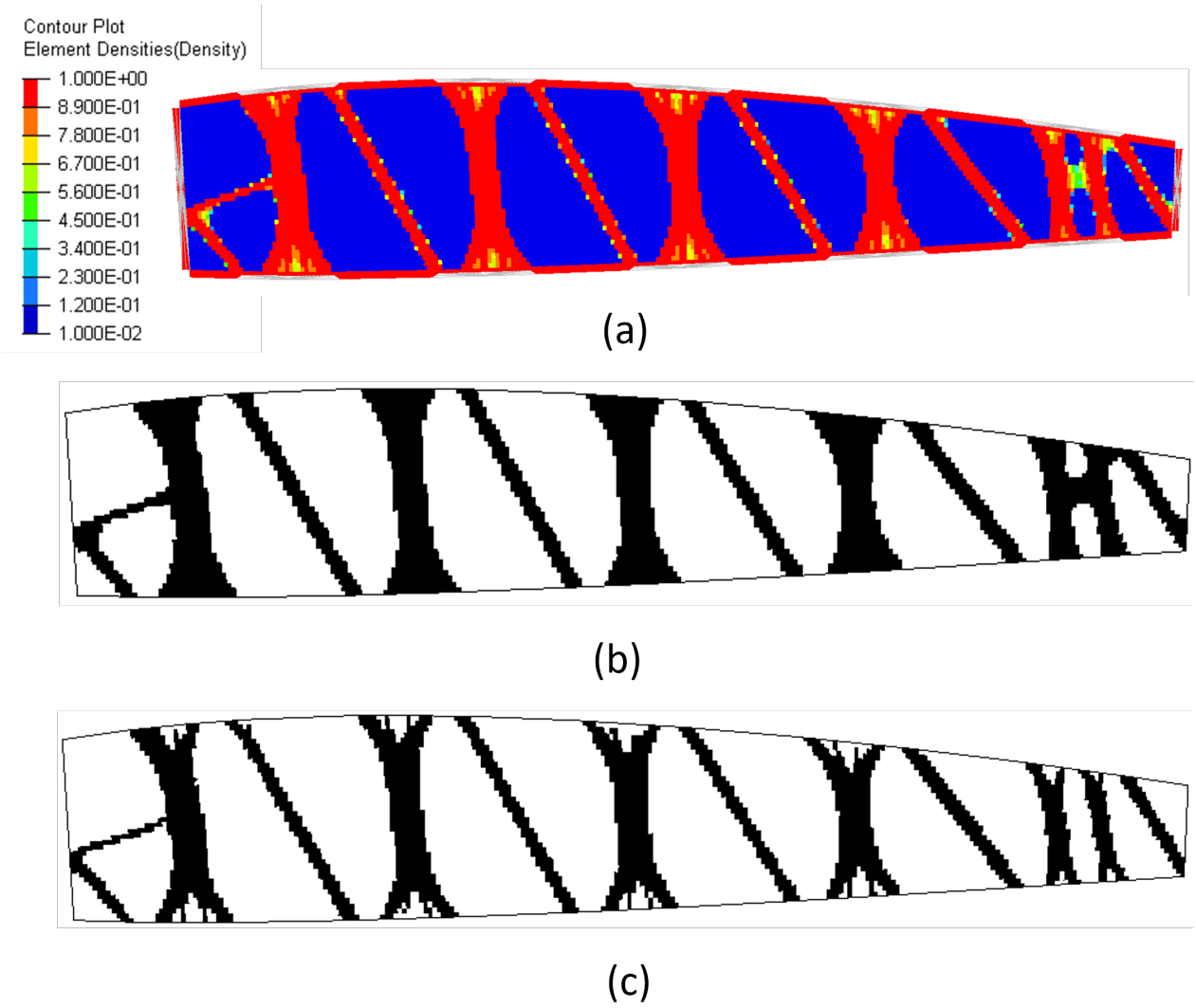


Figure 4.13 Binarization of ribs material distribution. (a) Optimal material distribution using Optistruct (b) Binarization of material distribution with a low threshold (All pixels with density value over 0.01) (c) Binarization of material distribution with a high threshold (All pixels with density value over 0.98)

and do a buckling analysis. Since this is high level abstraction, analytical solutions will easily work such as the margin of safety calculation methods used in the aeronautic industry.

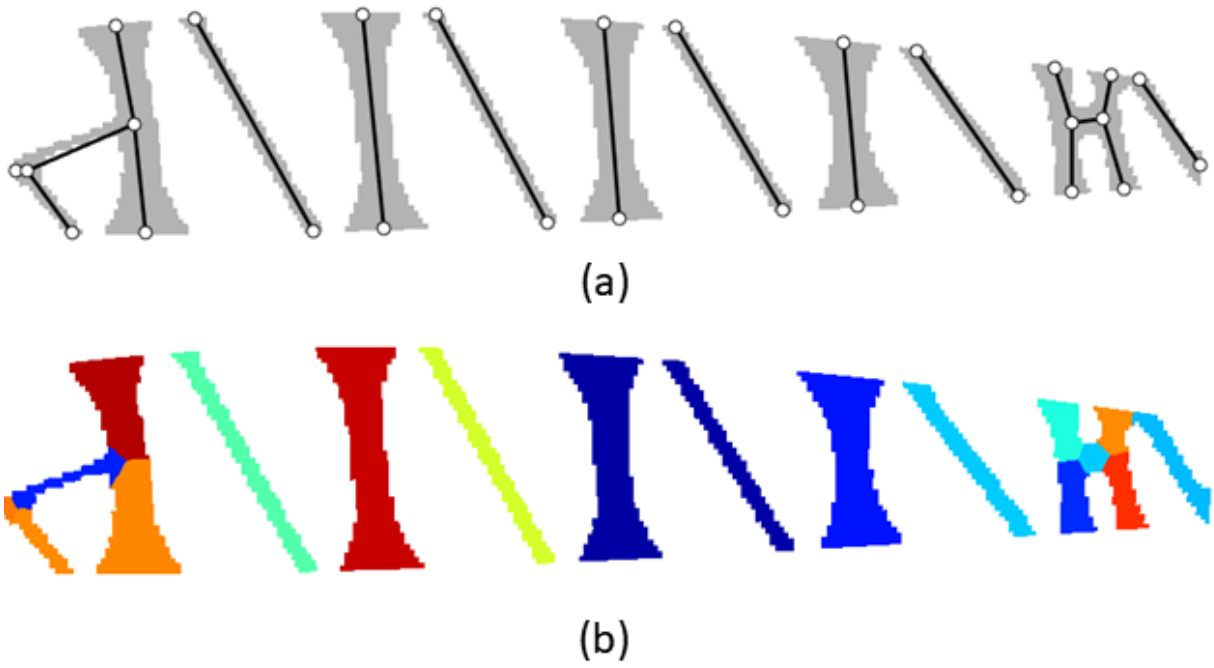


Figure 4.14 Rib's material distribution connectivity with low threshold. (a) Connectivity results (b) Image segmentation

The next results, presented in fig. 4.15, illustrate the truss recognition for the high threshold solution.

Since the threshold is higher, only features with a high density are recognized. The major differences can be seen on the ends of the "X" shaped sections. The extremities of the regions are split into multiple small trusses; the algorithm can recognize the nuances of the large sections. The information from the layout can be merged with the information from the low threshold segmentation to better know how the structure behaves. It becomes possible to associate the vertical stiffeners of the first step with the "X" shape of the second step, while recognizing it as either a single entity or not. The association is useful for feature analysis and comparison since it makes it possible for the design engineer to associate features with optimization and recognition parameters.

Just like any optimization result, it is not recommended to use only one single result since an optimization is about exploring a design space in an intelligent way. As such, one result alone does not answer questions like, why are some trusses larger on the sides and smaller in the middle? An engineer could say that this is because an "X" is more efficient for the shear,

however, the algorithm does not know this information and might interpret it as a simple vertical bar. Therefore, the work presented in this paper puts emphasis on the interesting features of the OT that allow a more complete interpretation by a computer.

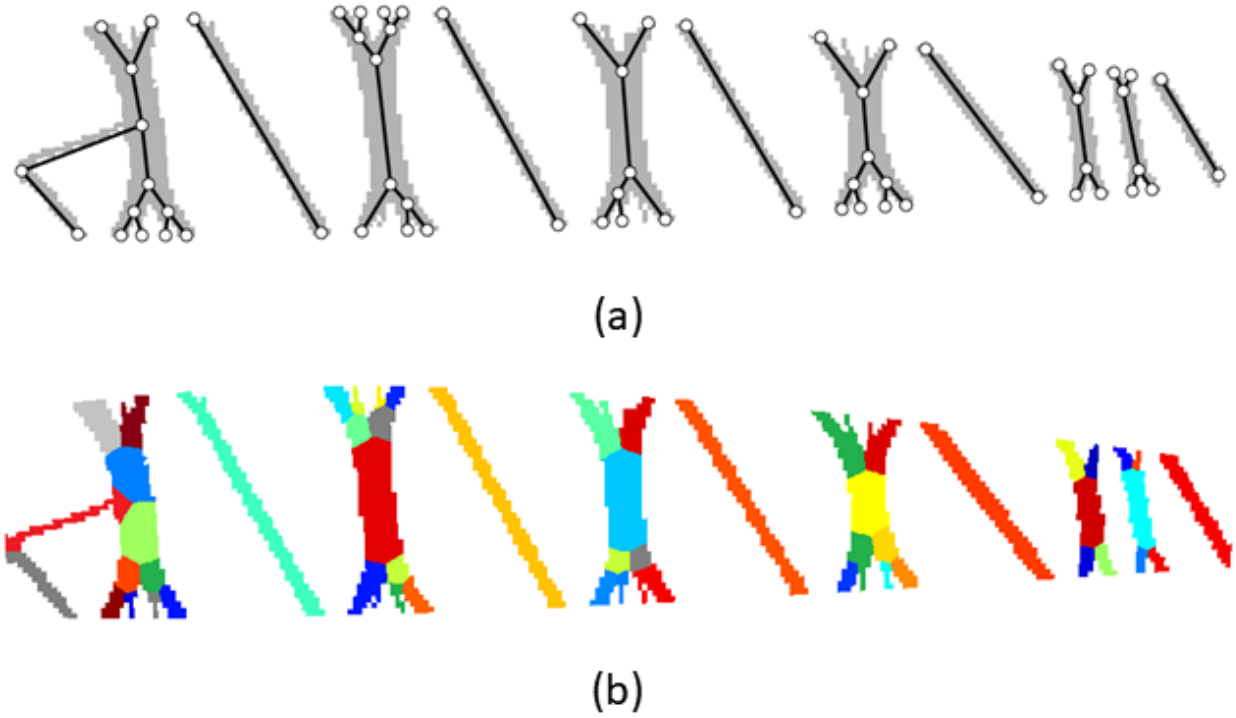


Figure 4.15 Rib's material distribution connectivity with high threshold. (a) Connectivity results. (b) Image segmentation.

Comparing the two results obtained through different density thresholds, it is clear that two different topologies are proposed. While both solutions might be local minima, they could also propose two infeasible solutions. The next step of this project is destined to topology analysis and synthesis where the feasibility and quality of the proposed structures will be evaluated.

4.6 Conclusion

This paper presented a truss recognition algorithm that recognizes the different skeletal components of low volume fraction optimized topology obtained with topology optimization using a novel computer vision skeletonization method.

The novel skeletonization method presented in this work removes the limitations of other skeletonization methods in truss recognition by focusing specifically on the optimized topology. It solves four limitations seen in the skeleton-based method; the high dependence on the quality of material distribution, the issues encountered due to jagged edges, the maintenance of boundary conditions and the independent recognition of superimposed trusses.

This makes the skeleton image usable in a truss recognition algorithm that is compatible with any topology optimization results presented in a binary image. Also, a comparison with the literature shows that this method gives excellent results with classic problems such as the cantilever beam.

With the proper binary image skeleton, it becomes possible to recognize the trusses of the skeletal structure appropriately. As shown with the case study of the airplane wing box rib, it works very well with a real-world scenario.

Finally, with the recognized branches in the image and the appropriate image skeleton, it is possible to get a stabilized skeletal structure and associate different information from the FEM with the extracted structure. The recognized structure may then be further used in a design support tool. Furthermore, the segmentation allows the different branches data to be enhanced by multiple OTs with different parameters. This is an important step for a more complete design support tool for topology optimization interpretation that incorporates the industrial knowledge and axiomatic design.

The work presented in this paper was limited to low volume fraction problems which can be interpreted as truss-like structures. High volume fraction OT shouldn't be interpreted with a skeletal structure, and will be the subject of future work. Additionally, another step that is required is a feature analysis module which will define the role of each recognized component.

CHAPTER 5 Article 2: On Generating Stiffening Layouts with Density-Based Topology Optimization Considering Buckling

Jean-François Gamache[a], Aurelian Vadean[a], Nicolas Dodane[b], and Sofiane Achiche[a]

[a]Polytechnique Montreal, 2900 Edouard Montpetit Blvd, Montreal, Québec, Canada
[b]Stelia Aéronautique Canada, Research & Technology, 12000 rue Henry Giffard, Mirabel, Québec, Canada.

Submitted to *CEAS Aeronautical Journal*, on May 11th, 2020.
Revised and Resubmitted on June 16th, 2021.

Abstract

This work includes a complete optimization, design, sizing and validation application of density-based topology optimization for a single stiffened panel from the upper skin of a commercial aircraft wing. In this work, topology optimization is carried with Optistruct from Altair. The initial values of the density variables are shown to have the biggest impact on the optimized material distribution. This effect is used in a random restart approach to explore multiple local minima, and thus to find different material distributions. Different material distribution obtained with topology optimization have shown the same buckling resistance within the implicit model used for optimization. However, the stiffened panel models created from the different material distributions show very different strength when they are sized with a subsequent optimization and validated using quasi-static non-linear analysis. Besides, the optimization results are almost all simple orthogrid solutions. Finding these layouts with topology optimization has proven to be difficult and highlights the fact that the technology is not mature for the design of new layouts for stiffened panels.

5.1 Introduction

Stiffened panels are the main structural components of large vehicles, such as aircraft and ships, due to their high strength and relatively low weight [29]. A low weight is very important for these components as to reduce the consumption of fuel as well as to increase the overall efficiency of airplanes [214]. There has been a significant effort in the aircraft industry to reduce the weight of the structures, with advances at all design stages but especially at the conceptual and preliminary phases. Wing box design has an inherent multidisciplinary

nature [215]. Recent literature often ideally include the modeling of not only structure but also aerodynamics, loads, flutter, etc. directly in the conceptual and preliminary design tools [216, 217]. Still, current architecture has not been easy to challenge in terms of reducing its weight [196].

Stiffened panels have long been used in the aviation industry as their properties and failure modes are well understood and described in widely used handbooks [26, 58]. The stability of these thin components is one of the main concerns of design for stiffened panels, as any imperfection can initiate the buckling of the assembly [26, 58]. The handbook design method for stiffened panel is based on experimental data, analytical equations and the experience of engineers. This somewhat limits the design freedom when trying to improve the layout of stiffened panels, as almost all experimental data has been developed for the orthogrid configuration [26, 58]. The orthogrid layout is an arrangement of stiffeners built orthogonally, which are straightforward to design and analyze. They also have a great strength with regard to buckling, post-buckling and fatigue [26, 58].

Further reducing the weight of stiffened panels by improving the stiffening layout is proving to be challenging [82,84,88]. Advances in manufacturing methods and numerical tools provide engineers with new capabilities to achieve this weight reduction as there is now the possibility to manufacture and analyze much more complicated patterns [82].

5.1.1 Aerospace Applications of Topology Optimization

Topology optimization (TO) is a powerful structural optimization tool that is capable of generating innovative structural components by evolving a material distribution to comply with design requirements [2]. TO seeks an optimized material distribution within a user-defined design space while considering loads and boundary conditions [2]. The design freedom of TO is larger than the more common parametric optimization. However, this comes at the cost of an implicit generation of the structure which can lead to solutions which are complex to design and manufacture.

Topology optimization has been used in aircraft structure design for different use cases, including stiffened panel assemblies [13, 218]. TO is generally used early in the design process to help designers create new concepts to reduce the weight of structural components [196].

There is a constant interest in the optimization of aircraft wing boxes, as they are complex structures with many loading conditions. Two approaches are applied to topology optimization of wing boxes, the global and local approach. The global approach being an optimization with the whole structure defined as the design space and the local approach focuses on a sin-

gle component. Regarding the global approach, the results have usually been that the layouts proposed were, at best, just as efficient as the traditional layouts [39, 219]. The best achieved weight savings were obtained with the local approach on hinges, ribs, pylons, etc., rather than complete assembly optimization [13, 38, 219].

TO publications regarding aircraft stiffened panels generally do not consider buckling during the TO phase [13]. Buckling is sometimes verified in a subsequent interpretation and design step [13]. It is acknowledged in the literature that considering buckling during TO should lead to better stiffening layout, as the layout of the stiffeners has a significant impact on buckling strength [13, 155, 220].

5.1.2 Topology Optimization

There are different types of algorithms and formulations for structural TO. The most prevalent method is Solid Isotropic Material with Penalization (SIMP) which is used in most commercial finite-element model (FEM) software such as Optistruct from Altair [13, 78]. Optistruct is the solver used in this work [78]. Using the SIMP method, one can avoid the common problem associated with early TO algorithms that would require discrete "full" and "void" variables. SIMP associates a continuous density value to each finite element of the design space. The continuous density variable allows for efficient gradient-based solvers to be used. To limit the effect of intermediate values which have no physical significance, the intermediate values are penalized as described in equation 5.1 [2].

$$E_x = \rho^P E_0 \qquad \rho\epsilon[0,1] \tag{5.1}$$

where E_0 is the material young modulus, ρ the element density, P the SIMP penalization factor and E the young modulus of the element [2]. The factor P penalizes intermediate density values and helps the optimization converge toward clean full/void material distributions [2].

The most common TO formulation focuses on minimizing compliance by evolving the material distribution, given a certain volume fraction constraint [141]. Compliance is defined as the inverse of stiffness, generally measured as the total strain energy [2].

Manufacturing constraints for TO have seen a lot of development. Useful examples are the minimum and maximum member size, symmetry, extrusion and casting constraints, etc. [209]. These constraints allow some control of the behavior of the TO. Still, their impact is not significant for stiffened panel TO as shown in the section 5.2.2.

For the design of aircraft structures, buckling is usually evaluated using semi-empirical formulas found in handbooks [26, 58]. These formulas can prove very useful as the different

buckling modes of each sub-components can be evaluated individually, thus ensuring margins of safety for each component, and each mode. Note that imperfections can modify the behavior of each individual mode, which makes it important to understand the strength of each component. However, the handbook methods are only applicable for the orthogrid layout. As TO is a FEM-based optimization tool, buckling is measured using this same FEM. To measure the buckling critical loads of a given structure with FEM, it is possible to compute the eigenvalues of the stiffness matrix [63].

The first computation step, as for any FEM, is to compute the equilibrium equation for displacement [63]:

$$\mathbf{K}\mathbf{u}_0 = \mathbf{P} \tag{5.2}$$

where $\mathbf{K}$ is the stiffness matrix, $\mathbf{u_0}$ the equilibrium displacement vector and $\mathbf{P}$ the load vector.

From the static solution, we then solve a generalized eigenvalue problem [63]:

$$(\mathbf{K} + \lambda\mathbf{K}_\sigma(\mathbf{u_0}))\varphi = 0 \qquad \varphi \neq 0 \tag{5.3}$$

where $\mathbf{K}_\sigma(\mathbf{u_0})$ is the stress stiffness matrix and the eigenpairs (λ_j, φ_j) are respectively the buckling load factors and its associated nodal displacement of the j^{th} buckling mode [63].

The first buckling mode is of interest, as it defines the critical mode for which it is possible to define the critical load:

$$\mathbf{P}_{cr} = \lambda_1\mathbf{P} \tag{5.4}$$

where $\mathbf{P}_{cr}$ is the magnitude of the load at which the equilibrium bifurcation occurs and $\mathbf{P}$ the external force [63].

The occurrence of multiple buckling modes is a challenge of FEM-based buckling optimization [57]. There are global and local panel buckling modes; stiffeners and skin modes and even combined skin-stiffener modes [57]. The complexity of buckling modeling and optimization for stiffened panels comes from coupling effects of the respective geometries of each component interacting with one another. The orthogrid layout has shown an important property: the coupling is minimized when stiffeners are orthogonal. More importantly, when the orthogrid layout is not used, there are notable in-plane and of out-of-plane coupling effects that can arise to make the optimization even more difficult. Finally, mode shifting can also exacerbate the challenges of buckling optimization by creating low to medium densities as spurs or disconnected areas [57].

These challenges are still present in TO when introduction buckling eigenvalue constraints. There has been some recent work on improving buckling eigenvalue constraints to the density-

based TO [191]. However, most work has focused on the buckling TO of truss or truss-like structures, for which the challenges are to capture both local and global modes [191].

Using buckling constraint in TO for stiffener layout has been tried a few times. The work of Chin and Kennedy (2016) has incorporated a constraint on the first 10 buckling eigenvalues with a mesh of the order of 10^5 design variables [155]. Dunning et al. (2015) used a level-set TO method to incorporate a full-wing optimization, with buckling constraints on the skins [221]. However, both do not discuss any weight savings and did not include a validation of the proposed solutions.

Buckling optimization with a FEM is already considered challenging to use for stiffened panels, due to the coupling between skin, stiffeners and skin-stiffener buckling modes. TO helps reduce this coupling but new challenges associated with TO with a buckling constraint, mainly due to the important mode shifting during optimization and the impact of optimization parameters on the final material distribution [221].

5.1.3 This Work

Some limitations have now been identified in the literature for TO of aircraft stiffened panels. One can find multiple publications for which aircraft structure application of TO, but no verification is done on the results to assess their quality. As such, this work seeks to understand if density-based TO is capable of actually improving, or at least find results with a reasonable quality for stiffened panel design when a buckling constraint is included. We also discuss the effect of optimization parameters to help find the feasible results.

We go a step further than most studies and assess the effect of adding the buckling constraint to the TO. From there, we verify the quality of the results by interpreting the results and sizing the new layouts and validating their stability with a non-linear quasi-static analysis. This is not a multi-step optimization, the topology and sizing optimizations are done sequentially.

Preliminary work by both our research team and our industrial partners has been done to study TO for a structural wing-box. It first focused on TO of components such as the ribs, spars and skin with complex load conditions. It was found that current models are too complex to allow a good understanding of the behavior of TO with a buckling constraint, which does not confer confidence in the material distribution. This complexity was observed as a sensitive, erratic behavior, i.e., small modifications to the optimization objective, constraints or parameters yielded very different results with no obvious reasons. Erratic behavior through small variations are often considered design complexity in design science [47,222]. To enhance this confidence in the optimization process, only a section of a certified aircraft wing box is

used as a baseline. The detailed model is based on a wing-box general finite-element model provided by our industrial partners. Due to publication limitations, we use similar loads and dimensions, but not the actual ones.

The scope is limited to a wing upper skin panel where the buckling margins are identified as critical. Multiple runs have been done manually to explore the impact of parameters on TO results, more details on this can be found in section 5.2.2.

The optimized material distributions are used in a subsequent interpretation and size optimization. This step allows the different stiffened panels to be sized properly, ensuring enough strength with respect to buckling and stress. The sized stiffened panels are then analyzed with a FEM non-linear quasi-static analysis to validate that their critical stability is higher than the applied "ultimate load." The ultimate load being a conservative estimation of the worst possible case associated with a specific load case such as an up gust or catastrophic landing. This FEM quasi-static model was validated with a non-FEM based handbook empirical method, as described in previous work [223]. This path of generating new concepts, interpreting and sizing, then validating is carried out multiple times (see fig. 5.1). Each design and optimization process allow for a better assessment and understanding of the impact of TO parameters on the strength of the layout of stiffened panels. Once the optimization parameters are well understood, we run 500 TO of the panel with different starting points to explore the local minima of the design space.

5.1.4 Case Study

The studied panel is a portion of the upper plank of the wing of an existing commercial airplane. This section of the wing is chosen due to its high compressive stress that leads to a critical buckling margin, which makes it an interesting case study.

The stiffened panel is made up of a skin web and “J” stiffeners, which are built as one component. The geometry is defined with the same modeling hypothesis made for the margin of safety calculations, as used in the industry or as defined in [26, 58]. First, the panel is considered flat, in the X-Y plane. Secondly, only the ribs provide out-of-plane support (in the Z direction). Finally, we consider only the effect of in-plane loads and make the assumption that bending effect is negligible for buckling evaluation. The stiffened panels and its subcomponents are illustrated in fig. 5.2.

Aircraft face multiple complex loading conditions; from a crash landing to a wind gust, everything needs to be well-thought-out. There are more than a hundred loading conditions that need to be considered for validation. To simplify this study, only one load case is selected

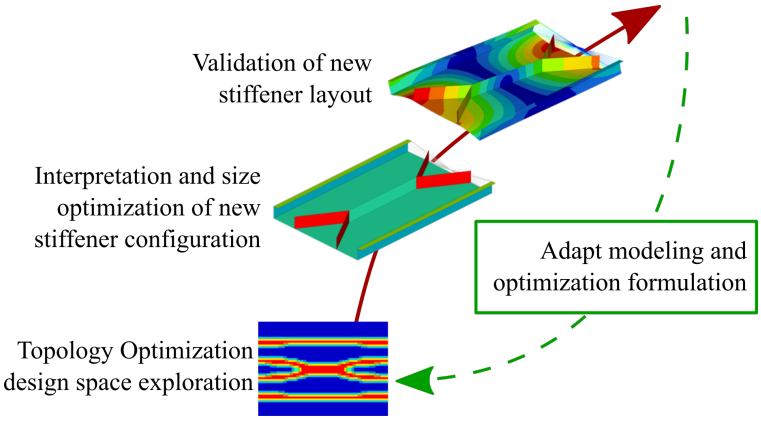


Figure 5.1 Research method used in this research project. Including validation of stiffened panels has shown that topology optimization need to consider buckling.

for its critical buckling margin, that is the up-gust load case that causes a high compressive load on the upper skin. Although it is possible to include multiple load cases in SIMP, demonstrating this capability for stiffened panels considering buckling is out of the scope of this current study. Further research would be required to test such capabilities.

The boundary conditions are modeled as clamped on the loaded side ($U_z = 0, R_y = 0$) to simulate the stiffness of ribs, see 5.3a. The main compressive force is applied through a rigid ($RBE2$) element to ensure a constant displacement in the X axis (CPU_X). A displacement constraint is set on the opposite side ($U_X = 0$).

Local load values are extracted from a linear static analysis of the global wing FEM, using the "endloads" of selected elements. This is a common practice for the margin of safety calculations in the aeronautic industry [26]. his load extraction uses the hypothesis used in semi-empirical calculations that the panels behave in the wing box similarly to the panels

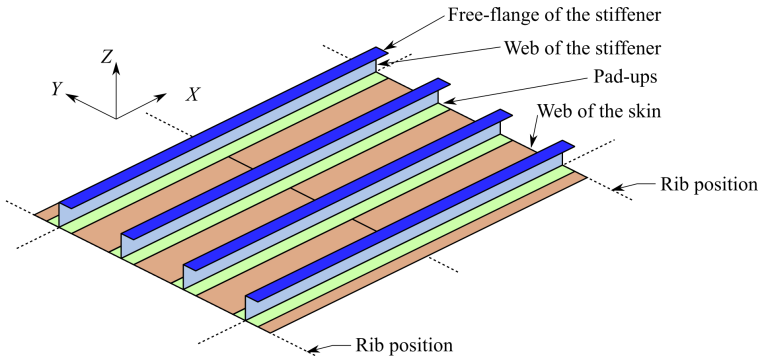


Figure 5.2 Sub-Components of the Stiffened Panel

used in the tests done by NACA [58]. A safety factor of 1.5 is considered on the applied loads. This safety factors value is used in the remainders of the paper. The load cases are locally modeled as a combination of three loads: span-wise compression, chord-wise compression and shear. The loads are applied as shown in fig. 5.3b, and their value can be found in the table 5.4. The main compressive force is applied on the independent node of the rigid element and the other loads are applied directly to the skin.

The material used for this case study is aluminum 7075 (see fig. 5.2), a widely used material for aeronautics structures, for which non-linear properties are considered [59].

Two different sizing are used to define the baseline, from different optimization methods. The first is the one obtained with handbook design optimization. Multiple collapse modes were used as constraints: skin buckling, Euler, crippling and post-buckling Euler-Johnson. Furthermore, all plasticity effects of cladding were considered. This method allows for the separation of the stable skin buckling and unstable global buckling, thus letting the skin buckle earlier to save weight.

The second sizing is obtained with only the FEM with simple weight optimization considering the eigenvalues and stress. A summary can be found in the table 5.1. Doing optimization with FEM doesn't allow for a specific control for each component, as such the buckling constraint can only be applied globally. This results in the difference in weight between the handbook and FEM sizing, as the handbook sizing allows for earlier skin buckling. Depending on the value of the load, allowing skin to buckle early can save up to 20% of weight depending on loads and locations [26], but the difference is relatively small in our specific case study.

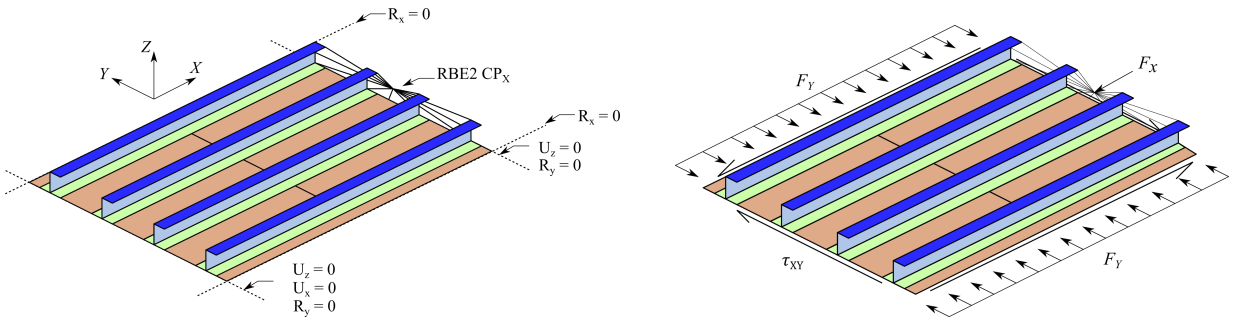
The dimensions of the panels are described in fig. 5.4 and table 5.3. The weight and strength found in the table 5.5. These properties will be used to validate if the new layouts proposed by TO are at least equivalent to the baseline in terms of strength and weight.

5.2 Setting Up Topology Optimization

The goal of TO for stiffened panel is to find an optimal material distribution that shows an optimal placement of the stiffeners. For our application, it is possible to remove any "void"

Table 5.1 Sizing optimization formulation

	Parameter	**Function**
Objective	Weight [lb.]	Minimize
Constraint	Buckling [-]	$\lambda_1 \geq 1.0$
Constraint	Stress [ksi]	$\sigma_{VM} \leq F_{cy}$



(a) (b)

Figure 5.3 Boundary and loading conditions of the case study. U_x,U_y,U_z are the displacement conditions and R_x,R_y,R_z the rotation conditions. F_y is the chord-wise compression, F_x is the span-wise compression, τ_{xy} Shear.

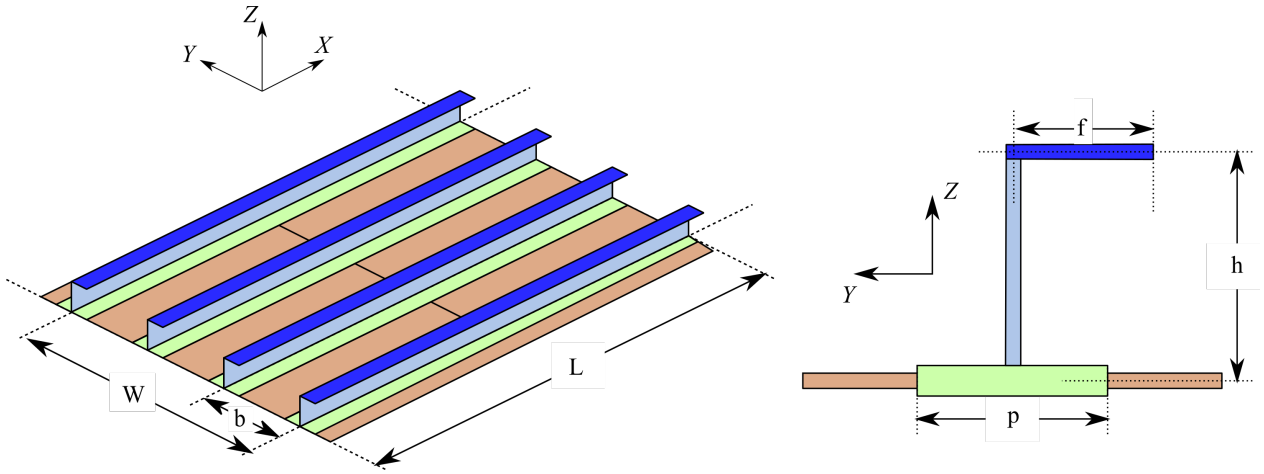


Figure 5.4 Baseline Dimensions. Where is W the panel width, b the bay width, L the panel length, p the pad-up width, h the stiffener height, f the free-flange width.

Table 5.2 Aluminum 7075 properties [59]

Property	**Value**
Young's Modulus (E_0) [ksi]	10,700
Poisson's ratio (ν) [–]	0.33
Yield limit (F_{cy}) [ksi]	68
Material Density $\left[\frac{lb.}{in^3}\right]$	0.1
Ramberg-Osgood factor (n) [-]	13

Table 5.3 Baseline dimensions [in.] from different optimization methods

Dimensions	**Handbook Sizing**	**Baseline Sizing**
L	20	20
W	12.5	12.5
b	4.2	4.2
f	0.9	0.9
h	1.45	1.45
p	1.50	1.50
t_{skin}	0.09	0.08
t_{pad-up}	0.05	0.12
t_{web}	0.08	0.06
$t_{free-flange}$	0.09	0.07

Table 5.4 Baseline load values, with integrated safety factors.

Load type	**Applied Load**
Axial Compression [lbf]	120,000
Transverse Compression [lbf]	9,000
Shear [lbf/in]	60

Table 5.5 Baseline properties with a 4-stiffener orthogrid layout. Two sizing optimization were completed, with the handbook sizing allowing for a controlled skin buckling.

Property	**Handbook Sizing**	**FEM Sizing**
Weight [lb.]	5.2	5.3
Compliance [lb.in.]	5100	5000
Maximum Stress [ksi]	46	45
Linear Buckling [λ_1]	0.7	1.0

elements by defining a base thickness in the design space. This avoids the problem where "void" elements have virtual buckling modes [224]. As such, only the stiffeners are part of the design space and are modeled as variables of density in a thick sandbox (fig. 5.5). This puts forward one major limitation of the density-based model as it will only be able to model the buckling of the skin and miss potential buckling of the stiffeners. For TO, the loads and boundary conditions are modeled similarly to the baseline on the design space, see fig. 5.6. Again, the base thickness and the design space in set in the X-Y plane, and the stiffeners are models in the extruded design space in the Z direction.

5.2.1 The Reference Material Distribution

Generally in topology optimization applications compliance is used as the optimization objective. Compliance is defined as the inverse of rigidity, generally measured as the strain energy. It is particularly useful as it is not dependent on the scale of the loads, which makes the whole design space convex. However, buckling evaluation is dependent of the value of the load. This requires a test to measure the effect of the loads on buckling evaluated using the density-based model. The results of this test are presented here, as we define a reference material distribution. This reference is a hand-built model that uses the same implicit modeling as SIMP, with the objective of imitating the behavior of the baseline explicit model. With the reference material distribution, we have an idea of the minimum expected properties for the implicit density-based model.

In the reference model, the stiffeners have been modeled as thin and dense material distributions, at the same positions as in the baseline (fig. 5.7). A thickness optimization of this panel has allowed the model to replicate the buckling strength of the baseline, see the table 5.6.

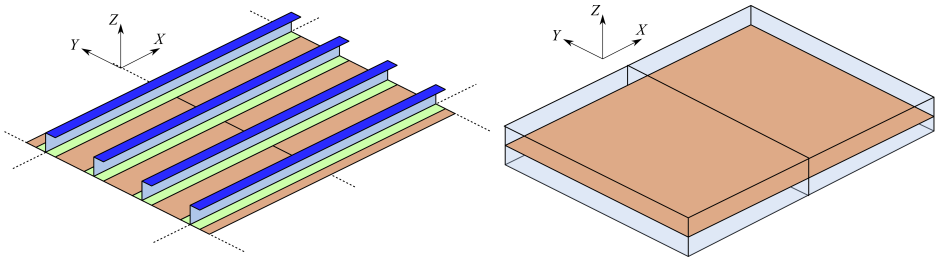


Figure 5.5 Stiffened panel topology design space. (a) The baseline with four stiffeners. (b) The topology optimization design space defined from the existing design. The illustration includes the skin and the bounding box of the design space. The stiffeners can be placed anywhere in this design space.

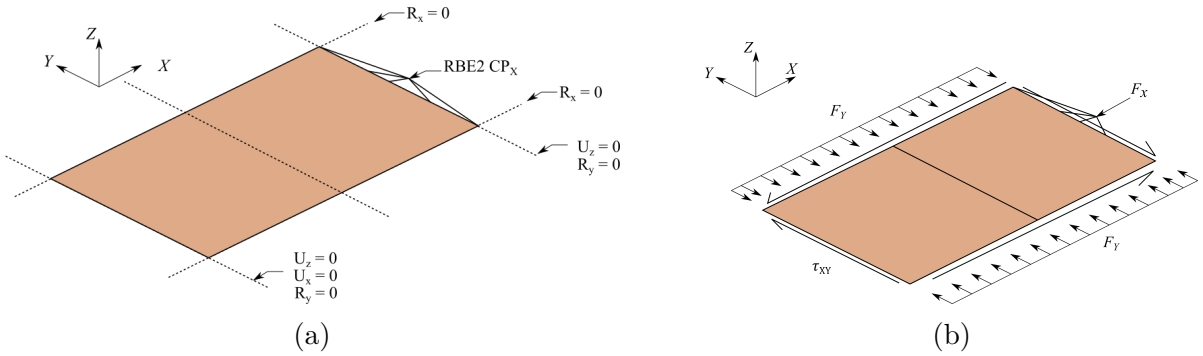


Figure 5.6 Boundary and loading conditions of the design space for topology optimization of the panel. (a) Boundary conditions on the design space. (b) Loading conditions on the design space. Where F_y is chord-wise compression, F_x is span-wise compression, τ_{xy} is shear, U_x,U_y,U_z are displacement conditions, R_x,R_y,R_z are rotation conditions

In this model, the plane is in the X-Y plane, and the design space is an extrusion in the Z direction. It is important to note that this modeling technique is implicit; thus it is far from a perfect representation of the behavior of the stiffened panel. However, it is required to give full design freedom to the optimization process. As such, for the same buckling strength, almost twice as much mass is required, taking the weight from 5.3 lb. to 9.9 lb. Of course, this has an impact on the measured stress (which is cut by about 50%) and compliance which also decreases 50%. As expected, there is a linear relationship between weight, stress and compliance for a given topology. The added weight reduces significantly the stress captured in the density-based model which shows that for a given topology the stress in the density-based model is not representative of the stress obtained with an explicit model.

From the reference model, the optimization constraints are defined to achieve similar properties between the reference material distribution and the baseline, see the table 5.6. The TO constraints are not set directly to be the same as the reference material distribution in to allow the optimization some freedom during optimization.

5.2.2 Parameter and Formulation Analysis

Multiple test runs of TO were carried out to study the impact of the optimization parameters on the material distributions. Optimization parameters include filters, solver parameters, objectives and constraints. The post-processing of the results showed significant but unpredictable impact for most optimization parameters on the material distributions. Changing the optimization parameters mainly influences the behavior of the optimization in the first few iterations and thus the final material distribution.

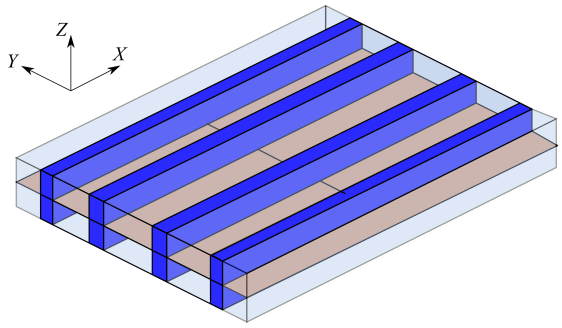


Figure 5.7 Reference material distribution. Implicit stiffener generation (in blue) in the design space (in gray).

Table 5.6 Comparison of baseline and reference material distribution, which are used to define TO constraints

Properties	**Baseline**	**Reference Material Dist.**	**TO constraints**
Max Stress [ksi]	45	29	30
Linear Buckling [λ_1]	1.0	1.0	1.0
Weight [lb.]	5.3	9.9	10.0
Compliance [lb.in.]	5000	3100	N/A

An interesting aspect that comes out of this parameter study is that the effect of the initial value of the density variables is dominant in respect to other parameters. Therefore, changing only the initial values of the density variables leads to several feasible material distributions. This shows a lack of robustness of SIMP in this application to stiffened panels, and there is, for now, no clear strategy to improve the robustness for SIMP with buckling constraints. Still, this lack of robustness is leveraged in this work to explore different minima of TO without changing other optimization parameters or constraints. This allows for more design exploration and generation of more solutions that could be used in the next design phases, as more design constraints are introduced.

For a correct optimization setting, it is still necessary to set some optimization parameters. The decisions related to some important parameters are discussed below.

1. Type of elements
2. Manufacturing filters
3. Mesh Size
4. Symmetry
5. Secondary design variable
6. Stress constraints
7. Other parameters

According to the literature, it is usually preferred to use the $\mathcal{Q}_4$ elements instead of $\mathcal{Q}_8$ elements, as it allows more design freedom while maintaining relatively low computation time [37]. However, we found that with linear buckling, $\mathcal{Q}_8$ usually finds more discrete void/full solutions in less iterations. A recent paper goes in the same direction and proposes a $\mathcal{Q}_6$ element that is a good compromise between speed and accuracy [191]. Since those elements are not available in Optistruct, $\mathcal{Q}_8$ elements are used in this work.

The only useful manufacturing filters for our 2D TO are the minimum and maximum member size. Other manufacturing filters, such as extrusion or casting constraints, are not applicable for 2D TO. As recommended by Altair, the minimum member size should be at least three times the mesh size [78]. Using the minimum member size also removes checkerboard artifacts. Maximum member size is not used. From our experiences, it over-constrains the problem and creates optimization artifacts.

The mesh size has a significant impact on TO. A mesh size too coarse does not allow the optimization to converge toward light solutions. A mesh too fine (with similar member size

filter) yields non-manufacturable material distributions. From experience, for stiffener layout optimization, a mesh size of approximately the thickness of stiffeners yields clean full/void material distributions. From the baseline, the stiffeners are expected to have a thickness of about 0.6 inch. Consequently, a mesh size of 0.2 inch is used.

Using a symmetry constraint along the x axis helps the optimization converge faster, as the number of design variables is significantly reduced.

The thickness of the design space is defined as a secondary design variable. This has generally helped the optimization converge toward clean a void/full material distribution.

From the *reference material distribution*, it was noted that the stress is not properly captured with the 2D shell elements. However, it was found that using stress constraints helps the optimization converge toward clean void/full solutions.

The size of the base thickness has an important impact on both mass and shear resistance. This parameter would ideally be part of the optimization.

Other parameters have no significant or random effects.

5.2.3 Randomized Initial Values Topology Optimization

To demonstrate the effect of the initial values on TO, the parameters presented in the table 5.7 are used, as discussed in subsection 5.2.2.

Preliminary results shown in fig. 5.8 show the effect of combining random initial values on different TO material distributions. As expected, when observing only compliance for the simple test case, the result is a uniformly thick plate (fig. 5.8.A and 5.8.B). To the best of our knowledge, this is after all the stiffest solution possible for a simple panel. However, this result is not optimal for buckling resistance and does not have the minimum mass we are looking for either. Adding only the buckling constraint, the optimization finds only a non-feasible optimum (fig. 5.8.C). By introducing random initial values with the buckling constraint, the optimization becomes able to converge toward feasible results (fig. 5.8.D). Still, the material distribution is highly dependent on the initial density values.

To study the effect of randomized initial values, 500 optimizations have been completed. A sample of some material distributions are shown in fig. 5.9. The effect of the random initial values is significant; it allows the TO with buckling to converge toward different solutions. Still, this shows that it is not possible to achieve global optimum with this technique. From a design perspective, the availability of multiple material distribution is favorable, as it proposes different solutions that may trigger new creative ideas and more easily adapt to the integration of other systems.

Table 5.7 Optimization parameters for random initial value TO

Optimization formulation	**Objective**	Minimize Compliance
	Buckling	$\lambda_1 \geq 1.0$
	Weight [lb.]	$w \leq 10$
	Stress [ksi]	$\sigma_{VM} \leq 30$
Design variables	**Density**	for each finite element of the design space
	Thickness	for the design space (1 continuous variable)
Optimization parameters	**Symmetry**	2-plane symmetry around the middle point
	Minimum member size	3 times the size of the smaller element [0.60 in]
	Base thickness	0.075 in

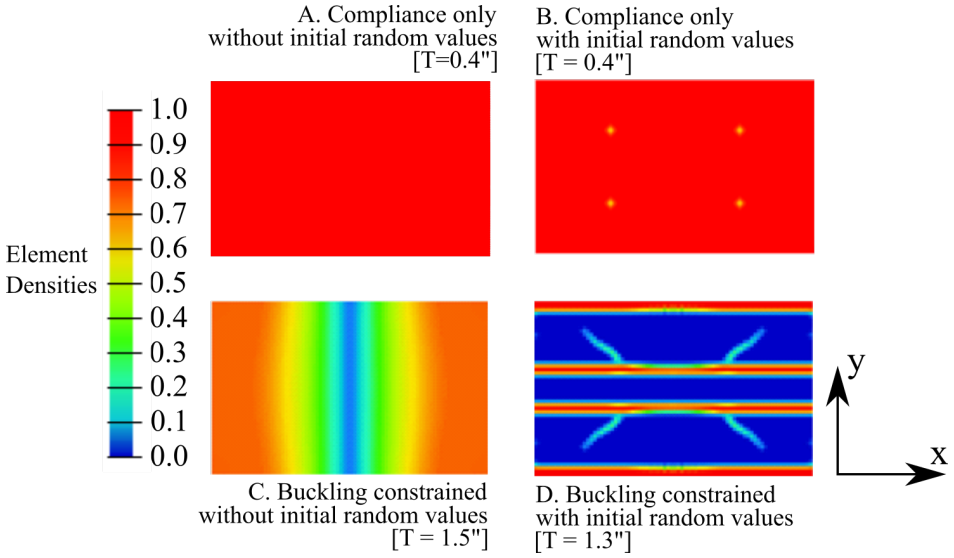


Figure 5.8 Material distributions of compliance only optimization (a) modeling compared to the optimization with an additional buckling constraint (c). The results with random initial density values with compliance only (b) and added buckling (d). Where T is the design space thickness.

Another interesting aspect of density-based buckling TO is the apparition of "spurs." Finding the right penalization factor of SIMP is delicate with buckling, as too high a penalization doesn't allow convergence but too low a penalization will have a significant number of intermediate density in all of the design space. This intermediate and distributed material greatly increase the buckling resistance in the implicit density-based modeling.

For the 500 TO runs, 500 minima have been obtained when compared elements by elements. This shows that from a mathematical point of view, there are as many different material distribution than there are initial value distributions. This is not surprising considering the very high number of design variables in a TO problem, the non-convexity of the buckling problem and the fact that TO uses a gradient-based solver [78, 191]. With these results, one can conclude that using solely gradient-based solvers is not enough to achieve the global minima. The gradient-based solvers are the only available optimization tools able to converge quickly and reliably in the large design space of topology optimization [2, 225]. Especially in compliance only optimization where the design space remains convex, which is not the case with buckling constraints. Still, as the implicit density-based modeling does not completely capture the full behavior of a stiffened panels anyway, simply finding multiple minima could be sufficient to find usable material distribution capable of improving creativity of engineers.

Even if there are multiple material distributions, it is possible to group together different solutions to create families of stiffening layouts. The solutions with two stiffeners are grouped together, the same for three stiffeners, etc. The different families of material distribution and their occurrences are aggregated in fig. 5.10. An example of grouping for the "four stiffeners" family is illustrated in fig. 5.11a with their respective buckling modes in fig. 5.11b. The buckling modes of each material distributions show a similar buckling pattern for a similar material distribution.

The family distribution leans toward orthogrid solutions, which represent almost all proposed solutions. This could be an indication that simple solutions are easier to achieve, or it could be an indication that these topologies are better. Considering the simplicity of the test case and the applied loads, these results are coherent.

From these results, it is possible to notice the impact of initial values on the proposed results, even without changing optimization parameters. This approach can be used to generate different results and explore the design space for different types of solutions, which could help designers find even more efficient stiffening layouts.

Fig. 5.12 shows that the different topologies behave similarly during optimization in terms of strength and weight. Indeed, for a given weight, if the material distribution connects both sides of the span-wise compression, the compliance and buckling strength are directly linked

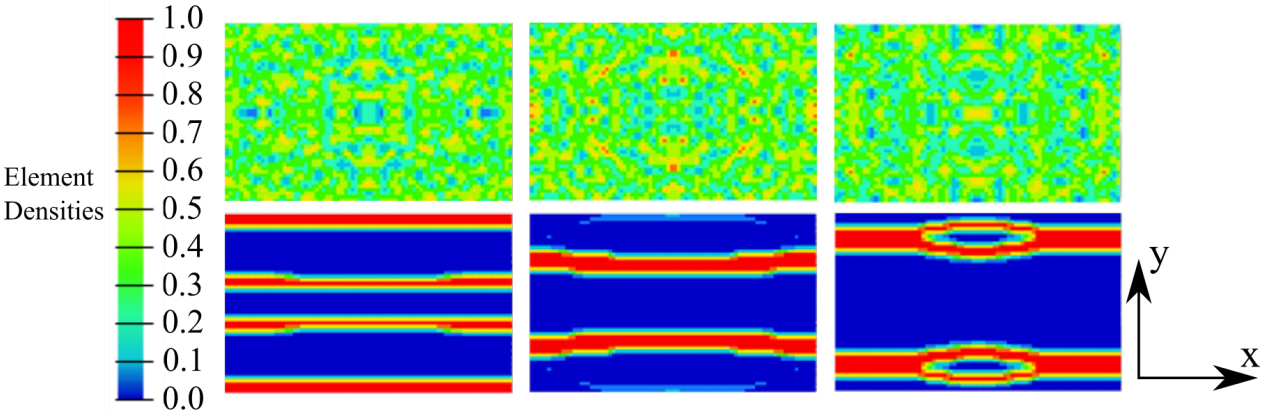


Figure 5.9 The effect of three different fully random initial values on TO. On top, the random initial value distribution of three examples. On the bottom line, their respective optimized material distribution.

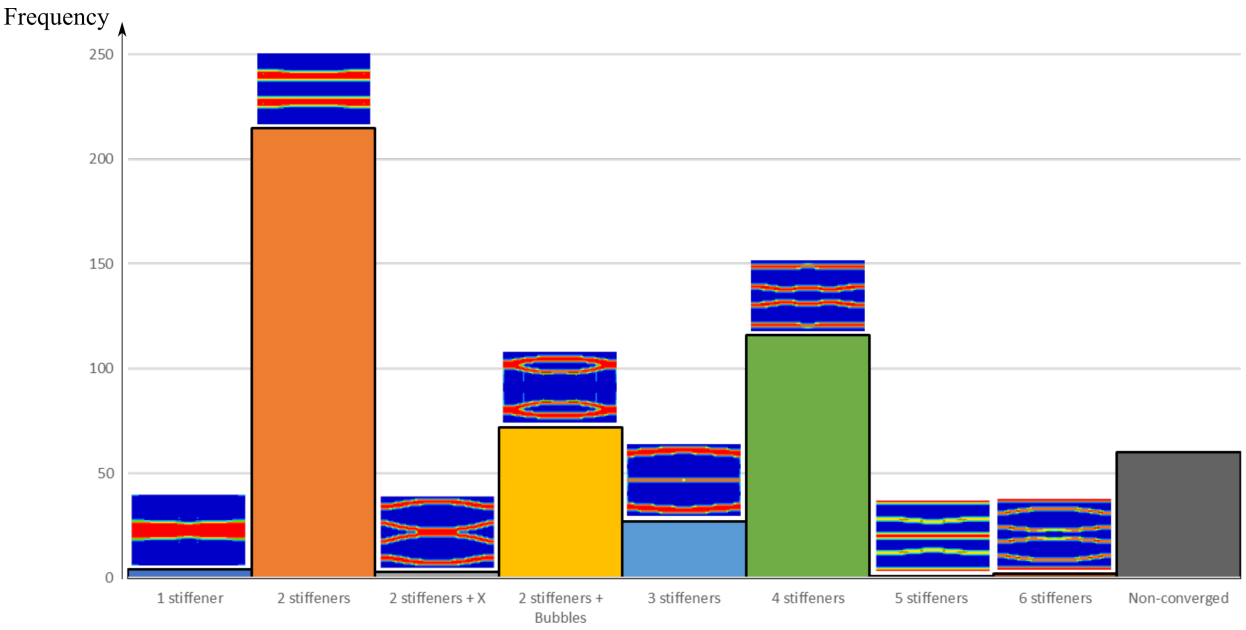
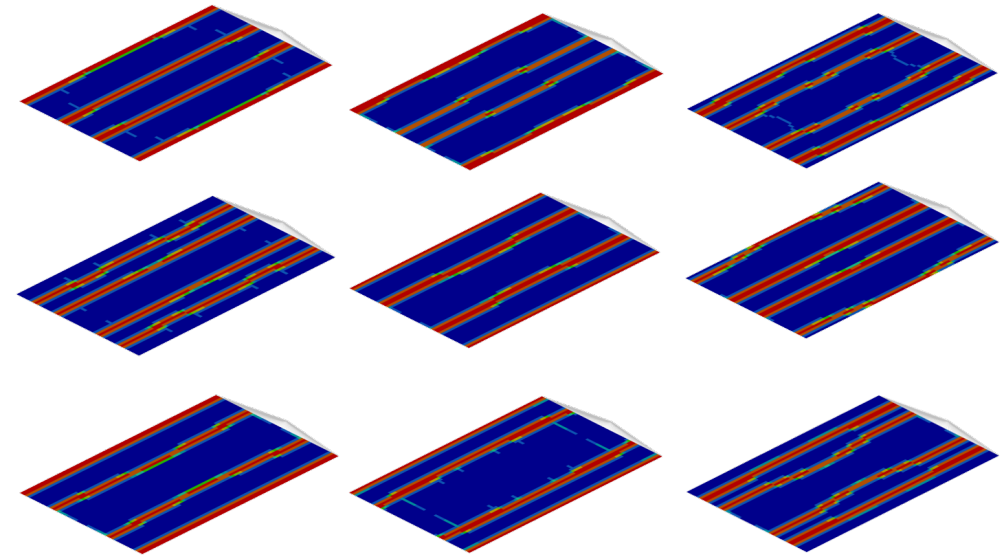
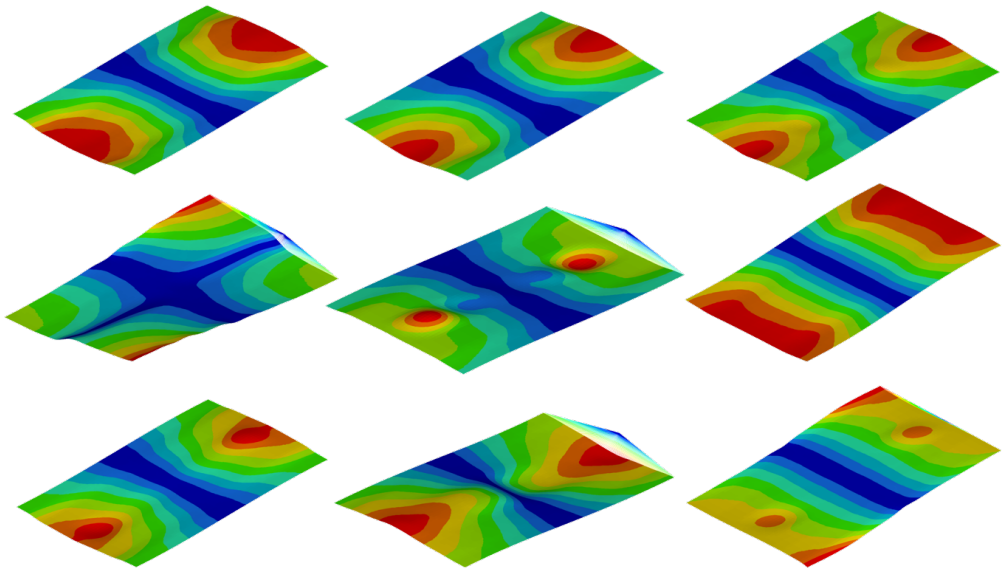


Figure 5.10 Frequency of different families of topology distribution for 500 random initial values



(a)



(b)

Figure 5.11 A sample of the family of “4 stiffeners” material distribution. These material distributions all have the same topology. (a) A sample of "4-stiffeners" material distributions. (b) First buckling modes of respective "4-stiffeners" material distribution. The total displacement of each node is illustrated.

to the weight of the panel. Constant strength does not remain true for the layouts once they have been interpreted as stiffened panels. More information on this can be found in the validation section, which will show that the strength of the stiffened panels is more linked to its layout than what would be inferred from fig. 5.12.

This section focused on the analysis of the impact of buckling constraints on TO of stiffened panels, which led to a design space exploration method that uses random initial values. It allows the optimization to reach multiple minima without changing the parameters. Even though the design space is very large due to the large number of design variables, the possible number of layouts remains limited.

5.3 Interpretation, Sizing and Validation

Layout families obtained using random initial values in section 2 are interpreted as FEM of stiffened panels. Two solutions inspired by the work of Houston & al. are also added for more design space exploration [3]. They consist of buckling containment features (BCF) that should help buckling resistance while reducing weight [88]. They are proposed as the FourLBCF and ThreeLBCF solutions. The BCFs are simple, smaller stiffeners with much lower inertia than the main stiffeners. Their role is to increase skin buckling, without compromising post-buckling. All interpreted stiffened panels are illustrated in fig. 5.13.

Whenever possible, all stiffeners were modeled as “J” to limit variability and ease comparison. However, the *One Hat* solution, uses a hat section because of the larger width of the material distribution, that makes the use of a single stiffener unsuitable.

5.3.1 Sizing the "New" Stiffened Panels

To compare the layouts, a size optimization is done to find the minimum weight associated with each stiffening layout. The same buckling limit as the baseline is used as a constraint. The sizing process objective and constraints are respectively the weight and buckling, as defined in the table 5.8. The sizing optimization is also completed with Optistruct using the sequential quadratic programming (SQP) algorithm [78]. The variables of the optimization are the thickness of each stiffeners. One might notice a difference between the topology and sizing optimization formulations. A reason for this modification is the poor convergence of topology optimization with a buckling constraint, especially as it is modeled as a thick shell. The design space of the sizing optimization is less complex, and as such can include a more challenging optimization problem such as mass minimization, which is closer to the design problem we want to solve.

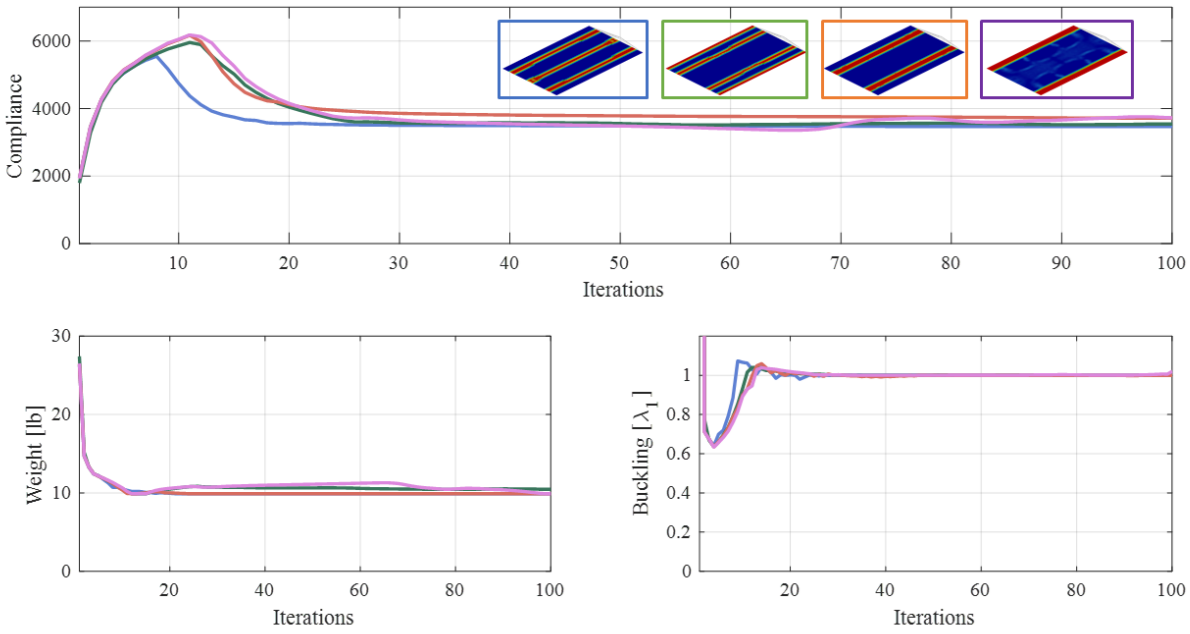
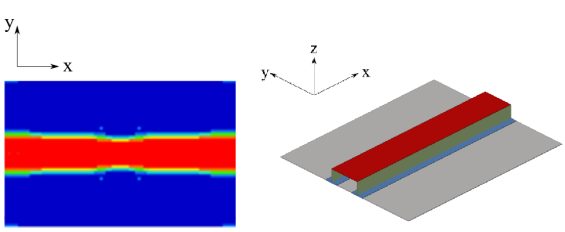


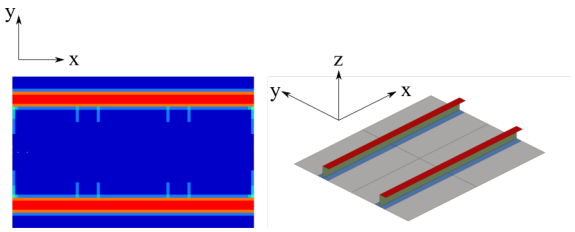
Figure 5.12 The effect of initial values on the convergence of TO with buckling constraints. The color of each curve is related to each material distribution (box of the same color).

Table 5.8 Sizing optimization formulation

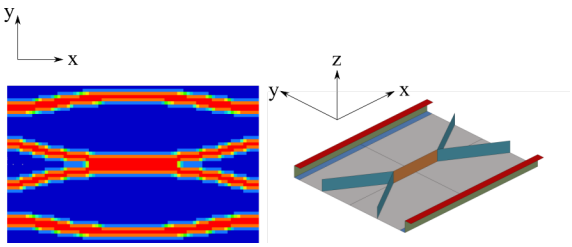
	Parameter	**Function**
Objective	Weight [lb.]	Minimize
Constraint	Buckling [-]	$\lambda_1 \geq 1.0$
Constraint	Stress [ksi]	$\sigma_{VM} \leq F_{cy}$



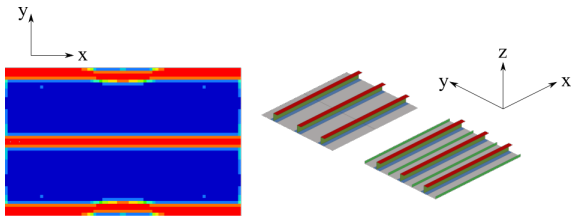
(a) One Hat



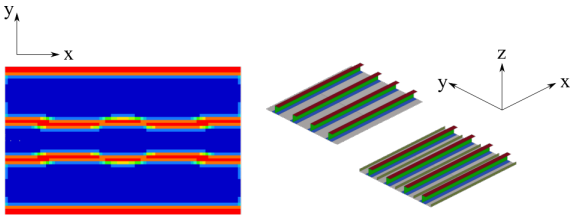
(b) TwoL & TwoLSplit



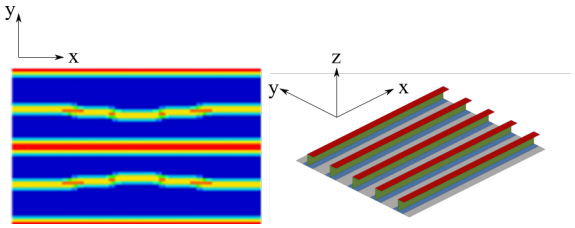
(c) XBars



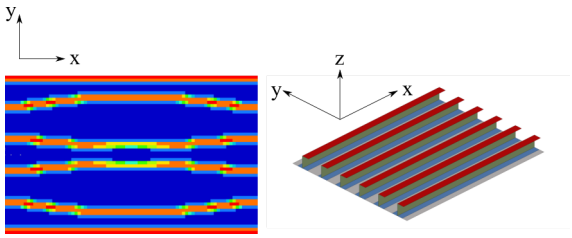
(d) ThreeL & ThreeLBCF



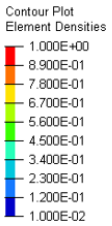
(e) FourL & FourLBCF



(f) FiveL



(g) SixL



(h) Density Scale

Figure 5.13 Interpretation into Stiffened Panels of the different Layout Families

From this size optimization, the suitable dimensions and properties associated with each layout are obtained. The properties of each layout are presented in table 5.9.

The results from the size optimization show that stiffening layouts have a significant impact on the buckling strength of stiffened panels. From the density-based model, it would have been expected to have similar performances from each topology, but size optimization results show that an inappropriate choice of layouts can make a panel much heavier for a similar strength. Furthermore, it turns out that the layout obtained the most in the exploration (see fig. 5.10), the *TwoL* turns out to be one of the heaviest solution.

Linear buckling does not always capture the interaction between the different buckling modes and material non-linearity. As such, a non-linear validation step is necessary to accurately assess the capabilities of the different stiffening patterns.

5.3.2 Validating the Stiffening Layouts

A quasi-static non-linear FEM analysis considers both the geometrical and material non-linearity. However, it is computationally expensive, a single run may take up to several minutes of calculations for a simple panel. As such, it should not be used for optimization. Still, it will be used for the validation of the strength of stiffening layouts obtained with TO. The non-linear analysis in Optistruct using the arc-length methods and the Riks adaptive load-stepping algorithm [78].

The difference between linear static analysis and non-linear quasi-static analysis is that the non-linear analysis progressively applies the loads [78]. As such, a load-stepping technique is required. For quasi-static analysis, where dynamic effects are negligible, the implicit method is preferred [78]. This method calculates for each load step the stiffness matrix of the FEM and

Table 5.9 Properties of each interpreted panels

Name	**Linear buck.** [λ_1]	**Compliance** [**lb.in.**]	**Max. stress** [**ksi**]	**Weight** [**lb.**]	**Weight diff.** [**%**]
One Hat	1.0	2750	25	9.8	85%
TwoL	1.0	3600	32	7.6	43%
XBars	1.0	3900	68	7.2	36%
ThreeL	1.0	4410	39	6.1	15%
ThreeLBCF	1.0	5600	49	4.8	-10%
FourL (Baseline)	**1.0**	**5000**	**45**	**5.3**	**–%**
FourLBCF	1.0	6200	55	4.3	-19%
FiveL	1.0	5500	49	4.9	-8%
SixL	1.0	5294	47	5.1	-4%

updates it iteratively until it finds equilibrium. During the first linear phase, the load steps are larger, as the position of the next load steps is easy to predict. However, after buckling, the non-linear effects are harder to predict, which requires progressively smaller load steps. For our comparative study, we limit the number of load steps to 100 as it allows a good comparative view of the problem while limiting the computation time. Another important aspect of non-linear analysis is the impact of imperfections. The analysis could have a hard time finding the buckling divergence point without imperfections and jump over it. As such, it is important to model imperfection into the mesh of the FEM. The recommended approach is to first conduct a linear buckling analysis and deform the model using some of the first buckling modes [78].

It should also be noted that the effect of material non-linearity is non-negligible. In preliminary works by our research group, the material used was aluminum 2024 alloy that has a yield limit of around 45 ksi. This is close enough to the buckling limit of the panel that there is a coupling of material and geometrical non-linearity that makes the stiffened panel unstable before the linear buckling. This was the reason behind the choice of the aluminum 7075 alloy that has a higher yield limit of 68 ksi, which removes some of the coupling of material and geometrical non-linearity.

As an example, in fig. 5.14, we see the analysis for the handbook design where skin buckling and collapse are separated. The effect of buckling is seen on the left figure, where both top and bottom layers of the stiffeners become more stressed due to the buckling of the skin which redistributes the load to the stiffeners. This effect is also seen in the change of the slope of the applied force on the figure on the right. The non-linear analysis is able to continue until collapse, close to the value of the applied load of $1.2 * 10^5$ lbf. The collapse of the panel is illustrated in fig. 5.15.

In this section, we validate the sizing method to confirm (or refute) that the panels are indeed as resistant as the linear buckling analysis suggests. First, the sizing optimization ensures the linear stability of the panel up to the ultimate load (1.0 of the load ratio) for every topology. Table 5.10 and fig. 5.16 show the effect of the layouts on the non-linear analysis. It indicates that not all layouts are actually capable of reaching the ultimate load without collapsing.

The non-orthogrid design show significant premature collapse, even the BCFs. The addition of non-uniform stiffeners enhances the coupling between the different components of the stiffeners panels, which increases the effect of geometric non-linearity. For the design with BCFs, the use of design map instead of FEM optimization could reduce this problem [88].

This shows a major limitation of using only FEM and linear information for the design and optimization of stiffened panels. The coupling effect of in-plane and out-of-plane forces

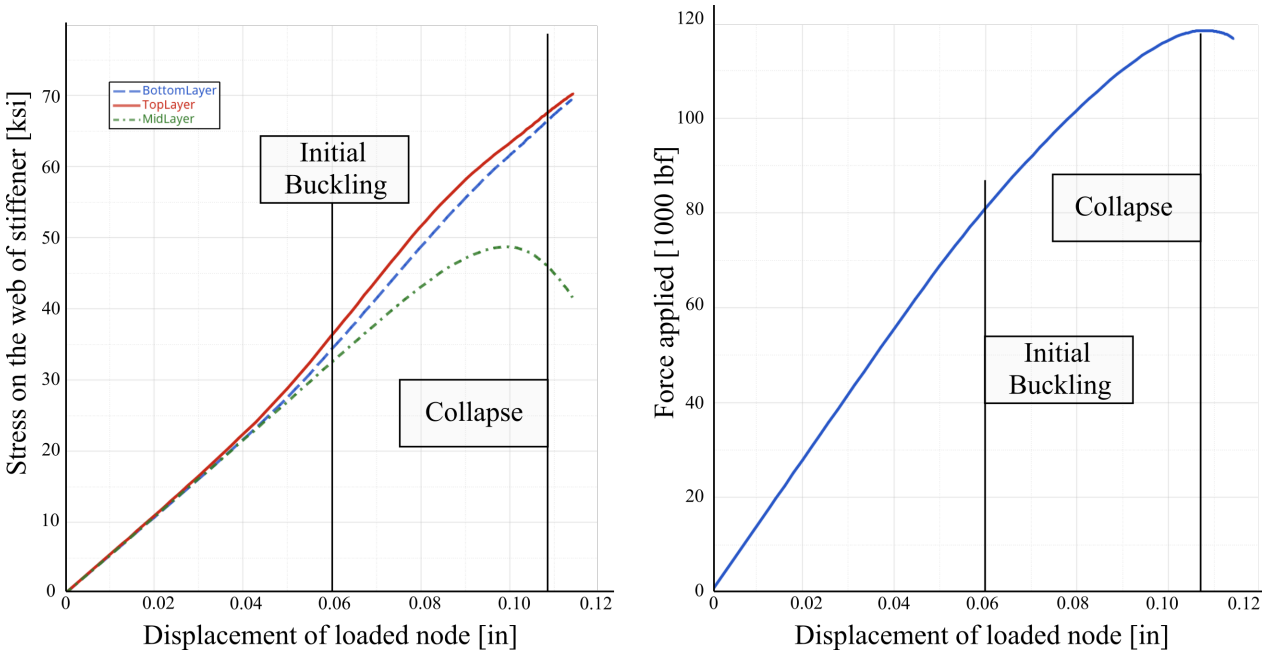


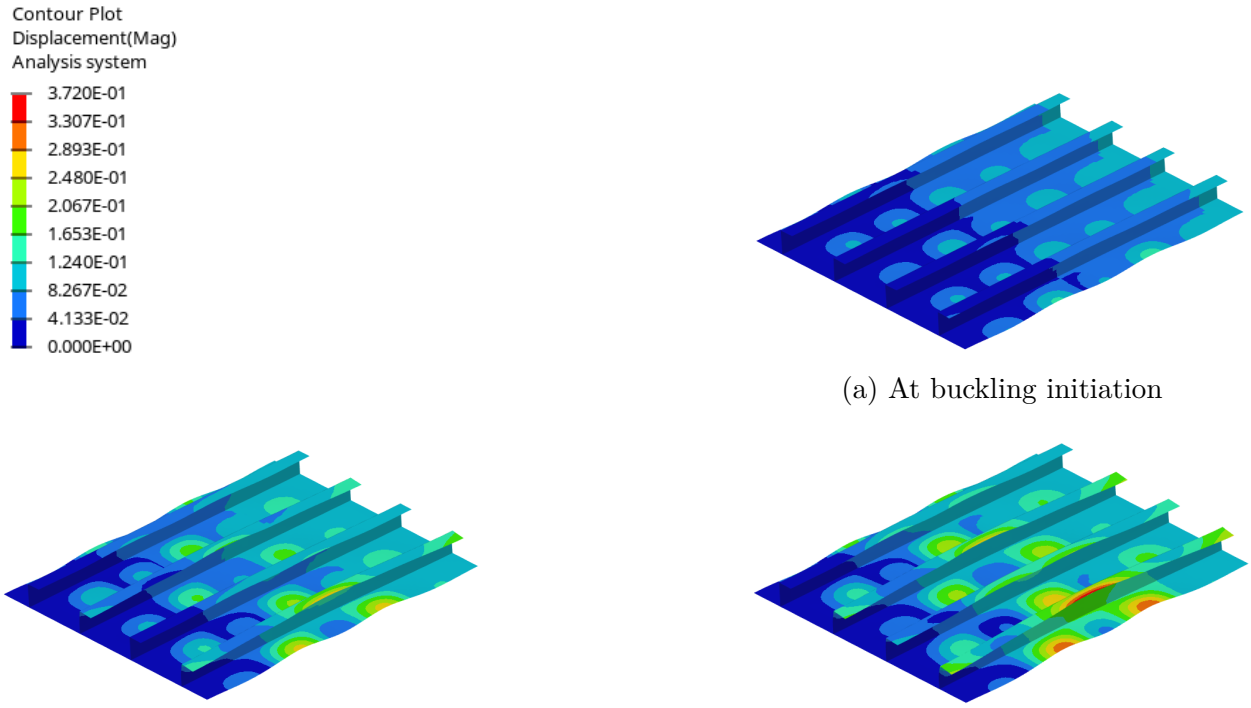
Figure 5.14 Non-linear analysis using the RIKS method for the baseline with sized with handbook methods. Note that there is a separation between initial buckling and collapse, this is the stable post-buckling.

combines to create geometrical non-linearity. Furthermore, the generally non-linear material used in aeronautics has to be considered during design to ensure non-premature collapse.

5.4 Conclusion

This work has shown that the combination of buckling constraints with random initial values allows TO to converge toward feasible material distributions. However, the density model does not allow for a proper assessment of the strength and weight of different stiffening layout. All the panels had very similar properties when evaluated with the density-based model, but this does not hold true when it comes to the interpreted stiffened panels.

The layout of the stiffeners has a significant impact on the strength and weight of the stiffened panels. This shows that the modeling of buckling with the density-based TO is not accurate. Modeling the stiffeners into stripes of very thick shell elements, in the same plane as the skin and loads, was the assumption made in order to smear the stiffeners into an equivalent model. In turn, this allowed great design freedom and simplification for optimization, but it seems it lowers too much the fidelity of the analysis. Still, current TO with a buckling constraint can generate feasible solutions that may then be used to provide new insights. If, and only if, a proper validation is done on the panels.



(a) At buckling initiation

(b) At full load

(c) During collapse

Figure 5.15 Evolution of the displacement of the handbook optimized baseline during non-linear analysis. Axis in inches.

Table 5.10 Non-linear validation of each interpreted panels in name order

Name	**Lin. Buckling** $[\lambda_1]$	**Load Ratio at Collapse**
XBars	1.0	0.85
One Hat	1.0	0.97
TwoL	1.0	0.85
ThreeL	1.0	1.0
FourL (Baseline)	**1.0**	**0.98**
FourLBCF	1.0	0.88
ThreeLBCF	1.0	0.91
FiveL	1.0	0.96
SixL	1.0	1.03

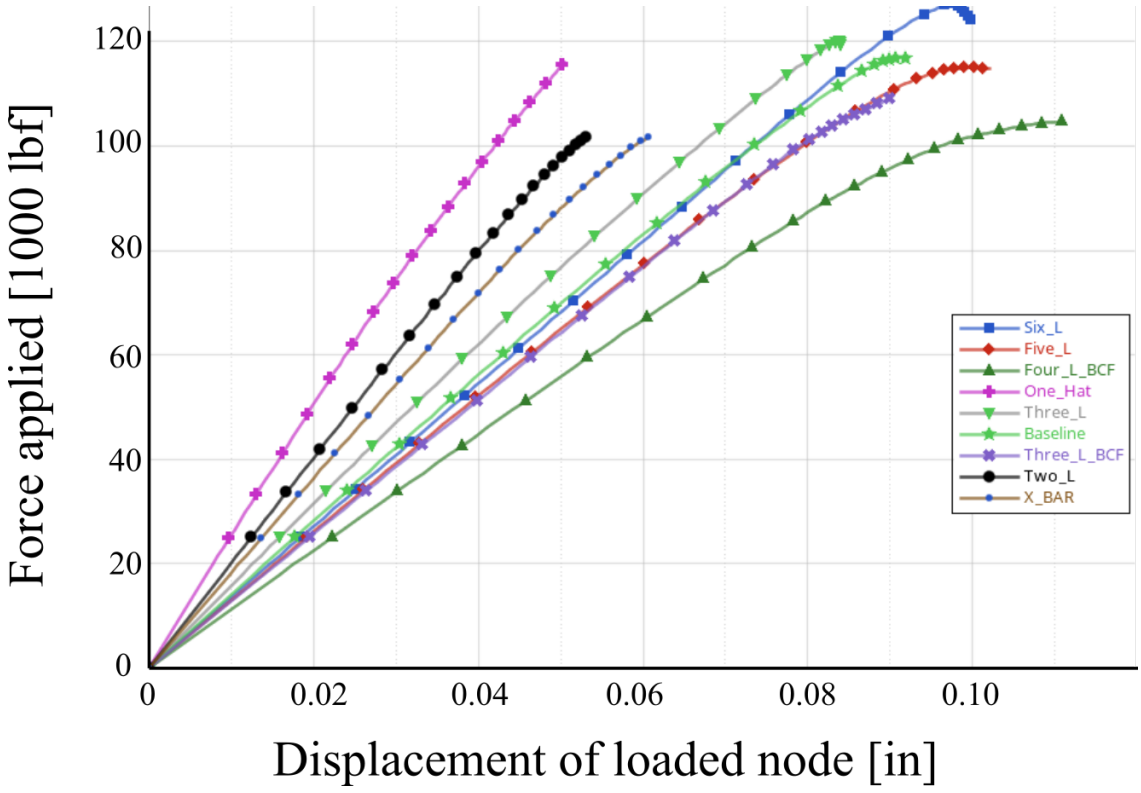


Figure 5.16 Non-linear relation between displacement and applied load for all layouts. The analysis stops at numerical instability or when collapse is reached. See fig. 5.13 for definition of layouts.

From these results, the first observation is that the design space is very large: for 500 different starting points, there are 500 different minima. The second observation is that the number of layout families is finite. From the results of a batch of five hundred TO, only 8 different families of layout were obtained and compared.

Those layout families have been interpreted into stiffened panels. The sizing results show that orthogrid is better than more organic shapes when sized with FEM optimization. Since the orthogrid layout is also proposed by TO, it may be concluded that TO with a buckling constraint and random initial values is a method capable of generating feasible solutions.

Also, the non-linear analysis shows that not all layouts are equivalent in terms of the strength/weight ratio but that at least the linear buckling approximation is good enough to find feasible layouts. It was shown that the effect of the topology on strength is significant but not captured completely with the implicit generation of density-based method. Depending on the topology, for the same buckling strength, the weight ranges from a 85% increase to 19% decrease when compared to the baseline topology. There is currently no clear link between the strength of the density model and its interpreted model. More work could be carried out to incorporate stable post-buckling in the FEM-based sizing process.

As such, when it comes to generate stronger or lighter solutions than the already existing aeronautic solutions, the results in this work show that TO with buckling constraints does not result in new layouts for this case study. Furthermore, computation time is excessive (multiple hours per solution) even though the case study has been reduced to its simplest form. The current handbook design methods still offer an easier, more complete approach by considering non-linear aspect using semi-empirical equations. Still, since the material distributions have been shown to be at least feasible, it could also be interesting to push this work further and automate the family layout analysis with a vision-based recognition tool as the one developed by the authors in [151].

Additional work may improve the TO formulations with buckling constraints or objectives. It is shown that modeling stiffeners as thick shell elements for TO does not capture buckling properly, as shown in the differences between material distribution properties versus the interpreted stiffened panels. It appears that the implicit generation of stiffeners as density variables is not an appropriate approximation of the physics of panel buckling, which makes the optimization converge simply toward coherent, but not optimized material distribution. More work is required to improve the representation of buckling with the density-based method. Another research avenue could be to implement other topology optimization algorithms, such as the ground structure or moving morphable components [5, 226].

CHAPTER 6 Article 3: Topology Optimization for Stiffened Panels: A Ground-Structure Method

Jean-François Gamache[a], Aurelian Vadean[a], Nicolas Dodane[b], and Sofiane Achiche[a]

[a]Polytechnique Montreal, 2900 Edouard Montpetit Blvd, Montreal, Québec, Canada
[b]Stelia Aéronautique Canada, Research & Technology, 12000 rue Henry Giffard, Mirabel, Québec, Canada.

Published in proceedings of ASME2020, conference *IDETC-DAC*, August 2020.

Abstract

Reducing the weight of structures remains a major challenge in the aviation industry in order to reduce fuel consumption. The stiffened panel is the main assembly method for primary structures in aircraft, e.g. fuselage or wing. Density-based topology optimization has been used in research and in industry as a tool to help create new stiffening patterns for aircraft components, such as ribs, spars, bulkheads or even floor design. One critical aspect of stiffened panel design for wing structures is the buckling resistance. However, most work found in the literature does not include buckling analysis during optimization which leads to sub-optimal results when the stiffening layout is validated for buckling. Including buckling as a constraint for the density-based topology optimization has proven to be a complex task, mainly caused by the fact that the buckling of the stiffeners is not captured accurately. As such, this work presents an optimization method for stiffened panels based on the ground structure approach usually used for truss topology optimization. The main novelty of the method is the use of a Stiffener Activation Variable (SAV) to activate only one variable at a time, either the height or density variable associated with each stiffeners of the ground structure. This work shows that while ground structure topology optimization requires more setup time and limiting the degrees of freedom of the optimization, it finds the best stiffening layout efficiently when compared to the density method.

6.1 Introduction

For the design of aircraft, it is important to reduce the weight of components as much as possible to reduce fuel consumption. As such, the structures built with stiffened panels have been used extensively in the aircraft industry due to their high strength and their relative

low weight [29].

The failure and collapse of traditional stiffened panels are well studied and understood, stiffened panels are made of thin metallic components and are thus sensitive to buckling collapse [26, 58]. The traditional stiffening pattern has stiffeners placed orthogonally to each other in what is called the orthogrid configuration. The usual structural optimization method uses semi-analytical calculations for buckling constraints, but is limited to the orthogrid configuration [26, 58].

In the recent years, new manufacturing techniques and new optimization methods were developed, broadening the possibilities for the design of stiffened panels. One research avenue extensively exploited is to use topology optimization to explore new stiffening configurations for the design of lighter aircraft components, such as wings and fuselages [38, 155, 196, 218].

Optimizing for new stiffening configurations faces two main challenges among others. The first challenge is related to the modeling and buckling optimization. Since the accepted method uses semi-analytical formulas, proposing new layouts requires more flexible analysis tools, such as the FEM. The second challenge is related to the high number of design variables of topology optimization problems.

There is no easy solution to address these challenges, as they compete against each other. Ideally, one would need a quick mean of assessing buckling accurately coupled to a fast method of exploring the design space.

The most used method for topology optimization is the density-based method, especially the SIMP method [13, 37, 141]. Density-based methods also includes (B)-ESO and Level-set [141]. Another approach is the ground-structure approach, also called truss topology optimization, that is usually used for completely discrete assembled structures, such as cranes and bridges [227, 228]. More recently, the MMC, has also been proposed recently where discrete components are free to move in the design space using displacement and morphing variables [5, 229].

Of all these methods, only the SIMP method is widely implemented into commercial software packages, such as HyperWorks or ANSYS Workbench [78, 79]. Therefore, most industrial applications of topology optimization for aircraft design use the SIMP method [13].

Despite its wide use, there are very few publications that includes a validation of their new stiffening layouts for buckling. Therefore it has been difficult to assess which design methods and tools actually result in feasible solutions [13, 38]. Furthermore, only [155, 221] have included buckling as an optimization constraint. Consequently, in a previous work [223], our research group has shown that the material distribution buckling resistance is not directly

correlated with the buckling resistance of the stiffened panel. It was highlighted that the modeling of buckling of the density-based method is not a good approximation of stiffeners [223]. Still, the density-based method remains a well-performing topology optimization method that deals, in a reasonable amount of time, with a large number of design variables, while exploring a vast design space [141].

Both MMC and ground-structure are interesting approaches to eliminate the buckling modeling problem, but only the ground-structure approach could be quickly implemented directly into a commercial package, such as Optistruct.

This work presents a topology optimization method for stiffened panels based on the ground structure approach that also uses the SIMP material interpolation. The main novelty of the method in this work is the introduction of a Stiffener Activation Variable (SAV) that greatly improves the convergence of the optimization towards manufacturable solutions.

6.1.1 Optimization with a Buckling Constraint

All the topology optimization methods listed in the last section uses FEM to capture displacement, stress and buckling of the structure. Our main design driver for stiffened panel being buckling, this section discusses how to capture it with FEM. It is possible to approximate the buckling critical loads of a given structure by computing the eigenvalues of the stiffness matrix. The first step, as for any FEM, is to compute the equilibrium equation [230]:

$$\mathbf{K}\mathbf{u_0} = \mathbf{P} \tag{6.1}$$

where $\mathbf{K}$ is the stiffness matrix, $\mathbf{u_0}$ the equilibrium displacement vector and $\mathbf{P}$ the load vector.

From the static solution, it is possible to solve a generalized eigenvalue problem associated with buckling:

$$(\mathbf{K} + \lambda\mathbf{K}_\sigma(\mathbf{u_0}))\varphi = 0, \text{ for } \varphi \neq 0 \tag{6.2}$$

where $\mathbf{K}_\sigma(u_0)$ is the stress stiffness matrix for which the computed eigenpairs (λ_j, φ_j) are respectively the buckling load factors and its associated nodal displacement of the j^{th} buckling mode [230].

The first buckling mode is of interest, as it defines the critical mode for which it is possible to define the critical load:

$$\mathbf{P_{cr}} = \lambda_\mathbf{1}\mathbf{P} \tag{6.3}$$

where P_{cr} is the critical of buckling load associated with the 1^{st} buckling mode λ_1 and $\mathbf{P}$ the external force [230].

With the computed first eigenvalue of the FEM, it becomes possible to quickly assess and constrain the buckling strength of the stiffened panels during optimization.

6.1.2 Ground Structure Topology Optimization for Stiffened Panels

In opposition to the density-based method that is a continuous topology optimization method, the ground structure approach uses a pre-defined discretization of the design space. This pre-defined design space is called the ground structure.

The ground structure approach is generally used for the design of truss assemblies, for bridges or building designs [2]. The classic ground structure approach uses continuous design variables where the area of the cross-section of trusses is used as variables. The ground structure approach may also use a discrete formulation for the design variables, where they either exist or don't. This formulation usually uses evolutionary optimization solvers, such as the genetic algorithm.

Challenges with the ground structure approach for buckling optimization arises from the fact that most of literature studies only truss assemblies. This creates three challenges. First, for truss assemblies, the local buckling of the thin trusses is easily evaluated locally as each truss may buckle individually. However, the evaluation of global buckling modes remains an open challenge [165]. Second, as for stress constrained optimization, a buckling constraint creates a disjointed and non-convex design space [231]. Finally, there are challenges related to the jump in buckling length [227]. This problem is related to the nature of truss ground structure, as the length of the independent trusses depends on the existence of the adjacent trusses, which creates non-linearities in the design space [227].

These challenges are alleviated for the optimization of stiffened panels by introducing a combination of certain geometrical variables. Furthermore, as this method is specific to stiffened panel topology optimization, there is always a continuum of material (web of the skin) connecting the boundary conditions, which removes the problems associated with individual free trusses.

To test and illustrate the proposed method, a section of the upper plank of the wing of an existing aircraft is used.

6.2 Case Study

The studied panel is a section of a typical wing upper plank of an existing commercial airplane, see fig. 6.1. This section is chosen due to its high compressive load that leads to a

critical buckling margin.

The Detailed FEM (DFEM) of the stiffened panels uses the double half-bay modeling technique, described in [68] to ensure the modeling of both odd and even buckling modes. The material used is a 7075-aluminum alloy with the properties defined in table 6.1 [232].

Aircraft have multiple complex loading conditions; from crash landing to wind gusts, everything is considered. There are more than a hundred loading conditions that need to be considered for validation, but to simplify the optimization, only one critical load case is selected. Load values are extracted from a linear static analysis of the aircraft General FEM (GFEM). This is a common practice for the margin of security calculations in the aerospace industry [26, 58]. The load case is modeled as a combination of three loads: Axial compression, transverse compression and shear, see fig. 6.2. The properties of the baseline design are presented in table 6.2 and will be used to compare the new layouts.

In terms of topology optimization, it will be useful to define a comparison with the density-based method. Density-based topology optimization has been used in the past by our research team [223]. One of the conclusions of this work is that the evaluation of buckling during topology optimization is not captured accurately by the density-based model [223].

From this work, multiple topology optimization has been carried, the two results that come most often are the two- and three-stiffener layouts. The four to six stiffeners layouts represent a much smaller number of the results. However, as shown in table 6.3, the five- and six-stiffener layouts are much more efficient in terms of buckling strength.

6.3 Ground Structure Method for Stiffened Panels Design

This section details the method used for the optimization of stiffened panel, using the ground structure approach. Firstly, the setup is described, which includes the geometry and variable equations. Secondly, the optimization process and the results for the case study are presented. Finally, a validation is performed on the best solution to ensure that buckling was correctly

Table 6.1 Aluminum 7075 properties [232]

Property	**Value**
Young's Modulus E_0 $[ksi]$	$10,700$
Poisson ratio $[-]$	0.33
Yield limit (F_{cy}) $[ksi]$	68
Material Density $\left[\frac{lb.}{in^3}\right]$	0.1

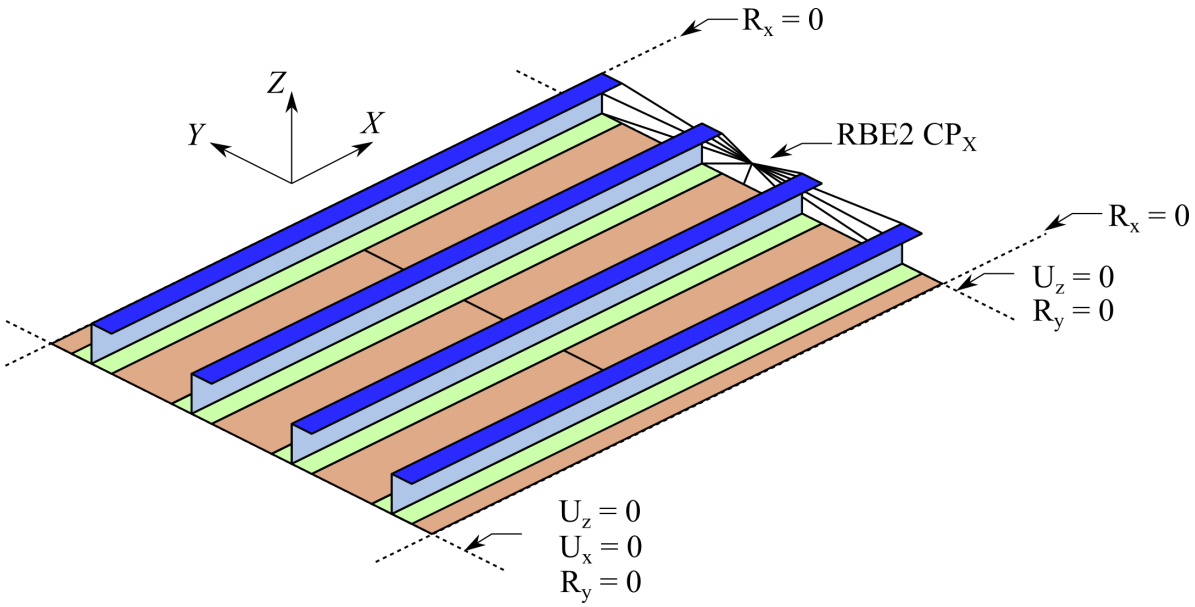


Figure 6.1 Four-stiffeners (Baseline) sub-components of the stiffened panel

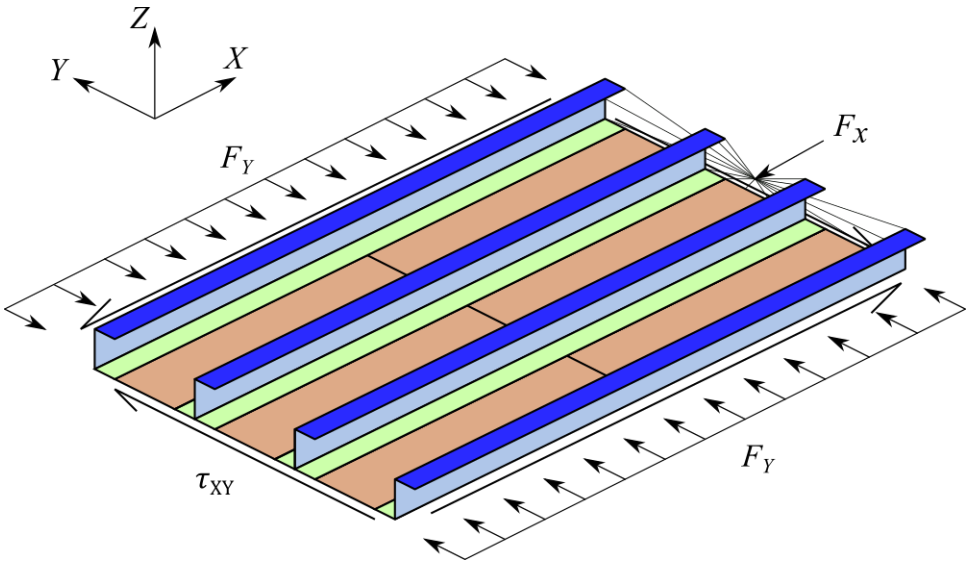


Figure 6.2 Loads applied on the baseline stiffened panel

Table 6.2 Baseline properties

Property	**Value**
Weight [*lb.*]	5.2
Compliance [*lb.in.*]	4900
Maximum Stress [*ksi*]	45
First buckling mode [λ_1]	1.08

Table 6.3 Properties of some layouts obtained with density-based optimization compared to the baseline obtained with handbook methods.

Name	**Weight** [*lb.*]	**Weight difference** [%]
TwoL	7.7	48%
ThreeL	6.5	24%
FourL [Baseline]	5.2	[−]
FiveL	4.6	−12%
SixL	4.5	−14%

considered during optimization. There is multiple software available to leverage both FEM and optimization at the same time. The authors are familiar with the Altair HyperWorks suite, so HyperMesh is used to create the ground structure and Optistruct is used to solve the optimization problem [78].

The optimization is defined as followed:

Objective *Minimize Weight*

Buckling $\lambda_1 \geq 1.08$

Von Mises Stress $\sigma_{VM} \leq 60.0$

The objective is to reduce the weight of the panel, while ensuring that it is fail-safe. The buckling constraint is set to have the same strength as the baseline (1.08) as to make comparison easier with new stiffener layouts. The stress constraint is set lower than the yield limit (68 ksi) of the material to be able to differentiate the effects of geometric and material non-linearities.

To find feasible solutions quickly, a gradient-based solver is used. It is usually a good solution for continuously derivable solutions. It is also the default solver for Optistruct, which uses the sequential quadratic programming (SQP) solver [78]. This is combined with a design space exploration that uses a design of experiment (DOE) that creates evenly spaced random initial values.

6.3.1 Setting-up Ground Structure Topology Optimization

The design of the ground structure was made to have as much degrees of freedom as possible without requiring a restricting number of design variables.

The ground structure for the proposed method consists of straight stiffeners arranged in a grid, as shown in fig. 6.3. Most possible stiffeners are positioned axially (in the X direction).

The case study is simple, consequently it is expected that the solver finds only axial stiffeners. Diagonal and transverse stiffeners have been added as design variables to verify that the proposed method is able to remove useless stiffeners.

One of the disadvantages of the ground-structure method, is the prerequisite work necessary to define said ground-structure. Hereby, the resulting solution is highly dependent on the design of the ground-structure. The current ground-structure is limited to a simple and restricted design area. Multiple new stiffeners possibilities were defined in the X direction and some on the diagonal and transverse directions. This forms a basis of manufacturable stiffeners that can be added or removed from the solution. More transverse and diagonal stiffeners could have been considered, but a simple ground-structure has been initially chosen to validate the method.

Another challenging aspect of developing a ground structure method for stiffened panels is to find a variable formulation that does not create any unusual numerical behavior.

The first iteration formulation, as like most ground structure approaches, uses the cross-section as the design variable. So, for our case study, it means associating a height, thickness or combination of both as design variables. The details on the geometrical variables are presented in 6.4.

Topology optimization seeks to find the best stiffening layout, while deciding which stiffeners are kept and which can be eliminated. Therefore, the different variables describing the stiffeners need to approach zero. For buckling optimization, this becomes critical as even small values of thickness or height have a significant impact on buckling strength.

In the case of stiffener thickness as the design variable, small thicknesses will buckle very early. This makes the solver add thicknesses for all the possible stiffeners which tends to create heavy non-optimal solutions. Using only the height of stiffeners as the design variable

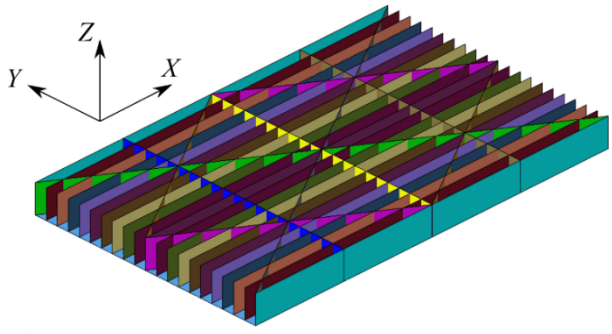


Figure 6.3 The stiffened panel ground-structure

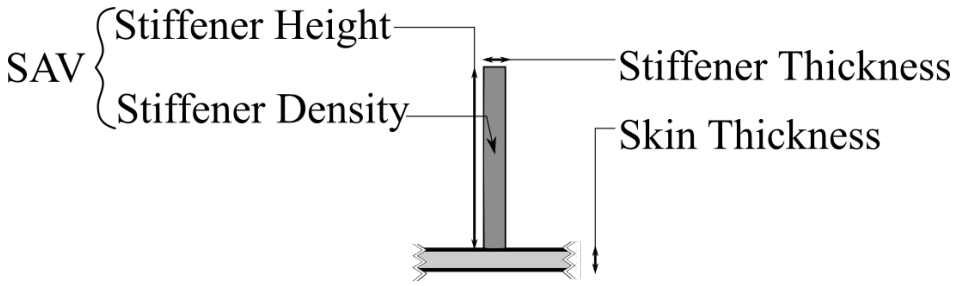


Figure 6.4 The design variables for the ground-structure topology optimization.

creates singularities and high mesh distortion for very low height. As such, the solver is not able to go toward a light feasible solution. Combining size and height only increases the weaknesses of both variable formulations. Therefore, a comparison with these formulations is not added to this work, as the solutions obtained are not feasible.

Inspired by the continuous density-based topology optimization, a density variable is assigned to each stiffener. Just like the SIMP method proposes, this density variable affects the young modulus (E_x) of each stiffener, as shown in eq. 6.4 [2].

$$E_x = \rho_x^p E_0, \text{ where } \rho_x \in [0, 1] \tag{6.4}$$

where ρ_x is the density of the x^{th} stiffener, P the penalization factor and E_0 the young modulus of the applied material. As discussed in [2], a penalization factor P of 2 or 3 results in the elimination of most intermediate densities.

The use of density variables greatly helps the optimization towards lighter and stronger stiffening layouts. However, it introduces multiple local minima, which results in a general convergence toward heavy stiffening layouts for a gradient-descent optimization.

Instead of working with the height and density as independent variables, we define a new independent stiffener activation variable (SAV_x). This allows to define density (ρ_X) and height (H_x) as dependent variables from the SAV_x to activate only one variable at a time. The activation of a variable is defined as when the value may change between iterations. Inversely, an inactive variable is constant between iterations.

This is very useful as the density variable is only active when the height of the stiffener is at its lowest and inversely the height variable is only active when the stiffener is at full density. The relationship between the different variables are defined in eq. 6.5, 6.6, and 6.7, and illustraed in fig. 6.5 and table 6.4.

$$SAV_x \in [-1, 1] \tag{6.5}$$

$$\rho_x = -max(0, -SAV_x) + 1 \tag{6.6}$$

$$H_x = Amax(0, SAV_x) + B \tag{6.7}$$

	ρ_x	H_x
$SAV_x \leq 0$	Variable	$H_x = B$ [0.5 in]
$SAV_x > 0$	$\rho_x = 1$ [Full]	Variable

Table 6.4 The relation between density (ρ_x) and height (H_x) variables for each stiffener (SAV_X) variable

where A is the range of the height variable ($A = 1$ in) and B the minimum of the height variable ($B = 0.5$ in) to limit the effect of mesh deformations due to morphing. This formulation allows ρ_x to be only active when $SAV_x \in [-1, 0]$ and H_x when $SAV_x \in [0, 1]$. The minimum height B (0.5 in) was chosen to limit the effect of virtual buckling modes and avoid the effect of mesh deformations. The maximum height $A + B$ (1.5 in) was chosen to ensure that the stiffeners stay within the existing envelope of the aircraft.

By using these relations, each stiffener has the possibility to fade in and grow or shrink and fade out. This has allowed us to have an optimization model that converges toward light feasible minima.

With the newly design variables defined, the complete optimization problem becomes:

Optimization formulation	Objective [lb]	Minimize weight
	Buckling constraint	$\lambda_1 \geq 1.08$
	Von mises stress [ksi]	$\sigma_{VM} \leq 60$
Design variables	Stiffener existence (SAV_x) [-]	[-1.0, 1.0]
	Stiffener thickness (T_x) [in]	[0.050, 0.250]
	Skin thickness (T_s) [in]	[0.050, 0.250]

6.3.2 Solving Ground-Structure Topology Optimization

The challenge of working with aeronautics structures is that they have already been optimized extensively. This means that only finding feasible results is generally not enough; a global

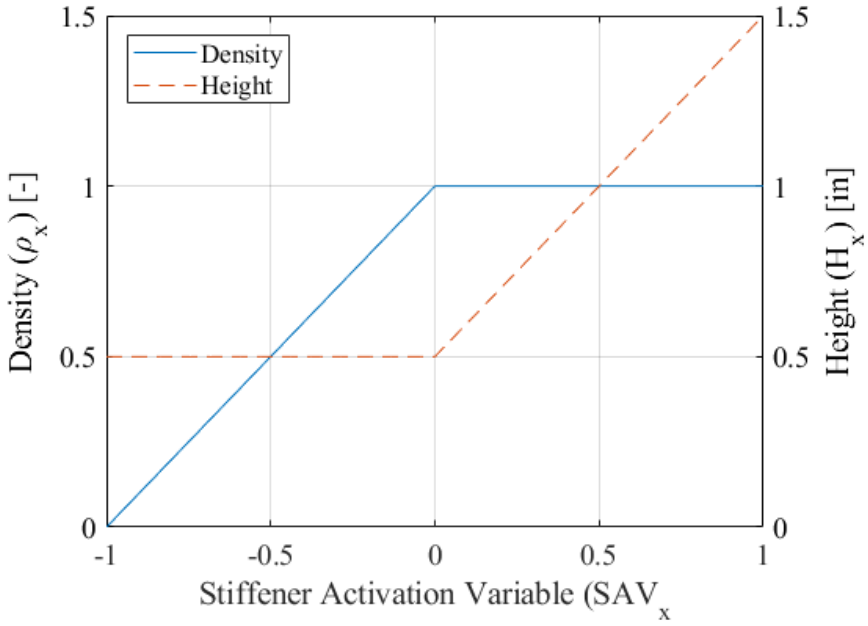


Figure 6.5 The relation between density (ρ_x) and height (H_x) variables for each stiffener (SAV_X) variable

minimum is what we are searching for. However, due to the nature of topology optimization, global search algorithms such as the surface response method or evolutionary optimization are still computationally expensive. This is another reason that a gradient-descent solver is used in this work.

To help the solver find the global minima, multiple optimizations are necessary, although it does not guarantee a global minimum. To explore the design space thoroughly, the initial values are changed using a Latin Hypercube DOE of a hundred gradient descents. A graph of the results of each gradient-descent is presented in fig. 6.6.

The graph shows that most of the gradient descent (93/100) can find a feasible solution. The graph also shows that the quality of the feasible solutions varies greatly. We face the same problem as any optimization considering buckling; there are multiple local minima. The weight of the feasible solutions ranges from 5.1 to 8.5 lb. The active constraint, for all feasible solution, is the buckling constraint. All solutions have stress levels under 45 ksi, very far from the yield stress, which shows that the buckling constraint is driving the optimization and not stress constraint, for the test case.

The four lightest stiffening layouts are illustrated in fig. 6.7. They are equivalent to the baseline in terms of strength and weight. However, they do not have free flanges which

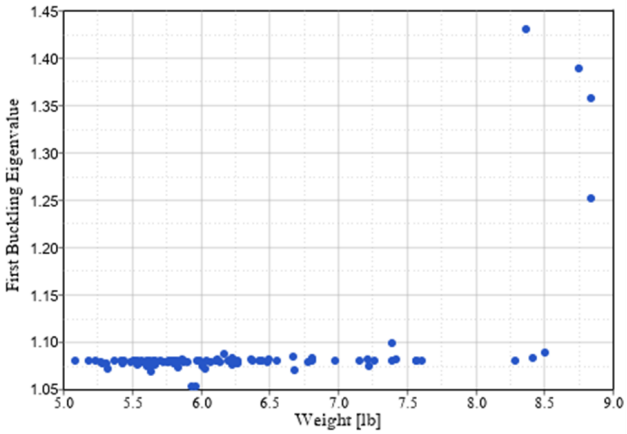


Figure 6.6 Distribution of results from a 100 random initial values ground-structure topology optimization.

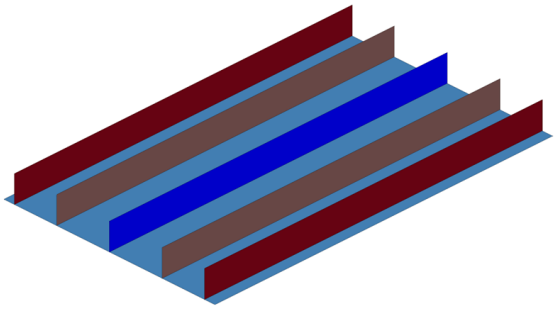
should help reduce their weight. The best solutions show that the solver can eliminate parasite diagonal and transverse stiffeners. The best minima are all simple layouts, with only a few stiffeners, all at maximum height.

6.3.3 Interpreting and Sizing Proposed Layouts

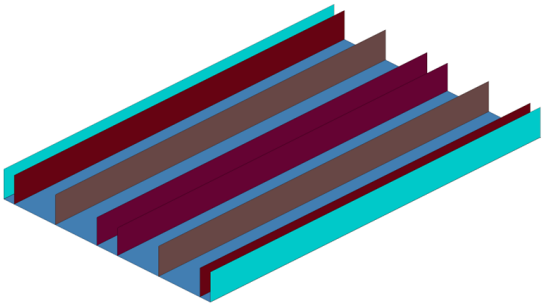
As described in the last subsection, to simplify the topology optimization a few hypotheses were required. The first element that needs verification is that the effect of small or intermediate density values have, at most, a small impact on the buckling and weight values. To verify this, the sizing optimization of the panels is carried out by removing the stiffeners completely with very small SAV_x values. The four best solutions are directly sized to demonstrate the effect of small SAV_x values.

Furthermore, just as density-based topology optimization, an interpretation of the variables helps to find true optimal results. A few iterations of the interpretation show that iso-spaced stiffeners offer a more efficient structure.

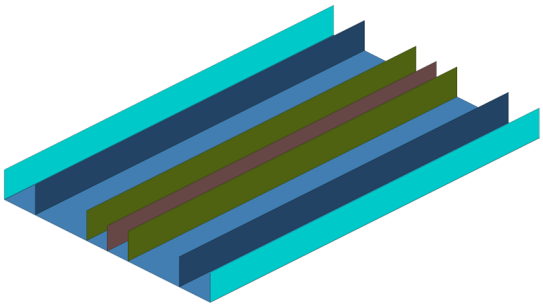
This could not always be the case for all stiffened panels, especially for more complex structures, but it proved effective for the test case. The interpretations of the optimization results are shown in fig. 6.8.



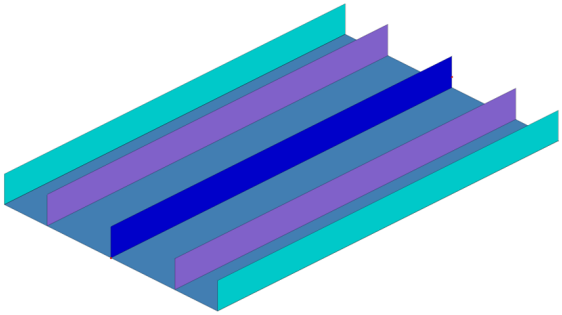
(a) Ground structure A, weight = 5.1 lb. (**GSA**)



(b) Ground structure B, weight = 5.2 lb. (**GSB**)

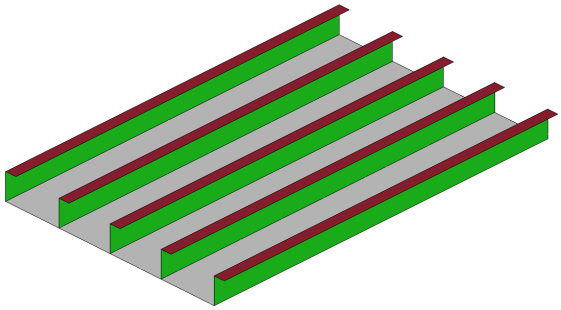


(c) Ground structure C, weight = 5.2 lb. (**GSC**)

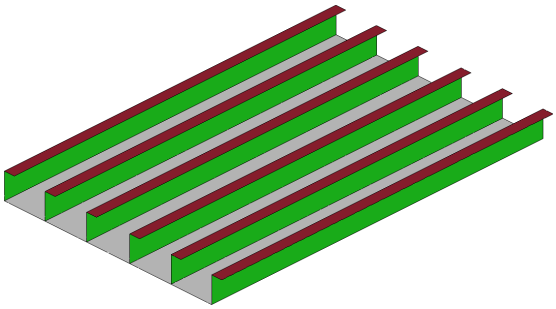


(d) Ground structure D, weight = 5.3 lb. (**GSD**)

Figure 6.7 Ground-Structure lightest layouts, color indicate regions affected by different variables.



(a) ISO-SPACED A. (**ISA**)



(b) ISO-SPACED B. (**ISB**)

Figure 6.8 Interpretation of stiffening layouts. The interpretation process uses engineering knowledge to modify the results towards more classical solutions. ISA has 5 stiffeners and is interpreted from GSA and GSD and ISB has 6 stiffeners and is interpreted from GSB and GSC.

A sizing optimization is done on all selected layouts. The sizing formulation is shown here:

Optimization formulation	Objective [lb]	Minimize weight
	Buckling constraint	$\lambda_1 \geq 1.08$
	Von mises stress [ksi]	$\sigma_{VM} \leq 60$
Design variables	Stiffener thickness (T_x) [in]	[0.050, 0.250]
	Stiffener Height (H_x) [in]	[0.5, 1.5]
	Skin thickness (T_s) [in]	[0.050, 0.250]

From the sizing optimization, it is possible to compare the effect of the small density values on the weight of the panel, see table 6.5. The effect of the small density values seems negligible, as the difference between the ground structure model and the interpreted model is less than 5%.

Stiffening Layout	Weight [lb]		
	Optimized Ground Structure	W\O Intermediate Densities	With Free Flange
GSA	5.1	5.3	5.0
GSB	5.2	5.5	5.1
GSC	5.2	5.4	4.9
GSD	5.3	5.5	5.0
ISA	[NA]	4.6	4.6
ISB	[NA]	4.5	4.5
Baseline	[NA]	5.6	5.6

Table 6.5 Comparison of stiffening layouts. See fig. 6.7 and 6.8 for stiffening layout definitions.

Also, from the sizing results, the weight of the best layouts is within accuracy margin of error, which shows that the best layouts are close together in terms of efficiency. This gives a good number of possibilities for the designer to find good stiffening patterns that may accommodate for the installation of systems or other attachments. Of course, for more complex shapes and loading conditions, new concepts could come challenge the existing straight stiffeners. Still, it shows that the method can find optimal solutions.

Another interesting effect is that the iso-spaced solutions are much lighter than the baseline of the ground structure results. It shows that a using purely optimization, just as for the density-based method, is not enough to really optimize the layout of stiffened panels.

6.4 Discussion

This section discusses the method and results from the optimization of the case study presented in the previous section. The method is compared qualitatively with the density-based

method for the three main design steps: setting-up, solving and post-processing. Improvements of the method are further explored.

6.4.1 Topology Optimization Setup

Setting-up ground structure topology optimization compared to the density-based method is more straightforward but requires many manipulations. It is more straightforward in the sense that it does not require any modeling hypothesis, building the ground structure is simply about adding more possibilities and more variable to the design space, whereas modeling for the density-based method requires multiple modeling hypotheses and parameters tuning. Our work has found that to find good solutions, ground structure was easier and quicker to put in place.

In terms of setup, the challenge of the ground structure method is more in terms of scalability. For the density-based method, once the modeling hypothesis and optimization parameters are set, the setup of the problem is independent of the scale. For the ground structure method, when the problem gets more complex much more time is required for setting-up the ground structure, as much more design variable needs to be created. Though, this could be scripted which would make the creation of ground structures much easier.

6.4.2 Computing Topology Optimization

The main disadvantage of the ground structure method is its limited design of freedom compared to the density-based method. Where the density-based method is completely free to propose any shape and path for the stiffeners, the ground structure is limited to the possibilities proposed in the design space. However, with a good sense and knowledge of the problem, it is not a complex task to propose a good ground structure.

For the same case study, the ground structure method takes around 5 hours per gradient-descent on a given computer, whereas a SIMP run on Optistruct takes about 2 hours per gradient-descent on the same computer. The two methods converge under a hundred iterations. For both methods, a hundred different initial values gave a good overview of the possible stiffening layouts.

Both methods use a gradient-descent solver, so they are very sensitive to the initial values of the variables. They are also capable of finding feasible solutions about 90% of the time, depending on the initial values of the variables. However, the ground structure method globally finds excellent layouts more efficiently than the density-based method.

6.4.3 Interpretation and Sizing

The interpretation of the ground structure results is straightforward, remove the stiffeners with a small density value and group together long and thin stiffeners that are close together. By nature, the results of the ground structure method are easily manufacturable as only these solutions are made available in the ground structure. The interpretation for the density-based method is the complete opposite, where good care and understanding of the results is necessary to interpret the material distribution correctly. This difficulty is mainly caused by the fact that density-based topology optimization usually results in very organic material distributions if not parameterized correctly.

This is emphasized by the fact that density-based topology optimization is not accurate in modeling the effect of stiffeners on the buckling of the panel, as shown in [223]. This is where the ground structure method shows its main advantage: its results can be directly translated into good light and strong stiffening layouts, with minimum interpretation is required to obtain lightest design.

As discussed in the introduction, the use of the density-based method resulted into few five- or six-stiffener configuration. It could easily have been missed by the design space exploration, whereas all the best solutions of the ground structure may be interpreted into a five- or six-stiffener configuration which are globally the best solutions.

6.4.4 Possibilities of Improvement

For the design of stiffened panels both the density-based method and this work's ground structure method has shown strength and weaknesses for which more research could help mitigate.

In the case of the density-based topology optimization, each increment of maturity of the method requires a lot of research, as it allows an overwhelming number of possible topologies. However, in terms of adding complexity in terms of model responses or automating interpretation it is very limited.

For the ground structure method, even though the design freedom is limited, there are a lot of improvements that could easily be incorporated. Due to the semi-discrete approach, it would be easier to implement analytical constraints to the optimization, such as crippling or controlled skin buckling. For design automation purposes, the ground structure process setup is simpler due to the already discrete components easily interpretable in the ground structure.

6.5 Conclusion

In conclusion, optimizing the topology of the stiffeners of a stiffened panel remains a challenge. With the ground structure method, it is possible to define a feasible design set of stiffeners and allow the optimization to find the placement and sizing in a single optimization run. The combined density-height variable, the stiffener activation variable, allows the gradient-descent to avoid the numerical errors associated with both independent variables.

The stiffened panels sizing optimization has shown that, compared to the density-based method, the ground structure method converge to the lightest solutions more often. The results are also easier to interpret and shows an excellent potential for complex design space and complex optimization constraints. Future work will integrate this method in a full wing-box optimization problem with multiple load cases.

CHAPTER 7 Article 4: Complexity-Driven Conceptual Exploration for Aircraft Structures (CD-CEAS)

Jean-François Gamache[a], Aurelian Vadean[a], Mario Capo[a], Thomas Rochefort-Beaudoin[a], Nicolas Dodane[b] and Sofiane Achiche[a]

[a]Polytechnique Montreal, 2900 Edouard Montpetit Blvd, Montreal, Québec, Canada
[b]Stelia Aéronautique Canada, Research & Technology, 12000 rue Henry Giffard, Mirabel, Québec, Canada.

Submitted to *Design Science*, on June 18th, 2021.

Abstract

Stiffener layout optimization for stiffened panels is currently an active area of research. Multiple works have used parametric and topology optimization to develop new layouts that seek to reduce the weight of the panels in aircraft assemblies. This work introduces a new algorithm based on generative design to propose new and efficient layouts quickly by leveraging lessons from generative design systems, topology optimization, axiomatic design and stochastic search. Generative design has three main properties that require an application of specific properties of generation, representation and exploration. The proposed algorithm leverages a novel functional complexity measure to rebalance the layout optimization process towards a more explicit generation, more accurate representation and increased diversification of the exploration. Two case studies of commonly used stiffened panels are done to showcase the performance of the algorithm. The results have shown that using complexity to drive exploration allows our algorithm to converge quickly to simpler and stiffer stiffener layouts.

7.1 Introduction

Reducing the weight of structures is an active challenge of the aviation industry, with the goal to reduce fuel consumption and thus increase the efficiency of aircraft transportation. The stiffened panel is the basic structural component from which assemblies are built, such as the fuselage, wings, control surfaces, etc. In industrial applications, stiffened panels are reinforced using orthogonally placed stiffeners, in what is called the orthogrid layout.

New analysis, optimization, design and manufacturing methods, such as electron beam free-forming, additive manufacturing and integrally machined stiffeners, have opened new oppor-

tunities for innovation in structural design. These new manufacturing methods offer a much larger design freedom for stiffener placement than traditionally assembled stiffened panels.

With traditional design and manufacturing methods, the only available layout is the orthogrid panels, which consists of orthogonally placed stiffeners. This layout has proven very effective in multiple industrial applications [58]. There are very few new layouts used in aircraft design, in part due to an increase in analysis and validation complexity and limited number of empirical data available for such layouts. Some good examples of new layouts are the buckling containment features (BCF) and the curvilinear stiffeners. BCFs were found to increase the strength to mass ratio of stiffened panels in certain regions of a commercial wing box [3]. BCFs and curvilinear stiffeners have been proposed from experience and intuition of engineers and researchers to improve the design of stiffened panels [27, 88].

The topological design space is large and complex to navigate. Consequently, traditional design and optimization tools are having trouble finding innovative ways to leverage the new manufacturing techniques. Since finding new effective layouts from experience has proven to be challenging, new numerical tools have been developed to explore the design space systematically and effectively. Some examples are the EBF3 optimization framework for curvilinear layouts [30] as well as the use of density-based topology optimization [38, 39]. Another proposed approach has been the use of grids of curvilinear stiffeners [84, 233].

In this line, the algorithm we propose will support the automation of the conceptual design phase of the layout of stiffened panels. Our algorithm is based on generative design, topology optimization, stochastic search, and complexity measures. We seek to improve on current topology and parametric optimization methods while proposing an efficient and effective technique.

7.1.1 Generative Design

In this work, we define generative design as the overall design process that leverages conceptual automation tools to assist the synthesis of conceptual design [54]. Said otherwise, generative design is an approach that leverages generative systems to explore and navigate a large and complex design space. The generative systems, for which we include computational design synthesis [115], topology optimization [2] and other generative design systems [54], are computational tools that can generate conceptual solutions from simple set of rules. Generative systems have the following properties:

1. They can generate complexity (the systems use base components to create emergent properties of the assembly);

2. They can generate solutions which have forms that are interconnected with their environment;
3. They can self-maintain and self-repair (i.e. it can adapt to changing environment);
4. They can generate innovative shapes or forms [54].

Many different generative systems exist, each with different capabilities. Out of the many ways of classifying them, we adapted the key properties proposed in [54] specifically for generative systems of structures. The three proposed properties are defined as follow:

Generation refers to the way the algorithm infers the architecture or structure of the solution from the description of the topological variables. Generative systems can use a range from implicit to explicit topological variables for generation.

Representation refers to the degree of fidelity used for performance evaluation of the generative system. A balance exists between low-fidelity and high-fidelity models, since capturing more complicated physics comes at the cost of increased computational costs.

Exploration refers to the balance between exploiting a small but promising region of the search space (Exploitation), and searching through a larger region for possible better optimum (Exploration). Using stochastic search vocabulary, exploration is discussed in terms of exploitation vs. exploration or also in terms of diversification vs. intensification [234].

These three properties are linked and the challenge is to balance them towards a specific need and application. Balancing the generative systems properties is about finding a compromise between them, as the decisions pertaining to these properties have a large impact on computation time and convergence. For example, using implicit variables makes for an easier implementation of gradient-based solvers, but at the cost of making high-fidelity representation more difficult and with a focus on exploitation rather than exploration.

In summary, generative design is about leveraging computational power and a generative system to explore a complex design space, which includes topological changes, with the goal of finding new innovative solutions from simple design rules. For layout optimization, there are many types of generative systems that could be used for generation, with topology optimization currently being widely used to inspire engineers [143]. To the best of our knowledge, conventional generative design techniques have not been used for the layout design of reinforcement in stiffened panel applications.

7.1.2 Topology Optimization

In structural engineering, topology optimization is currently used widely in multiple academic and industrial research projects [76, 141]. More specifically, it has been used for the design of many aircraft components such as wing, fuselage and sub-sysems [13, 38, 39]. Topology optimization is generally used during the conceptual design phase to inspire engineers towards new ways of designing structural components [102]. In current design practices, the Solid Isotropic Material with Penalization (SIMP) method is by far the most commonly used and is implemented in many commercial software [78, 79].

As a generative system, SIMP has to compromise on the same three properties described in the last section, generation, representation and exploration. This balance is discussed here. SIMP uses an implicit generation, so the topological variables are implemented as a density variable assigned to each finite element of the optimization model. This is the main strength of SIMP, as this implicit generation makes the optimization setup very adaptable and flexible to any type of structural problems. However, this also means that the representation is generally low fidelity, as higher fidelity models are more difficult to implement [191]. There are few publications that effectively leverage higher fidelity physics such as buckling, fatigue or non-linear geometric properties during SIMP optimization [235]. The use of lower fidelity models can make SIMP converge towards sub-optimal solutions for applications such as stiffened panels [236]. As for the exploration capability of SIMP, it is fairly limited. Users are only able to modify the optimization parameters, filters and boundary conditions to expect different optimized material distribution. As done in [236], using different initial values is the only way to expect different layout. Meanwhile, this method is inefficient in terms of exploration, often the same layouts are produced. As SIMP uses a gradient-based solver, it is predictably more exploitation focused. Using SIMP for design, the topology is inferred from the implicit optimized material distribution to create a more explicit model for further analysis, where higher fidelity models can be used more easily.

In our research we have found that the low fidelity representation and the low exploration of SIMP has led to underperforming results for the design of stiffened panels which are very sensitive to non-linear constraints such as stress and buckling constraints, but also to imperfections [236]. To improve this, our research group also tried implementing a ground-structure approach, which offers a slightly more explicit generation and a higher fidelity representation but requires much more computing time for exploration [237].

More recent topology optimization techniques are the level-set method (LSM) and the moving morphable component (MMC) [4, 5]. They both use more explicit generation techniques, but still with low-fidelity representation and gradient-based solvers with low exploration

capabilities. The LSM method uses an explicit description of the material boundaries and the MMC method an explicit description of the sub-components [4, 5]. All of the current topology optimization techniques don't have completely explicit generation capabilities, as the connectivity of the sub-components are always inferred and controlled only indirectly with density, thickness, boundaries or subcomponents. A completely explicit generation techniques would be to use graphs to include connection data during generation. We will discuss this in more depth in the section 7.4.

The main limitation to exploration for topology optimization is related to the use of gradient-based solvers which are not effective for exploration, as they are more effective for exploitation [73]. In most application cases, topology optimization leverages a compliance-based optimization formulation, with compliance defined as the inverse of stiffness and measured as the total strain energy [141,238]. The compliance formulation has a convex design space for which gradient-based solvers can effectively find the global minima independently of the initial variable values [2]. For the case of stiffened panels, however, the proposed material distribution is often highly complex and challenging to interpret and manufacture. Furthermore, in the case where non-linear constraints are added, the solver can only find local minima [236,237].

7.1.3 Conventional and Performance-based Generative Systems

Conventional generative systems are defined by their lack of performance evaluation driving the generation of concepts, that is the performance is still evaluated, but only once all the concepts have been generated [54]. As such, the biggest advantage of conventional generative systems is that they are able to quickly generate solutions respecting design rules without using computationally expensive performance evaluations [53]. However, these systems require a "filter and select" algorithm to navigate the solution space [105]. For generation, there are many techniques used in conventional generative systems, such as the shape, design or graph grammars, L-systems, cellular automata, etc. [54]. Grammars are tools used often in the architecture, engineering and construction industry, in which their ability to create new interesting shapes that respond to specific requirements has great potential [54].

Performance-based generative systems offer more robustness than conventional generative systems by using performance analysis throughout the design exploration [127]. Focusing on performance allows the system to generate mostly feasible solutions, making the job of engineers during the synthesis for concepts much easier, with less filtering and selecting [127]. Still, evaluating performance accurately comes at the cost of much more computing power which reduces the total number of solutions. Depending on the generative system, slowing down for accuracy can greatly reduce the innovation and exploration of the systems.

Meta-heuristic optimization algorithms, such as the genetic algorithm and particle swarm optimization, are widely used in performance-based generative systems for design exploration [128].

There are few works that leverage lessons from generative systems with topology optimization applications. A good example of a generative system as topology optimization is the work of Hooshmand & al. [136], where they leverage a graph-grammar with context-sensitive heuristic rules to drive the exploration towards optimized topologies for the design of truss and cable assembly.

7.1.4 Scope of this Work

This work focuses on the development of a generative system that has the ability to do layout optimization of the reinforcement of stiffened panels. We mainly focus on finding a balanced approach in terms of generation, representation and exploration. To achieve this balance, we leverage lessons from many engineering disciplines.

For the generation, we use a graph-grammar which can create many reinforcement layouts from action and rules. This allows for a quick explicit generation of layouts that also ensures significant topological changes for each generation. In this work, the generation is implemented in Matlab. [239].

As the generation is done via an explicit method, the choice of the fidelity of the representation is flexible. We use an automation script to create a finite-element model for each proposed solution. As the model can be output automatically, any fidelity level can be used, from simple linear static to non-linear geometric analysis. We limit our case studies to linear static displacement and linear buckling evaluation, as to keep computation time low. HyperMesh and Optistruct from Altair are used to create and evaluate each model [78]. The automation is implemented via the TCL scripting capabilities of HyperMesh [78]. Furthermore, to ease the comparison process, we couple the evaluation with a sizing optimization, as this ensures layouts are comparable to each other for a given property, be it weight, compliance or linear buckling.

Finally, as for exploration, this work uses a novel relative functional complexity measure as one of the objectives to drive the design space exploration. This ensures that novel design proposed by generative design can be easily applied in an industrial context. The multi-objective search is done using the basic Burst algorithm, a stochastic search approach for graph-grammars [8]. The exploration is also implemented in Matlab [239].

We have named the generative system we developed the “Complexity-Driven Conceptual Ex-

ploration for Aircraft Structures", CD-CEAS for short. In summary, CD-CEAS is a two-step optimization process, with the layout optimization being done using an exploratory stochastic approach completed with a sizing optimization to measure and compare the performance and complexity of each layout. The general algorithm and data exchange structure of the CD-CEAS algorithm are illustrated in fig. 7.1.

In this paper, we will first discuss the source and usage of the proposed functional complexity measure. We then develop how the generic complexity measure is applied for the specific case of layout optimization of stiffened panels. This is presented in parallel with the description of the inner sizing optimization loop. From there, the discussion focuses on the graph-grammar generation algorithm. Our implementation of the basic Burst algorithm is explained with the adaptation necessary for complexity-driven search. Finally, two case studies of common usage of stiffened panels are proposed to showcase the efficiency of CD-CEAS. The first focuses on a rectangular pressure bulkhead and the second on a highly compressed and buckling sensitive panel.

7.2 Complexity Measures for Optimization

In the topology optimization community, some research groups have implemented complexity constraints to topology optimization. In density-based topology optimization, size filters are considered complexity limits [240]. In the ground-structure method, the number of nodes, edges and connections are used to measure and constrain geometric complexity [241]. In LSM, the complexity is calculated depending on the number of basis functions [177]. Finally, for MMC, complexity is measured by the number of effective components [242] In summary, in the topology optimization community, complexity is only measured with regard to the geometry of the solution.

Measuring design complexity is an active area of research, with perspectives from many different disciplines [47, 243–246]. In this work, we focus on the definitions used in axiomatic design for conceptual design [47]. As such, complexity is not only related to geometry, it also becomes dependent on the specific problem. Thus, the measure we propose is relative and allows for an easier synthesis of multiple solutions with respect to a specific problem. The complexity measure leverages the concepts of functional requirements (FR), design parameters (DP) and the design matrix of the sizing sub-problem, rather than the geometry of the solution alone. This allows for functional complexity that is relative to the specific design problem. Before introducing the complexity measure, it is necessary to introduce some key concepts of axiomatic design.

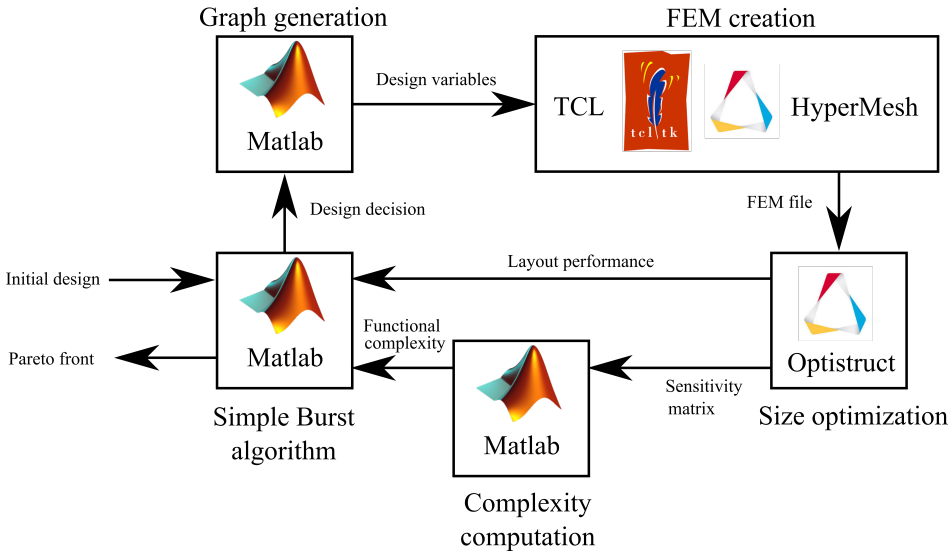


Figure 7.1 General process of the CD-CEAS approach.

7.2.1 Introduction to Axiomatic Design

Axiomatic design is born out of a need to create a systematic approach for the design process [47]. Since its introduction, axiomatic design has been used in a wide variety of product design, from software to engineering systems [47]. Axiomatic design is offering an alternative to the trial and error approach and is part of the first-time right paradigm [46]. It is used for both product creation and concept improvements, focusing mainly on efficiency and robustness [247]. In summary, axiomatic design provides a framework to understand the effect of design on the quality of the product. In other words, it makes sure that *you do the right things and that you do things right* [46].

One of the main aspects of axiomatic design is the separation of the design activity into four domains, with the following properties:

Customer attributes (CA) The needs and desires of the customer,

Functional requirements (FR) The well-defined required function and sub-functions of the product that will fulfill the CAs,

Design parameters (DP) The solutions selected to address the FRs,

Process variables (PV) The process (e.g. manufacturing, implementation, or resources) through which the DPs are realized.

For the complexity measure, we focus on the relationship between the FRs and DPs, which is characterized and given by the design matrix (**A**). The design matrix can help identify the

types of Information that is present in the current concept. (see eq. 7.1). The design matrix may be built in two different ways, either as a set of linear equations or using the differential relationship of each FRs with respect to each DPs (see eq. 7.2). In this work, we use the differential design matrix.

$$[\mathbf{FR}]_m = \mathbf{A}[\mathbf{DP}]_n \qquad (7.1) \qquad A_{ij} = \frac{\delta FR_i}{\delta DP_j} \qquad (7.2)$$

In addition to the domains, there are two identified axioms that stand as the basis of axiomatic design: the Independence and the Information axioms [47]. The first axiom stipulates that a good design maintains independence between the FRs. The second axiom puts emphasis on the need to minimize the Information content of the design. Here, the Information content is defined as the probabilistic relation related to the number of combinations which leads to uncontrolled FRs with respect to the DPs [47]. Said otherwise, the Information content of a design reflects the probability of DPs not satisfying every FRs.

Using these axioms as starting points, Suh has defined complexity as the difficulty to fulfill these two axioms in a single design [47]. Further work by Puik & al. has extended this idea, by developing a design complexity theory that uses Information content as its focus point [222]. Their theory separates design Information into different categories, providing a framework to understand complexity:

Unrecognized Information is the unrecognized coupling between FRs and DPs that leads to unexpected complexity. This Information content becomes recognized when erratic behavior happens during product testing,

Recognized Information is the recognized coupling relations between FRs displayed in the design matrix,

Axiomatic Information is the uncoupled or decoupled information that is due to a difference in design and system ranges. It deals with the probability of DPs to satisfy the FRs. Is usually addressed by robust design and optimization techniques,

Superfluous Information has no effect on the relations of FRs and DPs,

Useful Information the total information that affects the relations of FRs and DPs [222].

We seek to propose a functional complexity measure that can be used for our problem to compare different solutions to the same problem, thus have the same set of functions (FRs).

Traditionally, the visualization of the design matrix allows engineers to categorize solutions between coupled (challenging), decoupled (acceptable) and uncoupled (ideal) solutions [47]. See eq. 7.3, 7.4 and 7.5 for the possible coupling levels observable in the design matrix. Uncoupled solutions are the easiest solutions to implement, as no coupling between DPs can perturb the FRs of the design thus making design straightforward.

Uncoupled Matrix

$$\begin{bmatrix} X & 0 & 0 \\ 0 & X & 0 \\ 0 & 0 & X \end{bmatrix} \tag{7.3}$$

Decoupled Matrix

$$\begin{bmatrix} X & X & X \\ 0 & X & x \\ 0 & 0 & X \end{bmatrix} \tag{7.4}$$

Coupled Matrix

$$\begin{bmatrix} X & X & X \\ x & X & x \\ X & x & X \end{bmatrix} \tag{7.5}$$

In axiomatic design literature, there are two measures based on the design matrix for assessing the coupling of the design matrix: re-angularity (eq. 7.6) and semi-angularity (eq. 7.7) [248]. Re-angularity measures the coupling of each FRs, with respect to all DPs [248]. In the design matrix, each row represents a FR vector and each column a DP vector [248].

Re-angularity measures for each pair FR vector the angle between them. As such, if the FR vector is the same as another the value of the pair becomes 0, indicating coupling. As the re-angularity multiplies the angle of each pair of FR vectors, any value indicating coupling (thus 0) makes the measure 0, thus showing a coupled system [248].

In a similar fashion, semi-angularity can detect if a system is decoupled or uncoupled [248]. It measures the relative size of the diagonal members of the design matrix, with other DPs of a given FR vector [248]. If all DPs have similar effects on a given FR, there are no dominant DP. Otherwise, if only a single DP has a significant effect on a given FR, then it is considered dominant. If only one vector FR_i measures a non-dominant DP_j, then the semi-angularity measure quickly tends to zero [248].

$$\mathbf{R} = \prod_{\substack{i=1,n-1 \\ j=i+1,n}}^{n} \left[1 - \frac{(\sum_{k=1}^{n} A_{ki} A_{kj})^2}{(\sum_{k=1}^{n} A_{ki}^2)(\sum_{k=1}^{n} A_{kj}^2)} \right]^{1/2} \tag{7.6}$$

$$\mathbf{S} = \prod_{j=1}^{n} \frac{\|A_{jj}\|}{(\sum_{k=1}^{n} A_{kj}^2)^{1/2}} \tag{7.7}$$

Both of these measures are not meant to measure the relative complexity of a given system, it merely classifies the design matrix in one of the three coupling categories. Still, we keep in mind what they are trying to measure: the coupling of FRs, or simply the recognized Information content in Puik's framework.

7.2.2 Complexity Measure for Complexity-Driven Exploration

This work uses the Information complexity framework proposed by Puik & al., which was discussed in section 7.2.1 [222]. Note that our goal is not to directly measure the Information content of each design, but to develop indirect approximations that correlate with the Information content. Unrecognized Information cannot be identified using only analytical data, but the three other types (recognized, superfluous and axiomatic) can be approximated to reduce unnecessary complexity.

In this section, the three approximations are introduced, with the symbol Ψ representing a complexity approximation. These approximation will be aggregated using a simple euclidean norm to approximate the useful (or total) Information content, see eq. 7.8.

$$\Psi_U = \sqrt{\Psi_A^2 + \Psi_R^2 + \Psi_S^2} \tag{7.8}$$

where Ψ_U is the useful Information content, Ψ_A the axiomatic Information content, Ψ_R the recognized Information content and Ψ_S the superfluous Information content.

Let's start by approximating the recognized Information content, which is the coupling of the FRs with respect to DPs. Said in mathematical terms, we seek to measure the collinearity of the FR vectors in the design matrix. A good tool to measure the collinearity of vectors is the matrix conditioning number. In this work, we start from a generic definition (see eq. 7.9) [249]. This conditioning number uses the singular value decomposition (SVD) to measure is any collinearity in the design matrix. For our implementation, we can use the function *cond()* natively provided in Matlab [239].

$$cond(\mathbf{A}) = \frac{max(SVD(\mathbf{A})}{min(SVD(\mathbf{A}))} \tag{7.9}$$

However, this definition only uses the extreme (min and max) measures of the matrix and as such can only identify if there is any collinearity or not at all. It is a very useful measure of the complexity of computing the inverse of an arbitrary matrix, but not a good measure of recognized Information. Consequently, as a recognized Information measure, we propose a normalized sum of all SVD components, see eq. 7.10.

$$\Psi_R = \frac{\sum_{i=1}^{n} \left[1 - \left(\frac{SVD(\mathbf{A})_i}{max(SVD(\mathbf{A}))}\right)^2\right]}{rank(\mathbf{A})} \tag{7.10}$$

where Ψ_R is the recognized complexity, the SVD operation returns the singular value de-

composition vector and the *rank* operation is the size of the design matrix. This measure of recognized Information content is relative. When Ψ_R goes to zero, there is no collinearity, as all the SVD terms are one. If there are multiple collinearity detected, then the measure goes up to one.

Another aspect that is useful to measure is the axiomatic Information, that returns how difficult it is to realize the functions with a given set of DPs. It is an indirect measure of the robustness of the DPs with respect to the FRs. To measure axiomatic Information, we use the condition number of a non-linear function [249], as defined in eq. 7.11. The condition number of a non-linear function reflects the sensitivity of the FRs with respect to the DPs [249].

$$\Psi_A = \frac{\|J(\mathbf{x})\|}{\|f(\mathbf{x})\| \,/\, \|\mathbf{x}\|} \tag{7.11}$$

where Ψ_A is the axiomatic complexity, $J(x)$ the Jacobian matrix of the sizing problem at the local optimum, $f(x)$ the performance at the local optimum and x the DPs at the local optimum. The euclidean norm was used for this equation, but any matrix and vector norm can be used. As we use the differential notation of the design matrix $\mathbf{A}$, we can simply replace the design variable as the Jacobian $J(x)$ in the axiomatic complexity equation. From our experiences, Ψ_A usually varies between 0 and 5. When Ψ_A goes closer to zero, it means that big variations of DPs have a low impact on FRs. As it gets higher, the impact of DPs get bigger on FRs, making the design more complicated to manage.

Finally, superfluous Information can arise when some DPs have no impact on the FRs, they just make optimization more difficult. As such, we define the amount of superfluous Information using a threshold (we use 10%) on the norm of the vector of the influence of each DPs, as shown in eq. 7.12.

$$\Psi_S = 1 - \frac{rank(\mathbf{A}_{reduced})}{rank(\mathbf{A})} \tag{7.12}$$

where $\mathbf{A}_{reduced}$ is the reduced design matrix, from which DP vectors with a norm below 10% of the maximum vector norm of A are removed.

Unrecognized Information is not captured in the design matrix, and as such we are not able to measure it. Still, solutions with low complexity, that is with a low recognized, axiomatic and superfluous Information will have an easier time managing the added Information that can arise during testing, production and maintenance.

In summary, all of these Information content approximation and be used to approximate a relative complexity measure. Useful information as a complexity measure can be used for

any design problem where the design matrix can be computed in its differential form. In the next section, we introduce how panels with different layout reinforcements are sized and evaluated and also how we use this sizing step to create the differential design matrix used for complexity assessment.

7.3 Performance Evaluation Implementation for Stiffened Panels

For the CD-CEAS algorithm, we need to be able to measure performance and complexity automatically for any layouts created. In order to do so, we present here how we deal with the FRs, constraints and performance of stiffened panels using the finite-element method. Stiffened panels are composed of multiple subcomponents; the main component is the skin to which stiffeners are added in order to increase strength, stiffness and stability [26]. The stiffeners can be built in different ways, but generally have a pad-up section attached to the skin, a web that is perpendicular to the skin and a free flange to increase the stability of the stiffener (see fig. 7.2). The panels are periodically attached to bigger assembly components such as the spars and ribs [26].

As the stiffened panels are built using thin sheet metal or laminated composite components, buckling stability, imperfections and out-of-plane forces are the main concerns for their design [58]. The most used design method for stiffened panels is based on handbooks [26, 58] which contains important relations and equations for the orthogrid configuration. For example, analytical and semi-empirical equations exist to predict skin and Euler buckling, as well as Euler-Johnson's post-buckling collapse [26, 58].

Current evaluation methods for stiffened panels uses semi-empirical equations, which are only adapted for orthogrid panels [58]. In this work, we require a more flexible modeling approach to be able to model any layouts. This is why we are using the finite-element method, which

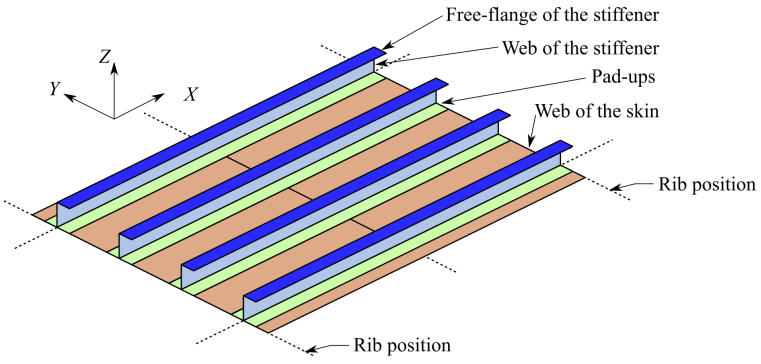


Figure 7.2 Sub-Components of the Stiffened Panel

is very flexible and adaptable [78]. The modeling is done using HyperMesh and the solving with the Optistruct FEM solver [78].

To help with the synthesis and comparison of the different layouts, a sizing optimization was added to the performance evaluation. For this, we also use Optistruct, which includes a family of efficient gradient-based solvers. The sequential quadratic programming (SQP) method is used for the sizing problem. Even though the constraints of the sub-problem are non-linear, our experiences have shown a good convergence toward the global minima of the sub-problem, showing that the problem is rather convex.

The objective of the sizing optimization can vary depending on the problem. It can be a weight minimization with regard to non-linear constraints, or a simple compliance minimization given a certain weight constraint. The exact formulation of the sizing optimization depends on the case study, which we will discuss in section 7.6. At the optimum obtained from the sizing, it is possible to measure complexity as described in section 7.2.2. We use the optimization module of Optistruct to run and extract the sensitivity matrix. Optimization responses and variables are used as approximations of FRs and DPs.

Compliance, the inverse of stiffness, is often used in topology optimization as the main optimization objective [2]. It allows for a fast convergence towards not only stiff, but coherent concepts [2]. In topology optimization, a coherent concept ensures structural stability (e.g. no unexpected possible displacement) and connectivity of boundary conditions. A minimal compliance for a given volume is a good indicator of the capacity of a structure to maintain integrity. While topology optimization commonly measures the compliance of the whole structure by measuring the total strain energy, we instead deal with local skin and stiffener segments. As such, in this work we define the FRs of the stiffened panel as the stability of each component, that is each skin and stiffener sections (measured as their local compliance). The DPs of a given layout are defined as the thickness of each sub-components. Any other responses, such as weight, stress, buckling or fatigue, can be considered constraints and consequently they are not required to adhere to the design axioms [47].

Using local compliance measures as the FRs allows the algorithm to build the design matrix simply by using the sensitivity analysis of the sizing optimization with regard to the thicknesses and compliance of each sub-component, see eq. 7.13.

$$\mathbf{A_{SP}} = \begin{bmatrix} \frac{\delta C_1}{\delta t_1} & \cdots & \frac{\delta C_1}{\delta t_n} \\ \vdots & \ddots & \vdots \\ \frac{\delta C_m}{\delta t_1} & \cdots & \frac{\delta C_m}{\delta t_n} \end{bmatrix} \tag{7.13}$$

where $\mathbf{A_{SP}}$ is the design matrix of a given stiffened panel, C_i denotes the compliance of each sub-component and t_j their thickness. With this applied design matrix, it is possible to use the complexity measure presented in sec 7.2.2. The sensitivity matrix of the sub-sizing problem is used as the design matrix, the FRs as the local compliance measures ($\mathbf{C}$) and the DPs as the thickness ($\mathbf{T}$) of each sub-components. See the updated equations 7.14, 7.15, 7.17 and 7.17.

$$\Psi_{R,SP} = \frac{\sum_{i=1}^{n} \left[1 - \left(\frac{SVD(\mathbf{A_{SP}})_i}{max(SVD(\mathbf{A_{SP}}))}\right)^2\right]}{rank(\mathbf{A_{SP}})} \tag{7.14}$$

$$\Psi_{A,SP} = \frac{\|\mathbf{A_{SP}}\|_2}{\|\mathbf{C}\|_2 \,/\, \|\mathbf{t}\|_2} \tag{7.15}$$

$$\Psi_{S,SP} = 1 - \frac{rank(\mathbf{A}_{SP,reduced})}{rank(\mathbf{A_{SP}})} \tag{7.16}$$

$$\Psi_{U,SP} = \sqrt{\Psi_{A,SP}^2 + \Psi_{R,SP}^2 + \Psi_{S,SP}^2} \tag{7.17}$$

Until now, we have described a general functional complexity measure and then how it can be used for a sizing optimization problem of a stiffened panel with any layout.

7.4 Graph-Grammar for Stiffened Panels

In generative design, graph-grammars are used to generate design concepts from explicit design actions and rules that affect each component and their relationships. There are multiple types of graph-grammars. In this work we have chosen to work on a set grid with a simple graph-grammar composed of only one possible type of action and few rules. We use a fixed grid for two reasons. First, it allows for an easy implementation of a "bar code," which is a unique ordered string that describes the topology of the layout. This bar code ensures that the search algorithm does not explore the same solution twice, via different decisions. Secondly, fixed-grid solutions are much easier to work with for a reinforcement learning algorithm, which will be studied in the future in our research group.

Using this grid, the only available action for our grammar is named "CreateStiffener," which has to respect certain rules before being applied. This action creates an edge and connects two nodes on an existing grid, activating each node it passes through. See fig.7.3 for an example of actions with a 5x5 grid. To define the rules of our implementation, each node of

the fixed grid has a specific status. They are either “active,” “offset,” “side” or “inactive.” "Active" and "Inactive" refer to nodes with or without a connected edge respectively “Side” nodes are a special case of “active” nodes, i.e., they are always considered active but will only allow the action “CreateStiffener” between nodes of different sides. “Offset” nodes are semi-active nodes, in the sense that if a stiffener passes in their area of influence, the “offset” node becomes available for connection and their position is modified to be at the crossing of the new stiffener. Implement the “offset” nodes allows the identification a graph independently of the sequence of rules required to get there.

With this single action and rules, the graph-grammar can create a graph representation of any piecewise linear stiffening layout. From this graph representation, we can convert the position of nodes and edges connectivity into a parametric file that is passed to a TCL script that builds a FEM model of the given layout using HyperMesh automation capabilities [143]. The TCL script also calls Optistruct for the sub optimization problem. Also, as the node positions are described on a grid from 0 to 1 in 2D, the TCL script can easily extrude the stiffeners with respect to the normal of any planar or curved plane using a bilinear projection.

This graph-grammar is more explicit than the discrete ground-structure approach for a simple reason: The decisions are not made for each single edge, the graph is not fixed, only the grid. The algorithm is able to create stiffeners, by connecting edges without preexisting connections. This ensures that significant topological changes are made at each decision. A major advantage of the graph-grammar is that the description of the layout is independent of the sequence of rule application, which makes for a much easier design exploration. In the future, this means that more complex actions could be built, such as places a grid, copy an existing pattern, mirror a set of patterns or even use curvilinear stiffeners.

Still, one limitation is to be noted. As the grid is fixed, where more than one stiffener passes near an “offset” node, the offset is removed and all the edges connect at the fixed node. This ensures that a given layout is the same, independent of the order of previous decisions. So, for a more “precise” description, a finer grid of nodes can be used, although it significantly increases the design space. For this current study, a limit to 10x10 grids is set, which is still more than enough to find interesting solutions for simple stiffened panels. We also implemented a symmetry option, which helps reduce the size of the problem.

The graph-grammar is implemented as a class in Matlab. This class is capable of returning a list of possible actions that responds to the design rules, and in the next section we describe the algorithm used to choose which actions to take in this list.

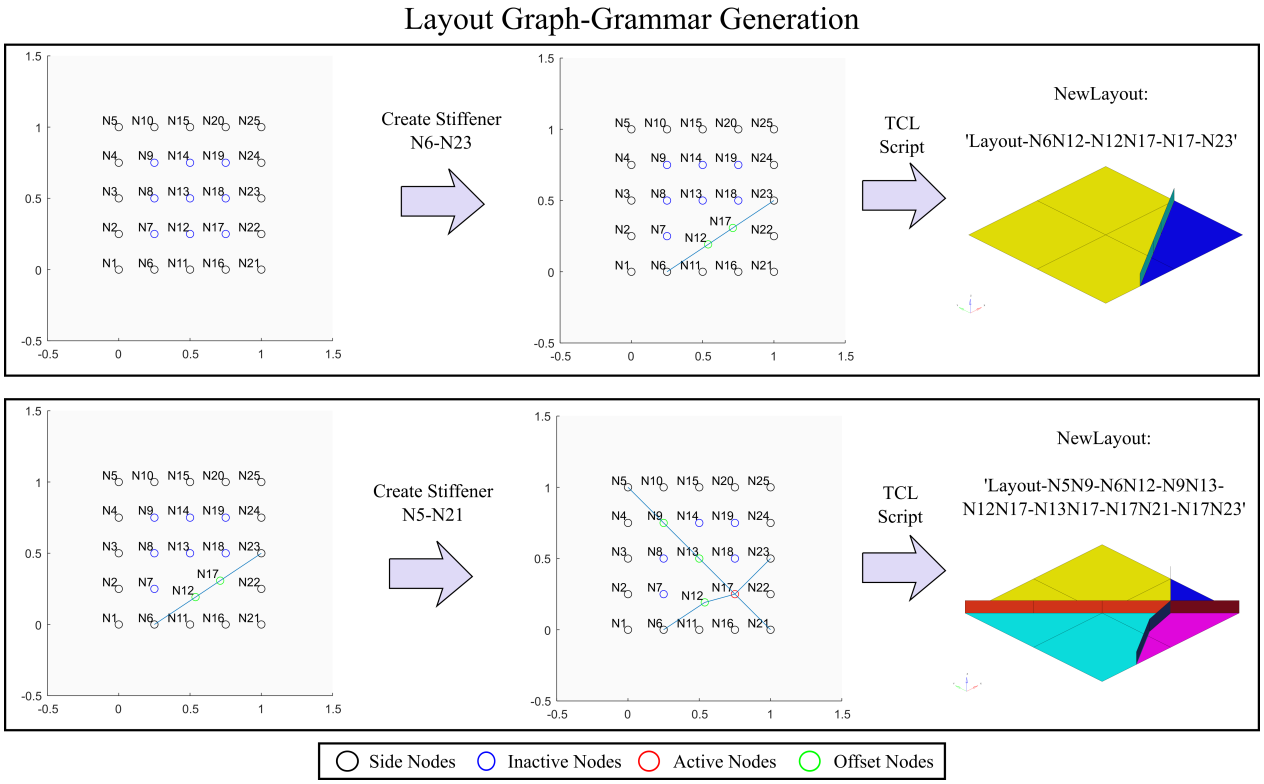


Figure 7.3 Generation of graph representation and conversion to FEM from the application of the action “CreateStiffener”. We show the application of the same action on two different nodes. On top, we see that there are no intersections, as such the grammar rules allows the grid to adapt to the stiffener with "Offset Nodes". On the bottom, two stiffeners intersect, and the grammar rule forces the node to get back to its initial position as an "Active node". The illustrated model has an aspect ratio of 1:1, but it is possible to easily change the conversion to other surfaces.

7.5 Complexity-Driven Basic Burst-Algorithm

The list of possible actions for any layouts is large. Therefore, the stochastic search process is about searching effectively through a decision tree with controlled random decisions that reduces the total amount of required performance evaluations. Commonly used stochastic search algorithms are the greedy search, random search, random walk, evolutionary algorithms, etc [234]. The choice of a search algorithm is driven by the need to balance randomized and goal-directed search, that is decide which is more important in terms of exploration vs. exploitation or in terms of diversification vs. intensification [234]. For our case of multi-objective graph-grammar search, we found that the Burst algorithm provided simple parameters that can be leveraged to find this balance [8]. A basic and advanced version of the Burst algorithm are proposed in [8]. Simply put, the burst algorithm is a stochastic search that explores in "bursts", in a similar fashion to a greedy search. Its particularity is the Pareto front it uses to solve a multi-objective problem. Furthermore, the use of "burst" makes the algorithm easy to run with parellel computing.

For the sake of simplicity, this work uses our own implementation of the basic Burst algorithm. A possible future improvement for CD-CEAS could be to implement the advanced Burst algorithm which improves search by using a similarity measure between graphs [8].

Our implementation of the basic Burst algorithm is illustrated in fig. 7.4. The algorithm is initialized with any number of initial layouts that are placed in the archive. Throughout the search, the archive will contain all layouts and their properties. At each iteration, the algorithm randomly chooses a "burst" of decisions available in the grammar, thus generating N new layouts. For each of the new layouts the performance and complexity is computed in parallel and added to the archive. N can easily be scaled to the number of cores available in the user's computer or server. A Pareto Front is then built or updated from the layouts in the archive. In our implementation, we used the script available from the MathWorks file exchange [250]. We added a condition to ensure that each layout of the Pareto front is chosen at least once for improvements at each iteration. As we found the Pareto front to be too small at the beginning of the search, a relaxation mechanism was used; if the number of layouts on the Pareto front is smaller than $N * r$, where r is the relaxation parameter, we redo the Pareto evaluation on the remaining non-dominant layouts. This step is repeated until there are at least $N * r$ layouts in the active search set. In our test cases, it was found that using $r = 1/3$ yields a good balance between exploration and exploitation. In short, N and r are search parameters that can be used to tune exploration vs. exploitation and diversification vs. intensification. If we increase the values of N, there are going to be more decisions made from a single set of layouts without looking at performance. This can increase exploration

and diversity, at the cost of more evaluations that might lead to uninteresting layouts. At the opposite, small values of N will make the algorithm behave more like a greedy search, thus improving the intensification, at the cost of diversification. The only other search parameter is the stopping criteria $Archive_{max}$ which is simply the maximum number of created layouts.

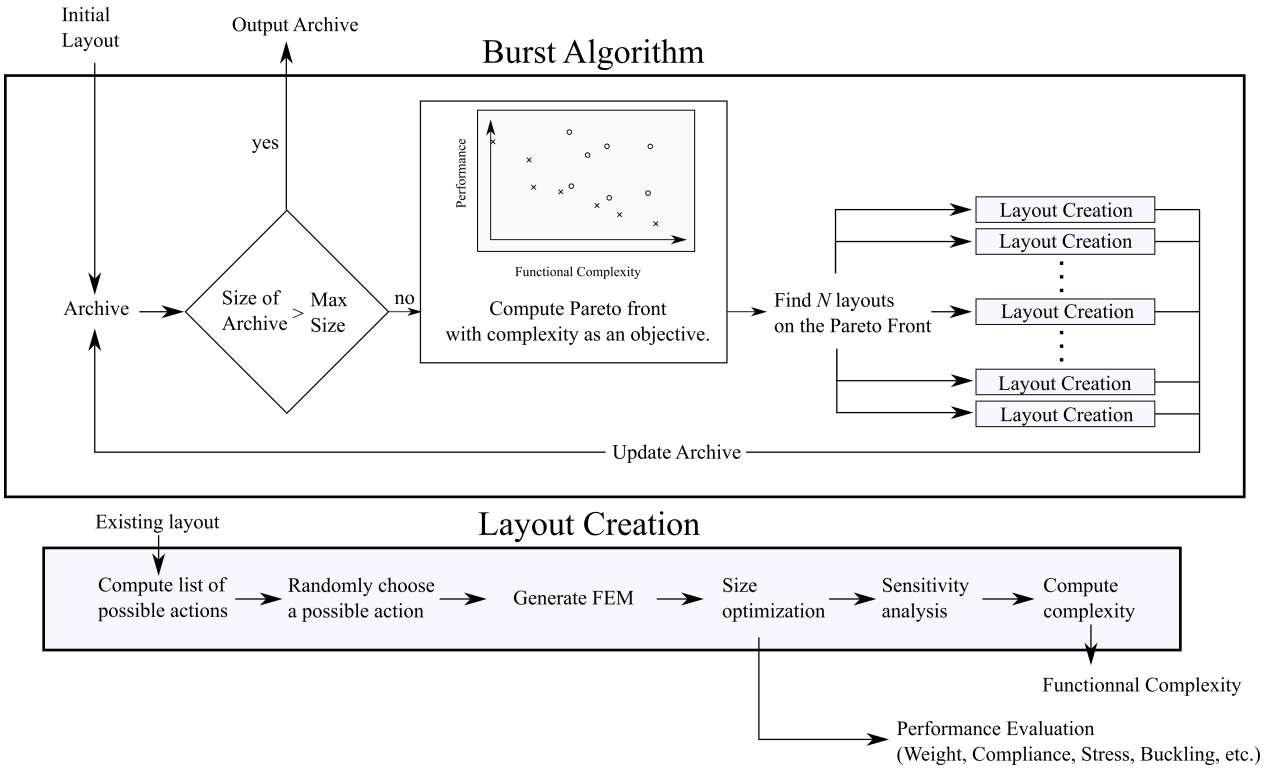


Figure 7.4 Our implementation of the basic Burst algorithm. [8]

In summary, CD-CEAS introduces a combination of many interesting mechanics that together have a great balance of generation, representation and exploration. The relative complexity measure is used to focus on exploration as well as to encourage the search algorithm to find simple solutions. The graph-grammar allows for a generation of solution that is uncoupled from the performance evaluation, as the representation of the problem is done using a simplified size optimization for each proposed layout. And finally, our implementation of the basic Burst algorithm is used to explore the design space, with a good balance of diversification vs. intensification.

The next section will demonstrate the capabilities of the algorithms of some difficult topology optimization problems for which our research teams have had many challenges in the past [196, 237].

7.6 Case Studies of CD-CEAS

In this section, we propose two different case studies of common loading conditions of stiffened panels: a pressurized bulkhead and a highly compressed wing section panel of a wing section.

The only element that changes between the examples are the boundary and load conditions. Even then, the case study have very different design spaces but for which CD-CEAS can find adequate results. Furthermore, a comparison with the SIMP method for the pressurized bulkhead and handbook optimization for the compressed wing section are presented.

7.6.1 Pressure Bulkhead with Out-of-plane Loading

The pressure bulkhead is a known difficult challenge for topology optimization [196]. In aircraft, bulkheads are at the front and back of fuselages to keep a stable pressure in the cabin during flight operations. It is usually round, but was kept as a square panel in this study for the sake of simplicity.

Description of the problem

The graph-grammar actions and rules are the same as presented in the section 7.4. The plate is flat on the X-Y plane and the boundary conditions are simply supported ($U_Z = 0$) on all sides, see fig. 7.5. Pressure is applied evenly on all the plate as a distributed normal force. For the sizing optimization, the weight constraint is set to 5.0 lb. with a compliance minimization objective. The value of the pressure is arbitrarily set to 10 psi. An arbitrary pressure doesn't have any impact on the solution in the case of compliance minimization, as compliance measure is directly proportional to the applied loads. Aluminum 7075 was used and its properties are found in table 7.1.

As a layout reference, we ran the SIMP method with Optistruct [78] and converted the results to an explicit stiffened panel, see fig. 7.6. The results for the SIMP results can be found in table 7.2. Finally, the Burst and graph-grammar parameters are defined as follow for the pressure bulkhead case:

Evaluation per iterations $[N]$: 8
Maximum Evaluation $[Archive_{max}]$: 500
Relaxation $[r]$: 3
Graph Grid Size : 10x10
Symmetry : From the center line in both X and Y axis

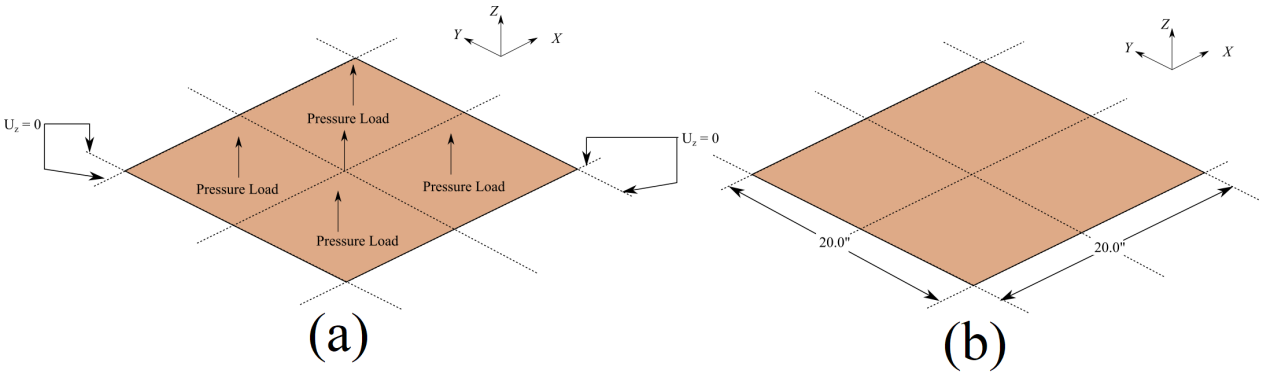


Figure 7.5 Test case of a stiffened panel with a uniform pressure, with simply supported boundary conditions. (a) The pressure load is applied uniformly on the whole panel. (b) The panel dimensions. Where U_z is the imposed displacement.

Table 7.1 Aluminum 7075 properties [59]

Property	**Value**
Young's Modulus (E_0) $[ksi]$	$10,700$
Poisson's ratio (ν) $[-]$	0.33
Yield limit (F_{cy}) $[ksi]$	68
Material Density $\left[\frac{lb.}{in^3}\right]$	0.10

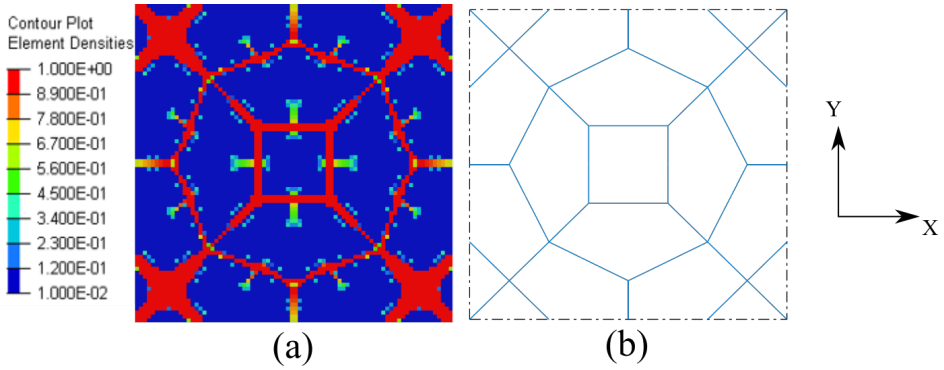


Figure 7.6 (a) Material Distribution using SIMP (b) Interpretation as a stiffened panel, shown as a graph.

Table 7.2 Properties of the model created from an SIMP interpretation

Property	**Value**
Weight [lb.]	5.0
Compliance [lb.in.]	57
Functional Complexity (Ψ_U)	1.8

Based on our extensive tests, these parameter offer a good balance between exploration and exploitation. With these parameters, computation time is 25 minutes with an AMD Ryzen 7 3700X @4.0GHz, running the eight layout evaluation in parallel on the eight cores.

CD-CEAS Results for the Pressure Bulkhead

The results of CD-CEAS for the pressure bulkhead are presented in different ways. First, the layouts of the final Pareto set are presented in fig. 7.7. Then, the performance of the entire archive is presented in fig. 7.8a. Finally, the convergence plot of the compliance is shown in fig. 7.8b. It is possible to see that convergence is obtained quickly, in fewer than 20 iterations.

Of course, using a stochastic search approach is highly dependent on the random choices the algorithm makes during exploration. It is possible to see in fig. 7.7 that the obtained layouts share some similar patterns. We have rerun the search with the exact same parameters and initial layout, for which the solutions of the Pareto front are illustrated in fig. 7.9.

The best CD-CEAS result has a compliance of 37 lb.in., a reduction of 35% in comparison to the layout found with SIMP. However, it comes at the cost of a much more complex solution. If we chose a layout similar in complexity at $\Psi_U \approx 1.7$, the third layout of fig. 7.7 with $\Psi_U = 1.62$ has a compliance of 41 lb.in., still a reduction of 28% in compliance for a similar relative complexity. Thus, in both cases, CD-CEAS is able to find solutions that are both stiffer and less complex than the results obtained with SIMP.

Furthermore, the Pareto set of the pressure bulkhead problem shows a clear compromise between complexity and compliance. These results can empower designers to easily choose adequate level of compliance and complexity that should allow for a much easier detailed design phase. These trade-off can be translated as a clear hierarchy of the primary and secondary stiffening components, with components of simple solutions offering the most effective compromise of complexity-stiffness. The results show a clear advantage with respect to exploration when compared to gradient-based topology optimization. Furthermore, results obtained with SIMP are often organic and complex, which creates design challenges down the road, especially with respect to unrecognized Information.

In summary, CD-CEAS can rapidly generate simple and efficient solutions, even offering better results than SIMP for the case of the pressure bulkhead. A major advantage of CD-CEAS against topology optimization, such as SIMP and LSM, is the fact that the stiffeners are explicitly generated, ensuring a proper representation of the stiffened panel. Besides, using the Pareto front as the starting points of each iteration allows the Burst algorithm not to stay in place in the design space of complex solutions, as the design space is smaller in

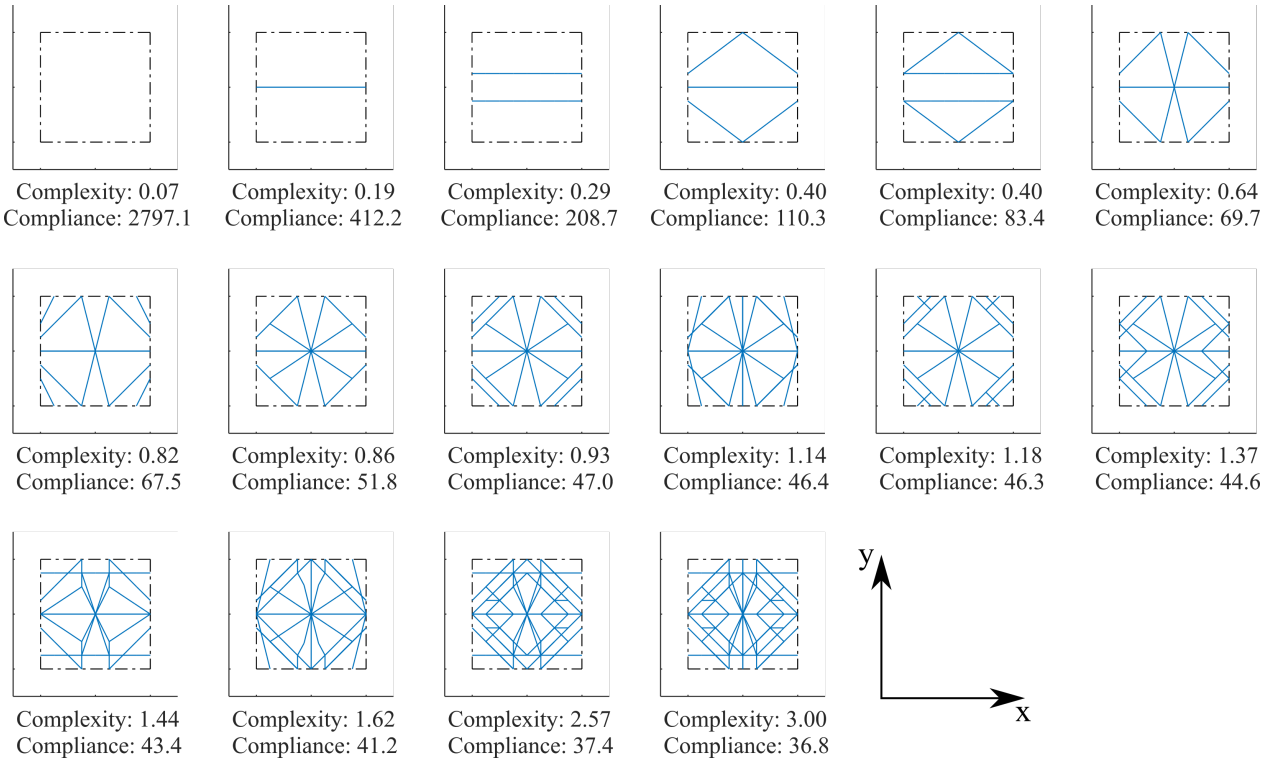
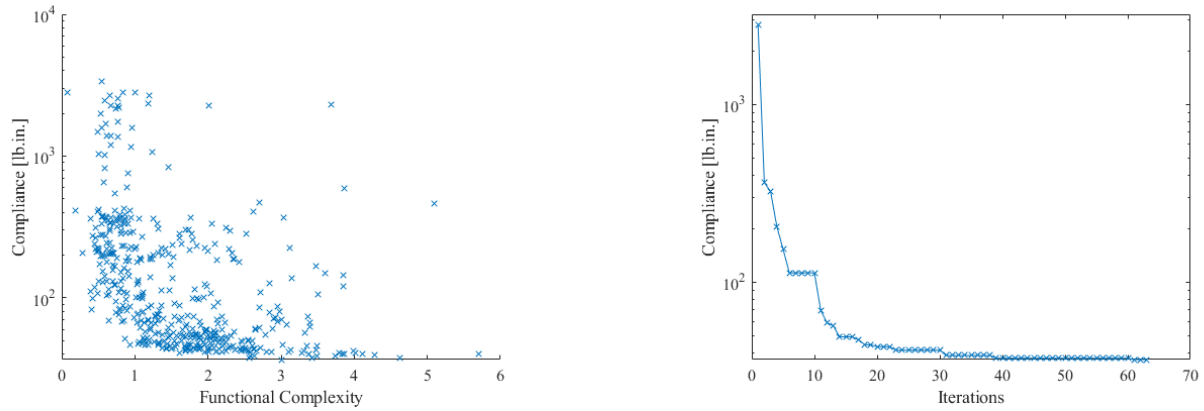


Figure 7.7 Solutions on the Pareto front for the pressurized stiffened panel exploration.



(a) (b)

Figure 7.8 Results of the compliance-based run for the pressure case study. For this run, the sizing optimization uses a compliance minimization with a weight constraint of 5.0 lb. Burst size: 8, Archive has 500 layouts, relaxation is set to 3 and the grid size is 10x10. Symmetry on both axis is active. (a) Pareto front for the pressurized stiffened panel exploration. (b) Convergence of compliance for the Pressure Bulkhead.

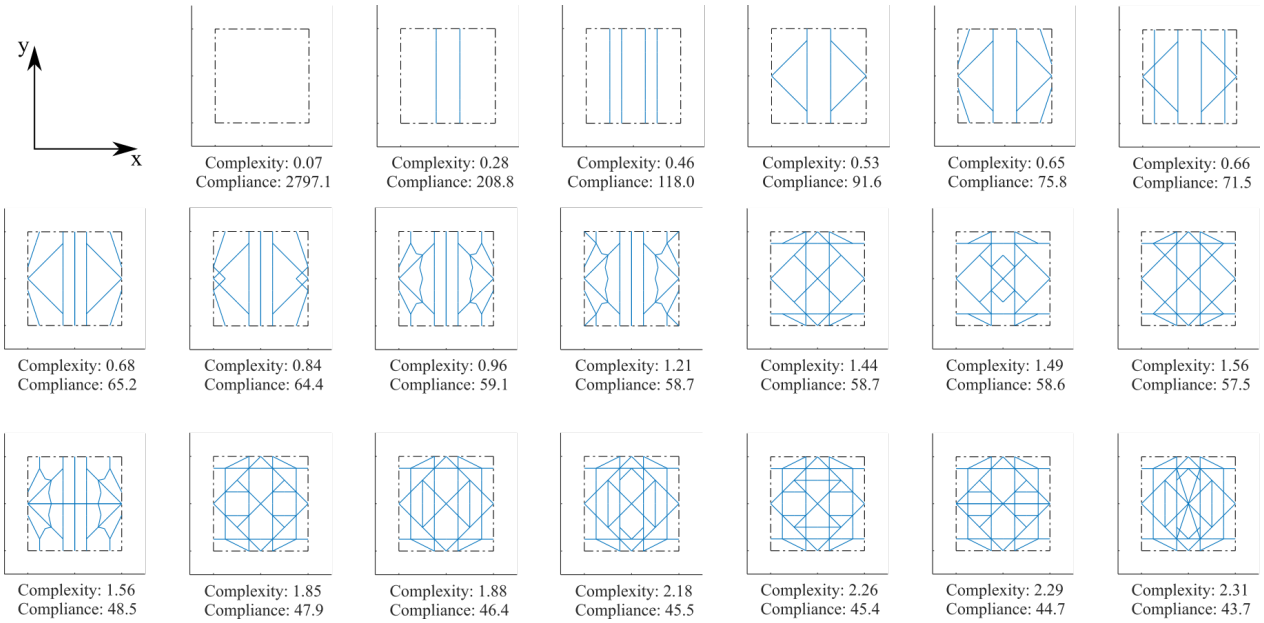


Figure 7.9 Second set of solutions of the Pareto front for the pressurized stiffened panel exploration. The optimization parameters are the same as of fig. 7.8

the simple space than the complex space.

The next section discusses the compressed panel case study as an in-plane loading.

7.6.2 Compressed Stiffened Panel, with In-plane Loading

The design of compressed stiffened panel is also an active challenge of topology optimization, mainly due to convergence difficulty created by buckling constraints [151, 153, 251]. These panels are found on the outer skins of the wing, mainly on the upper skin. The bending action of the lift and gust forces on the wing creates high compressive loads on the panels.

In the industry, these panels are currently designed and optimized using a handbook method [26, 58]. Relations and equations found in these handbooks are only for the orthogrid configuration and are based on analytical models and empirical data to model the collapse of the panels in terms of buckling, crippling and post-buckling. The handbook design method is very efficient for large-scale problems and can easily be automated once the layout is fixed. As such, in this section, we will compare the results of CD-CEAS with the results of the design with the handbook method.

Description of the Problem

The same graph-grammar actions and rules that were presented in section 7.4 are used, with the only possible action is "CreateStiffener." Again, the plate is flat on the X-Y plane and the boundary conditions are simply supported ($U_z = 0$), see fig. 7.10. This time, the compressive load is applied on one side via a rigid (RBE2) element, in the X direction. The load value is set at 120,000 lb. The RBE2 is only active in the X direction. On the opposite side, the displacement ($U_x = 0$) is set to resist the compressive load. We use the same aluminum 7075 alloy that was used in the pressure test case.

For the sizing optimization, we propose here two formulations. The first is the same as for the pressure bulkhead, with a compliance minimization and a weight constraint. For the second one, we use a weight minimization and a buckling constraint. These two formulations are used to demonstrate that non-linear constraints such as buckling barely change the resulting topologies. As for the Burst algorithm parameter, we use the same as for the pressure bulkhead case.

Evaluation per iterations : 8
Graph Grid Size : 10x10
Maximum Evaluation : 500
Symmetry : From the center line of the X and Y axis

For the pressure case, we have used SIMP to create an optimized baseline. However, for compressed stiffened panels, there no clear results that can be obtained with SIMP. Consequently, we define the baseline as a current layout used in a commercial aircraft, as illustrated in fig. 7.11. In the table 7.3, the result of a FEM-based sizing optimization is presented. The optimization considers the eigenvalues of the linear buckling as a constraint and minimize the weight of the panel.

Table 7.3 Baseline properties

Property	**FEM Sizing**
T_{Skin} [in.]	0.11
T_{Stiff} [in.]	0.15
Weight [lb.]	5.3
Compliance [lb.in.]	5000
Maximum Stress [ksi]	45
Complexity [ksi]	0.27
Linear Buckling [λ_1]	1.0

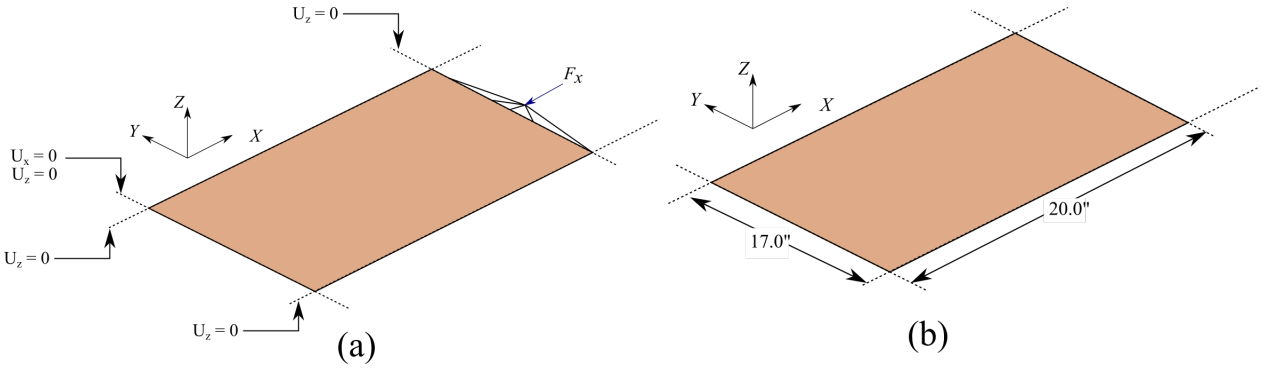


Figure 7.10 Test case of an axially compressed stiffened panel, with simply supported boundary conditions. (a) The applied load. (b) The design space dimensions. Where, U_z, U_x are imposed displacement, and F_x is the applied force on a RBE2.

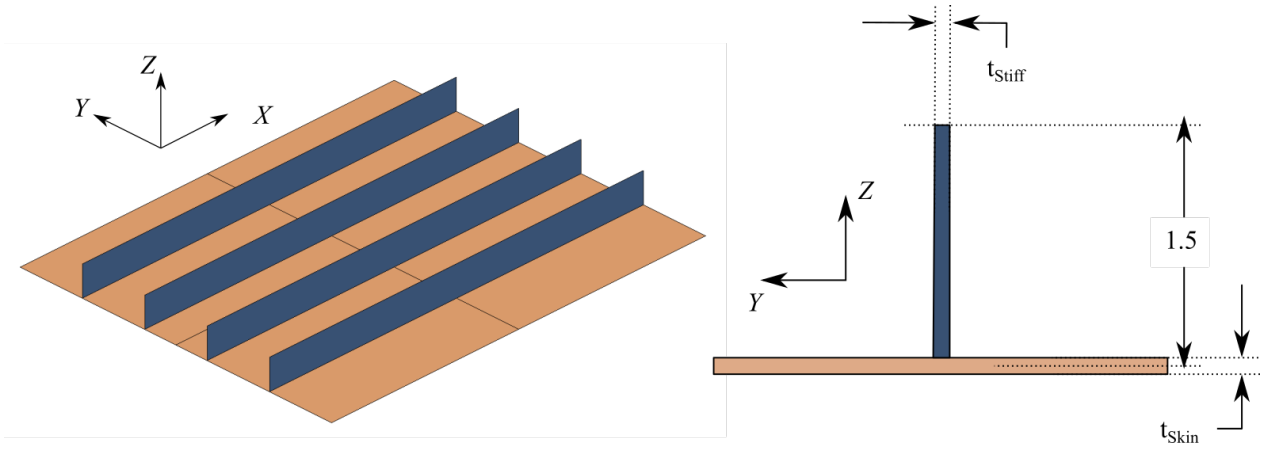


Figure 7.11 Compression baseline layout from a commercial aircraft, sized with handbook methods. Where t_{Stiff} and t_{Skin} are respectively the thickness variables for stiffeners and skin sections.

Compliance-based results for the Compressed Stiffened Panels

In this run, we define the sizing optimization as a compliance minimization with a weight constraint, set to 5.0 lb. It took 22 minutes to create, size and evaluate the 500 layouts. The layouts found on the Pareto front of this run are illustrated in fig. 7.12, the full archive is presented as a scatter plot in fig. 7.13a and the convergence of compliance in fig. 7.13b.

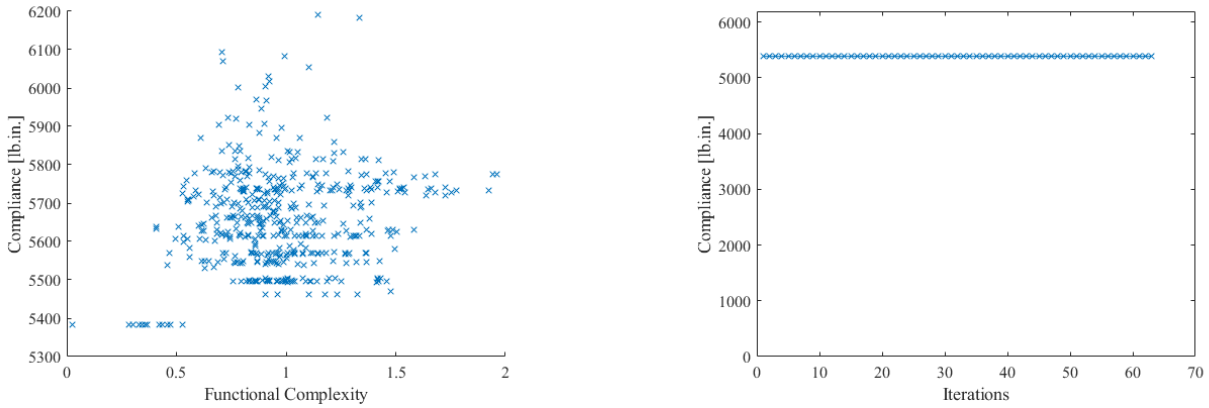
The results of this run are interesting, as they reflect a particularly difficult case for topology optimization. As shown in the scatter of the results in fig. 7.13a, there is a plateau in the solution space. Any other solutions that do not provide stiffeners parallel to the load will both increase complexity and compliance. As such, for topology optimization algorithms using implicit generation (SIMP, Level-Set, MMC), it is very difficult to make any decisions that will not have a negative impact on compliance. The only topology optimization algorithm that is capable of easily finding a solution for this case is the ground-structure method, but it is computationally very expensive due to the evaluation of buckling and the use of finite-difference evaluations [237].

Still, CD-CEAS easily finds a range of efficient solutions at different complexity levels. However, as noted earlier, buckling is actually the main driver for the design of compressed stiffened panels. Thus, to verify the strength of the proposed layout, we use a sizing subproblem including buckling. The linear eigenvalue constraint is set to $\lambda > 1.0$. The objective is to reduce the weight of the panel, given the buckling constraint. See fig. 7.14 for the results of each layout.

As these panels are sized, it appears that when properly sized for buckling, the proposed layout is unable to surpass the baseline. The best layout proposed by CD-CEAS has a weight of 5.5 lb., whereas the FEM sized baseline weight 5.3 lb. This is to be expected as the distribution of the stiffeners on the panel does not affect the compliance, but does significantly impact the buckling. Still, by using CD-CEAS, any unnecessary components that add com-



Figure 7.12 Layouts on the Pareto front for the compliance-based compression case.



(a) (b)

Figure 7.13 Results of the compliance-based run of the compression case study. For this run, the sizing optimization uses a compliance minimization with a weight constraint of 5.0 lb. Burst size: 8, Archive has 500 layouts, relaxation is set to 3 and the grid size is 10x10. Symmetry on both axis is active. (a) Scatter of the archive of all layouts created in this compliance-based run. (b) Layouts on the Pareto front for the compliance-based compression case.

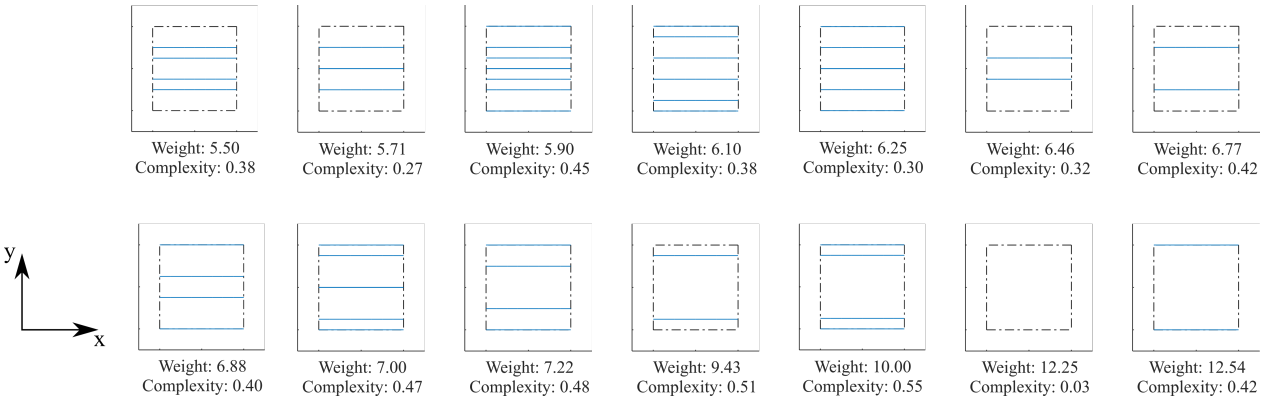


Figure 7.14 Sizing optimization with weight minimization and a buckling constraint ($\lambda_1 = 1.0$ for all layouts) for the layouts proposed by CD-CEAS for the search with compliance only.

plexity are ignored. Some work by the engineers is still required to adapt the layouts and distribution of stiffeners, but as the computation time is low, it can explore feasible solutions quickly. Other works by the authors have shown that the ground-structure algorithm using buckling obtained similar results, with much more computation time [237].

In the next section, we use the buckling sizing optimization during the CD-CEAS search to compare with the compliance-based search.

Buckling-based results for the Compressed Stiffened Panels

The addition of buckling during the search greatly increased the computation time of CD-CEAS. On the same processor, for 500 layouts creation, sizing and evaluation it took 5.8 hours. Still a somewhat reasonable amount of time, as it can easily be run overnight, which is the norm for structural optimization [56]. Furthermore, compared to SIMP or the ground-structure method this is a significant improvement in computation time. As discussed in [236], SIMP is relatively difficult to use, exploration can hardly be controlled and it requires multiple days of computation to obtain only some efficient layouts. As for the ground structure, a single gradient descent requires more than 5 hours of computation [237] for the same problem. Parallelism could reduce slightly computation time, but it would still be longer than CD-CEAS. Furthermore, exploration is only controlled by changing the initial optimization variables.

For the CD-CEAS run, the layouts found on the Pareto front are illustrated in fig. 7.15, the full archive is presented as a scatter in fig. 7.16a and the convergence of weight in fig. 7.16b.

Compared to the compliance-based search, using buckling shows a cleaner convergence. Also, the scatter plot shows that there are some great solutions with low complexity. Furthermore, this time the best results has a weight of 5.03, lower than the baseline with a trade-off of increased complexity. The next best solution at 5.06 still beats the baseline while having a similar complexity value to the baseline.

Choosing whether to use buckling or not during CD-CEAS search is up to the available time

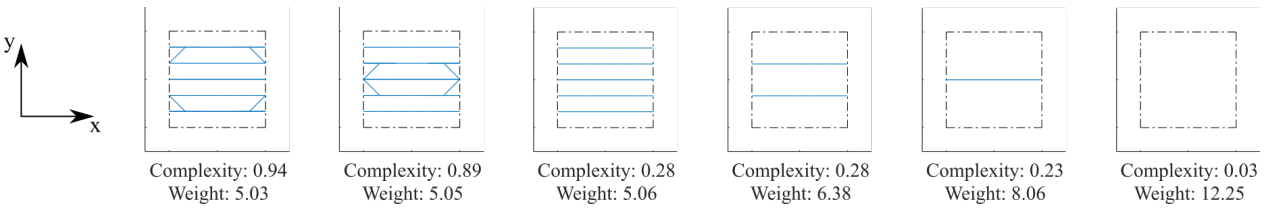
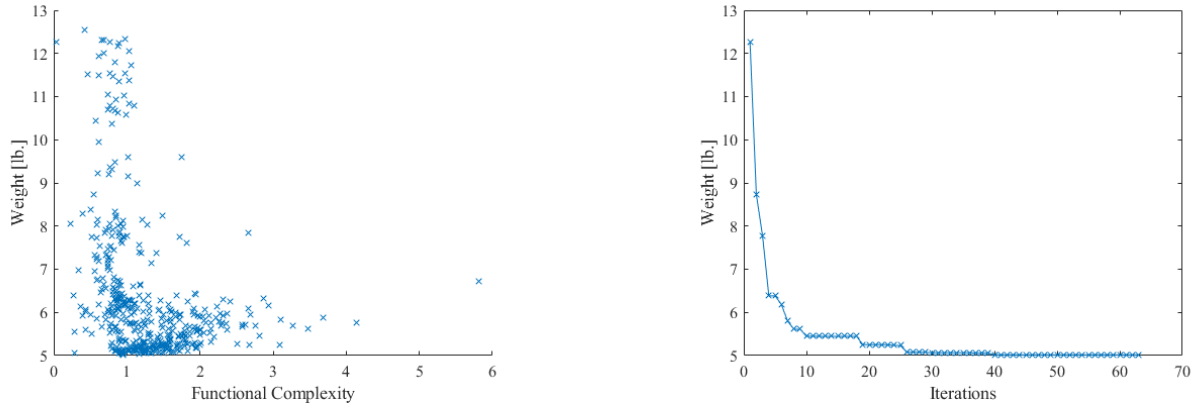


Figure 7.15 Layouts on the Pareto front for the buckling-based compression case.



(a) (b)

Figure 7.16 Results of the buckling-based run of the compression case study. For this run, the sizing optimization uses a weight minimization with a buckling constraint of $\lambda > 1.0$ and a weight constraint of 5.0 lb. Burst size: 8, Archive has 500 layouts, relaxation is set to 3 and the grid size is 10x10. Symmetry on both axis is active. (a) Scatter of the archive of all layouts created in the buckling-based run. (b) Convergence of weight in the buckling-based run.

and the problem at hand. Still, both formulations are capable of generating feasible results with a performance similar to the ones created by experienced engineers. The compromise proposed on the Pareto front is clear and offers interesting information to the users with regards to the impact of layouts. In summary, the results obtained show a better or equal performance to the ones proposed by topology optimization, with SIMP or ground-structure, while requiring less computation time. More importantly, the generation used by CD-CEAS is explicit, making the representation of buckling more accurate and the exploration focused search shows an efficient and diversified search.

7.7 Discussion and Limitations

There are multiple advantages to using functional complexity measures, rather than some heuristics to limit the complexity of new layouts. First, the functional complexity is context-dependent, and quick to assess. By using the functional complexity to drive layout optimization, it becomes possible to identify three main types complexity measures with recognized (coupling), axiomatic (sensitivity) and superfluous Information content and therefore reducing the challenges of detailed design down the road. This effect is shown in the compressed stiffened panel case, where using only compliance still yields results that are relatively efficient in terms of buckling. Secondly, as the complexity measure is relative, there is no arbitrary

threshold to set. As the algorithm explores and build the Pareto front at each iteration from the whole archive of solutions, it will organically set a threshold on complexity by ignoring layouts that are both complex and with low performance, as shown in both case studies. Finally, as shown by the case studies, CD-CEAS is more effective than current topology optimization algorithms for exploration, as it does not get stuck in local minima. This is helped by the complexity measure that act as a relaxation of the optimization, which allows the Burst algorithm to keep looking around existing layouts with low performance, as long as they stay simple. Eventually, this allows the algorithm to find solutions that have both high performance and low relative complexity.

As discussed in the introduction, we classify generative systems according to three main properties; generation, representation and exploration. In this work, generation is carried out using the graph-grammar algorithm, ensuring an explicit representation of components and their relations through the graph. In addition, the use of the archive and the "bar-code" ensures that the exploration does not evaluate the same layout twice. Moreover, the explicit generation is capable of creating evaluation models with a good representation. In this work, the representation of each layout is provided by an automatically created sub-optimization problem as a FEM model. This sub-optimization model provides everything needed for performance and complexity assessments. As such, in terms of representation, CD-CEAS does not propose anything new, but uses automation to accelerate the process. Finally, the exploration of CD-CEAS is done using our implementation of the basic Burst algorithm, using both a complexity measure and any performance assessment as an objective. The combination of these two measures is central to the strength of the algorithm, as already discussed. In summary, by adjusting the balance towards exploration rather than exploitation, CD-CEAS offers a more flexible approach to layout optimization. It quickly finds great layouts, which are clear compromises of simplicity and performance. In other terms, this allows the use of more flexible generation and representation.

In the future, there are many ways in which CD-CEAS could be improved. With regard to generation, the current implementation has only one action and few design rules. It is possible to imagine actions that add more stiffeners in a single action, such as the creation of a grid, actions that modify a grid by moving connections or still actions that combine different graphs. For example, the action "createGrid" could take as input a "spacing", "length" and "width" parameters and create many stiffeners at once, using the same design rules as we already defined. Moreover, curvilinear stiffeners have been studied in multiple works recently, and the possibility to add them could be interesting [30]. Another possible improvement is the implementation of primary/secondary stiffeners with different heights, such as the buckling containment features (BCF) proposed in [88]. It could also be possible to use multiple different

cross-sections.

The current case studies have been used only on flat panels. It would be interesting to test on different types of surfaces, such as the single curvature which could be found in an aircraft fuselage. For the moment, the limitation is related to the capability of the TCL interpreter to create the FEM optimization models automatically. It can be imagined that CD-CEAS could be used for bigger assemblies, such as a complete wing box with ribs, spars and stiffeners.

As we use an explicit generation, it is possible to easily implement high-fidelity models for the evaluation of new layouts. In this work we implemented compliance and buckling, but one could imagine more studies that include fatigue, stress or even non-linear material or geometrical non-linearity for post-buckling.

Finally, for the exploration, the use of the basic Burst algorithm has shown its capabilities. Still, there are certainly other stochastic search algorithm that could prove to be more efficient in searching the design space by leveraging the complexity measure.

7.8 Conclusion

In this work we propose a new tool for the generation of stiffened panel layout based on generative design, topology optimization and design science. Leveraging knowledge acquired from this research area, the CD-CEAS algorithm is a two-level optimization process that improves upon topology optimization of layout design for the generation, representation and exploration properties. The generation is done using a graph-grammar with a single possible action and few design rules. The main novelty aspect of CD-CEAS is the fact that complexity, as a relative and approximate measure of Information content, is used to drive the exploration. This allows for much simpler designs. As an example, a trade-off of less than 1% of weight can reduce complexity from 0.94 to 0.28, as observed in the case of the buckling-based stiffened panels. We think this shows that current topology optimization algorithm, as they only focus on a given objective function, will make any sacrifice necessary to complexity as to get those 1 or 2 final percentage of performance. As CD-CEAS also takes into account, it becomes possible to select slightly underperforming solutions, in exchange for much less complexity. Furthermore, CD-CEAS has shown an improvement on both computation time and performance with respect to widely used topology optimization algorithms. We demonstrate these improvements with two case studies that are compared with previous work of the authors regarding topology optimization for stiffened panels. In the pressure case study, we have shown an improved exploration, a stiffer layout (44 vs. 57 lb.in.) and multiple good compromise solutions (with multiple interesting results, instead of just one). As for

the compression case study, we have shown the numerical challenge of such a problem and discussed how different search formulations (compliance or buckling-based sub-problem) can offer efficient results. In this particular case, previous work had identified a very difficult use with SIMP, whereas CD-CEAS has shown a consistent convergence towards a more efficient minimum. Future work to explore more challenging case study will be required to assess the full potential of CD-CEAS, and more broadly the use of complexity measures in design automation algorithms.

CHAPTER 8 GENERAL DISCUSSION

At the preliminary stage of the project, SO1 and SO3 were built upon the hypothesis that SIMP was an effective design exploration tool for stiffened panels. Consequently, to ease the exploration process, we have implemented automation for the density-based approach, with SIMP used in chapter 4, answering the SO2. Computer vision is leveraged to take the implicit material distribution from SIMP into an explicit graph representation that can easily create high-fidelity models for subsequent sizing and validation. This SO was completed first, as it was initially thought it would be the most challenging aspect.

For SO1, we have characterized existing, state-of-the-art topology optimization methods for stiffened panel layout optimization. Chapters 5 and 6 contain comprehensive applications of the original SIMP and a modified Ground-Structure method. SIMP was used through a commercial software and tested for different optimization formulations and parameters. We found out that in order to reduce the complexity of the material distribution to feasible results, there was only a very narrow set of formulations and parameters required. As such, we have concluded that for stiffened panel layout optimization, SIMP is highly sensitive to parameters leading to unexpected and erratic results. Complexity rose from the implicit generation that could not capture panel buckling accurately with semi-density values. As for the modified ground-structure method, the improvements made for the application for stiffened panels allowed for a more straightforward approach, as the behavior was more predictable and efficient to find feasible results. Still, the computation cost was too high to allow for an effective design exploration, as multiple days of computing yield only a few optimized layouts.

With the results of SO2, it has become clear that density-based methods and even the ground-structure approach were not easily adapted for design exploration. Consequently, the work in analysis and synthesis of layout complexity grew from a **complexity filter into a complexity-driven algorithm** which was presented in chapter 7. From the ground up, we implemented a complexity-driven layout optimization technique using the Generative Design Framework: CD-CEAS. This algorithm has shown that it is an effective balance of generation, representation and exploration, thus creating an easy-to-use search and synthesis algorithm perfectly adapted for the conceptual design of stiffened panels.

Looking back at the main objective, it is clear that the development of the Generative Design Framework was built from many lessons learned through the achievements of the three secondary objectives. It evolved into including the selection, application, validation and de-

velopment of generative systems. We identified three key properties of the generative systems: representation, generation and exploration. The complexity measures for design synthesis in SO3 led to a complete topology optimization tool, which answers the development aspect of the main objective.

Within the proposed set of framework, tools and algorithms, the objective to minimize the weight of existing stiffened panels is partially met. The proposed methods, with specific formulations, are able to find many feasible and efficient layouts of stiffened panels. Although, the best proposed layouts are the already widely adopted orthogrid, which means that our algorithms did not meet the objective to reduce stiffened panels weight.

Still, with the developed tools, new research avenues are envisioned for general structure optimization, and more critically for the development of novel forms of aircraft structures where the orthogrid layout might not be optimal.

8.1 Industrial Deliverable

As this project is in collaboration with industrial partners, we have delivered different automation scripts and documented optimization methods.

The work of chapter 4 is implemented in Matlab and leverages its computer vision library. In the future, using Python and OpenCV would allow for an easier industrial implementation. The Matlab code is considered a proof of concept. The SIMP characterization of chapter 5 was delivered in the format of a technical report delivered in June 2019 to Stelia Aéronautique Canada. The conclusions of the report which discussed the several limitations of SIMP with respect to stiffened panel optimization led to reducing the efforts in topology optimization by the research team at Stelia. The ground-structure method presented in chapter 6 has been delivered as an HyperMesh model and is also considered a proof of concept. Finally, the work of chapter 7 is implemented in Matlab for the generation and search algorithms, and as a TCL script for sub-model generation. Once again, this is a proof of concept that would benefit from further development to improve scalability and modularity.

8.2 Contributions and Importance of Research

In summary, this thesis has multiple research contributions to the research communities of topology optimization, aircraft structure design and design science. We first considered topology optimization not only as an optimization tool but positioned it in a comprehensive design framework. This allows one to characterize and develop topology optimization as a

generative system and thus improve its balance in terms of generation, representation and exploration for our application in layout optimization of stiffened panels.

By using the Generative Design Framework to improve conceptual computational design, we explain how and why the exploitation of topology optimization for aircraft structures had focused too narrowly on a structure only global optimum. Said simply, topology optimization has been developed with a simple, convex design space. In industrial applications, the non-linear constraints (e.g. stress, buckling) create a complicated, non-convex design space for which gradient-based solvers are ill-suited. Moreover, structure design is seldom independent of other disciplines, especially in wingbox design. Accordingly, proposing multiple feasible solutions directly during the structure conceptual design allows for a quicker response to changing requirements from other disciplines. We are convinced this insight will drive the development of algorithms seeking to explore the many local minima of the non-convex design space.

With these important lessons, we developed CD-CEAS, a proof of concept of a generative system for layout optimization balanced towards exploration. This represents an important achievement as CD-CEAS is the first implementation of a generative system including a novel complexity measure to drive exploration. CD-CEAS has shown significant improvements with respect to layout weight minimization and simplicity while also largely improving exploration efficiency compared to the density-based and the ground-structure methods. An important outcome of this thesis is the new and different ways to approach automation in the context of the conceptual design phase and more specifically how to use it for aircraft structure design.

There are multiple publications of the work carried out during my PhD. In addition to the four chapters of this thesis, I contributed and participated to many international conferences. Table 8.1 contains a list of all publications done during the PhD, including work completed with colleagues from our research group in design and mechatronics.

Moreover, the research discussed in this thesis contains contributions to three research communities: topology optimization, aircraft structure design and design science. Table 8.2 present a summary of key contributions and their respective specialized communities.

8.3 Limitations

There is an increasing amount of interest in generative systems in multiple engineering disciplines and we are convinced that thinking in terms of generation, representation and exploration will improve the quality of newly developed generative systems. Thinking of generative design as a conceptual automation tool allows developers to imagine more efficient

Table 8.1 All scientific publications completed during this PhD.

1	**Gamache, J.-F.**, Vadean, A., Capo, M., Rochefort-Beaudoin, T., Dodane, N., Achiche, S., 2021. Complexity-Driven Conceptual Exploration for Aircraft Structure (CD-CEAS), Submitted to *Design Science* on June 18th, 2021.
2	Capo, M., **Gamache, J.-F.**, Rochefort-Beaudoin, T., Vadean, A., Achiche, S., 2021. A Novel use of the Ground Structure Topology Optimization for the Design of Pressurized Stiffened Panels, in ICTAM Milano 2020+. [Accepted: Poster, Video Presentation and Extended Abstract]
3	**Gamache, J.-F.**, Vadean, A., Dodane, N., Achiche, S., 2020. On Generating Stiffening Layouts with Density-Based Topology Optimization Considering Buckling, Submitted to *CEAS Aeronautical Journal* on May 11th, 2020.
4	Coulombe, C., **Gamache, J.-F.**, Barron, O., Descôteaux, G., Saussié, D., Achiche, S., 2020. Task Taxonomy for Autonomous Unmanned Aerial Manipulator: A Review, in: IDETC-CIE2020. Volume 9: 40th Computers and Information in Engineering Conference (CIE). https://doi.org/10.1115/DETC2020-22297
5	**Gamache, J.-F.**, Vadean, A., Dodane, N., Achiche, S., 2020. Topology Optimization for Stiffened Panels: A Ground Structure Method, in: IDETC-DAC2020. Volume 11A: 46th Design Automation Conference (DAC). https://doi.org/10.1115/DETC2020-22103
6	**Gamache, J.-F.**, Vadean, A., Achiche, S., 2019. Validating Novel Stiffened Panel Configuration Generated with Topology Optimization using Non-Linear Analysis, in: Proceedings of AERO '19. Presented at the CASI - Aero 2019.
7	**Gamache, J.-F.**, Vadean, A., Achiche, S., 2018. Topology Optimization for the Design of Stiffened Panels for Wing Box. In Proceedings of Design Science Research 2018: Data-Driven Design and Learning (DSR 2018), Montreal, Canada, 23-25.08.2018. [Oral Presentation & Extended Abstract]
8	**Gamache, J.-F.**, Vadean, A., Noirot-Nérin, É., Beaini, D., Achiche, S., 2018. Image-based truss recognition for density-based topology optimization approach. Structural and Multidisciplinary Optimization. https://doi.org/10.1007/s00158-018-2028-x
9	Coulombe, C., **Gamache, J.-F.**, Mohebbi, A., Chouinard, U., Achiche, S., 2017. Applying robust design methodology to a quadrotor drone, in: DS 87-4 Proceedings of the 21st International Conference on Engineering Design. Presented at the ICED 17, Vancouver, pp. 395–404.

and focused generative systems. The main limitation associated with this work is that it was developed for a single, specific use case. An application of these concepts outside of stiffened panels structural generation would give more weight to the framework. All implementations discussed in this thesis are proof of concepts and consequently there is still more work to validate their usefulness in the industrial context of industrial aircraft development. The scope and challenges related to an application in aircraft development are still out of reach for the

Table 8.2 Major contributions by communities

Community	**Contributions**	**Pub.#**
Topology Optimization	-Developed a novel computer-vision based recognition tools for continuous topology optimization, reducing the challenge of combining topology, shape and size optimization in a single tool.	2
	-Developed the Stiffener Activation Variable (SAV) for the Ground-Structure Method for stiffened panels.	5
	-Characterized the effect of randomized starting values in topology optimization (SIMP and Ground-Structure).	5,7
	-Developed a graph-grammar of stiffened panels in CD-CEAS, a new explicit topology generation tool.	9
Aircraft Structure	-Proposed a data-based exploration approach for stiffened based with topology optimization.	3
	-Validated that post-buckling of stiffened panels can be accurately evaluated with nonlinear FEM analysis.	4
	-Applied and validated our modified Ground-Structure Method to stiffened panels optimization with buckling.	5
	-Identified the low performance of SIMP when including buckling in SIMP for stiffened panels.	7
	-Implemented CD-CEAS, an automated stiffened panel conceptual layout design tool.	9
Design Science	-Introduced a relative complexity measure based on the sizing sub-optimization problem of stiffened panels.	9
	-Introduced the Generative Design Framework to analyze and develop topology optimization methods.	Thesis

current versions of the proposed work. Still, the results of CD-CEAS show a promising future to the use and development of generative systems in the industry.

With respect to representation in stiffened panels generative systems, the work of this thesis uses FEM-based models. First as an implicit material distribution in SIMP then as a composite shell structure in the Ground-Structure method and in CD-CEAS. However, in industry the design of stiffened panels is still validated using empirical data within semi-empirical calculations, with all data available only for the orthogrid panels. The scope of industry calculation tools are limited to orthogrid panels as their behavior is very difficult to capture in numerical models. Therefore, even as the developed generative systems can potentially find improved layouts, the complete validation of these new layouts would still require significant new experimental data to be integrated and certified for aircraft development.

CHAPTER 9 CONCLUSION & FUTURE WORK

This project was originally rooted in the optimization of aircraft structures, specifically for a wing box multidisciplinary optimization framework (MuFoX). Topology optimization, more specifically the commercial version of the Solid Isotropic Material with Penalization (SIMP) method, was envisioned to create innovative structures that could be rapidly implemented back in Bombardier's and Stelia's Multidisciplinary Optimization framework for a complete optimization of the wing box considering in addition to structure: aerodynamics, loads and systems.

With the roadblocks and challenges identified throughout the project, the scope gradually evolved to more specifically develop a method to integrate conceptual design and structural optimization in the same design tool. Layout complexity, design integration and buckling representation were the main identified challenges. At this point, we introduced the Generative Design Framework and its systems for applications in aircraft structure design.

Three key properties of generative systems (generation, representation and exploration) were the drivers for research and improvement of this thesis. We characterized existing topology optimization algorithms, such as the density-based and ground-structure methods, throughout the lens of these properties. The challenges of using topology optimization in layout design are mainly associated with the implicit generation which requires expert interpretation and perfect tuning of optimization parameters and formulations. Challenges are amplified as layout and buckling of stiffened panels are tightly connected. Neglecting buckling during topology optimization yields complex and weak layouts. Still, including buckling in topology optimization reveals a highly complex design space with many similar performing local minima. We have shown that density-based and ground-structure methods are very efficient at finding local minima, as expected of gradient-based algorithms, but not adequate to explore many local minima, which would be a step-up in industry. Finally, the characterization of the topology optimization algorithm through a full sizing and validation process has shown that the density-based representation does not accurately capture buckling of stiffened panels.

Still, all the generative systems throughout this thesis have been improved with respect to either generation or exploration. The objective is to balance these properties towards exploration and make it more in sync with the industrial design process. For each of these

key properties, we summarize the contributions covered in this thesis:

Representation This thesis has discussed representation in both continuous and truss topology optimization. We have shown that the implicit generation and current representation with density approximations make it impossible to capture the effect of stiffeners on buckling resistance. Choosing the Ground-Structure method offered a better representation by using a 3D shell modeling of the stiffeners. CD-CEAS used a similar representation and added a sizing sub-optimization problem within the global optimization loop. If the present work rather contributed on the effect of generation rather than the accuracy of representation, a complementary work is carried out on the latter by our research team.

Generation Characterization with the density-based and ground-structure algorithm has shown that an explicit generation generally makes representation more accurate. In the density-based approach, the generation of solutions is only implied from the material distribution, which means the exploration algorithms has no knowledge of real position and relationship between components. With this information, we took advantage of the more explicit Ground-Structure Method, for which the exploration algorithm knows the position of components, but not their relationship. The semi-explicit generation allowed for a more accurate representation of buckling in the stiffened panels, but still requires the gradient-based exploration and thus does not allow for controlled exploration. Lessons learned from SIMP and Ground-structure led to the development of a graph-grammar which is completely explicit on positions and relationships between components.

Exploration The main contribution of this thesis is the development of a complexity measure to drive exploration in CD-CEAS. In both SIMP and Ground-Structure, it was noted that finding some feasible solutions is possible, although finding efficient one is challenging. Only a very narrow balance of optimization parameters allowed simple and accurate solutions to appear in both topology optimization methods. Using complexity in CD-CEAS has allowed a narrower exploration towards simple and efficient solutions first, ensuring less computation power is lost in the complex area of the design space. This has potential for more difficult design problems.

In summary, by improving on current industrial usage of topology optimization in aircraft development and implementing this knowledge and expertise in modern tools, we have shown that our Generative Design Framework is an effective method to structure the development

of generative systems, such as topology optimization. Still, future work could leverage the lessons learned and improve upon each contribution of this thesis. A summary of possible future improvements per tool is discussed below.

Truss Recognition The current implementation of the truss recognition based on computer vision has yet to be expanded to more surfaces and to 3D. It currently still needs many manipulations to take pictures of the material distribution and the implementation to CAD and FEA software packages.

Density-Based Topology Optimization During my thesis, there have been multiple academic publications that have shown improvements of the algorithm, especially for buckling analysis. However, most of them are still to be implemented in the commercial software that was used in this thesis. An obvious step forward for our research team would be an in-house implementation of SIMP, which would allow for an easier integration of novel methods found in the literature.

Ground-Structure Method The method we proposed to exploit the ground-structure uses finite differences to evaluate the gradient. A more efficient approach would use an explicit equation to describe the gradient. Furthermore, the representation with mixed finite elements could allow for more efficient evaluations of buckling. Work in this direction is currently being pursued in our research group.

CD-CEAS This novel algorithm has combined multiple disciplines to create an efficient layout optimization framework for stiffened panels based on complexity. Still, the combination is novel and few cases were studied. More case studies are required to improve the confidence in using the tool. Further improvement is noted for all three key generative system properties. First, for the generation, more complex actions and rules could be implemented to increase flexibility, such as the introduction of curvilinear stiffeners and secondary reinforcements. Secondly, for the representation, it is possible to imagine the use of higher-fidelity models such as nonlinear analysis or the implementation of robust or reliability optimization in the sub-optimization problem. Finally, only the basic Burst algorithm is currently implemented, which means that exploiting other search algorithms could potentially improve the efficiency of CD-CEAS. In our research group, there is research carried out to introduce reinforcement learning for exploration.

REFERENCES

[1] L. Wang, W. Shen, H. Xie, J. Neelamkavil, and A. Pardasani, "Collaborative conceptual design—state of the art and future trends," *Computer-Aided Design*, vol. 34, no. 13, pp. 981–996, 2002.

[2] M. P. Bendsøe and O. Sigmund, *Topology optimization: theory, methods, and applications*. Berlin ; New York: Springer, 2003.

[3] G. Houston, D. Quinn, A. Murphy, and F. Bron, "Wing panel design with novel skin-buckling containment features," *Journal of Aircraft*, vol. 53, no. 2, pp. 416–426, Mar. 2016. [Online]. Available: http://arc.aiaa.org/doi/10.2514/1.C033540

[4] N. P. van Dijk, K. Maute, M. Langelaar, and F. van Keulen, "Level-set methods for structural topology optimization: a review," *Structural and Multidisciplinary Optimization*, vol. 48, no. 3, pp. 437–472, Sep. 2013. [Online]. Available: http://link.springer.com/10.1007/s00158-013-0912-y

[5] X. Guo, W. Zhang, and W. Zhong, "Doing topology optimization explicitly and geometrically—a new moving morphable components based framework," *Journal of Applied Mechanics*, vol. 81, no. 8, p. 081009, Aug. 2014.

[6] M. Bremicker, M. Chirehdast, N. Kikuchi, and P. Papalambros, "Integrated topology and shape optimization in structural design," *Journal of Structural Mechanics*, vol. 19, no. 4, pp. 551–587, 1991.

[7] M. Gedig, "A framework for form-based conceptual design in structural engineering," Ph.D. dissertation, University of British Columbia, 2010.

[8] C. Königseder and K. Shea, "Strategies for topologic and parametric rule application in automated design synthesis using graph grammars," in *International Design Engineering Technical Conferences and Computers and Information in Engineering Conference*, vol. 46315. American Society of Mechanical Engineers, 2014, p. V02AT03A007.

[9] M. Janić, "Aviation and externalities: the accomplishments and problems," *Transportation Research Part D: Transport and Environment*, vol. 4, no. 3, pp. 159 – 180, 1999. [Online]. Available: http://www.sciencedirect.com/science/article/pii/S1361920999000036

[10] E. Terrenoire, D. Hauglustaine, T. Gasser, and O. Penanhoat, "The contribution of carbon dioxide emissions from the aviation sector to future climate change," *Environmental research letters*, vol. 14, no. 8, p. 084019, 2019.

[11] N. Zazulia, "UTC's hybrid-electric regional plane promises 30 percent fuel savings," *Aviation Today*, Mar. 2019. [Online]. Available: https://www.aviationtoday.com/2019/03/28/utc-hybrid-ev-regional/

[12] J. Bachmann, C. Hidalgo, and S. Bricout, "Environmental analysis of innovative sustainable composites with potential use in aviation sector—a life cycle assessment review," *Science China Technological Sciences*, vol. 60, no. 9, pp. 1301–1317, 2017.

[13] J.-H. Zhu, W.-H. Zhang, and L. Xia, "Topology optimization in aircraft and aerospace structures design," *Archives of Computational Methods in Engineering*, vol. 23, no. 4, pp. 595–622, Dec. 2016. [Online]. Available: http://link.springer.com/10.1007/s11831-015-9151-2

[14] Y. Kim, J. Lee, and J. Ahn, "Innovation towards sustainable technologies: A socio-technical perspective on accelerating transition to aviation biofuel," *Technological Forecasting and Social Change*, vol. 145, pp. 317–329, 2019.

[15] L. R. M. Pérez, M. C. Lara, and H. J. Ríos, "Design of a delta wing aircraft," in *2017 International Conference on Mechatronics, Electronics and Automotive Engineering (ICMEAE)*. IEEE, 2017, pp. 93–97.

[16] A. Barke, C. Thies, S. P. Melo, F. Cerdas, C. Herrmann, and T. S. Spengler, "Socio-economic life cycle assessment of future aircraft systems," *Procedia CIRP*, vol. 90, pp. 262–267, 2020.

[17] E. S. Hendricks, R. D. Falck, and J. S. Gray, "Simultaneous propulsion system and trajectory optimization," in *18th AIAA/ISSMO Multidisciplinary Analysis and Optimization Conference*, 2017, p. 4435.

[18] F. Afonso, J. Vale, F. Lau, and A. Suleman, "Performance based multidisciplinary design optimization of morphing aircraft," *Aerospace Science and Technology*, vol. 67, pp. 1–12, 2017.

[19] P. S. Prakasha, L. Boggero, M. Fioriti, B. Aigner, P. D. Ciampa, K. Anisimov, A. Savelyev, A. Mirzoyan, and A. Isianov, "Collaborative system of systems multidisciplinary design optimization for civil aircraft: AGILE EU project," in *18th AIAA/ISSMO Multidisciplinary Analysis and Optimization Conference*, 2017, p. 4142.

[20] J. T. Bowen, *The Economic Geography of Air Transportation: Space, Time, and the Freedom of the Sky.* Routledge, 2010.

[21] T. Pardessus, "Concurrent engineering development and practices for aircraft design at airbus," in *Proceedings of the 24th ICAS Conf., Yokohama, Japan*, vol. 1, no. 2, 2004.

[22] R. Curran, X. Zhao, and W. J. Verhagen, "Concurrent engineering and integrated aircraft design," in *Concurrent Engineering in the 21st Century.* Springer, 2015, pp. 571–605.

[23] F. Mas, J. Menéndez, M. Oliva, and J. Ríos, "Collaborative engineering: an airbus case study," *Procedia Engineering*, vol. 63, no. 2013, pp. 336–345, 2013.

[24] A. Mohebbi, S. Achiche, and L. Baron, "Multi-criteria fuzzy decision support for conceptual evaluation in design of mechatronic systems: a quadrotor design case study," *Research in Engineering Design*, vol. 29, no. 3, pp. 329–349, 2018.

[25] T. Vuletic, A. Duffy, L. Hay, C. McTeague, L. Pidgeon, and M. Grealy, "The challenges in computer supported conceptual engineering design," *Computers in Industry*, vol. 95, pp. 22–37, 2018.

[26] T. H. G. Megson, *Aircraft structures for engineering students*, 6th ed., ser. Elsevier aerospace engineering series. Oxford ; Burlington, MA: Butterworth-Heinemann, 2017.

[27] R. Kapania, J. Li, and H. Kapoor, "Optimal design of unitized panels with curvilinear stiffeners," in *AIAA 5th ATIO and16th Lighter-Than-Air Sys Tech. and Balloon Systems Conferences.* Arlington, Virginia: American Institute of Aeronautics and Astronautics, Sep. 2005. [Online]. Available: http://arc.aiaa.org/doi/10.2514/6.2005-7482

[28] A. Murphy, D. Q. Quinn, P. Mawhinney, M. Ozakca, and S. van der Veen, "Tailoring static strength performance of metallic stiffened panels by selective local sub-stiffening," in *47th AIAA/ASME/ASCE/AHS/ASC Structures, Structural Dynamics, and Materials Conference 14th AIAA/ASME/AHS Adaptive Structures Conference 7th*, 2006, p. 1944.

[29] O. Bedair, "Analysis and limit state design of stiffened plates and shells: A world view," *Applied Mechanics Reviews*, vol. 62, no. 2, p. 020801, Mar. 2009. [Online]. Available: https://asmedigitalcollection.asme.org/appliedmechanicsreviews/article/doi/10.1115/1.3077137/446401/Analysis-and-Limit-State-Design-of-Stiffened

[30] S. B. Mulani, W. C. Slemp, and R. K. Kapania, "EBF3PanelOpt: An optimization framework for curvilinear blade-stiffened panels," *Thin-Walled Structures*, vol. 63, pp. 13–26, Feb. 2013. [Online]. Available: https://linkinghub.elsevier.com/retrieve/pii/S0263823112002601

[31] E. A. Calado, M. Leite, and A. Silva, "Selecting composite materials considering cost and environmental impact in the early phases of aircraft structure design," *Journal of Cleaner Production*, vol. 186, pp. 113–122, 2018.

[32] R. A. Witik, F. Gaille, R. Teuscher, H. Ringwald, V. Michaud, and J.-A. E. Månson, "Economic and environmental assessment of alternative production methods for composite aircraft components," *Journal of Cleaner Production*, vol. 29, pp. 91–102, 2012.

[33] J. F. Caseiro, "On the elasto-plastic buckling of Integrally Stiffened Panels (ISP) joined by Friction Stir Welding (FSW)_ Numerical simulation and optimization algorithms," *International Journal of Mechanical Sciences*, p. 11, 2013.

[34] J. W. Yoon, G. Bray, R. Valente, and T. Childs, "Buckling analysis for an integrally stiffened panel structure with a friction stir weld," *Thin-walled structures*, vol. 47, no. 12, pp. 1608–1622, 2009.

[35] S. Negi, A. A. Nambolan, S. Kapil, P. S. Joshi, R. Manivannan, K. Karunakaran, and P. Bhargava, "Review on electron beam based additive manufacturing," *Rapid Prototyping Journal*, 2019.

[36] J. Plocher and A. Panesar, "Review on design and structural optimisation in additive manufacturing: Towards next-generation lightweight structures," *Materials & Design*, vol. 183, p. 108164, Dec. 2019. [Online]. Available: https://linkinghub.elsevier.com/retrieve/pii/S0264127519306021

[37] M. P. Bendsøe and O. Sigmund, "Topology optimization by distribution of isotropic material," in *Topology Optimization*. Berlin, Heidelberg: Springer Berlin Heidelberg, 2004, pp. 1–69. [Online]. Available: http://link.springer.com/10.1007/978-3-662-05086-6_1

[38] L. Krog, A. Tucker, M. Kemp, and R. Boyd, "Topology optimisation of aircraft wing box ribs," in *10th AIAA/ISSMO Multidisciplinary Analysis and Optimization Conference*. Albany, New York: American Institute of Aeronautics and Astronautics, Aug. 2004. [Online]. Available: http://arc.aiaa.org/doi/10.2514/6.2004-4481

[39] N. Aage, E. Andreassen, B. S. Lazarov, and O. Sigmund, "Giga-voxel computational morphogenesis for structural design," *Nature*, vol. 550, p. 84, Oct. 2017. [Online]. Available: https://doi.org/10.1038/nature23911

[40] G. Singh, V. Toropov, and J. Eves, "Topology Optimization of a Blended-Wing-Body Aircraft Structure," in *17th AIAA/ISSMO Multidisciplinary Analysis and Optimization Conference*. Washington, D.C.: American Institute of Aeronautics and Astronautics, Jun. 2016. [Online]. Available: http://arc.aiaa.org/doi/10.2514/6.2016-3364

[41] E. Hunter, "Alternate detail part design and analysis: Topology, size, and shape optimization of ch-47 chinook underfloor structure," in *ANNUAL FORUM PROCEEDINGS-AMERICAN HELICOPTER SOCIETY*, vol. 62, no. 1. American Helicopter Society, Inc, 2006, p. 260.

[42] O. Shai and Y. Reich, "Infused design. i. theory," *Research in Engineering Design*, vol. 15, no. 2, pp. 93–107, 2004.

[43] A. Hatchuel and B. Weil, "Ck design theory: an advanced formulation," *Research in engineering design*, vol. 19, no. 4, pp. 181–192, 2009.

[44] W. J. V. e. Josip Stjepandić, Nel Wognum, *Concurrent Engineering in the 21st Century: Foundations, Developments and Challenges*, 1st ed. Springer International Publishing, 2015.

[45] A. Mammela, J. Riekki, A. Kotelba, and A. Anttonen, "Multidisciplinary and historical perspectives for developing intelligent and resource-efficient systems," *IEEE Access*, vol. 6, pp. 17 464–17 499, 2018. [Online]. Available: http://ieeexplore.ieee.org/document/8318568/

[46] A. M. Farid and N. P. Suh, Eds., *Axiomatic Design in Large Systems*. Cham: Springer International Publishing, 2016. [Online]. Available: http://link.springer.com/10.1007/978-3-319-32388-6

[47] N. P. Suh, *Complexity: theory and applications*. Oxford University Press on Demand, 2005.

[48] E. Puik and D. Ceglarek, "Axiomatic product design in three stages: A constituent roadmap that visualises the status of the design process by tracking the knowledge of the designer," in *Volume 15: Advances in Multidisciplinary Engineering*. Houston, Texas, USA: American Society of Mechanical Engineers, Nov. 2015, p.

V015T19A003. [Online]. Available: https://asmedigitalcollection.asme.org/IMECE/proceedings/IMECE2015/57588/Houston,%20Texas,%20USA/262527

[49] E. Puik, J. van Duijn, and D. Ceglarek, "Guidelines for application of the constituent roadmap of product design based on axiomatic design," *MATEC Web of Conferences*, vol. 127, p. 01013, 2017. [Online]. Available: http://www.matec-conferences.org/10.1051/matecconf/201712701013

[50] C. Königseder and K. Shea, "Comparing strategies for topologic and parametric rule application in automated computational design synthesis," *Journal of Mechanical Design*, vol. 138, no. 1, 2016.

[51] A. Hooshmand, *Solving engineering design problems through a combination of generative grammars and simulations*, ser. Produktentwicklung. München: Dr. Hut, 2014, oCLC: 931607788.

[52] J. Mountstephens and J. Teo, "Progress and challenges in generative product design: A review of systems," *Computers*, vol. 9, no. 4, p. 80, 2020.

[53] S. Krish, "A practical generative design method," *Computer-Aided Design*, vol. 43, no. 1, pp. 88–100, 2011.

[54] S. BuHamdan, A. Alwisy, and A. Bouferguene, "Generative systems in the architecture, engineering and construction industry: A systematic review and analysis," *International Journal of Architectural Computing*, p. 147807712093412, Jun. 2020. [Online]. Available: http://journals.sagepub.com/doi/10.1177/1478077120934126

[55] A. Nordin, "Challenges in the industrial implementation of generative design systems: An exploratory study," *Artificial Intelligence for Engineering Design, Analysis and Manufacturing: AI EDAM*, vol. 32, no. 1, p. 16, 2018.

[56] S. Venkataraman and R. T. Haftka, "Structural optimization complexity: what has moore's law done for us?" *Structural and Multidisciplinary Optimization*, vol. 28, no. 6, pp. 375–387, 2004.

[57] X.-Y. Ni, G. B. Prusty, and A. K. Hellier, "Buckling and post-buckling of isotropic and composite stiffened panels: A review on optimisation (2000-2015)," in *Transactions of the Royal Institution of Naval Architects Part A: International Journal of Maritime Engineering*, vol. 158, Jun. 2016, pp. 251–267.

[58] E. F. Bruhn, *Analysis and Design of Flight Vehicle Structures*. Indianapolis: Jacobs Pub., 1973, oCLC: 928252817.

[59] R. C. Rice, J. L. Jackson, and S. Bakuckas, J.and Thompson, "Metallic materials properties development and standardization (MMPDS)," Department of Transportation Federal Aviation Administration, Tech. Rep., January 2003. [Online]. Available: https://ntrl.ntis.gov/NTRL/dashboard/searchResults/titleDetail/PB2003106632.xhtml

[60] D. Stamatelos, G. Labeas, and K. Tserpes, "Analytical calculation of local buckling and post-buckling behavior of isotropic and orthotropic stiffened panels," *Thin-Walled Structures*, vol. 49, no. 3, pp. 422–430, 2011.

[61] Y. Xu, Y. Tong, M. Liu, and B. Suman, "A new effective smeared stiffener method for global buckling analysis of grid stiffened composite panels," *Composite Structures*, vol. 158, pp. 83–91, 2016.

[62] B. Liu, Y. Garbatov, W. Wu, C. G. Soares *et al.*, "Study on ultimate compressive strength of aluminium-alloy plates and stiffened panels," *Journal of Marine Science and Application*, pp. 1–19, 2020.

[63] R. D. Cook *et al.*, *Concepts and Applications of Finite Element Analysis*. John Wiley & Sons, 2007.

[64] J. Deng, X. Wang, Z. Yuan, and G. Zhou, "An efficient technique for simultaneous local and overall buckling analysis of stiffened panels," *Advances in Engineering Software*, vol. 131, pp. 36–47, May 2019. [Online]. Available: https://linkinghub.elsevier.com/retrieve/pii/S0965997818311955

[65] M. Mert and A. Kayran, "Post-buckling load redistribution of stiffened panels in aircraft wingbox structures," in *57th AIAA/ASCE/AHS/ASC Structures, Structural Dynamics, and Materials Conference*, 2016, p. 1974.

[66] M. Bruyneel, B. Colson, and A. Remouchamps, "Discussion on some convergence problems in buckling optimisation," *Structural and Multidisciplinary Optimization*, vol. 35, no. 2, pp. 181–186, 2008.

[67] M. C.-Y. Niu, *Airframe structural design: practical design information and data on aircraft structures*, 2nd ed. Hong Kong: Conmilit Press, 2002, oCLC: 248812908.

[68] P. Fenner, A. Watson, and C. Featherston, "Modelling infinite length panels using the finite element method," *International Journal of Structural Stability and Dynamics*, vol. 16, no. 07, p. 1750038, Sep. 2016. [Online]. Available: https://www.worldscientific.com/doi/abs/10.1142/S0219455417500389

[69] K. Tian, B. Wang, P. Hao, and A. M. Waas, "A high-fidelity approximate model for determining lower-bound buckling loads for stiffened shells," *International Journal of Solids and Structures*, vol. 148, pp. 14–23, 2018.

[70] F. S. Liguori, A. Madeo, D. Magisano, L. Leonetti, and G. Garcea, "Post-buckling optimisation strategy of imperfection sensitive composite shells using Koiter method and Monte Carlo simulation," *Composite Structures*, vol. 192, pp. 654–670, 2018.

[71] C. Fleury, M. Bruyneel, B. Colson, and A. Remouchamps, "Buckling optimization of composite stiffened panels: some important issues," *Proc. 2nd ICEO, Lisbon, Portugal*, 2010.

[72] S. S. Chauhan and J. R. Martins, "Low-fidelity aerostructural optimization of aircraft wings with a simplified wingbox model using OpenAeroStruct," in *International Conference on Engineering Optimization*. Springer, 2018, pp. 418–431.

[73] S. S. Rao, *Engineering optimization: theory and practice*. John Wiley & Sons, 2019.

[74] K. Svanberg, "The Method of Moving Asymptotes—a new method for structural optimization," *International journal for numerical methods in engineering*, vol. 24, no. 2, pp. 359–373, 1987.

[75] K. Svanberg, "A globally convergent version of MMA without linesearch," in *Proceedings of the first world congress of structural and multidisciplinary optimization*, vol. 28. Goslar, Germany, 1995, pp. 9–16.

[76] O. Sigmund and K. Maute, "Topology optimization approaches: A comparative review," *Structural and Multidisciplinary Optimization*, vol. 48, no. 6, pp. 1031–1055, Dec. 2013. [Online]. Available: http://link.springer.com/10.1007/s00158-013-0978-6

[77] S. G. Johnson, "The NLopt nonlinear-optimization package." [Online]. Available: http://github.com/stevengj/nlopt

[78] Altair Engineering Inc., "Altair OptiStruct 2019 Reference Guide," https://www.altair.com/optistruct/, Altair Engineering Inc., 2019.

[79] "Ansys© Workbench," USA, Apr. 2020.

[80] G. G. Wang, Z. Dong, and P. Aitchison, "Adaptive response surface method-a global optimization scheme for approximation-based design problems," *Engineering Optimization*, vol. 33, no. 6, pp. 707–734, 2001.

[81] S. Le Digabel, "Algorithm 909: NOMAD: Nonlinear optimization with the MADS algorithm," *ACM Transactions on Mathematical Software (TOMS)*, vol. 37, no. 4, pp. 1–15, 2011.

[82] S. B. Mulani, D. Havens, A. Norris, R. K. Bird, R. K. Kapania, and O. Robert, "Design, optimization, and evaluation of Al–2139 compression panel with integral T-stiffeners," *Journal of Aircraft*, vol. 50, no. 4, pp. 1275–1286, Jul. 2013. [Online]. Available: http://arc.aiaa.org/doi/10.2514/1.C032199

[83] T. D. Dang, R. K. Kapania, W. C. Slemp, M. Bhatia, and S. P. Gurav, "Optimization and postbuckling analysis of curvilinear-stiffened panels under multiple-load cases," *Journal of Aircraft*, vol. 47, no. 5, pp. 1656–1671, 2010.

[84] H. Chen, Y. Xu, J. Hu, and X. Wang, "Optimization of lightweight sub-stiffened panels with buckling analysis and imperfection sensitivity analysis," *Proceedings of the Institution of Mechanical Engineers, Part G: Journal of Aerospace Engineering*, vol. 233, no. 15, pp. 5507–5521, Dec. 2019. [Online]. Available: http://journals.sagepub.com/doi/10.1177/0954410019856782

[85] D. Quinn, A. Murphy, and L. Cervi, "Fatigue performance of aircraft panels with novel skin buckling containment features," *Proceedings of the Institution of Mechanical Engineers, Part G: Journal of Aerospace Engineering*, vol. 225, no. 7, pp. 791–806, Jul. 2011. [Online]. Available: http://journals.sagepub.com/doi/10.1177/0954410011399035

[86] D. Quinn, A. Murphy, W. McEwan, and F. Lemaitre, "Stiffened panel stability behaviour and performance gains with plate prismatic sub-stiffening," *Thin-Walled Structures*, vol. 47, no. 12, pp. 1457–1468, 2009.

[87] D. Quinn, A. Murphy, and C. Glazebrook, "Aerospace stiffened panel initial sizing with novel skin sub-stiffening features," *International Journal of Structural Stability and Dynamics*, vol. 12, no. 05, p. 1250060, 2012.

[88] G. Houston, D. Quinn, A. Murphy, and F. Bron, "Design rules for stiffened panel buckling containment features," *Thin-Walled Structures*, vol. 116, pp. 69–81, Jul. 2017. [Online]. Available: https://linkinghub.elsevier.com/retrieve/pii/S0263823117302586

[89] Y. Ye, W. Zhu, J. Jiang, Q. Xu, and Y. Ke, "Design and optimization of composite sub-stiffened panels," *Composite Structures*, vol. 240, p. 112084, 2020.

[90] M. Ozdemir, S. Sadamoto, S. Tanaka, S. Okazawa, T. Yu, and T. Bui, "Application of 6-dofs meshfree modeling to linear buckling analysis of stiffened plates with curvilinear surfaces," *Acta Mechanica*, vol. 229, no. 12, pp. 4995–5012, 2018.

[91] R. Vescovini, V. Oliveri, D. Pizzi, L. Dozio, and P. Weaver, "Pre-buckling and buckling analysis of variable-stiffness, curvilinearly stiffened panels," *Aerotecnica Missili & Spazio*, pp. 1–10, 2019.

[92] A. Saeedi, B. Hassani, and A. Farzam, "Simultaneous modeling and structural analysis of curvilinearly stiffened plates using an isogeometric approach," *Acta Mechanica*, vol. 231, no. 8, pp. 3473–3498, 2020.

[93] K. Singh, W. Zhao, M. Jrad, and R. K. Kapania, "Hybrid optimization of curvilinearly stiffened shells using parallel processing," *Journal of Aircraft*, vol. 56, no. 3, pp. 1068–1079, 2019.

[94] W. C. Slemp, R. K. Bird, R. K. Kapania, D. Havens, A. Norris, and R. Olliffe, "Design, optimization, and evaluation of integrally stiffened al-7050 panel with curved stiffeners," *Journal of aircraft*, vol. 48, no. 4, pp. 1163–1175, 2011.

[95] B. K. Stanford, C. V. Jutte, and C. A. Coker, "Aeroelastic sizing and layout design of a wingbox through nested optimization," *AIAA Journal*, vol. 57, no. 2, pp. 848–857, 2019.

[96] B. Keshtegar, P. Hao, Y. Wang, and Q. Hu, "An adaptive response surface method and gaussian global-best harmony search algorithm for optimization of aircraft stiffened panels," *Applied Soft Computing*, vol. 66, pp. 196–207, 2018.

[97] P. Hao, "Intelligent layout design of curvilinearly stiffened panels via deep learning-based method," *Materials and Design*, p. 16, 2021.

[98] D. Wang, "Buckling optimization design of curved stiffeners for grid-stiffened composite structures," *Composite Structures*, p. 11, 2017.

[99] D. Liu, P. Hao, K. Zhang, K. Tian, B. Wang, G. Li, and W. Xu, "On the integrated design of curvilinearly grid-stiffened panel with non-uniform distribution and variable stiffener profile," *Materials & Design*, vol. 190, p. 108556, 2020.

[100] A. Alhajahmad and C. Mittelstedt, "Design tailoring of curvilinearly grid-stiffened variable-stiffness composite cylindrically curved panels for maximum buckling capacity," *Thin-Walled Structures*, vol. 157, p. 107132, 2020.

[101] R. Savage, "Fusion 360 introduction to generative design," AutoDesk University, Tech. Rep., 2019. [Online]. Available: https://www.autodesk.com/autodesk-university/class/Fusion-360-Introduction-Generative-Design-2019#downloads

[102] E. Tyflopoulos, F. D. Tollnes, M. Steinert, A. Olsen *et al.*, "State of the art of generative design and topology optimization and potential research needs," *DS 91: Proceedings of NordDesign 2018, Linköping, Sweden, 14th-17th August 2018*, 2018.

[103] T. Briard, F. Segonds, and N. Zamariola, "G-DfAM: a methodological proposal of generative design for additive manufacturing in the automotive industry," *International Journal on Interactive Design and Manufacturing (IJIDeM)*, vol. 14, no. 3, pp. 875–886, Sep. 2020. [Online]. Available: http://link.springer.com/10.1007/s12008-020-00669-6

[104] M. Schnitger, "An Introduction to Generative Design," 2018. [Online]. Available: https://info.cadalyst.com/

[105] J. Matejka, M. Glueck, E. Bradner, A. Hashemi, T. Grossman, and G. Fitzmaurice, "Dream lens: Exploration and visualization of large-scale generative design datasets," in *Proceedings of the 2018 CHI Conference on Human Factors in Computing Systems*, 2018, pp. 1–12.

[106] N. O. Sönmez, "A review of the use of examples for automating architectural design tasks," *Computer-Aided Design*, vol. 96, pp. 13 – 30, 2018. [Online]. Available: http://www.sciencedirect.com/science/article/pii/S0010448517301781

[107] L. March, "Forty years of shape and shape grammars, 1971-2011," *Nexus Network Journal*, vol. 13, no. 1, p. 5, 2011.

[108] S. Oh, Y. Jung, S. Kim, I. Lee, and N. Kang, "Deep generative design: Integration of topology optimization and generative models," *Journal of Mechanical Design*, vol. 141, no. 11, 2019.

[109] P. Prusinkiewicz and A. Lindenmayer, *The Algorithmic Beauty of Plants*. Springer Science & Business Media, 2012.

[110] G. S. Hornby and J. B. Pollack, "The advantages of generative grammatical encodings for physical design," in *Proceedings of the 2001 Congress on Evolutionary Computation (IEEE Cat. No. 01TH8546)*, vol. 1. IEEE, 2001, pp. 600–607.

[111] J. McCormack, B. Porter, and J. Wetter, "A scriptable, generative modelling system for dynamic 3d meshes," *arXiv preprint arXiv:2004.10354*, 2020.

[112] A. Lobos, "Finding balance in generative product design," in *Norddesign 2018*. Linköping University, 2018.

[113] C. Königseder and K. Shea, "Systematic rule analysis of generative design grammars," *AI EDAM*, vol. 28, no. 3, pp. 227–238, 2014.

[114] M. I. Campbell, "A graph grammar methodology for generative systems," University of Texas at Austin, Tech. Rep., 2009.

[115] A. Chakrabarti, K. Shea, R. Stone, J. Cagan, M. Campbell, N. V. Hernandez, and K. L. Wood, "Computer-based design synthesis research: an overview," *Journal of Computing and Information Science in Engineering*, vol. 11, no. 2, 2011.

[116] P. Klint, R. Lämmel, and C. Verhoef, "Toward an engineering discipline for grammarware," *ACM Transactions on Software Engineering and Methodology (TOSEM)*, vol. 14, no. 3, pp. 331–380, 2005.

[117] J. Patel and M. I. Campbell, "An approach to automate and optimize concept generation of sheet metal parts by topological and parametric decoupling," *Journal of Mechanical Design*, vol. 132, no. 5, 2010.

[118] M. A. Zboinska, "Hybrid CAD/E platform supporting exploratory architectural design," *Computer-Aided Design*, vol. 59, pp. 64 – 84, 2015. [Online]. Available: http://www.sciencedirect.com/science/article/pii/S0010448514001985

[119] S. Khan, E. Gunpinar, and B. Sener, "GenYacht: An interactive generative design system for computer-aided yacht hull design," *Ocean Engineering*, vol. 191, p. 106462, Nov. 2019. [Online]. Available: https://linkinghub.elsevier.com/retrieve/pii/S0029801819306043

[120] C. M. Herr and R. C. Ford, "Cellular automata in architectural design: From generic systems to specific design tools," *Automation in Construction*, vol. 72, pp. 39–45, 2016.

[121] C. M. Herr and R. C. Ford, "Adapting cellular automata as architectural design tools," in *Emerging Experience in Past,Present and Future of Digital Architecture, Proceedings of the 20th International Conference of the Association for Computer-Aided Architectural Design Research in Asia CAADRIA*. Hong Kong: The Association for Computer-Aided Architectural Design Research in Asia (CAADRIA), 2015, pp. 169–178.

[122] A. Adamatzky, *Game of life cellular automata*. Springer, 2010, vol. 1.

[123] H. Erhan, I. Y. Wang, and N. Shireen, "Harnessing design space: a similarity-based exploration method for generative design," *International Journal of Architectural Computing*, vol. 13, no. 2, pp. 217–236, 2015.

[124] N. C. Brown and C. T. Mueller, "Quantifying diversity in parametric design: a comparison of possible metrics," *Artificial Intelligence for Engineering Design, Analysis and Manufacturing*, vol. 33, no. 1, p. 40–53, 2019.

[125] D. Mun, S. Han, J. Kim, and Y. Oh, "A set of standard modeling commands for the history-based parametric approach," *Computer-aided design*, vol. 35, no. 13, pp. 1171–1179, 2003.

[126] S. Vilgertshofer and A. Borrmann, "Using graph rewriting methods for the semi-automatic generation of parametric infrastructure models," *Advanced Engineering Informatics*, vol. 33, pp. 502–515, 2017.

[127] K. Shea, R. Aish, and M. Gourtovaia, "Towards integrated performance-driven generative design tools," *Automation in Construction*, vol. 14, no. 2, pp. 253–264, 2005.

[128] L. Zimmermann, T. Chen, and K. Shea, "A 3D, performance-driven generative design framework: automating the link from a 3D spatial grammar interpreter to structural finite element analysis and stochastic optimization," *Artificial Intelligence for Engineering Design, Analysis and Manufacturing: AI EDAM*, vol. 32, no. 2, p. 189, 2018.

[129] Y.-S. L.-K. Cio, Y. Ma, A. Vadean, G. Beltrame, and S. Achiche, "Evolutionary layout design synthesis of an autonomous greenhouse using product-related dependencies," *AI EDAM*, vol. 35, no. 1, pp. 49–64, 2021.

[130] D. J. Gerber, E. Pantazis, and A. Wang, "A multi-agent approach for performance based architecture: design exploring geometry, user, and environmental agencies in façades," *Automation in construction*, vol. 76, pp. 45–58, 2017.

[131] O. Krupnik, I. Mordatch, and A. Tamar, "Multi-agent reinforcement learning with multi-step generative models," in *Conference on Robot Learning*. PMLR, 2020, pp. 776–790.

[132] A. Ferdowsi and W. Saad, "Brainstorming generative adversarial networks (bgans): Towards multi-agent generative models with distributed private datasets," *arXiv preprint arXiv:2002.00306*, 2020.

[133] E. Francalanza, A. Fenech, and P. Cutajar, "Generative design in the development of a robotic manipulator," *Procedia CIRP*, vol. 67, pp. 244 – 249, 2018, 11th CIRP Conference on Intelligent Computation in Manufacturing Engineering, 19-21 July 2017, Gulf of Naples, Italy. [Online]. Available: http://www.sciencedirect.com/science/article/pii/S2212827117311514

[134] A. Lukin, S. Perepelkina, G. Demidova, D. Lukichev, A. Rassõlkin, T. Vaimann, and A. Kallaste, "Generative design in development of mechanical components for magnus effect-based wind turbine," in *2020 XI International Conference on Electrical Power Drive Systems (ICEPDS)*. IEEE, 2020, pp. 1–5.

[135] J. Lee, C. Mueller, and C. Fivet, "Automatic generation of diverse equilibrium structures through shape grammars and graphic statics," *International Journal of Space Structures*, vol. 31, no. 2-4, pp. 147–164, 2016.

[136] A. Hooshmand and M. I. Campbell, "Truss layout design and optimization using a generative synthesis approach," *Computers & Structures*, vol. 163, pp. 1–28, Jan. 2016. [Online]. Available: https://linkinghub.elsevier.com/retrieve/pii/S0045794915002692

[137] N. Shireen, H. Erhan, R. Woodbury, and I. Wang, "Making sense of design space," in *Computer-Aided Architectural Design. Future Trajectories*, vol. 724. Springer, 06 2017, pp. 191–211.

[138] T. Wortmann, "Efficient, visual, and interactive architectural design optimization with model-based methods," Ph.D. dissertation, Singapore University of Technology and Design, 2018.

[139] A. Konak, D. W. Coit, and A. E. Smith, "Multi-objective optimization using genetic algorithms: A tutorial," *Reliability Engineering & System Safety*, vol. 91, no. 9, pp. 992–1007, 2006.

[140] S. Buchanan and B. Aerospace, "Development of a wingbox rib for a passenger jet aircraft using design optimization and constrained to traditional design and manufacture requirements," in *Altair Engineering CAE Technology Conference*, 2007, p. 8.

[141] J. D. Deaton and R. V. Grandhi, "A survey of structural and multidisciplinary continuum topology optimization: Post 2000," *Structural and Multidisciplinary Optimization*, vol. 49, no. 1, pp. 1–38, Jan. 2014. [Online]. Available: http://link.springer.com/10.1007/s00158-013-0956-z

[142] M. Bendsoe, E. Lund, N. Olhoff, and O. Sigmund, "Topology optimization-broadening the areas of application," *Control and Cybernetics*, vol. 34, no. 1, p. 7, 2005.

[143] HyperWorks, *Detroit*. USA: Altair Engineering, 2018.

[144] M. P. Bendsøe, "Optimal shape design as a material distribution problem," *Structural optimization*, vol. 1, no. 4, pp. 193–202, 1989.

[145] D. J. Munk, G. A. Vio, and G. P. Steven, "Topology and shape optimization methods using evolutionary algorithms: a review," *Structural and Multidisciplinary Optimization*, vol. 52, no. 3, pp. 613–631, 2015.

[146] X. Huang and Y. M. Xie, *Evolutionary topology optimization of continuum structures: methods and applications*. Chichester: Wiley, 2010, oCLC: 730283590.

[147] O. Sigmund, N. Aage, and E. Andreassen, "On the (non-) optimality of michell structures," *Structural and Multidisciplinary Optimization*, vol. 54, no. 2, pp. 361–373, 2016.

[148] O. Sigmund, "A 99 line topology optimization code written in Matlab," *Structural and Multidisciplinary Optimization*, vol. 21, no. 2, pp. 120–127, Apr. 2001. [Online]. Available: http://link.springer.com/10.1007/s001580050176

[149] R. S. Iwamura and A. R. de Faria, "Topology optimization of multiple load case structures," in *Proceedings of International Symposium on Solid Mechanics, Porte Alegre, Brazil, April*, 2013.

[150] A. Sutradhar, J. Park, P. Haghighi, J. Kresslein, D. Detwiler, and J. J. Shah, "Incorporating manufacturing constraints in topology optimization methods: A survey," in *Volume 1: 37th Computers and Information in Engineering Conference*. Cleveland, Ohio, USA: American Society of Mechanical Engineers, Aug. 2017, p. V001T02A073. [Online]. Available: https://asmedigitalcollection.asme.org/IDETC-CIE/proceedings/IDETC-CIE2017/58110/Cleveland,%20Ohio,%20USA/259089

[151] J.-F. Gamache, A. Vadean, E. Noirot-Nerin, D. Beaini, and S. Achiche, "Image-based truss recognition for density-based topology optimization approach," *Structural and Multidisciplinary Optimization*, vol. 58, no. 6, pp. 2697–2709, Dec. 2018. [Online]. Available: http://link.springer.com/10.1007/s00158-018-2028-x

[152] J.-C. Cuillière and V. Francois, "Integration of CAD, FEA and Topology Optimization through a Unified Topological Model," *Computer-Aided Design*

and Applications, vol. 11, no. 5, pp. 493–508, Sep. 2014. [Online]. Available: http://www.cad-journal.net/files/vol_11/Vol11No5.html

[153] H. Layachi, Y.-m. Xu, and M. A. Bennaceur, "Topology Optimization and Design Guidelines of Sub-Stiffened Panels in Aerospace Applications," *MATEC Web of Conferences*, vol. 114, p. 03009, 2017. [Online]. Available: http://www.matec-conferences.org/10.1051/matecconf/201711403009

[154] Y. Zhou and Q. Fei, "Dynamic design of stiffeners for a typical panel using topology optimization and finite element analysis," *Advances in Mechanical Engineering*, vol. 7, no. 3, p. 1687814015572465, 2015.

[155] T. W. Chin and G. Kennedy, "Large-scale compliance-minimization and buckling topology optimization of the undeformed common research model wing," in *57th AIAA/ASCE/AHS/ASC Structures, Structural Dynamics, and Materials Conference*. San Diego, California, USA: American Institute of Aeronautics and Astronautics, Jan. 2016. [Online]. Available: http://arc.aiaa.org/doi/10.2514/6.2016-0939

[156] H. Jie, Z. Jihong, H. Fei, W. Zhang, and G. Wenjie, "Stiffeners layout design of thin-walled structures with constraints on multi-fastener joint loads," *Chinese Journal of Aeronautics*, vol. 30, no. 4, pp. 1441–1450, 2017.

[157] M. Stolpe, "Truss optimization with discrete design variables: a critical review," *Structural and Multidisciplinary Optimization*, vol. 53, no. 2, pp. 349–374, 2016.

[158] W. Dorn, "Automatic design of optimal structures," *J. de Mecanique*, vol. 3, pp. 25–52, 1964.

[159] A. R. Toakley, "Optimum design using available sections," *Journal of the Structural Division*, vol. 94, no. 5, pp. 1219–1244, 1968.

[160] T. Zegard, C. Hartz, A. Mazurek, and W. F. Baker, "Advancing building engineering through structural and topology optimization," *Structural and Multidisciplinary Optimization*, pp. 1–21, 2020.

[161] Y. Zhang, Y. Hou, and S. Liu, "A new method of discrete optimization for cross-section selection of truss structures," *Engineering Optimization*, vol. 46, no. 8, pp. 1052–1073, 2014. [Online]. Available: https://doi.org/10.1080/0305215X.2013.827671

[162] H. Fairclough and M. Gilbert, "Layout optimization of simplified trusses using mixed integer linear programming with runtime generation of constraints," *Structural and*

Multidisciplinary Optimization, vol. 61, no. 5, pp. 1977–1999, May 2020. [Online]. Available: http://link.springer.com/10.1007/s00158-019-02449-7

[163] M. Fenton, C. McNally, J. Byrne, E. Hemberg, J. McDermott, and M. O'Neill, "Discrete planar truss optimization by node position variation using grammatical evolution," *IEEE Transactions on Evolutionary Computation*, vol. 20, no. 4, pp. 577–589, Aug. 2016. [Online]. Available: http://ieeexplore.ieee.org/document/7335624/

[164] S. Roy, W. A. Crossley, B. Stanford, K. T. Moore, and J. S. Gray, "A mixed integer efficient global optimization algorithm with multiple infill strategy-applied to a wing topology optimization problem," in *AIAA Scitech 2019 Forum*, 2019, p. 2356.

[165] W. Yang, Z. Yue, L. Li, and P. Wang, "Aircraft wing structural design optimization based on automated finite element modelling and ground structure approach," *Engineering Optimization*, vol. 48, no. 1, pp. 94–114, Jan. 2016. [Online]. Available: http://www.tandfonline.com/doi/full/10.1080/0305215X.2014.995175

[166] W. Zhu, X. Yu, and Y. Wang, "Layout optimization for blended wing body aircraft structure," *International Journal of Aeronautical and Space Sciences*, vol. 20, no. 4, pp. 879–890, 2019.

[167] T. J. Ikonen and A. Sobester, "Ground structure approaches for the evolutionary optimization of aircraft wing structures," in *16th AIAA Aviation Technology, Integration, and Operations Conference*, 2016, p. 3286.

[168] M. Friswell, D. Baker, J. Herencia, F. Mattioni, and P. Weaver, "Compliant structures for morphing aircraft," *Proceedings of the ICAST2006, Taipei, Taiwan*, pp. 16–19, 2006.

[169] R. Van Dijk, X. Zhao, H. Wang, and F. Van Dalen, "Multidisciplinary design and optimization framework for aircraft box structures," in *Proceedings of the 3rd Aircraft Structural Design Conference, Delft, The Netherlands, 9-11 October 2012*. Royal Aeronautical Society, 2012.

[170] Z. Xia, Y. Wang, Q. Wang, and C. Mei, "GPU parallel strategy for parameterized LSM-based topology optimization using isogeometric analysis," *Structural and Multidisciplinary Optimization*, vol. 56, no. 2, pp. 413–434, Aug. 2017. [Online]. Available: http://link.springer.com/10.1007/s00158-017-1672-x

[171] L. Jiu, W. Zhang, L. Meng, Y. Zhou, and L. Chen, "A CAD-oriented structural topology optimization method," *Computers & Structures*, vol. 239, p. 106324, Oct. 2020. [Online]. Available: https://linkinghub.elsevier.com/retrieve/pii/S0045794920301279

[172] J. Liu and Y. Ma, "A new multi-material level set topology optimization method with the length scale control capability," *Computer Methods in Applied Mechanics and Engineering*, vol. 329, pp. 444–463, 2018.

[173] S. Townsend and H. A. Kim, "A level set topology optimization method for the buckling of shell structures," *Structural and Multidisciplinary Optimization*, vol. 60, no. 5, pp. 1783–1800, Nov. 2019. [Online]. Available: http://link.springer.com/10.1007/s00158-019-02374-9

[174] S. Kambampati, S. Townsend, and H. A. Kim, "Coupled aerostructural level set topology optimization of aircraft wing boxes," *AIAA Journal*, 2020.

[175] B. Li, H. Liu, and S. Zheng, "Multidisciplinary topology optimization for reduction of sloshing in aircraft fuel tanks based on sph simulation," *Structural and Multidisciplinary Optimization*, vol. 58, no. 4, pp. 1719–1736, 2018.

[176] J. A. Norato, "A geometry projection method for continuum-based topology optimization with discrete elements," *Comput. Methods Appl. Mech. Engrg.*, p. 22, 2015.

[177] W. Zhang, Y. Liu, P. Wei, Y. Zhu, and X. Guo, "Explicit control of structural complexity in topology optimization," *Computer Methods in Applied Mechanics and Engineering*, vol. 324, pp. 149–169, Sep. 2017. [Online]. Available: https://linkinghub.elsevier.com/retrieve/pii/S0045782516317443

[178] W. Zhang, D. Li, J. Zhang, and X. Guo, "Minimum length scale control in structural topology optimization based on the Moving Morphable Components (MMC) approach," *Computer Methods in Applied Mechanics and Engineering*, vol. 311, pp. 327–355, Nov. 2016. [Online]. Available: https://linkinghub.elsevier.com/retrieve/pii/S0045782516309835

[179] S. Zhang, A. L. Gain, and J. A. Norato, "Stress-based topology optimization with discrete geometric components," *Computer Methods in Applied Mechanics and Engineering*, vol. 325, pp. 1–21, Oct. 2017. [Online]. Available: https://linkinghub.elsevier.com/retrieve/pii/S0045782517304577

[180] X. Guo, W. Zhang, J. Zhang, and J. Yuan, "Explicit structural topology optimization based on moving morphable components (MMC) with curved skeletons," *Comput. Methods Appl. Mech. Engrg.*, p. 38, 2016.

[181] T. Cui, Z. Sun, C. Liu, L. Li, R. Cui, and X. Guo, "Topology optimization of plate structures using plate element-based moving morphable component (MMC)

approach," *Acta Mechanica Sinica*, vol. 36, no. 2, pp. 412–421, Apr. 2020. [Online]. Available: http://link.springer.com/10.1007/s10409-020-00944-5

[182] W. Zhang, J. Yuan, J. Zhang, and X. Guo, "A new topology optimization approach based on moving morphable components (mmc) and the ersatz material model," *Structural and Multidisciplinary Optimization*, vol. 53, no. 6, pp. 1243–1260, 2016.

[183] Z. Sun, R. Cui, T. Cui, C. Liu, S. Shi, and X. Guo, "An optimization approach for stiffener layout of composite stiffened panels based on moving morphable components (mmcs)," *Acta Mechanica Solida Sinica*, pp. 1–13, 2020.

[184] H. Liu, B. Li, Z. Yang, and J. Hong, "Topology optimization of stiffened plate/shell structures based on adaptive morphogenesis algorithm," *Journal of Manufacturing Systems*, vol. 43, pp. 375–384, Apr. 2017. [Online]. Available: https://linkinghub.elsevier.com/retrieve/pii/S0278612517300158

[185] B. Li, H. Liu, Z. Yang, and J. Zhang, "Stiffness design of plate/shell structures by evolutionary topology optimization," *Thin-Walled Structures*, vol. 141, pp. 232–250, 2019.

[186] D. J. Lohan, E. M. Dede, and J. T. Allison, "Topology optimization for heat conduction using generative design algorithms," *Structural and Multidisciplinary Optimization*, vol. 55, no. 3, pp. 1063–1077, 2017.

[187] B. R. Bielefeldt, D. J. Hartl, J. D. Hodson, G. W. Reich, P. S. Beran, A. M. Pankonien, and J. D. Deaton, "Graph-based interpretation of l-system encodings toward aeroelastic topology optimization of a morphing airfoil in supersonic flow," in *Smart Materials, Adaptive Structures and Intelligent Systems*, vol. 59131. American Society of Mechanical Engineers, 2019, p. V001T04A013.

[188] S. Y. Wang and K. Tai, "Graph representation for structural topology optimization using genetic algorithms," *Computers and Structures*, p. 14, 2004.

[189] A.-R. Short, B. L. DuPont, and M. I. Campbell, "A comparison of tree search methods for graph topology design problems," in *International Conference on-Design Computing and Cognition*. Springer, 2018, pp. 75–94.

[190] X. Gao, Y. Li, H. Ma, and G. Chen, "Improving the overall performance of continuum structures: A topology optimization model considering stiffness, strength and stability," *Computer Methods in Applied Mechanics and Engineering*, vol. 359, p.

112660, 2020. [Online]. Available: http://www.sciencedirect.com/science/article/pii/S0045782519305456

[191] F. Ferrari and O. Sigmund, "Revisiting topology optimization with buckling constraints," *Structural and Multidisciplinary Optimization*, vol. 59, no. 5, pp. 1401–1415, May 2019. [Online]. Available: http://link.springer.com/10.1007/s00158-019-02253-3

[192] J. París, F. Navarrina, I. Colominas, and M. Casteleiro, "Block aggregation of stress constraints in topology optimization of structures," *Advances in Engineering Software*, vol. 41, no. 3, pp. 433–441, 2010.

[193] P. D. Dunning, E. Ovtchinnikov, J. Scott, and H. A. Kim, "Level-set topology optimization with many linear buckling constraints using an efficient and robust eigensolver," *International Journal for Numerical Methods in Engineering*, vol. 107, no. 12, pp. 1029–1053, 2016.

[194] S. Johnsen, "Structural topology optimization: Basic theory, methods and applications," Master's thesis, Institutt for produktutvikling og materialer, 2013.

[195] A. Olason, "Methodology for Topology and Shape Optimization in the Design Process," Master's thesis, Chalmers University of Technology, Goteborg, Sweden, 2010.

[196] A. Dugré, A. Vadean, and J. Chaussée, "Challenges of using topology optimization for the design of pressurized stiffened panels," *Structural and Multidisciplinary Optimization*, vol. 53, no. 2, pp. 303–320, Feb. 2016. [Online]. Available: http://link.springer.com/10.1007/s00158-015-1321-1

[197] J. Zhang, B. Wang, F. Niu, and G. Cheng, "Design optimization of connection section for concentrated force diffusion," *Mechanics Based Design of Structures and Machines*, vol. 43, no. 2, pp. 209–231, 2015.

[198] P. Y. Papalambros and K. Shea, "Creating structural configurations," *Formal Engineering Design Synthesis, EK Antonsson, and J. Cagan, eds., Cambridge University, Cambridge, UK*, pp. 93–125, 2005.

[199] S. Mostafavi, M. Morales Beltran, and N. Biloria, "Performance driven design and design information exchange," in *Proceedings of the 31st International Conference on Education and research in Computer Aided Architectural Design in Europe*. Education and research in Computer Aided Architectural Design in Europe, 2013, pp. 117–126.

[200] A. Mandhyan, G. Srivastava, and S. Krishnamoorthi, "A novel method for prediction of truss geometry from topology optimization," *Engineering with Computers*, vol. 33, no. 1, pp. 95–106, 2017.

[201] G. Yi and N. H. Kim, "Identifying boundaries of topology optimization results using basic parametric features," *Structural and Multidisciplinary Optimization*, vol. 55, no. 5, pp. 1641–1654, 2017.

[202] Y.-H. Chou and C.-Y. Lin, "Improved image interpreting and modeling technique for automated structural optimization system," *Structural and Multidisciplinary Optimization*, vol. 40, no. 1, pp. 215–226, 2010.

[203] C. Lin and Y. Chou, "Automated structural optimization system for integrated topology and shape optimization," *Journal of the Chinese Institute of Engineers*, vol. 31, no. 5, pp. 745–756, Jul. 2008. [Online]. Available: http://www.tandfonline.com/doi/abs/10.1080/02533839.2008.9671429

[204] A. Yildiz, N. Öztürk, N. Kaya, and F. Öztürk, "Integrated optimal topology design and shape optimization using neural networks," *Structural and Multidisciplinary Optimization*, vol. 25, no. 4, pp. 251–260, Oct. 2003. [Online]. Available: http://link.springer.com/10.1007/s00158-003-0300-0

[205] Y.-L. Hsu, M.-S. Hsu, and C.-T. Chen, "Interpreting results from topology optimization using density contours," *Computers & Structures*, vol. 79, no. 10, pp. 1049–1058, Apr. 2001. [Online]. Available: https://linkinghub.elsevier.com/retrieve/pii/S0045794900001942

[206] A. Koguchi and N. Kikuchi, "A surface reconstruction algorithm for topology optimization," *Engineering with Computers*, vol. 22, no. 1, pp. 1–10, 2006.

[207] S. Larsen and C. G. Jensen, "Converting topology optimization results into parametric cad models," *Computer-Aided Design and Applications*, vol. 6, no. 3, pp. 407–418, 2009.

[208] L. Barbieri, F. Bruno, M. Muzzupappa, and U. Cugini, "Design Automation Tools as a Support for Knowledge Management in Topology Optimization," in *Volume 1: 34th Design Automation Conference, Parts A and B*. Brooklyn, New York, USA: ASMEDC, Jan. 2008, pp. 1227–1234. [Online]. Available: https://asmedigitalcollection.asme.org/IDETC-CIE/proceedings/IDETC-CIE2008/43253/1227/330872

[209] J. Liu and Y. Ma, "A survey of manufacturing oriented topology optimization methods," *Advances in Engineering Software*, vol. 100, pp. 161–175, Oct. 2016. [Online]. Available: https://linkinghub.elsevier.com/retrieve/pii/S0965997816302174

[210] Y. Mass and O. Amir, "Topology optimization for additive manufacturing: Accounting for overhang limitations using a virtual skeleton," *Additive Manufacturing*, vol. 18, pp. 58–73, 2017.

[211] A. Mandhyan, G. Srivastava, and S. Krishnamoorthi, "A novel method for prediction of truss geometry from topology optimization," *Engineering with Computers*, vol. 33, no. 1, pp. 95–106, Jan. 2017. [Online]. Available: http://link.springer.com/10.1007/s00366-016-0474-x

[212] M. Chirehdast and P. Papalambros, "A note on automated detection of mobility of skeletal structures," *Computers & Structures*, vol. 45, no. 1, pp. 197–207, Sep. 1992. [Online]. Available: https://linkinghub.elsevier.com/retrieve/pii/0045794992903576

[213] C. Arcelli, L. Cordella, and S. Levialdi, "Parallel thinning of binary pictures," *Electronics Letters*, vol. 11, no. 7, pp. 148–149, 1975.

[214] M. Kaufmann, D. Zenkert, and P. Wennhage, "Integrated cost/weight optimization of aircraft structures," *Structural and Multidisciplinary Optimization*, vol. 41, no. 2, pp. 325–334, Mar. 2010. [Online]. Available: http://link.springer.com/10.1007/s00158-009-0413-1

[215] S. S. Chauhan and J. R. R. A. Martins, "Tilt-wing eVTOL takeoff trajectory optimization," *Journal of Aircraft*, vol. 57, no. 1, pp. 93–112, Jan. 2020.

[216] M. Belardo, J. Beretta, A. D. Marano, G. Diodati, N. Paletta, and L. Di Palma, "On the preliminary structural design strategy of the wing of the next-generation civil tiltrotor technology demonstrator," *International Journal of Aeronautical and Space Sciences*, vol. 22, no. 3, pp. 613–624, 2021.

[217] M. Belardo, A. D. Marano, J. Beretta, G. Diodati, M. Graziano, M. Capasso, P. Ariola, S. Orlando, F. Di Caprio, N. Paletta *et al.*, "Wing structure of the next-generation civil tiltrotor: From concept to preliminary design," *Aerospace*, vol. 8, no. 4, p. 102, 2021.

[218] A. Remouchamps, M. Bruyneel, C. Fleury, and S. Grihon, "Application of a bi-level scheme including topology optimization to the design of an aircraft pylon," *Structural and Multidisciplinary Optimization*, vol. 44, no. 6, pp. 739–750, Dec. 2011. [Online]. Available: http://link.springer.com/10.1007/s00158-011-0682-3

[219] B. K. Stanford and P. D. Dunning, "Optimal topology of aircraft rib and spar structures under aeroelastic loads," *Journal of Aircraft*, vol. 52, no. 4, pp. 1298–1311, Jul. 2015. [Online]. Available: http://arc.aiaa.org/doi/10.2514/1.C032913

[220] R. Ansola, J. Canales, J. Tarrago, and J. Rasmussen, "Combined shape and reinforcement layout optimization of shell structures," *Structural and Multidisciplinary Optimization*, vol. 27, no. 4, pp. 219–227, 2004.

[221] P. D. Dunning, B. Stanford, and H. A. Kim, "Level-set topology optimization with aeroelastic constraints," in *56th AIAA/ASCE/AHS/ASC Structures, Structural Dynamics, and Materials Conference*. Kissimmee, Florida: American Institute of Aeronautics and Astronautics, Jan. 2015. [Online]. Available: http://arc.aiaa.org/doi/10.2514/6.2015-1128

[222] E. Puik and D. Ceglarek, "A different consideration on information and complexity in axiomatic design," in *Axiomatic Design in Large Systems*. Springer, 2016, pp. 105–129.

[223] J.-F. Gamache, A. Vadean, N. Dodane, and S. Achiche, "Validating novel stiffened panel configuration generated with topology optimization using non-linear analysis," in *Proceedings of Canadian Aeronautics and Space Institute AERO '19*. Canadian Aeronautics and Space Institute, May 2019.

[224] M. Zhou, N. Pagaldipti, H. Thomas, and Y. Shyy, "An integrated approach to topology, sizing, and shape optimization," *Structural and Multidisciplinary Optimization*, vol. 26, no. 5, pp. 308–317, 2004.

[225] O. Sigmund, "On the usefulness of non-gradient approaches in topology optimization," *Structural and Multidisciplinary Optimization*, vol. 43, no. 5, pp. 589–596, 2011.

[226] J.-F. Gamache, A. Vadean, and S. Achiche, "Topology optimization for the design of stiffened panels for wing box," in *Proceedings of Design Science Research 2018: Data-Driven Design and Learning*, Montreal, Canada, 2018.

[227] M. Zhou, "Difficulties in truss topology optimization with stress and local buckling constraints," *Structural Optimization*, vol. 11, no. 2, pp. 134–136, Apr. 1996. [Online]. Available: http://link.springer.com/10.1007/BF01376857

[228] G. I. N. Rozvany, "A critical review of established methods of structural topology optimization," *Structural and Multidisciplinary Optimization*, vol. 37, no. 3, pp. 217–237, Jan. 2009. [Online]. Available: http://link.springer.com/10.1007/s00158-007-0217-0

[229] W. Zhang, Y. Liu, Z. Du, Y. Zhu, and X. Guo, "A moving morphable component based topology optimization approach for rib-stiffened structures considering buckling constraints," *Journal of Mechanical Design*, vol. 140, no. 11, p. 111404, Nov. 2018. [Online]. Available: https://asmedigitalcollection.asme.org/mechanicaldesign/article/doi/10.1115/1.4041052/472606/A-Moving-Morphable-Component-Based-Topology

[230] R. D. Cook, D. S. Malkus, and P. R. J. Witt, *Concepts and applications of finite element analysis*, 4th ed. New York, NY: Wiley, 2001.

[231] G. Cheng and Z. Jiang, "Study on topology optimization with stress constraints," *Engineering Optimization*, vol. 20, no. 2, pp. 129–148, Nov. 1992. [Online]. Available: http://www.tandfonline.com/doi/abs/10.1080/03052159208941276

[232] A. International, J. R. Davis, and A. International, Eds., *Properties and Selection: Nonferrous Alloys and Special-Purpose Materials*, 10th ed., ser. ASM handbook. Materials Park, Ohio: ASM International, 2000, oCLC: 249055263.

[233] A. Alhajahmad and C. Mittelstedt, "Minimum weight design of curvilinearly grid-stiffened variable-stiffness composite fuselage panels considering buckling and manufacturing constraints," *Thin-Walled Structures*, vol. 161, p. 107526, 2021.

[234] H. H. Hoos and T. Stützle, *Stochastic local search: Foundations and applications*. Elsevier, 2004.

[235] L. Xia and P. Breitkopf, "Recent Advances on Topology Optimization of Multiscale Nonlinear Structures," *Archives of Computational Methods in Engineering*, vol. 24, no. 2, pp. 227–249, Apr. 2017. [Online]. Available: http://link.springer.com/10.1007/s11831-016-9170-7

[236] J.-F. Gamache, A. Vadean, N. Dodane, and S. Achiche, "On generating stiffening layouts with density-based topology optimization considering buckling," N.D., unpublished.

[237] J.-F. Gamache, A. Vadean, N. Dodane, and S. Achiche, "Topology Optimization for Stiffened Panels: A Ground Structure Method," in *IDETC-CIE2020*, Volume 11A: 46th Design Automation Conference (DAC), Aug. 2020, v11AT11A049. [Online]. Available: https://doi.org/10.1115/DETC2020-22103

[238] J. Zhu and T. Gao, *Topology optimization in engineering structure design*. Elsevier, 2016.

[239] MATLAB, *version 9.8.0 (R2020a)*. Natick, Massachusetts: The MathWorks Inc., 2020.

[240] O. Sigmund, "Morphology-based black and white filters for topology optimization," *Structural and Multidisciplinary Optimization*, vol. 33, no. 4-5, pp. 401–424, 2007.

[241] A. J. Torii, R. H. Lopez, and L. F. Miguel, "Design complexity control in truss optimization," *Structural and Multidisciplinary Optimization*, vol. 54, no. 2, pp. 289–299, 2016.

[242] W. Zhang, J. Zhou, Y. Zhu, and X. Guo, "Structural complexity control in topology optimization via moving morphable component (mmc) approach," *Structural and Multidisciplinary Optimization*, vol. 56, no. 3, pp. 535–552, 2017.

[243] U. Chouinard, S. Achiche, and L. Baron, "Integrating negative dependencies assessment during mechatronics conceptual design using fuzzy logic and quantitative graph theory," *Mechatronics*, vol. 59, pp. 140–153, 2019. [Online]. Available: https://www.sciencedirect.com/science/article/pii/S0957415819300376

[244] K. Bjarklev, T. Eifler, N. H. Mortensen, S. Linnebjerg, and M. Ebro, "Product behavior complexity metric for early prioritization of tolerance analysis tasks," *Design Science*, vol. 6, p. e1, 01 2020.

[245] K. Sinha, E. S. Suh, and O. de Weck, "Integrative Complexity: An Alternative Measure for System Modularity," *Journal of Mechanical Design*, vol. 140, no. 5, 03 2018, 051101. [Online]. Available: https://doi.org/10.1115/1.4039119

[246] G. Min, E. S. Suh, and K. Hölttä-Otto, "System Architecture, Level of Decomposition, and Structural Complexity: Analysis and Observations," *Journal of Mechanical Design*, vol. 138, no. 2, 12 2015, 021102. [Online]. Available: https://doi.org/10.1115/1.4032091

[247] G.-S. Shin, Y.-I. Kim, and G.-J. Park, "Decoupling process of a coupled design in axiomatic design using the triz," *Transactions of the Korean Society of Mechanical Engineers A*, vol. 31, no. 1, pp. 77–88, 2007.

[248] N. P. Suh, *The principles of design*, ser. Oxford series on advanced manufacturing. New York: Oxford University Press, 1990, no. 6.

[249] L. N. Trefethen and D. Bau, *Numerical Linear Algebra*. Philadelphia: Society for Industrial and Applied Mathematics, 1997.

[250] R. Tom, "Find multi-objective pareto front using modified quicksort," 2021, retrieved: 2021-03-03. [Online]. Available: https://www.mathworks.com/matlabcentral/fileexchange/73089-find-multi-objective-pareto-front-using-modified-quicksort

[251] S. Chu, S. Townsend, C. Featherston, and H. A. Kim, "Simultaneous layout and topology optimization of curved stiffened panels," in *AIAA AVIATION 2020 FORUM*, 2020, p. 3144.